Cloning and expression of Na^+, K^+-ATPase in the euryhaline bull shark, *Carcharhinus leucas*

Lara J. Meischke

Thesis submitted for the degree of Doctor of Philosophy
University of St Andrews

March 2006

Declaration

I, Lara Meischke, hereby certify that this thesis, which is approximately 55, 000 words in length, has been written by me, that it is the record of work carried out by me and that it has not been submitted in any previous application for a higher degree.

Date 23/03/06 Signature of Candidate

I was admitted as a research student in October 2001 and as a candidate for the degree of Ph. D. in Biology in (month year); the higher study for which this is a record was carried out in the University of St Andrews between 2001 and 2005.

Date 23/03/06 Signature of Candidate

I hereby certify that the candidate has fulfilled the conditions of the Resolution and Regulations appropriate from the degree of Ph. D. in Biology in the University of St Andrews and that the candidate is qualified to submit this thesis in application for that degree.

Date 23/03/06 Signature of Supervisor

In submitting this thesis to the University of St Andrews I understand that I am giving permission for it to be made available for use in accordance with the regulations of the University Library for the time being in force, subject to any copyright vested in the work not being affected thereby. I also understand that the title and abstract will be published, and that a copy of the work may be made and supplied to any bona fide library or research worker.

Date 23/03/06 Signature of Candidate

Acknowledgements

This work was funded by grant number NER/A/S/2000/01270 awarded by NERC. I was a tied research student on this project and as such was required to fulfil many of the objectives outlined in this grant proposal.

I would like to thank the following for their help and support during the course of my work in St Andrews.

Gordon Cramb, my Ph. D. supervisor, who was always available for questions, suggestions, encouragement and assistance.

All of my colleagues in the Biomolecular Osmoregulation Research Group, particularly Chris Cutler, Gillian Wilson, Iain McWilliam, Anne-Sophie Martinez and several undergraduate students carrying out their Honours projects in our lab. These people not only provided technical and laboratory expertise and assistance, but also enthusiasm, ideas and focus.

The collaborators on the bull shark project: Neil Hazon, Gary Anderson, Craig Franklin, Richard Pillans and Jon Good. I would like to especially thank Neil for contacting me in reference to this project, after I had sent numerous emails over the previous years enquiring about elasmobranch work in the UK.

The technical staff in the Bute Medical Buildings, Workshop, and Photographics who were always on hand to help when needed.

The teaching staff in the School of Biology who were kind enough to offer me teaching work in order to supplement my grant.

My family, who have always enthusiastically supported my endeavours without question. They strengthen my determination, provide emotional and financial support, and I hope I continue to make them proud.

My friends, who have offered ears and shoulders, advice and hospitality, diversion and amusement. A special thank you to Chris who continues to make a significant contribution to my sanity, happiness and well-being.

Finally, thank you to everyone involved in the production and distribution of the film Jaws (1975). This film sparked my interest in sharks and has ultimately led me to where I am today.

Contents

Figure List

Chapter 1: Introduction

Chapter 2: Materials and Methods

Chapter 3: Amplification, cloning and sequencing of Na^+, K^+-ATPase α and β subunit isoforms from the bull shark

Abbreviations List

AFA	Afferent filament artery
ALA	Aferent lamellar arteriole
ANOVA	Analysis of variance
AP	Adaptor primer
AQP	Aquaporin
ATL	Ascending thin limb of Henle
ATP	Adenosine triphosphate
ATS4B	Activated thiol Sepharose™ 4B
ACV	Afferent companion vessel
bp	Base pair
BSA	Bovine serum albumin
BW	Brackish water
BZ	Bundle zone
C	Capsule
CA	Carbonic anhydrase
cAMP	Cyclic adenosine monophosphate
CC	Corpus cavernosum
CCD	Charge coupled device
CCD	Cortical collecting duct (relating to kidney)
ccdB	Control of cell death B
cDNA	Complementary deoxyribonucleic acid
CF	Cystic fibrosis
CFTR	Cystic fibrosis transmembrane conductance regulator
cGMP	Cyclic guanosine monophosphate
CHIF	Corticosteroid hormone induced factor/channel inducing factor
CNP	C-type natriuretic petide
CNT	Connecting tubule
CTAL	Cortical thick ascending limb
CVS	Central venous sinus
dATP	Deoxyadenosine 5'-triphosphate
DCT	Distal convoluted tubule
dCTP	Deoxycytidine 5'-triphosphate
ddNTP	Dideoxyribonucleotide triphosphate
dGTP	Deoxyguanosine 5'-triphosphate
DTL	Distal thin limb of Henle
DNA	Deoxyribonucleic acid
dNTP	Deoxyribonucleotide triphosphate
DTT	Dithiothreitol
dTTP	Deoxythymidine 5'-triphosphate
E. coli	*Escherichia coli*
ECV	Efferent companion vessel
EDTA	Ethylene diamine tetra acetic acid
EFA	Efferent filament arteriole
EFF. AVA.	Efferent arterio-venous anastomosis
ELA	Efferent lamellar arteriole
ELISA	Enzyme-linked immunosorbent assay
EM	External medium
ENaC	Epithelial sodium channel

E	Epithelium
F	Flagellum
FITC	Fluorescein isothiocyanate
FW	Freshwater
FXYD	Protein of FXYD family, with 'FXYD' amino acid motif
G	Glomerulus
GFR	Glomerular filtration rate
GTP	Guanosine triphosphate
HEPES	N-2-hydroxyethylpiperazine-N'-2-ethanesulfonic acid
HPLC	High-Performance Liquid Chromatography
IgG	Immunoglobulin G
Int	Intermediate tubule
K	Connective tissue capsule
KLH	Keyhole limpet haemocyanin
L	Lumen
LB	Luria broth
LP	Lamina propria
Mat-8	Mammary tumour marker
MBS	m-maleimidobenzoyl-N-hydroxysuccinimide
MC	Marginal capillary
MCT	Medullary collecting duct
MIP	Major intrinsic protein
M-MLV RT	Moloney-Murine Leukaemia Virus reverse transcriptase
MOPS	3-[N-Morpholino]-propanesulphonic acid
MR	Mitochondria-rich
MRC	Mitochondria-rich cell
mRNA	Messenger RNA
MTAL	Medullary thick ascending limb
Na^+, K^+-ATPase	Sodium, potassium ATPase
NCBI	National Center for Biotechnology Information
NCC	Sodium 2 chloride transporter
NKCC	Sodium potassium 2 chloride cotransporter
OUC	Ornithine-urea cycle
PAGE	Polyacrylamide gel electrophoresis
PAS	Periodic acid-Schiff
PBS	Phosphate buffered saline
PCR	Polymerase chain reaction
PCT	Proximal convoluted tubule
PGF	Primary gill filament
PKA	Protein kinase A
PKC	Protein kinase C
PKG	Protein kinase G
PLMS	Phosholemman-like protein from shark
PLSD	Post analysis of significant difference
PMSF	Phenyl methyl sulfonyl fluoride
PST	Proximal straight tubule
PVDF	Polyvinylidene difluoride
Px	Proxmial Tubule
RACE	Rapid amplification of DNA ends
RAS	Renin-angiotensin system

RBC	Red blood cell
RC	Renal corpuscle
RIC	Relating to ion channel
RNA	Ribonucleic acid
ROMK	Renal outer medullary potassium channel
RT	Room temperature
RT-PCR	Reverse Transcriptase Polymerase Chain Reaction
S	Blood sinus
SDS	Sodium dodecyl sulphate
SL	Secondary lamellae
SNARE	Soluble N-ethyl-maleimide sensitive factor attachment protein receptor
SS	Septal sinus
SSC	Standard saline citrate
ST	Secretory tubule
SW	Seawater
SZ	Sinus zone
TAE	Tris acetate EDTA buffer
TB	Terrific Broth
TEMED	N, N, N, N tetramethylethylenediamine
TL	Total Length
TMAO	Trimethylamine oxide
UT	Urea transporter
UTR	Untranslated region
UV	Ultra violet
V	Villus
v/v	Volume/volume
VIP	Vasoactive intestinal peptide
vol	Volume
w/v	Weight/volume
wt	Weight

Abstract

The bull shark, *Carcharhinus leucas*, is rare amongst the elasmobranchs in that it is able to tolerate both seawater and freshwater environments. It is able to inhabit water ranging from 0 to 53 ppt by precisely controlling the composition of their body fluids. This requires the expression, function and coordination of several ion transporters and channels including the Na^+, K^+-ATPase. In this study, juvenile bull sharks were acclimated to either freshwater (0 ppt) or seawater (35 ppt). Using RT-PCR and 5'- and 3' RACE techniques, three α isoform subunits and one β isoform subunit of the Na^+, K^+-ATPase have been amplified, cloned and sequenced from the bull shark. The nucleotide and putative amino acid sequences have been analysed and compared to those published for other vertebrate species including stenohaline elasmobranchs. Northern blot and semi-quantitative RT-PCR analyses revealed that Na^+, K^+-ATPase α and β subunit isoform expression is unchanged in *C. leucas* rectal gland, kidney, gill and intestine following transfer from FW to SW. In addition, expression of Na^+, K^+-ATPase α_1 and β_1 subunit isoform proteins in *C. leucas* kidney, gill and intestine is unchanged following FW-SW transfer as determined by Western blotting. The distribution of Na^+, K^+-ATPase α_1 subunit protein in the osmoregulatory tissues of FW- and SW-acclimated *C. leucas* was investigated using immunofluorescence analysis. Na^+, K^+-ATPase immunoreactivity was found in mitochondria-rich (MR) cells of the gill lamellae and filaments in FW-acclimated sharks, but only in the filament MR cells of SW-acclimated sharks. Epithelial cells within the sub-capsular region of the rectal gland exhibits strong immunoreactivity of Na^+, K^+-ATPase compared with the central tubular region in both FW- and SW-acclimated sharks. These results indicate that the changes reported in Na^+, K^+-ATPase activity in the osmoregulatory tissues of the bull shark following FW-SW transfer must be post-translationally regulated, possibly by differential recruitment of subunits to the plasma membrane, direct phosphorylation of the α subunit or by interactions with other molecules, including FXYD proteins.

1

Introduction

1. Introduction

The definition of a euryhaline fish is one which is able to tolerate and acclimate to changes in environmental salinity from freshwater (FW) to seawater (SW) or vice versa (Motais and Garcia-Romeu, 1972). There are many well known and commonly studied euryhaline teleosts, e.g. the European eel, *Anguilla anguilla*, the European flounder, *Platichthys flesus*, the Atlantic salmon, *Salmo salar* and the killifish, *Fundulus heteroclitus* (Appendix 1: List of species names). Euryhaline elasmobranchs are far less common, with true euryhalinity being restricted to only a handful of species (see Section 1.3). These include the bull shark, *Carcharhinus leucas*, which spends most of its adult life in SW, but which enters reduced salinity environments to breed, and both the young which develop within river systems and the adults are able to tolerate FW (see Section 1.2). This life-history pattern is known as anadromy.

Studies of osmoregulation in elasmobranchs have largely been limited to examination of the rectal gland, a salt secreting organ unique to chondrichthian fish (Section 1.4.1). The only truly euryhaline elasmobranch species to have been studied at length is the Atlantic stingray, *Dasyatis sabina* (Piermarini and Evans, 1998; Piermarini and Evans, 2000; Piermarini and Evans, 2001; Piermarini *et al.*, 2003). This study is the first to examine the osmoregulatory biology of *C. leucas*, in particular the cell membrane bound transporters directly responsible for maintaining the ionic composition of the body fluids which make significant contributions to the plasma osmolality of these fish as, they acclimate from FW to SW. The characterisation, expression and distribution of these transport proteins, specifically the Na^+, K^+-ATPase (Section 1.6) will enhance our understanding of osmoregulation in euryhaline elasmobranchs.

1.1. Osmoregulation in Teleosts and Elasmobranchs

Teleosts and elasmobranchs deal with osmotic regulation in markedly different ways (*Figures 1.1 and 1.2*). The body fluids of FW teleosts are hyperosmotic to the external medium, so water is gained by osmosis, and ions are lost by diffusion. These ions must be replaced either by the diet and active transport systems working within the gills to sequester ion from the ion-poor waters. To prevent the edema associated with osmosis, copious

dilute urine is produced to compensate for water influx. In marine teleosts, body fluids are hyposmotic to the external medium so water is lost, and ions are gained. To prevent dehydration, marine teleosts must drink SW to replace the water lost. Water and ions are absorbed across the gut and enter the bloodstream. Mitochondria rich cells, located in the gills, actively pump sodium and chloride ions outward against a large concentration gradient, and the intake of water maintains the gradient of ions from sea to blood (Evans *et al.*, 1999).

In contrast to teleost fish, elasmobranch body fluids are hyperosmotic in both SW and FW environments (*Figure 1.2*). Marine elasmobranch body fluids are at a higher osmotic pressure than that of the external medium (Endo, 1984). Elasmobranchs in SW therefore reduce osmotic flow of water out of the body by maintaining the concentration of the body fluids nearer to that of SW. Elasmobranch plasma Na^+ and Cl^- concentrations are maintained around 50% of that in the SW (Bone *et al.*, 1999). Although these salt concentrations are much the same as other marine fish, other compounds are added to the body fluids to balance the osmotic gradient (*Figure 1.3*). By retaining urea, and other organic compounds such as trimethylamine oxide (TMAO), body fluids are slightly maintained hyperosmotic to the SW, and thus fish gain small amounts of water by osmotic diffusion. The presence of TMAO prevents the urea having a denaturant effect on proteins/enzymes within the elasmobranchs (Yancey and Somero, 1980). Elasmobranch gills are highly impermeable to urea, allowing urea retention, and kidney tubules actively reabsorb the compound. Marine elasmobranchs do experience ion influx, due to the relatively lower concentration of ions within the cells and body fluids. Although elasmobranch gills are less permeable to ions than teleost gills (Evans, 1984[a]), ions still diffuse into the body at the gill. To counteract this salt influx, elasmobranchs make use of the rectal gland, which secretes a highly concentrated solution of Na^+ and Cl^-, but which is isosmotic to the body fluids. In FW, rectal gland function is reduced and may become completely inactive, and water influx is balanced by increasing urine flow rate.

a) Seawater: ~1000 mOsm/kg

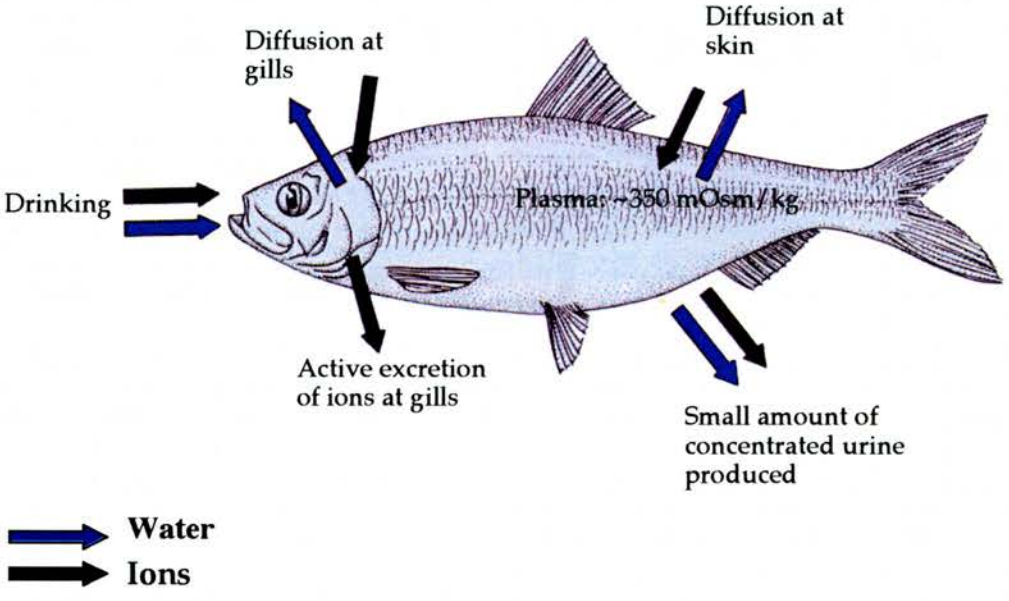

Water
Ions

b) Freshwater: <5 mOsm/kg

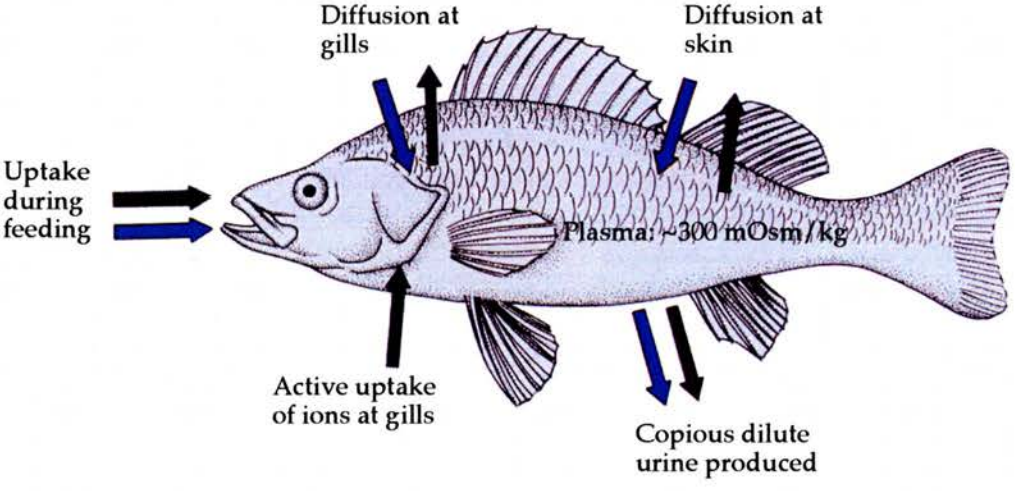

Figure 1.1: Schematic of water and salt exchange in teleost fish. a) seawater teleost **b)** freshwater teleost. (Adapted from Withers, 1992 and Jobling, 1995.)

a) Seawater: ~1000 mOsm/kg

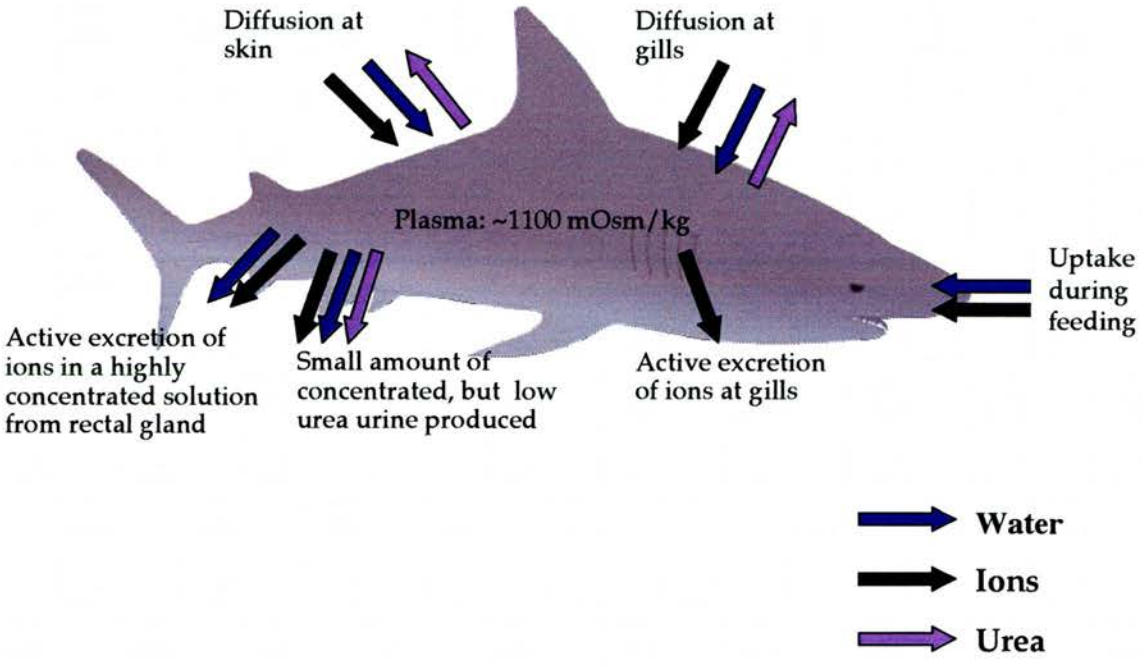

b) Freshwater: <5 mOsm/kg

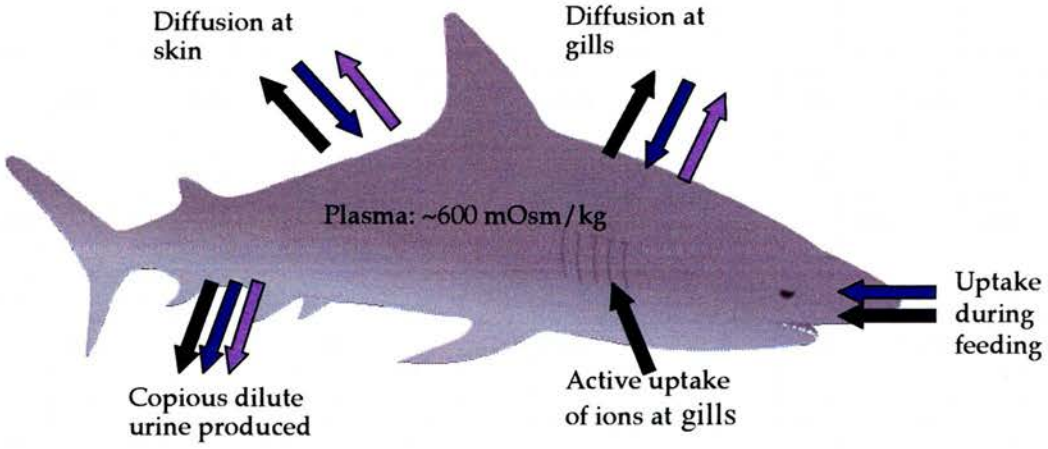

Figure 1.2: Schematic of water and salt exchange in elasmobranch fish. a) seawater elasmobranch **b)** freshwater elasmobranch. Urea is produced and retained in SW elasmobranchs to contribute to the total plasma osmolality, but is not retained to the same extent in FW elasmobranchs. The rectal gland is inactive in FW.

Species	Salinity	Osmolality mOsm.kg^{-1}	Na^+ mmol.l^{-1}	Cl^- mmol.l^{-1}	Urea mmol.l^{-1}
Euryhaline					
Carcharhinus leucas[a]	SW	1067	289	296	370
Carcharhinus leucas[b]	SW	940	304	315	293
Dasyatis sabina[c]	SW	1034	310	300	395
Dasyatis sabina[d]	SW	953	319	296	329
Carcharhinus leucas[a]	FW	642	208	203	192
Carcharhinus leucas[b]	FW	595	221	220	151
Dasyatis sabina[d]	FW	621	212	208	196
Seawater					
Scyliorhinus canicula[e]	SW	1003	-	308	302
Urolophus jamaicensis[f]	SW	1010	301	325	384
Leucoraja ocellata[g]	SW	930	246	232	398
Scyliorhinus canicula[e]	80% SW	776	-	231	212
Urolophus jamaicensis[f]	66% SW	704	240	265	168
Leucoraja ocellata[g]	50% SW	556	151	150	243
Freshwater					
Potamotrygon spp.[h]	FW	320	178	146	1.2
Potamotrygon spp.[i]	FW	308	146	135	1.1
Potamotrygon motoro[j]	FW	349	157	163	0.7
Himantura signifer[j]	FW	416	167	164	44
Potamotrygon spp.[i]	40% SW	391	185	175	1.3
Potamotrygon motoro[j]	66% SW	378	166	180	1.3
Himantura signifer[j]	66% SW	571	231	220	83

Figure 1.3: Total plasma osmolality and plasma concentrations of Na^+, Cl^- and urea in elasmobranchs from FW and SW environments. Plasma composition of the bull shark, *Carcharhinus leucas*; the Atlantic stingray, *Dasyatis sabina*; the European lesser spotted dogfish, *Scyliorhinus canicula*; the yellow stingray, *Urolophus jamaicensis*; the winter skate, *Leucoraja ocellata*; unknown species of Amazonian river ray, *Potamotrygon spp.*; the Amazonian motoro ray, *Potamotrygon motoro* and the Asian white-edge freshwater whip ray, *Himantura signifer*. Sources: [a](Pillans and Franklin, 2004); [b](Pillans *et al.*, 2005); [c](De Vlaming and Sage, 1973); [d](Piermarini and Evans, 1998); [e](Good, 2005); [f](Sulikowski and Maginniss, 2001); [g](Sulikowski *et al.*, 2003); [h](Wood *et al.*, 2002); [i](Gerst and Thorson, 1977); [j](Tam *et al.*, 2003).

Urea retention allows greater control of intracellular ion levels during periods of osmotic stress. Intracellular ion levels can be maintained whilst urea levels alter the net plasma osmolality (Ballantyne *et al.*, 1987). In both FW (Potamotrygonid rays) and euryhaline (*C. leucas*) elasmobranchs, urea levels are only present at very low concentrations (Thorson *et al.*, 1967). When *C. leucas* enters FW from SW, water diffuses into the body fluids, and must be removed. Since the urea is retained in order to increase the plasma osmolality when in SW, it is no longer required in FW. The stenohaline FW Potamotrygonids are not able to increase urea to cope with higher salinities, their gills are more permeable to urea than marine elasmobranchs, and their kidney tubules are less able to reabsorb urea (Piermarini and Evans, 1998). The relative volumes of body fluids of FW and marine sharks are similar in spite of differences in the external medium and in osmotic pressure of body fluids (Thorson, 1962).

1.1.1. Urea/TMAO

In SW elasmobranchs are osmo-conformers; they control the solute concentrations of their body fluids to maintain osmolality as near as possible to that of the environment. To do this, they retain high urea and trimethylamine oxide (TMAO) concentrations in the body fluids when in SW (Stolte *et al.*, 1977). Up to 40% of the plasma osmolality can be accounted for by urea concentrations as high as 680 mM (Ballantyne, 1997). Although these levels would be lethal in most organisms, they are not only tolerated but are essential to the marine elasmobranch (Thorson *et al.*, 1967); elasmobranch metabolism has adapted to function normally in this high urea concentration. The stenohaline FW rays however cannot retain urea and TMAO, and indeed have no need to, as high plasma osmolality would only hinder osmoregulation in a FW environment (Piermarini and Evans, 1998). Some deep sea teleosts, polar teleosts and the coelacanth, *Latimeria chalumnae*, are also able to retain urea and TMAO in the body fluids (Griffith *et al.*, 1973). Besides the obvious osmoregulatory benefits of retaining urea and TMAO, when in SW, these organic osmolytes also contribute significantly to positive buoyancy (Withers *et al.*, 1994).

High urea concentrations can only be tolerated due to the presence of TMAO, other methylamines and betaine (Yancey and Somero, 1979; Yancey

and Somero, 1980; Kleinzeller, 1985; Seibel and Walsh, 2002). These organic anions counteract the denaturing effects of urea on macromolecules such as proteins and nucleic acids. Urea destabilises many proteins by disrupting hydrogen bonds and hydrophobic interactions, and may also change the optimal substrate concentrations for some enzyme reactions (Kanoh *et al.*, 1999). TMAO best neutralises the effects of urea at a ratio of 2:1 (urea:TMAO), and this is the naturally occurring ratio found in the body fluids of marine elasmobranchs and the coelocanth, *L. chalumnae* (Yancey and Somero 1980). Although TMAO reduces the damaging effects of urea, it is probable that many proteins including the Na^+, K^+-ATPase have adapted to function at these higher urea concentrations.

Urea levels are maintained by a well developed urea production system coupled with several retention mechanisms, to prevent massive loss across epithelial surfaces to the external environment. Marine elasmobranchs synthesise urea via the hepatic ornithine-urea cycle (OUC), and excrete urea as an end product of nitrogen metabolism. OUC enzymes are present in little skate embryos (*Raja erinacea*) as early as 4 months, which correlates with the opening of their egg capsules and therefore their first direct contact with the marine environment (Steele, *et al.*, 2004). Urea may also be synthesised in the skeletal muscle (Steele *et al.*, 2005). Diet is also critical to the maintenance of urea levels; a high protein diet is necessary to maintain urea biosynthesis. The European lesser spotted dogfish, *Scyliorhinus canicula* fed on a low protein diet, (and thus lower rate of urea biosynthesis) were unable to increase plasma urea concentration when acclimated to hypersaline water, unlike those fed on a high protein diet (Armour *et al.*, 1993[a]). In *S. acanthias* and the black dogfish, *Centroscyllium fabricii*, Treberg and Driedzic (2002) were unable to detect any enzymes responsible for TMAO synthesis, indicating that TMAO in elasmobranchs is obtained solely from the diet.

The elasmobranch kidney can reabsorb more than 90% of the filtered urea from primary urine (Thorson 1967; Hyodo *et al.*, 2004), and models for passive reabsorption via morphological countercurrent systems and specialised urea transporters have been suggested (Boylan, 1972; Friedman and Hebert, 1990; Wright and Land, 1998; Smith and Wright, 1999; Hyodo *et al.*, 2004). Urea transport proteins have been found in the elasmobranch

kidney tissue of several elasmobranch species (Wright and Land, 1998; Smith and Wright, 1999; Janech *et al.*, 2003; Morgan *et al.*, 2003[a]; Hyodo *et al.*, 2004). There is also evidence of a Na^+ coupled secondary active urea transporter (Morgan *et al.*, 2003[b]). Elasmobranch gill membranes also help retain urea and are more impermeable to urea than those of teleost fish (Fines *et al.*, 2001; Zeidel *et al.*, 2005). The apical membrane is particularly impermeable to urea, ammonia and water (Hill *et al.*, 2004). However the basolateral membrane is up to 14 times more permeable to urea than the apical membrane. It is possible that this difference is caused by a basolateral active transporter carrying urea back into the blood against its concentration gradient, and therefore causing less of a apical urea gradient (Part *et al.*, 1998). Despite this low urea permeability, the combination of large surface area and high diffusional gradient amounts to the gill being the primary site of urea efflux in elasmobranch fish (Evans and Kormanik, 1985; Hazon *et al.*, 2003; Wood *et al.*, 1995).

Euryhaline species can decrease plasma urea concentration by reducing urea production when exposed to dilute environments. The effect is reversible, and urea levels rise upon re-entering SW (Goldstein and Forster 1971; Hazon *et al.*, 1997[a]). De Vlaming and Sage (1973) noted that when *D. sabina* was transferred from SW to a range of concentrations of dilute SW down to 35% SW, urea was maintained at 38-40% of the total plasma osmolality. When *D. sabina* was exposed to 26% SW however, urea was found to account for only 33% of the plasma osmolality. Renal urea clearance is increased on exposure to dilute SW in *R. erinacea* and the thorny skate, *Raja radiata*, whereas urea efflux from the gill is unchanged (Payan *et al.*, 1973). This increase in renal urea clearance may be due largely to increased urine production (Section 1.4.2). It is likely that the renal urea transporters described above play an important role in regulating plasma urea concentrations in euryhaline elasmobranchs. Down-regulation of the little skate renal urea transporter (skUT) was observed with exposure to decreased salinity (50% SW; Morgan *et al.*, 2003[a]). It is interesting that even in low-salinites, elasmobranchs remain ureotelic, with the exception of the exclusively FW Potamytrygonidae which are ammonotelic (Thorson *et al.*, 1967). When in FW, euryhaline elasmobranchs maintain plasma urea concentrations of 100-250 $mmol.l^{-1}$. Regulation of the OUC under salinity challenge has been examined with

conflicting results. On exposure to 75% SW, there was no change in the activity of OUC enzymes in *R. erinacea* embryos, however in adult *R. erinacea*, OUC enzyme activity showed a significant decrease (Steele *et al.*, 2004; Steele *et al.*, 2005).

1.2. The Bull Shark, *Carcharhinus leucas.*

C. leucas is of great interest when considering the problem of osmoregulation, as they are known to remain in both FW and SW for extended periods, and freely move between the two environments (Thorson *et al.*, 1973). This shark is a large (2-3m), heavy bodied species, grey in colour, with a characteristically short and rounded snout (*Figure 1.4*). The eyes are small, and the teeth are large, broad and triangular in the upper jaw, whereas more narrow teeth line the lower jaw. Both pectoral and dorsal fins are large. The size of the rectal gland, and the salt and urea concentration of the body fluids vary depending on environmental salinity, and are reduced in specimens taken in FW compared with marine specimens (Thorson *et al.*, 1973); (Thorson *et al.*, 1978); (Sosa-Nishizaki *et al.*, 1998). Urea levels in *C. leucas* range from 134-336 $mmol.l^{-1}$ in FW (Thorson and Gerst, 1972) up to around 800 $mmol.l^{-1}$ in SW (Sosa-Nishizaki *et al.*, 1998).

C. leucas is a relatively abundant species, especially in areas populated by humans, and is able to take large prey from many aquatic environments; this shark is quite probably the most dangerous shark to humans. In a study of shark attacks on the Natal coast, South Africa, between 1960 and 1990, *C. leucas* was found to be responsible for the majority of attacks. It is important to note however, that there were only 12 attacks attributed to *C. leucas* during this 30 year period, compared to a mean annual catch of 59 individuals of this species in the Natal anti shark nets (Cliff, 1991), and a total of 772 caught between 1978 and 1990 (Cliff and Dudley, 1991). Bull sharks caught in gill nets can often be released almost completely unharmed, unlike most sharks which die quickly on becoming entangled in the nets (Manire *et al.*, 2001). The International Shark Attack File has worldwide data on all shark attacks since 1580 to current. Only 101 attacks have been attributed to *C. leucas* during this 425-year period, although this number will be a gross underestimate since many attacks are not reported, or the shark involved misidentified. Of these 101 attacks, 71 were unprovoked (22 of which were

fatal), 20 were provoked, 6 were undetermined and 4 were attacks on boats (Burgess, 2005 and Burgess, G., 2005, pers. comm.).

C. leucas attains a size of several metres, with powerful jaws and large teeth relative to its size. It is not only able to inhabit bathing water on beaches, but also cruises along shallow banked rivers. This shark is often kept in aquaria, living more than 15 years in captivity (Compagno, 1984; Schmid *et al.*, 1990; Schmid and Murru, 1994). It may also be nocturnal; many experiments show a greater catch rate at night (Snelson *et al.*, 1984), although recent studies indicate that the sharks are simply utilising different areas of their habitat, but not altering activity according to time of day (Curtis, T., 2005, pers. comm.). They are opportunistic feeders; the diet mainly consists of bony fish and other elasmobranchs, the adults taking more elasmobranch and non-fish prey than juveniles due to size and prey availability. Lake and river dwelling groups are nearly always juveniles, feeding on small FW teleost fish (Snelson *et al.*, 1984). The adults in saltwater will take most prey available to them, including fish, invertebrates, sea turtles, birds, dolphins and whale offal. They are also a significant predator of other elasmobranchs, from the juveniles of their own and other species up to the large manta ray, *Manta birostris*. They are true scavengers, taking not only aquatic but also terrestrial mammals such as antelope, cattle, people, tree sloths, dogs and rats as well as slaughterhouse offal, and fish and other animals caught in fishing gear (Bass *et al.*, 1973; Compagno, 1984).

The maximum total length of adult *C. leucas* is estimated at 340 cm. Males mature at 160-230 cm and may reach 300 cm; females mature between 180 and 230 cm and may reach 330 cm. Data suggests that females attain a greater size due to their longer life span and greater age at maturity, 18+ years as opposed to 12. In a study based in the Gulf of Mexico, the largest male was 245 cm, and 21.3 years old, and the largest female, 268 cm, was 24.2 years old. The size at birth ranges between 55 and 80 cm (Thorson and Lacy, 1982; Compagno, 1984). Growth ring studies differ from these earlier estimates of age and growth, with the largest female at 221 cm (32 years), and the largest male at 216 cm (29 years). The age at maturity was also markedly different, with the smallest mature female at 197 cm (14 years) and smallest mature male at 196 cm (25 years; Wintner *et al.*, 2002). Age and growth

estimates must be reviewed regularly in order to manage this species. As with most sharks, the slow growth rate and age at maturity mean that this shark is vulnerable to overfishing (Branstetter and Stiles, 1987). *C. leucas* is a popular game fish, and due to its coastal distribution has long been a target for local fishermen and commercial fisheries (Compagno, 1984). Interestingly, a single bull shark was implicated in the food poisoning of 188 patients in Madagascar, leading to 50 fatalities (Boisier *et al.*, 1995).

Sharks are equipped with well-developed sensory systems. Hearing in bull sharks has been briefly examined with the finding that like teleosts, the auditory threshold is similar to that of humans, although the optimal frequency is lower (Kritzler and Wood, 1961). Perhaps the most interesting sense with regard to *C. leucas* is electroreception, via the ampullae of Lorenzini. These ampullae are composed of a collection of sensory cells and a canal opening as a pore in the epidermal surface, located primarily on the underside of the head. These allow the shark to detect and measure slight changes in potential difference between the external environment and the internal sensory cells of the ampullae. This sense has been implicated in prey detection and capture, and also orientation and navigation (Bleckmann and Hofmann, 1999). Given the turbidity of coastal, estuarine and river waters that *C. leucas* is known to inhabit, electroreception may play a crucial role in prey detection and capture. Indeed, the distribution of ampullary pores on the head of *C. leucas* indicates that it relies heavily on this sense for prey capture, rather than vision (Collin and Whitehead, 2004). However, because the ampullary system relies on detecting potential difference, it becomes obvious that the ionic composition of the external environment will affect this sense, and therefore any euryhaline elasmobranch would have to adapt this sense to account for any change in environmental salinity. The ampullae of Lorenzini in juvenile, euryhaline bull sharks are morphologically different to previously described stenohaline SW and FW elasmobranchs (Whitehead, 2002). However, the ampullae of juvenile *C. leucas* native to FW do share some structural adaptations with those from stenohaline FW rays such as the Asian white-edge freshwater whip ray, *Himantura signifer* (Raschi *et al.*, 1997) and rays of the genus *Potamotrygon* (Raschi and Mackanos, 1989) which are thought to optimise the ampullae for electrical detection in FW environments (Whitehead, 2002; Collin and Whitehead, 2004; Whitehead, D., pers. comm.,

2006). It has not yet been determined as to whether the structure changes when *C. leucas* enters SW, nor whether the adult *C. leucas* have electroreceptive ability when in reduced salinity environments.

Bull sharks inhabit tropical and sub-tropical continental coasts, estuaries, warm rivers and lakes (*Figure 1.5*). They are often found close inshore in marine habitats, from 1 m to 30 m deep, but also down to at least 150 m. They have been found in hypo-saline and hyper-saline marine habitats, in lagoons, bays, river mouths and passages between islands. They are the only species with such a large range that can freely invade FW rivers and lakes, and are able to stay there for considerable periods of time, although they do not remain there, returning to the sea to breed. Bull sharks inhabiting Lake Nicaragua were once thought to be a separate species, *C. nicaraguensis*, but this has since been disproved (Thorson, 1962; Compagno, 1988). This species was also formerly referred to as *C. zambezensis* in South Africa, leading to the common name Zambezi shark being used in some areas (Randall, 1986), and has been found in the Zambezi river system at distances up to 1,120 km from the sea (Bass *et al.*, 1973). A man-made landlocked FW lake gave the opportunity to examine the FW adaptation of the bull shark. Two dead female bull sharks were retrieved, at lengths of 222 and 226 cm, at which they should have been sexually mature. The reproductive organs were under-developed, which may have been caused by atrophy of the disused organs in the absence of males, or more likely the inability to mate in FW (Montoya and Thorson, 1982).

In most FW habitats *C. leucas* frequents, the permanent population consists almost entirely of newborns, yearlings and juveniles, up to around 200 cm, but sharks larger than this are rarely seen, apart from mature adults making transient visits (Snelson *et al.*, 1984). All confirmed records of bull sharks in FW in the U.S.A are juveniles (Blackburn, J., 2002, pers. comm.). There are unconfirmed reports of large adult bull sharks in FW such as the shark which attacked three people in Matawan Creek, New Jersey in 1916, over 15 miles (24 km) from the open ocean (Reader's Digest, 1994), and a bull shark which became trapped on the underside of a river transportation vessel in Brisbane, Queensland (Brisbane City Council, 2005, pers. comm.). Juveniles are seldom encountered outside of FW, 99% of more than 1,000 neonatal sharks

from one study were taken in the FW of the river mouth rather than higher salinities (Thorson *et al.*, 1973). It is believed that the young stay in FW to avoid predators. Adults usually tend to avoid diluted SW and FW conditions, although pregnant females may enter estuarine waters for short periods to give birth (Bass *et al.*, 1973). Although all life stages of *C. leucas* can survive in FW, reproduction tends to occur in brackish water along the coast (Thorson, 1982; Montoya and Thorson, 1982). These sharks are also capable of tolerating hypersaline conditions. In South Africa, these sharks can tolerate salinities of up to 53 ppt in the St. Lucia lake system, but tend to leave the lake during periods of such high salinities (Bass *et al.*, 1973). Sharks from these habitats are in poor condition despite food availability, suggesting these to be sub-optimal conditions (Compagno, 1984).

The method of reproduction in *C. leucas* is advanced viviparity, with yolk-sac placenta, estimated 10-11 month gestation, and 1-13 young per litter (Thorson and Gerst, 1972). Mating occurs in the late spring and summer, females often bearing scars. Pregnant females move into inshore or estuarine waters near river mouths (and FW lakes in Nicaragua) to pup in late spring and early summer (Thorson and Gerst, 1972; Curtis. T., 2005, pers. comm.; Blackburn, J., 2005, pers. comm.). The pups are free-swimming miniatures of the adult sharks, and they move into waters of reducing salinity, often into estuaries, coastal lagoons or FW rivers. A study of a Southwest Florida estuary revealed that the smallest sharks (68 – 127 cm), which are also the youngest sharks, up to approximately 1 year old, were found in lower salinity reaches of the estuary and river, at salinities of less than 25 ppt (mean salinity 10-15 ppt). No sharks of <1 year were found in salinities above 17.45 ppt. The sharks caught in the estuarine waters around the river mouths were 89 – 112 cm (1 – 3 years of age), and those caught in the area outside of the estuary ranged in size from 91 – 189 cm (1 – 10 years of age), with the majority larger than 105 cm (>2 years). These estuarine areas can range from 15 – 35 ppt. This study provides strong evidence that bull sharks spend their first year at very low salinities, often in rivers, their second in estuarine waters, after which they move out into high salinity estuaries or full strength SW (Simpfendorfer *et al.*, 2005). Tracking studies have also revealed that juvenile bull sharks move up or down river depending on rainfall and flow rate, the youngest sharks preferring to stay at salinities of 10 – 15 ppt

regardless of geographic location (Heupel, M., 2005, pers. comm.). Temperature was also a factor, with the younger sharks preferring warmer water (Simpfendorfer *et al.*, 2005). The use of inshore nursery areas is also observed in many other elasmobranch species, several of which have been shown to partition habitat utilisation according to size or age (Heupel and Simpfendorfer, 2005; Simpfendorfer and Milward, 1993). A recent observation showed that juvenile blacktip sharks, *Carcharhinus limbatus,* moved out of their normal nursery habitat and into deeper waters prior to the arrival of a tropical storm, and re-entered the nursery after the storm had passed. It is suggested that the sharks were able to sense a drop in barometric pressure preceeding the storm, and responded by seeking out safer conditions (Heupel *et al.*, 2003). Several juvenile bull sharks in the same area also left, however, younger bull sharks from the adjoining Caloosahatchee river stayed for the duration of the storm (Heupel, 2005, pers. comm.). It is possible that the salinity tolerance of the younger sharks was not sufficient for them to enter deeper, more saline waters, or that the riverine sharks either could not detect or were more used to changes in their environment, including atmospheric pressure, and therefore did not respond to the oncoming storm.

Fetal serum solute concentrations are similar to those of the mother, and the uterine fluid (uterine flushing does not occur). The mother takes on most of the osmoregulatory responsibility for the young, with the embryos not exposed to the external environment until close to parturition. Oviparous elasmobranch embryos must osmoregulate from a much earlier stage. This difference is one of the important adaptations in the evolution of viviparity (Kormanik, 1993). The full range of urea tolerance is present before birth, as are functional osmoregulatory mechanisms, but independent osmoregulation may not occur until birth (Thorson and Gerst, 1972). Embryos of the spiny dogfish, *Squalus acanthias,* may osmoregulate prior to birth; later stages have reduced ionic permeability and a functional rectal gland (Evans *et al.*, 1982). It is expected that pups would be able to osmoregulate from birth independent of environmental salinity (Thorson and Gerst, 1972).

It is not fully understood why bull sharks have developed the ability to tolerate FW, since euryhalinity is rare amongst elasmobranchs. *C. leucas* may use this peculiarity to gain access to food resources, reduce predation risk and to deliver their young in an area with fewer competitive predators (Sosa-Nishizaki *et al.*, 1998). The habitat partitioning of juveniles described above strongly supports the theory that bull sharks have evolved to utilise FW habitats in an attempt to reduce predation risk. Sharks themselves represent a significant predatory threat to smaller sharks, even intraspecific predation, and *C. leucas* is known to be cannibalistic (Snelson *et al.*, 1984). Therefore habitat partitioning based on size (and age) would reduce the predatory threat from members of their own species (Simpfendorfer *et al.*, 2005). Furthermore, no other large shark is capable of entering the reduced salinity waters of some estuaries and rivers. Since they are able to tolerate many different environmental conditions, it is surprising that bull sharks are not the dominant shark species along the coasts they inhabit. This may be due in part to the associated energetic costs of being tolerant to a wide variety of salinities. Habitat partitioning by salinity in the juveniles may allow them to minimise these energetic costs (Simpfendorfer *et al.*, 2005).

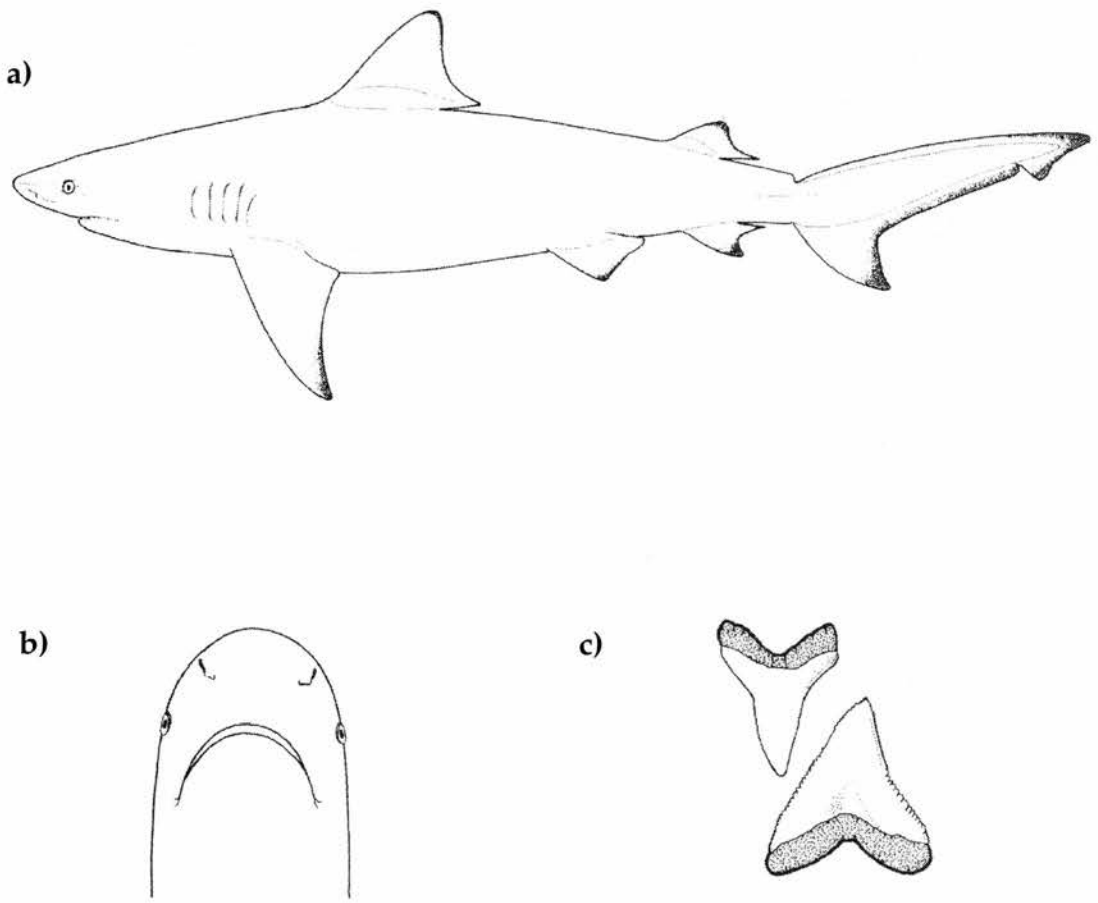

Figure 1.4: The bull shark, *Carcharhinus leucas*. a) *C. leucas*, lateral aspect, **b)** *C. leucas* anterior ventral view, **c)** *C. leucas* tooth morphology, upper and lower (Compagno *et al.*, 2005).

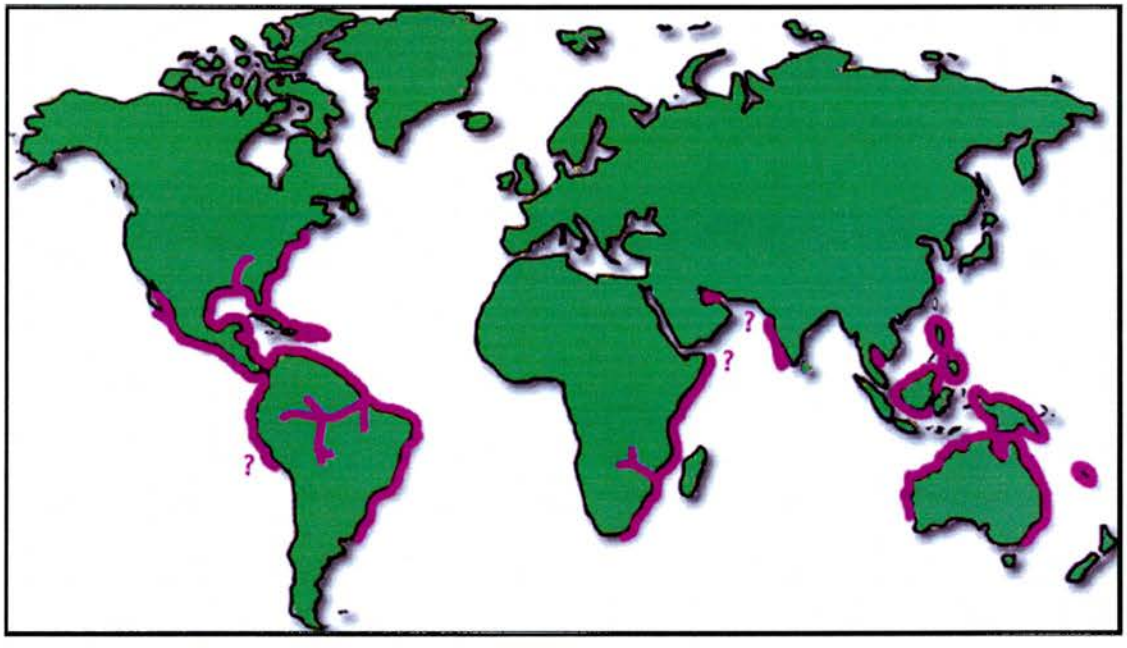

Figure 1.5: Geographical distribution of *C. leucas*. *C. leucas* geographical distribution indicated by purple shading (Compagno *et al.*, 2005).

1.3. Osmoregulation in the bull shark and other freshwater/euryhaline elasmobranchs

C. leucas is able to move between different salinities by using a number of coordinated responses. The main obstacle preventing marine elasmobranchs moving into FW is the high level of urea in their body fluids. Euryhaline species in SW have lower urea levels than stenohaline marine species, but still much higher than that of marine or FW teleosts. When encountering reduced salinity environments, they have mechanisms to lower urea retention, dropping body fluid urea content by 50-80%, decreasing osmotic concentration and limiting water influx. A increase in urea clearance and decrease in urea synthesis drops the plasma concentration to maintain osmotic balance (Thorson *et al.*, 1973; Wong and Chan, 1977). The ability to decrease plasma urea concentration whilst maintaining Na^+ and Cl^- contraction is vital for dilute SW tolerance. This has been demonstrated in many elasmobranch species, including *U. jamaicensis* (Sulikowski and Maginniss, 2001), and the winter skate, *Leucoraja ocellata* (Sulikowski *et al.*, 2003).

Several elasmobranchs, including the Port Jackson shark, *Heterodontus portusjacksoni*, the lemon shark, *Negaprion brevirostris, R. erinacea* and *C. plagiosum*, can be transferred between full strength SW and 50% SW (Thorson *et al.*, 1973; Wong and Chan, 1977; Cooper and Morris, 1998; Cooper and Morris, 2004). Many sharks which inhabit the intertidal zone may also have similar capabilities. Some elasmobranchs, such as *C. limbatus*, and sandtiger shark, *Carcharias taurus*, are able to swim into estuaries when strong tides increase the salinity (Bass *et al.*, 1973). However, it has not been possible to acclimate marine elasmobranchs that do not naturally encounter FW. Many survive low salinity SW, such as the stingaree, *Trygonoptera testacea*, but soon die when kept in FW (Thorson *et al.*, 1983; Cooper and Morris, 1998). It was previously thought that *S. canicula* could not tolerate diluted SW for any prolonged length of time (Thorson *et al.*, 1973), however later studies have managed to successfully maintain this species at reduced salinities (Hazon *et al.*, 2003, for review).

One group of elasmobranchs have made a complete and irreversible transition to FW. The family Potamotrygonidae of stenohaline FW rays are

only found in FW of South America, and are unable to tolerate salinities higher than 14 ppt. This group has made a significant number of adaptations to survive in FW. They can no longer reabsorb urea from the kidney tubules, plasma urea content is generally 1-3 $mmol.l^{-1}$ (Bittner and Lang, 1980) and low activity of the urea cycle enzymes renders them unable to produce enough urea to osmoregulate at higher salinities, although urea levels do rise (Thorson *et al.*, 1967). This puts their salinity tolerance on a par with stenohaline FW teleosts, and both groups regulate mainly by transporting electrolytes, and are therefore unable to tolerate the salt accumulation when transferred to high salinities (Carrier and Evans, 1973; Griffith *et al.*, 1973; Gerst and Thorson, 1977; Bittner and Lang, 1980). Rather than excreting urea as the chief component of nitrogenous waste, Potamotrygonids are ammoniotelic (Gerst and Thorson, 1977; Wood *et al.*, 2002). The majority of salt absorption in Potamotrygonids occurs at the gills, although the skin and kidney may play a role in salt transport. It is probable that the mechanisms for acid/base balance in marine elasmobranchs which allow also for osmoregulation became more suited for this purpose in FW rays (Wood *et al.*, 2002) The rectal gland is present in *Potamotrygon spp.*, but it has atrophied and become a vestigial organ (Shuttleworth, 1988). Another important feature of *Potamotrygon spp.* are the histological differences in the ampullae of Lorenzini, the electroreceptive organ, compared to the ampullae of stenohaline marine elasmobranchs allowing it to work in FW. This organ assists in prey location by detecting the weak electrical fields generated by all living things. Some other elasmobranchs frequenting FW also have this adaptation (Raschi and Mackanos, 1989). Another ray species, *H. signifer*, has been found predominantly in FW, and can tolerate brackish water (Tam *et al.*, 2003). This species has retained the capability to synthesise urea in significant quantities allowing it to increase plasma osmolality when exposed to brackish water, but cannot synthesise and retain sufficient urea to be able to tolerate higher salinities (Ip *et al.*, 2003). This species is not as well adapted for a completely FW lifestyle as the Potamotrygonids.

Apart from *C. leucas*, only a few other elasmobranch species have the ability to tolerate FW for extended periods (see Martin, 2005 for review). These include *D. sabina*, the smooth freshwater stingray (*Dasyatis garouaensis*), the honeycomb stingray (*Himantura uarnak*), the freshwater sawfish (*Pristis*

microdon), the smalltooth sawfish (*Pristis pectinata*) and the largetooth sawfish (*Pristis perotteti*) which are known to inhabit FW, but it is still unclear as to whether they can reproduce without returning to the sea (Bass *et al.*, 1973; Thorson *et al.*, 1983). The genus *Glyphis*, is represented by a possible six species, all of which are known from only a few examples found in estuarine or FW (Compagno *et al.*, 2005). It is interesting to note that, with the exception of the bull shark, many euryhaline species which are found in FW are in decline, for example *Glyphis spp.* (Compagno *et al.*, 2005) and *P. pectinata* (Simpfendorfer, 2005), the latter of which is listed as endangered by several conservation societies. It is possible that many more elasmobranch species can tolerate reduced salinities. Given that many marine elasmobranch species have now been maintained in reduced salinity environments for the purpose of laboratory experimentation, it is possible that many species thought to be stenohaline are in fact at least partially euryhaline. The physiological processes for controlling plasma osmolality by altering salt and urea levels are the same in both partially euryhaline and fully euryhaline species (Hazon *et al.*, 2003).

According to Thorson (1983), *C. leucas* has almost made a complete transition when considering elasmobranch FW adaptation. It is fully euryhaline, and able to survive in FW for long periods. However its life cycle is not completely adapted to FW and must return to higher salinities to breed (Montoya and Thorson, 1982). Despite this technicality, the bull shark can successfully inhabit both FW and SW, making it an ideal and interesting species for this study.

Recent studies have examined several physiological parameters with a view to better understanding osmoregulation in juvenile *C. leucas* in the Brisbane River (Pillans and Franklin, 2004; Pillans *et al.*, 2005). Juvenile *C. leucas* of 70-130 cm in length are found along the entire accessible length of the Brisbane River, but as observed in other similar river systems, smaller sharks remain in FW or estuarine water compared to their much larger sized SW dwelling conspecifics (*Figure 1.6*). There was no difference in rectal gland size between juvenile *C. leucas* captured in FW and estuarine water. This may be indicative of the extent of movement of the sharks along the salinity gradient during their development. Studies have already shown patterns of bull

shark movement in other systems where the sharks preferentially inhabit waters of 10-20 ppt (Section 1.2). Plasma osmolality increases slightly with increasing environmental salinity, and the internal body fluids are always hyperosmotic to the external environment (*Figure 1.7*). Na^+ and Cl^- concentrations remain relatively constant across all salinities observed, and it is the increase in urea concentration that contributes to the net increase in plasma osmolality in higher salinities (*Figure 1.8*). (Pillans and Franklin, 2004). However, this study utilised sharks caught at particular salinities, which may not provide a completely accurate picture since it is not known how rapidly or frequently these sharks move along the salinity gradient. It is impossible to know how long the sharks caught have inhabited these specified salinities, and whether they have previously been exposed to higher or lower salinity environments.

In contrast, further studies have examined juvenile *C. leucas*, caught in FW, and acclimated to either FW or SW in laboratory aquaria under controlled conditions. Although this is more controlled in that the sharks have been at a fixed salinity for a known period of time, it is not possible to account for any osmoregulatory contributions made by previous exposure to different salinities. Both Na^+ and Cl^- plasma concentrations were elevated in the SW-acclimated group, and the salt levels of both FW- and SW-acclimated groups were similar to those observed in the equivalent wild caught *C. leucas*. As in the wild caught sharks, plasma osmolality increases with increasing salinity, although the total plasma osmolality of both FW- and SW-acclimated sharks was 10-15% less than wild caught *C. leucas*. This deficit arises from a decrease in total urea plasma concentration in both captive groups, a phenomenon observed in other captive elasmobranchs as an effect of starvation (Section 1.1.1). The sharks in this study were fed, so presumably the urea levels are affected by stress due to captivity. Salt levels were apparently unaffected by captivity. A summary of the changes in plasma composition in both FW- and SW-acclimated fish is given in *Figure 1.9*. TMAO is also significantly elevated in SW-acclimated *C. leucas* compared to the FW-acclimated fish (Pillans *et al.*, 2005).

Na^+, K^+-ATPase activities were determined in the four major osmoregulatory tissues and was found to be much lower in gill and intestine compared to

rectal gland and kidney (*Figure 1.10*). There was no significant difference between Na^+, K^+-ATPase activity in gill and intestine from FW- and SW-acclimated fish. Given that current models imply the activity of Na^+, K^+-ATPase as a major facilitator of salt uptake in FW elasmobranch gills, it was expected that activity of this enzyme would decrease when exposed to higher salinities, as has been observed in *D. sabina* (Piermarini and Evans, 2000; Piermarini and Evans, 2001; Piermarini *et al.*, 2003). In the elasmobranch gill, the activity of Na^+, K^+-ATPase may remain constant, although the location of this enzyme may differ markedly, as has been observed in *D. sabina* (Piermarini and Evans, 2000). The intestine is not expected to play a large role in osmoregulation in elasmobranchs, therefore it is not surprising that there was no significant difference between treatment groups. Significant differences in Na^+, K^+-ATPase activities were only observed in rectal gland and kidney between treatment groups. In the rectal gland, Na^+, K^+-ATPase activity increased by ~50% following SW-acclimation, which is an expected result considering that the gland is known to secrete salt in marine elasmobranchs. Conversely, Na^+, K^+-ATPase activity decreased by ~100% in the kidney of *C. leucas* acclimated to SW. This highlights the importance of the kidney in FW-acclimation to reabsorb salts and produce copious dilute urine (Pillans *et al.*, 2005).

	Freshwater (0‰) n=21	Estuarine (11-28‰) n=10	Seawater (33‰) n=6
Mean size	867.8	873.4	1970.4
Minimum size	740	760	1550
Maximum size	1690	1043	2310

Figure 1.6: Average, minimum and maximum total length (mm TL) of *C. leucas* captured in FW, estuarine and marine environments (Pillans and Franklin, 2004).

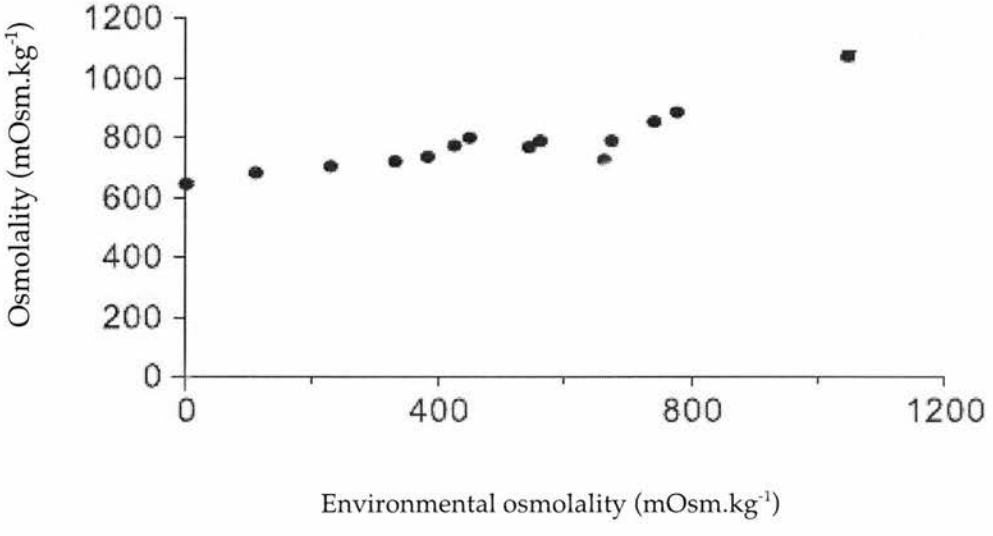

Figure 1.7: Plasma osmotic pressures of *C. leucas* captured along a salinity gradient in the Brisbane River against osmotic pressure of water from site of capture (Adapted from Pillans and Franklin, 2004).

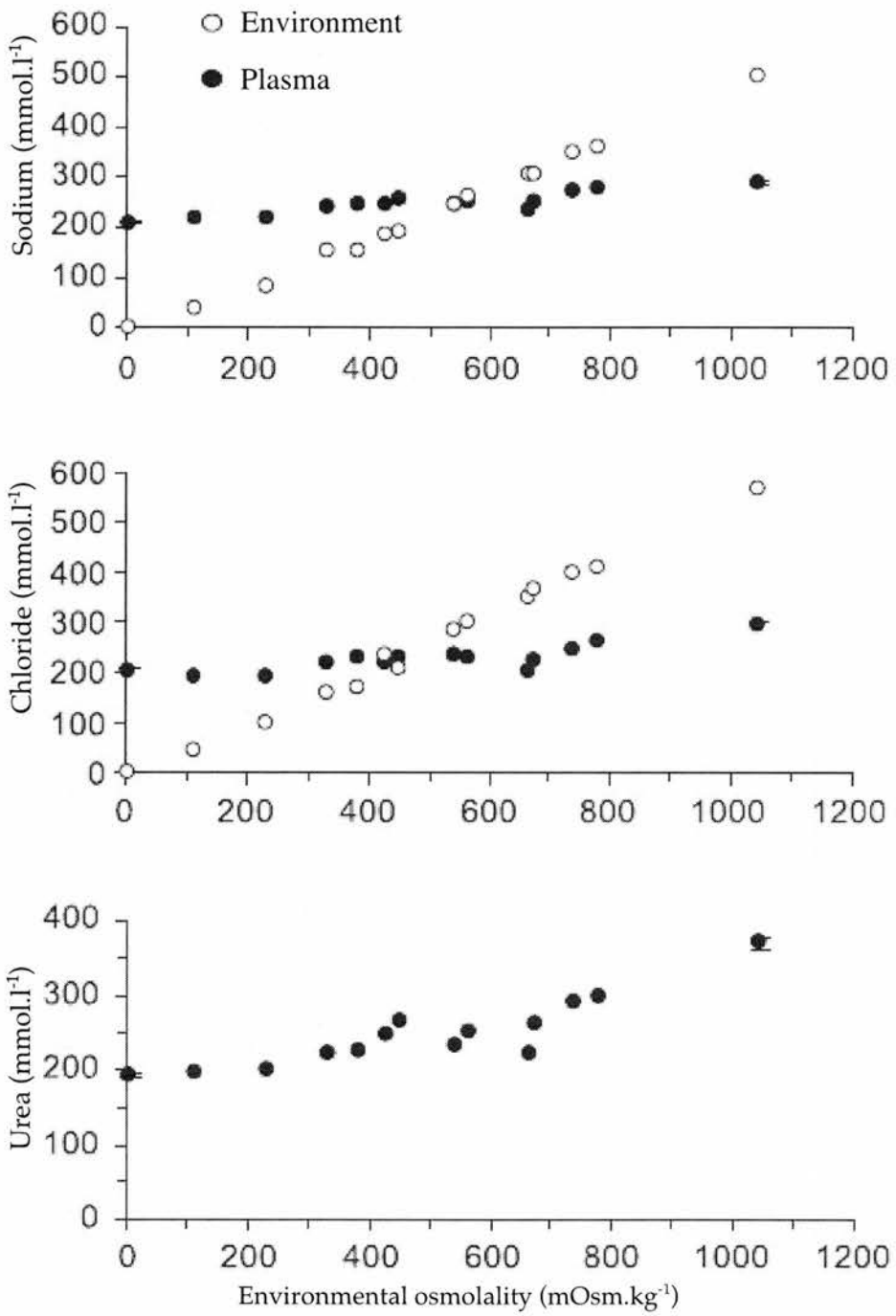

Figure 1.8: Plasma osmolyte concentrations of *C. leucas* plasma captured along a salinity gradient in the Brisbane River against osmolyte concentration from site of capture (Adapted from Pillans and Franklin, 2004).

	Freshwater (0‰) n=17	Seawater (33‰) n=11
Osmolality ($mOsm.kg^{-1}$)	595 ± 11	940 ± 10 *
Na^+ ($mmol.l^{-1}$)	221 ± 4	304 ± 3 *
Cl^- ($mmol.l^{-1}$)	220 ± 4	315 ± 3 *
K^+ ($mmol.l^{-1}$)	4.2 ± 0.2	5.8 ± 0.3 *
Mg^{2+} ($mmol.l^{-1}$)	1.3 ± 0.1	1.8 ± 0.1 *
Ca^{2+} ($mmol.l^{-1}$)	3.0 ± 0.1	4.4 ± 0.3 *
Urea ($mmol.l^{-1}$)	151.0 ± 5.0	293 ± 9 *
TMAO ($mmol.l^{-1}$)	19.1 ± 1.3 (6)	47.3 ± 4.5 (5) *

Figure 1.9: Plasma osmolality, ion and urea concentrations from bull shark, *C. leucas* acclimated to FW and SW for 1 week. Values are means ± SEM. Numbers in parentheses for TMAO represent sample size. *: significant difference (P<0.05) between FW- and SW-acclimated animals (Adapted from Pillans *et al.*, 2005).

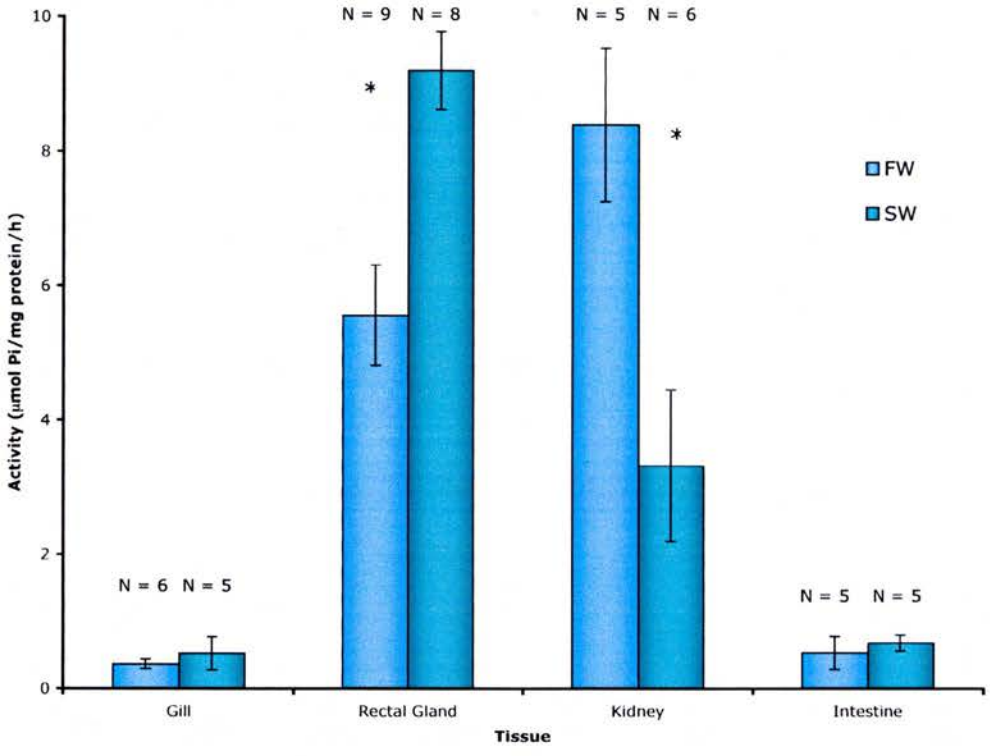

Figure 1.10: Maximal Na^+, K^+-ATPase activity of gill, rectal gland, kidney and intestine from *C. leucas* acclimated to FW and SW for 1 week. Asterisk indicates significant difference (P<0.05) between FW- and SW-acclimated animals (Adapted from Pillans *et al.*, 2005)

1.4. Osmoregulatory tissues

The cells of all vertebrate tissues contain Na^+, K^+-ATPase. For the purpose of studying the role of Na^+, K^+-ATPase in the osmoregulatory biology of the bull shark, particular emphasis is placed upon the rectal gland, kidney, gill and intestine. Osmoregulation is carried out by specialised cells (mitochondria rich cells or MR cells; Section 1.5) in the epithelia of osmoregulatory tissue. These cells contain numerous transport proteins including the Na^+, K^+-ATPase, the sodium, potassium, two chloride cotransporter (NKCC; Section 1.7.1) and the cystic fibrosis transmembrane conductance regulator (CFTR; Section 1.7.2). The following sections will summarise what is known about the anatomy, osmoregulatory function and control of each of these organs, with reference to studies in elasmobranchs, teleosts, and other vertebrates.

1.4.1. Rectal Gland

In 1899, Crawford described the rectal gland as looking very much like it had an excretory function, and may act as a supplementary kidney (as cited in Thorson *et al.*, 1978). Today the tubular epithelial cells of the gland are considered to be an excellent model tissue for the study of epithelial salt secretion. Salt secretion from the blood to the external environment depends on the movement of at least 3 different ions, utilising the functions of several transporters and channels (Riordan *et al.*, 1994). The rectal gland secretes a fluid that has often double the salt concentration of the plasma, but is isosmotic to SW (Burger and Hess, 1960; Anderson *et al.*, 1995). The gland has also been implicated in the excretion of certain xenobiotics (Miller at al., 1998; Miller *et al.*, 2002).

The rectal gland itself is a compound tubular gland (Shuttleworth, 1988), situated towards the caudal end of the body cavity (Hazon *et al.*, 1997[a]), suspended from the body wall by a mesentry (*Figure 1.11a*). The gland develops from the epithelium of the posterior intestine in the embryo, and by repeated folding of this epithelium (Chan and Phillips, 1966; Fishelson *et al.*, 2004). It is supplied with oxygenated blood by the posterior mesenteric artery, with the blood then exiting via the dorsal intestinal vein. The blood is distributed to the gland via the circumferential vessels within the capsule which penetrate into the gland to supply the secretory tubules. However,

there is a route whereby blood flow entering the gland can be redirected to essentially bypass the gland, indicating that secretory function is inherently linked to blood flow (Kent and Olson, 1982; *Figure 1.11b*). A cross section of the gland reveals three distinct layers: the peripheral capsule composed of connective tissue, the tubular region containing tubules consisting of cuboidal epithelial cells, and the central duct (Chan and Phillips, 1967; *Figure 1.12*). The secretory tubules of the rectal gland empty into the single central collecting duct (Riordan *et al.*, 1994), which opens into the lower intestine, just anterior to the rectum (*Figure 1.11a*). The gland (in *S. acanthias*, *D. sabina* and the white shark, *Carcharodon carcharias*) is covered in a layer of smooth muscle, which can alter the shape of the gland, and this may also affect the rate of secretion of the gland (Evans and Piermarini, 2001).

The subcellular components of rectal gland tubule cells were examined in the yellow stingray, *Urolophus jamaicensis*, a species which is able to tolerate reduced salinities. In *U. jamaicensis*, there are numerous vacuoles in the apical region, basal infoldings, and complex lateral membrane interdigitations with adjacent cells (Doyle, 1962). The rectal gland of *S. acanthias* was also found to have complex and numerous basal membrane infoldings, in addition to extensive lateral interdigitations (Bulger, 1963). The complex but 'leaky' lateral interdigitations are consistent with the model of salt secretion in the gill whereby sodium ions pass between MR cells and adjacent developing MR cells or accessory cells (Ernst *et al.*, 1981; Forrest *et al.*, 1982). The gross and fine structures of the gland in elasmobranchs are identical to that of the related chondrichthian sub-class, the holocephali (Lagios and Stasko-Concannon, 1979). The size of the gland itself increases allometrically, smaller sharks have large glands in comparison to their body weight, and the rate of growth of the gland is less than the growth of the fish. This is to be expected since smaller sharks have a larger surface area to volume ratio, and therefore would be subject to greater ion uptake requiring a rectal gland of sufficient size and activity to remove these salts (Anderson *et al.*, 2003).

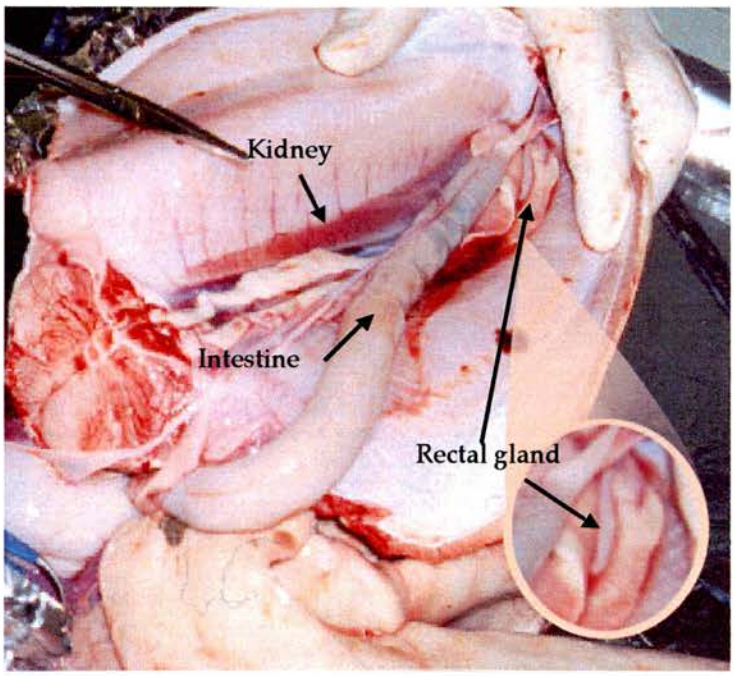

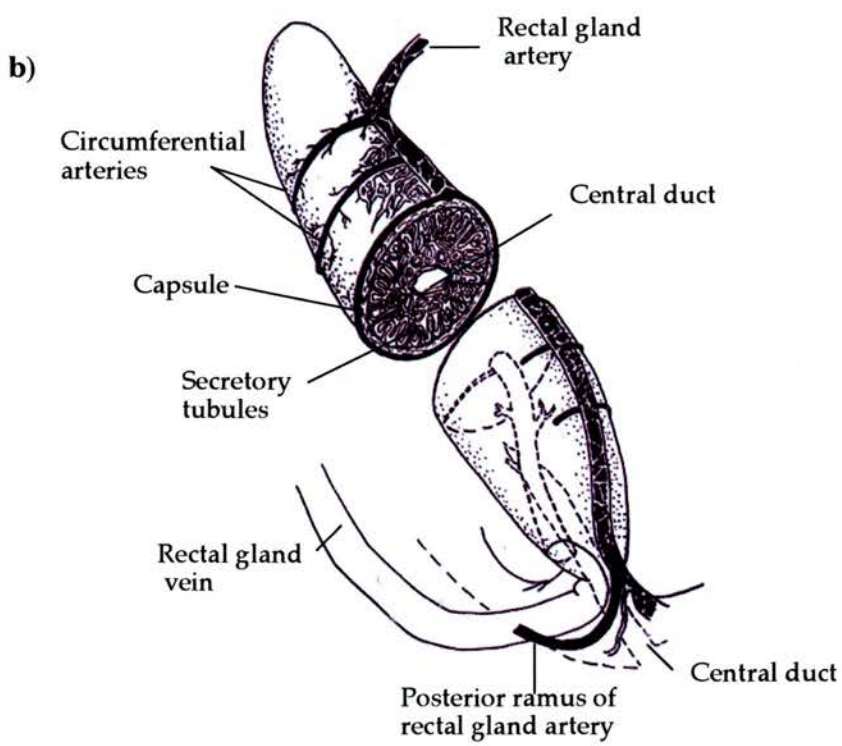

Figure 1.11: Position and structure of the elasmobranch rectal gland. a) Position of rectal gland, kidney and intestine in the body cavity of juvenile *C. leucas*. **b)** Vasculature and structure of the rectal gland (Adapted from Kent and Olson, 1982).

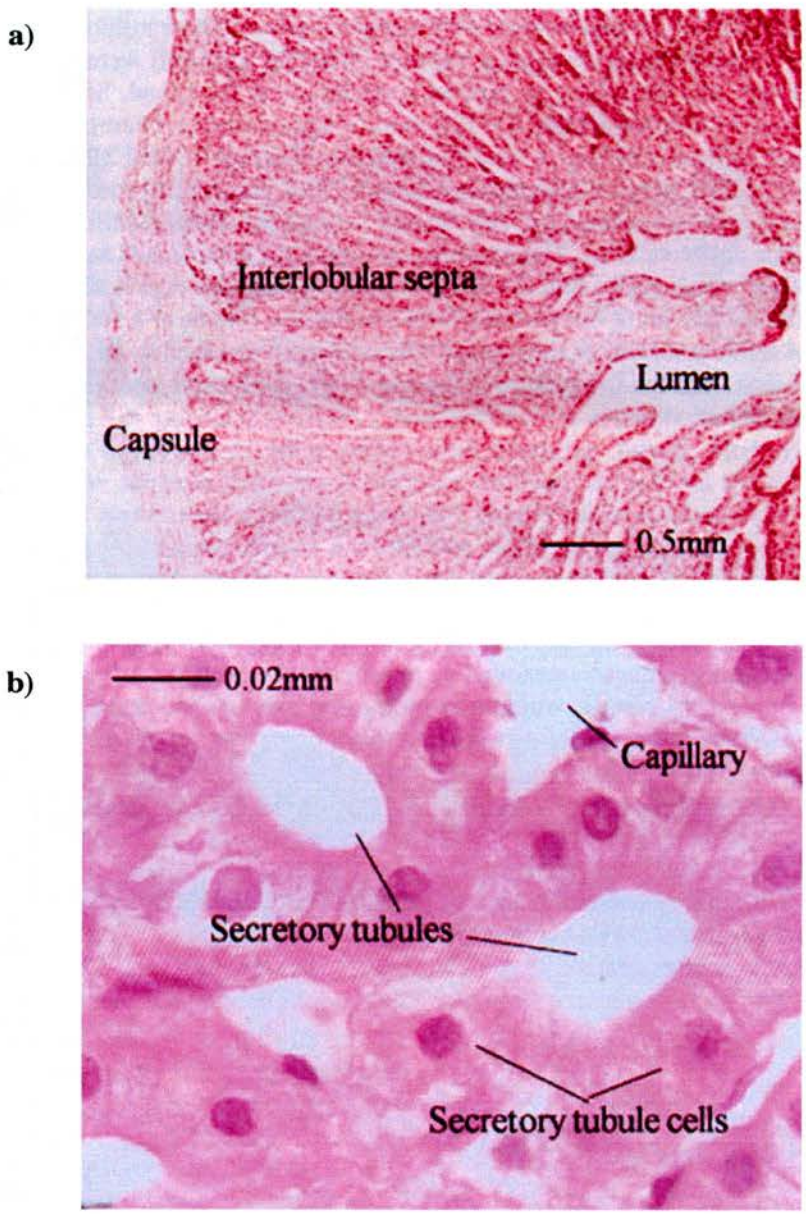

Figure 1.12: Light micrograph sections showing the structure of the rectal gland in *H. portusjacksoni*. **a)** Low power micrograph of the rectal gland. **b)** Secretory tubules (Newbound and O'Shea, 2001).

As such an important and unique osmoregulatory structure, many studies have been carried out on the cells of this gland. Investigation into the mechanisms of salt secretion in this gland has led to the proposal of Na^+, K^+-ATPase (Silva *et al.*, 1977; Greger and Schlatter, 1984[a]; Greger and Schlatter, 1984[b]; Riordan *et al.*, 1994), and NKCC (Forbush *et al.*, 1992) expression on the basolateral membrane of rectal gland epithelial cells and CFTR situated on the luminal membrane (Hannafin *et al.*, 1983). This arrangement of transporters is also observed in SW teleost gill MR cells (Sections 1.4.3 and 1.5). High Na^+, K^+-ATPase activity was found in the rectal glands of nine elasmobranchs (Bonting, 1966). Localization studies confirmed the basolateral positions of the Na^+, K^+-ATPase (Goertmiller and Ellis, 1976; Lear *et al.*, 1992) and the NKCC cotransporter (Lytle *et al.*, 1992). A basolateral K^+ channel was also identified (Gogelein *et al.*, 1987[a]; Greger *et al.*, 1987[a]) and characterized (Waldegger *et al.*, 1999; Kerst *et al.*, 2001). There are two luminal chloride channels, one of which may be the CFTR cloned from shark rectal gland, sCFTR (Gogelein, *et al.*, 1987[b]; Greger *et al.*, 1987[a]; Greger *et al.*, 1987[b]; Hanrahan *et al.*, 1993).

Experimental studies in vitro have shown that the secretory activity in the rectal gland can be stimulated by cAMP, and by hormones using cAMP as a second messenger (Greger and Schlatter, 1984[a]; Greger and Schlatter, 1984[b]; Greger *et al.*, 1984; Lytle and Forbush, 1992[a]). Addition of cAMP to rectal gland preparations stimulates rectal gland activity and oxygen consumption, as does theophylline, by inhibiting the breakdown of cAMP (Stoff *et al.*, 1979; Stoff *et al.*, 1977; Shuttleworth and Thompson, 1980; Marver *et al.*, 1986; Anderson *et al.*, 1995). The steroid 1-α-hydroxycorticosterone stimulates rectal gland activity; removal of the interrenal gland causes a decrease in both the volume and NaCl concentration of the fluid secreted (Holt and Idler, 1975). A conflicting study on the effects of 1-α-hydroxycorticosterone in *S.canicula*, suggest that it may decrease Na^+ (and Cl^-) excretion in the kidney and rectal gland (Armour *et al.*, 1993[b]). Several other biological factors have been demonstrated to affect the activity of the rectal gland or rectal gland cell cultures including C-type natriuretic peptide (CNP; Solomon *et al.*, 1992; Gunning *et al.*, 1993; Silva *et al.*, 1993[a]), guanylin (Karnaky *et al.*, 1999) and certain peptides isolated from the intestine, such as vasoactive intestinal peptide (VIP) and Scyliorhinin II (Anderson *et al.*, 1995).

It was believed that vasoactive intestinal peptide (VIP) stimulated rectal gland secretion by raising the intracellular levels of cAMP. This was seen in experiments on the spiny dogfish, *S. acanthias*, (Stoff *et al.*, 1979; Holmgren and Nilsson, 1983; Greger *et al.*, 1988). Somatostatin inhibits the accumulation of cAMP caused by VIP therefore blocking secretion (Solomon *et al.*, 1984[a]; Silva *et al.*, 1985; Stoff *et al.*, 1988). Bombesin, found in rectal gland nerve fibres, induces release of somatostatin into the gland from rectal gland neurosecretory nerve terminals, and therefore also inhibits the effects of VIP (Silva *et al.*, 1990). However, VIP only stimulated secretion in explanted rectal glands from *S. acanthias*, but not other experimental species, such as *S. canicula*, or *R. erinacea*, (Anderson *et al.*, 1995; Shuttleworth and Thorndyke, 1984). Therefore it was proposed that VIP was unlikely to be involved the control of rectal gland secretion in vivo (Shuttleworth and Thorndyke, 1984).

Another intestinal peptide was isolated, distinct from VIP, which caused stimulation in the rectal gland not only of *S.acanthias*, but also *S. canicula* and *R. erinacea*. This peptide, provisionally named rectin, was thought to be related to the urotensins, a group of peptides known to control salt and water balance in teleosts (Thorndyke and Shuttleworth, 1985). More recent studies have led to the assumption that rectin is in fact Scyliorhinin II, a gut peptide of the tachykinin family, isolated from *S.canicula*, as it has the same amino acid sequence and elicits the same response (Conlon *et al.*, 1986). Scyliorhinin peptides are absent from teleosts suggesting a specific role in elasmobranchs, including rectal gland stimulation (Anderson *et al.*, 1995).

CNP is found in the shark heart, brain and pituitary gland. Small amounts are also expressed in the kidney, liver and intestine (Suzuki *et al.*, 1994). CNP acts via several different pathways to result in increased rectal gland chloride secretion (Anderson *et al.*, 2002[a]). It acts on guanylyl cyclase to produce cGMP which is thought to activate the apically located CFTR chloride channel (Silva *et al.*, 1999). Similarly, CNP stimulates the release of VIP which acts on adenylyl cyclase with a resultant increase in intracellular cAMP, which again activates CFTR via stimulation of protein kinase A (Silva *et al.*, 1999). CNP also triggers the release of catecholamines such as noradrenaline in *S. acanthias* (McKendry *et al.*, 1999), which may increase

blood flow to the gland, and thus cause an increase in secretion due to cell volume expansion (Solomon *et al.*, 1984[b]; Solomon *et al.*, 1985; Gunning *et al.*, 1993).

Activities and mRNA expression of Na^+, K^+-ATPase α and β subunits, and mRNA expression of NKCC, and CFTR were examined in the rectal gland of *S. canicula* following a feeding event. Feeding temporarily enforces a salt load on the shark so it would be expected that there would be increase secretory activity in the rectal gland. The mRNA expression of all four transcripts increased, but only 1-2 days after the feeding event. However Na^+, K^+-ATPase activity began to increase only 3 hours after the feeding event and peaked at 9 hours when it was 40 times greater than the activity prior to the feeding event. This study indicates that feeding-induced increases in rectal gland Na^+, K^+-ATPase activity are not initially dependent on an increase in mRNA expression and are regulated by alternate mechanisms, which are possibly hormonally mediated (MacKenzie *et al.*, 2002).

Stenohaline FW elasmobranchs have a smaller or inactive rectal gland, as they no longer need to excrete salt in a low salt environment (Piermarini and Evans, 1998). This means that the rectal gland from a FW elasmobranch is more difficult to identify, due to its size, and is often mistaken for myeloid tissue (Thorson *et al.*, 1978). The gland also shows a reduction in the number of tubules for salt secretion (Gerzeli *et al.*, 1976; Piermarini and Evans, 1998). In a euryhaline species, such as *C. leucas*, total Na^+, K^+-ATPase activity in the gland of sharks taken from FW is less than those taken from marine environments (Pillans *et al.*, 2005). There was also no difference in mass of the rectal gland between FW and estuarine *C. leucas* (Pillans and Franklin, 2004). Similar results were found in *D. sabina*, where activities were highest in saltwater acclimated fish. The size and weight of the gland did not alter, but this may have been compensated for in SW-acclimated rays by an increased flow rate through the gland, or by the action of other osmoregulatory organs (Piermarini and Evans, 2000).

The gland has been successfully removed in several species, including *S. acanthias*, the whitespotted bambooshark, *Chiloscyllium plagiosum* and the

pyjama shark, *Poroderma africanum*, and although this may increase plasma salt levels temporarily, they either return to normal or reach a higher equilibrium point. This indicates that there is another site of salt secretion open to elasmobranchs (Haywood, 1975; Evans *et al.*, 1982). FW populations of *D. sabina* can be successfully acclimated to SW, and although their rectal glands are much smaller than fish in the marine population, size does not increase significantly indicating that activity in the gland must be increased or salt secretion is also carried out by the gill and kidney (Piermarini and Evans, 1998). After removal of the rectal gland, it was found that the kidney of *S. acanthias* produced more concentrated urine in order to excrete sufficient salts (Burger, 1962). However, Na^+, K^+-ATPase expression did not differ in the kidney or gill of *R. erinacea* after removal of the gland (Piermarini *et al.*, 1999).

A fragment of the Na^+, K^+-ATPase was originally cloned from the rectal gland of *S. acanthias* (Benz *et al.*, 1992). The 429 base pair fragment was reported to be most similar to the sequence of mammalian Na^+, K^+-ATPase α_3 isoform (89%), with reduced similarity to both α_1 (76%) and α_2 (73%) isoforms. Using this fragment as a DNA probe for Northern blotting, a mRNA band of 3.8 kb was found in the rectal gland and also to a lesser extent in other tissues (Benz *et al.*, 1992). Hansen (1999) attempted to further characterise the Na^+, K^+-ATPase in *S. acanthias* rectal glands. In this study, isoform specific antibodies were hybridised with Na^+, K^+-ATPase isolated from *S. acanthias* rectal glands. Antibodies designed from the intracellular domain of the rat for the α_1 and α_2 isoforms did not cross react with *S. acanthias* Na^+, K^+-ATPase, however the antibody designed from the same region of α_3 isoform did cross react with *S. acanthias* Na^+, K^+-ATPase (Hansen, 1999). From these results it was assumed that there was only one isoform of Na^+, K^+-ATPase, the α_3 isoform, present in elasmobranch rectal glands.

1.4.2. Kidney

The type of kidney, and the urine it produces, is of great importance when considering ion balance. In FW, the fish kidney must produce copious amounts of dilute urine to compensate for the influx of water. Large glomeruli and high glomerular filtration rate (GFR) allow production of

profuse amounts of urine, and salts are reabsorbed to prevent massive ion loss. Active reabsorption of Na^+ by renal tubules is essential for survival of FW teleosts (Jampol and Epstein, 1979). In the kidneys of marine fishes, small glomeruli and low glomerular filtration rate enable a small amount of highly concentrated urine to be produced, retaining water and losing ions. The elasmobranch kidney, although not the main site of salt secretion, appears to be rather versatile, with different tubules either secreting or absorbing ions and water (Karnaky, 1998). The kidney and gills certainly play a much greater role in osmoregulation in euryhaline and stenohaline FW elasmobranchs. Urine flow rate in FW *D. sabina* was 2.5 to 10 times higher than in FW teleosts, and 9 – 15 times higher than in marine elasmobranchs so it is clear that the kidney responds to reduced salinities by increasing urine production to counter the high levels of water influx (Janech and Piermarini, 2002; Choe and Evans, 2003).

The elasmobranch kidney is paired, consisting of two elongated organs situated on the dorsal body wall on either side of the vertebral column (*Figure 1.11a*). The functional unit of the kidney is the nephron, which is notably longer in elasmobranchs than in teleosts (Lacy and Reale, 1985[a]). The complex organisation of an elasmobranch nephron is revealed by *Figure 1.13*. This nephron can be split into sections which are the renal corpuscle or glomerulus, neck segment, proximal tubule, intermediate segment, distal tubule and collecting duct (Endo 1984; Lacy and Reale, 1985[a]). Kempton (1962) examined the nephron of the marine lesser electric ray, *Narcine brasiliensis*, and divided it morphologically into a heavily flagellated neck segment, a very long proximal segment which varies in thickness and has long flagella extending into the lumen, and a short distal tubule. This was anatomically similar to the nephrons in *S. acanthias* and the dusky smoothhound, *Mustelus canis*. Later studies by Lacy and Reale (1985[a], 1985[b], 1986) examined the structure of the kidney of both *S. acanthias* and *R. erinacea*. The gross anatomy of the kidney could be divided into two distinctly different regions, the bundle zone and the sinus zone (*Figure 1.14*). The bundle zone contains segment loops of the nephron enclosed in a peritubular sheath, whereas the sinus zone shows less organisation, and no clear distinction between segments from each nephron. The only tubule segments which can be observed in histological sections of the sinus zone are

proximal III and IV, and intermediate I and VI, and all other segments can be seen in sections of the bundle zone. Renal corpuscles are situated on the border between bundle and sinus zones, so they can be seen in sections from both zones (Lacy and Reale, 1985[b]). Many cells of the nephron epithelium are ciliated, and some also bear long flagellar ribbons. This is particularly marked in the neck and proximal segments where rows of flagella form into ribbon-like structures which are visible under light microscopy (*Figure 1.15*). These tubules are predicted to promote the movement of glomerular filtrate along the nephron (Lacy *et al.*, 1989).

The positive identification of tubule segments and sub-segments relies on selective staining and high magnification light and electron microscopy. The neck and proximal segments are comprised of cells with and without long flagellar ribbons. Those without flagellar ribbons have few apical projections and cell microfilaments. The size and shape of the mitochondria varies between flagellated and non-flagellated cells, with small mitochondria in flagellated and large mitochondria in non-flagellated cells (Lacy and Reale, 1991[a]). Proximal segments are easily recognizable as absorptive epithelia, with characteristic pinocytic invaginations (Endo, 1984). In the intermediate and distal segments and the collecting duct, there are also the two cell types, flagellated and the more abundant non-flagellated cells. Secretory and absorptive functions may vary between sub-segments of the same segment, for example, proximal III has an enlarged basolateral surface area by virtue of large projections into the intercellular space and intermediate VI has extensive basolateral membrane infolding indicating a secretory function (Lacy and Reale, 1991[a]; Lacy and Reale, 1991[b]). However, the interdigitations and large intercellular spaces of other sub-segments of intermediate, distal and collecting tubules suggest absorption may occur in these segments (Endo, 1984; Lacy and Reale, 1991[b]). The collecting duct of the mammalian kidney has been demonstrated to absorb Na^+, at the apical surface via ENaC and at the basolateral surface via Na^+, K^+-ATPase (Feraille *et al.*, 2003).

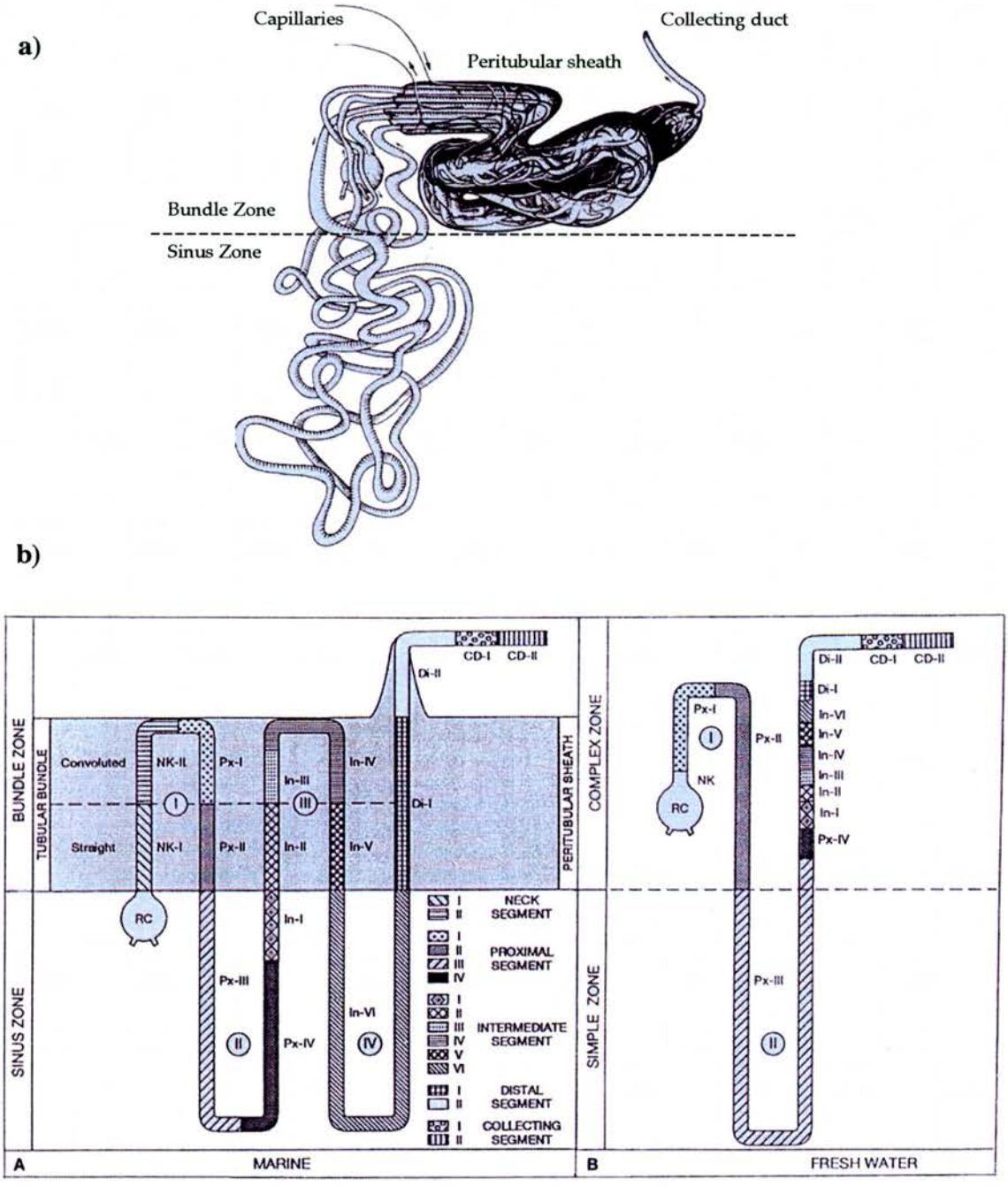

Figure 1.13: Drawing and schematic diagram of the elasmobranch nephron. **a)** Drawing of the nephron configuration in the bundle and sinus zones of the skate kidney (Adapted from Lacy and Reale, 1985[b]). **b)** Models of marine and freshwater elasmobranch renal tubule showing the sequence and position but not the length of tubular segments and their sub-divisions. RC, renal corpuscles (Lacy and Reale, 1999).

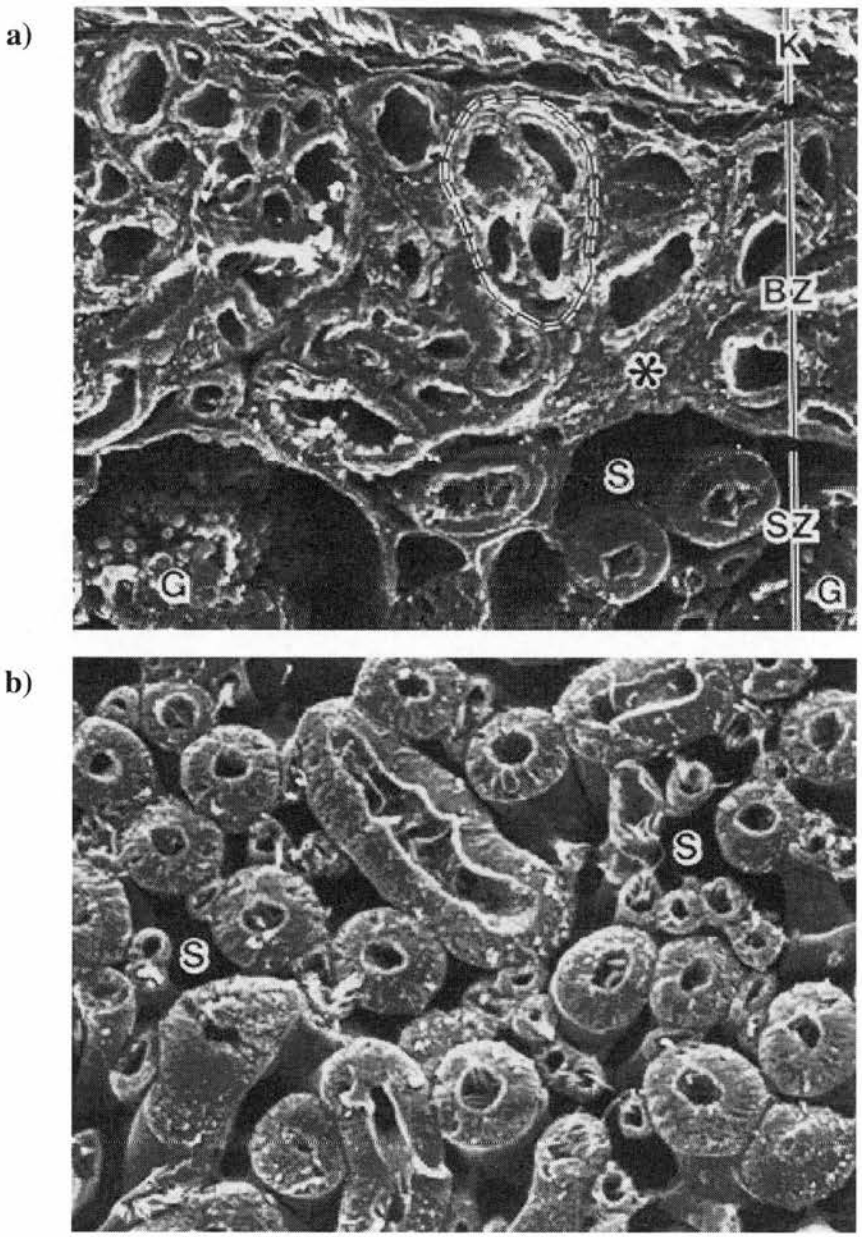

Figure 1.14: Structure of the elasmobranch kidney. **a)** Scanning electron micrograph (x 160) of cross section of skate kidney showing connective tissue capsule, K; bundle zone, BZ; glomeruli, G; sinus zone, SZ; blood sinus, S. Dashed line indicates a discrete bundle of nephron segments. Asterisk lies in the connective tissue between tubular bundles. **b)** Scanning electron micrograph (x 160) of cross section of skate kidney showing sinus zone. Tubules of various diameters, most with cilia, lie in large interconnecting blood sinuses, S (Lacy and Reale, 1985[a]).

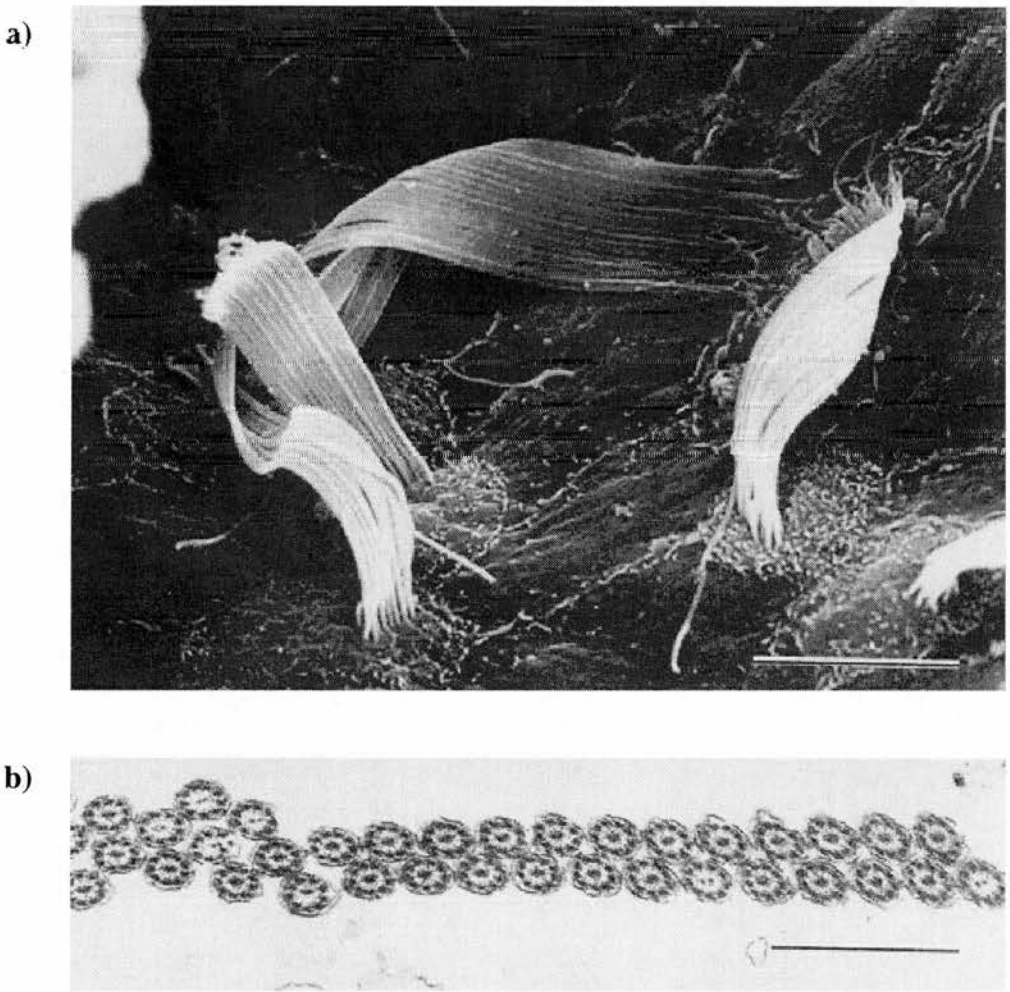

Figure 1.15: Flagellar ribbons in scanning and transmission electron microscopy. **a)** Flagellar cells of the Bowman's capsule in the little skate under scanning electron microscopy; scale bar: 10 μm **b)** Transmission electron micrograph showing the alignment of the flagella in compact rows; scale bar: 1 μm (Lacy and Reale, 1999).

The tubule of *S. acanthias* is electrophysiologically similar to those of mammals and amphibians, and may be involved in urea reabsorption (Hebert and Friedman 1990). The tubules and capillaries in the peritubular sheath are arranged in a parallel counter-current system similar to that observed in mammalian kidneys (Lacy *et al.*, 1985; Lacy and Reale, 1985[b]). The barrier provided by the peritubular sheath is proposed to help maintain the environment needed for the counter-current exchange system to operate efficiently (Lacy and Reale, 1986). Additionally, the structure of the renal corpuscle is similar to that of immature mammals and lower vertebrates (Lacy *et al.*, 1987)

Like the kidneys of other vertebrates, it is expected that different segments of the nephron will perform absorption or excretion of salts and water. The proximal segment may account for around 75% of the total glomerular filtrate reabsorption in the nephron of *S. canicula* (Brown and Green, 1987), with the Na^+, K^+-ATPase mediating this reabsorption of Na^+ (Blanco and Mercer, 1998). However, secretion also occurs in this region with Cl^- secretion being reported to occur in the elasmobranch proximal tubule (Sawyer and Beyenbach, 1985). The late intermediate and distal segments allow apical Na^+ uptake mediated by the NKCC, and Cl^- absorption similar to the absorption mechanisms studied in the mammalian kidney (Friedman and Hebert, 1990; Hebert and Friedman, 1990). Studies on the mammalian kidney have shown that although basolateral Na^+, K^+-ATPase is present throughout the length of the nephron, the apical transporters vary between segments. These apical transporters include NKCC, Na^+/H^+ exchanger, ENaC and a NCC transporter (Knepper *et al.*, 2003).

In marine elasmobranchs, much of the salt secretory activity is carried out by the rectal gland (Hayslett *et al.*, 1973). Compared to FW teleosts, relatively low levels of Na^+, K^+-ATPase activity and large amounts of carbonic anhydrase are found in the distal segment and collecting duct of marine teleosts and elasmobranch kidneys, suggesting the Na^+/H^+ exchanger accounts for much of the apical Na^+ reabsorption in the kidney, as in the gill (Endo, 1984). The collecting duct is the main site of urinary dilution. Most electrolytes in elasmobranch urine are at greater concentrations than in the plasma; with the exception of Na^+ and Cl^- which both have lower

concentrations (Stolte *et al.*, 1977). Since most elasmobranch kidney studies have investigated the kidney of marine fish, mechanisms of salt re-absorption in the FW teleosts may provide a good model for this process in the elasmobranch kidney. A high density of Na^+, K^+-ATPase has been located on the luminal surface of the distal segment and collecting duct of FW teleosts and this plays a part in Na^+ retention (Ura *et al.*, 1997). Kidney Na^+, K^+-ATPase activity in black sea bream, *Mylio macrocephalus*, decreases in brackish water compared to high levels in FW, SW and hypersaline SW (Kelly *et al.*, 1999). The Antarctic fish, *Notothenia neglecta*, also shows a decrease in renal Na^+, K^+-ATPase activity when transferred to half strength SW (Romao *et al.*, 2001). Highest levels of kidney Na^+, K^+-ATPase expression and activity are observed in FW-acclimated thick-lipped grey mullet, *Chelon labrosus*, and spotted green pufferfish, *Tetraodon nigroviridis* suggesting the importance of this enzyme in salt reabsorption (Gallis *et al.*, 1979; Lin *et al.*, 2004).

The control of kidney function has been more widely studied in mammals. Insulin, epinephrine and norepinephrine have been shown to regulate the activity of Na^+, K^+-ATPase in proximal tubules of the mammalian kidney (Bertorello and Aperia, 1989; Feraille and Doucet, 2001). Dopamine inhibits Na^+, K^+-ATPase activity and also the Na^+/H^+ exchanger in the proximal tubule (Feraille and Doucet, 2001). Aldosterone and vasopressin stimulate recruitment of Na^+, K^+-ATPase to the basolateral membrane and activity in the collecting duct. Insulin also increases the activity of Na^+, K^+-ATPase in this region (Feraille *et al.*, 2003). Other regulatory hormones include adrenalin, noradrenalin, calcitonin and thyroxine (Henderson *et al.*, 1998). Many of these hormones may also control kidney function in elasmobranchs. Adrenalin added to nephrons from SW *S. canicula* increases proximal water reabsorption and distal tubule water secretion (Brown and Green, 1987). The renin-angiotensin system (RAS), including the hormone angiotensin II, operates in elasmobranch fish, playing a major role in the control of the kidney function, as well as blood pressure and drinking rate (Hazon *et al.*, 1989; Tierney *et al.*, 1997[a]; Tierney *et al.*, 1997[b]; Hazon *et al.*, 1997[b]; Hazon *et al.*, 1999; Anderson *et al.*, 2001[a]). Receptors for angiotensin II have been found in the kidney, as well as gill, rectal gland and blood vessels of *S. canicula* and *T. scyllia* (Tierney *et al.*, 1997[b]; Hazon *et al.*, 1997[b]; Hazon *et al.*, 1999; Anderson *et*

al., 2001[a]). Administration of angiotensin I and II leads to a significant increase in drinking rate in *S. canicula* (Anderson *et al.*, 2001[b]).

1.4.3. Gills

Although several structures are associated with osmoregulation in fishes, the gill (*Figure 1.16*) is often considered the primary site of ion transport and balance, particularly in teleosts. Fish gills are the main site of gaseous exchange, modified to maximise the surface area available for O_2 and CO_2 diffusion, and minimize the diffusion distance between the water and the blood (Evans *et al.*, 1999). In the gills of elasmobranchs there are two vascular pathways, a respiratory and non-respiratory pathway. The respiratory pathway carries blood from the afferent branchial arteries through the afferent filament arteries, corpus cavernosum, afferent lamellar arterioles, secondary lamellae, efferent lamellar arterioles, and efferent filament arteries to the efferent branchial arteries (*Figure 1.17*). This carries blood through the gills to remove CO_2 from the blood and take up O_2. The non-respiratory pathway is associated with the respiratory pathway, and takes blood from the afferent to efferent branchial arteries but takes the route through the central venous sinus (Metcalfe and Butler, 1986).

The functional unit of the gill is the filament. The surface area of each filament is vastly increased by virtue of numerous projections, or lamellae, from the primary filament. The gill epithelium is composed of two major cell types, pavement cells and MR cells. In SW fish, MR cells are mainly found on the primary filament, in the interlamellar region. This area also shows a higher amount of Na^+, K^+-ATPase positive cells (Witters *et al.*, 1996). In the hagfish, *M. glutinosa*, the density of cells expressing Na^+, K^+-ATPase is highest in the afferent filamental epithelium, and at lower densities in the lamellar epithelium (Choe *et al.*, 1999).

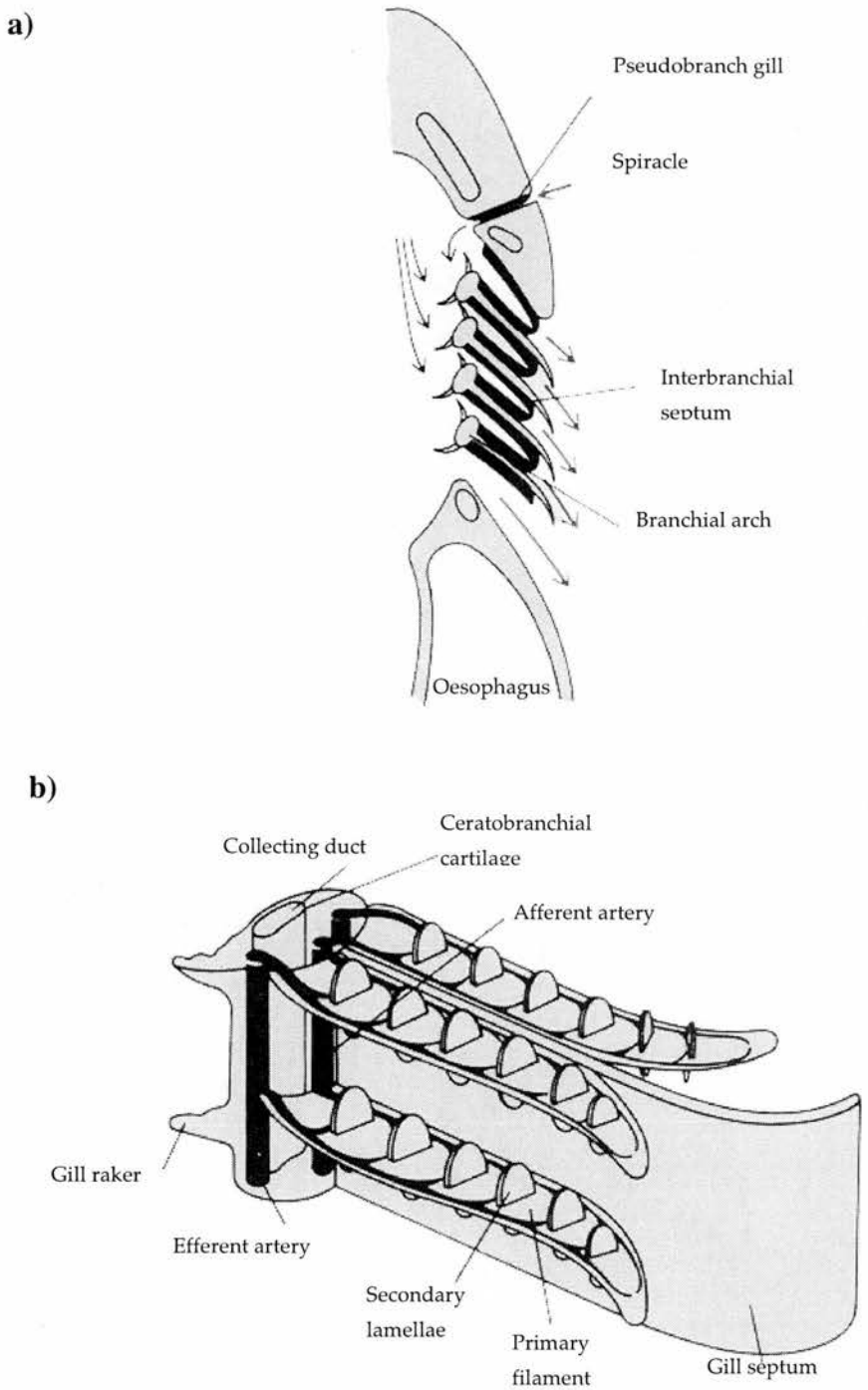

Figure 1.16: Structure of the elasmobranch gill. **a)** Drawing of the head region of a shark to demonstrate position and gross morphology of the gill (Withers, 1992). **b)** The structure of the gill (Withers, 1992).

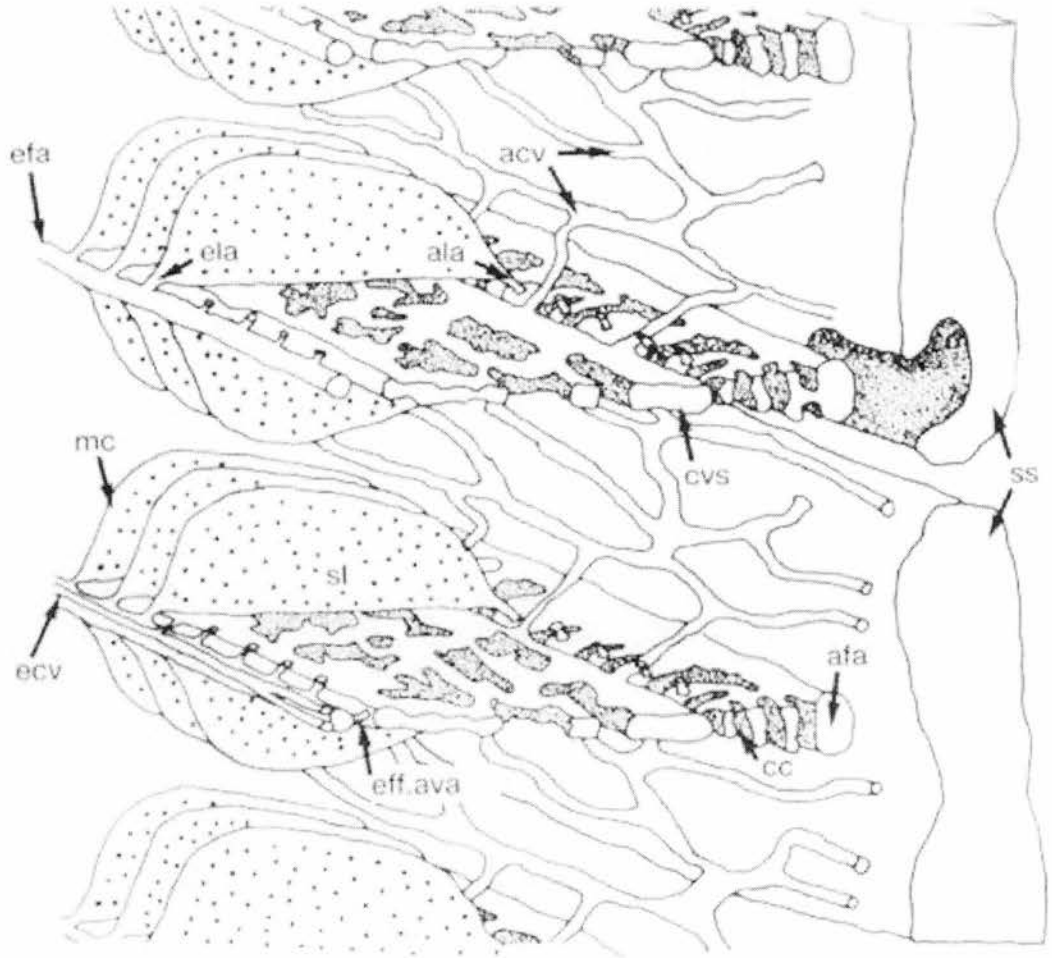

Figure 1.17: Gill vascular anatomy of an elasmobranch. a) Diagram of the solid cast of the blood vessels of two consecutive gill filaments in the gill of the dogfish, *S. canicula*. afa, afferent filament artery; cc, corpus cavernosum; ala, afferent lamellar arteriole; sl, secondary lamellae; ela, efferent lamellar arteriole; efa, efferent filament artery; eff. ava, efferent arterio-venous anastomosis (observed infrequently); cvs, central venous sinus; acv, afferent companion vessel; ecv, efferent companion vessel; mc, marginal capillary; ss, septal sinus (Metcalfe and Butler, 1986).

The teleost gill is of major importance in salt excretion. However, elasmobranchs possess a rectal gland to secrete salt; therefore the evidence for salt secretion in the gill is limited to the observation that removal of rectal gland does not cause osmoregulatory stress (Evans *et al.*, 1999; Piermarini and Evans, 2000; Wilson *et al.*, 2002). Elasmobranch gills express Na^+, K^+-ATPase, but this does not automatically imply salt secretion. After removal of the rectal gland, the number, structure and Na^+, K^+-ATPase activity of the gill MR cells is unchanged which indicates that the gills do not appear to compensate for the loss of salt secretion by the rectal gland (Wilson *et al.*, 2002). It is more likely that kidney takes over and secretes additional salts in elasmobranchs (Evans *et al.*, 2005).

FW teleosts and elasmobranchs are able to absorb ions from the ion-poor water via the gills. FW adapted *F. heteroclitus* take up Cl^- by the gills, although this may take over 48 hours to begin (Marshall *et al.*, 1997). It is thought, however that this may be an advantageous side effect of maintaining acid-base balance. In the fish gill, many of the transporters that are involved in ion transport are also vital to acid-base regulation (Pritchard, 2003). The mechanisms for ion uptake are present in both marine and FW fishes (Na^+/H^+ or NH_4^+ and Cl^-/HCO_3^- exchangers), and possibly evolved prior to fish entering FW habitats (Evans, 1984[b]). This ability to independently excrete H^+ and HCO_3^- maintains the pH and salt balance of the body fluids when in FW (Payan and Maetz, 1973; Conley and Mallatt, 1988). Carbonic anhydrase is an important component of this system, and is often found co-distributed in the gills with these exchangers, particularly in euryhaline species. Not only does it catalyse the hydration of CO_2 to H^+ and HCO_3^-, and vice versa, but also supplies H^+ and HCO_3^- to the exchangers to allow uptake of ions (Conley and Mallatt, 1988; Randall and Brauner, 1998; Piermarini and Evans, 2000). Functional carbonic anhydrase has been immunolocalised in both filament and lamellar epithelial MR cells in the gills of *S. acanthias* (Wilson *et al.*, 2000).

Many of the control systems in the gill MR cells are thought to be similar to those controlling the MR cells of the rectal gland, for example natriuretic peptide receptors are found on the epithelia and blood vessels of gill filaments, indicating CNP may regulate blood flow to the elasmobranch gill

(Donald *et al.*, 1997). Blood flow to the gills can also be controlled by catecholamines, causing vasodilation, and acetylcholine, causing vasoconstriction particularly of the efferent vasculature (Davies and Rankin, 1973). Cortisol is a well known stress response hormone, and this does indeed increase branchial Na^+, K^+-ATPase activity in some species (Forrest *et al.*, 1973; Gjevre and Naess, 1996; Shrimpton and McCormick, 1999). *F. heteroclitus* have a rapid cortisol response of less than an hour when transferred from FW to higher salinities. Over the next 8-48 hours this leads to increase in expression of the killifish CFTR (kfCFTR) channel proteins in MR cells in order to facilitate chloride secretion rather than absorption (Marshall *et al.*, 1999). Prolactin can be used to decrease Na^+, K^+-ATPase activity, and gill MR cell size in several marine teleosts, and may be an important hormone in the adaptation of marine fish to FW. (see Evans *et al.*, 2005 for review) Prolactin is vital to many fish for acclimation to FW since salt absorption is only possible in the gills in the presence of prolactin and cortisol (Evans *et al.*, 2005). Na^+, K^+-ATPase mRNA expression in silver sea bream (*Sparus sarba*) could be controlled by cortisol and prolactin in both SW or hyposmotic (6 ppt) water (Deane *et al.*, 1999). Feeding events also impact the Na^+, K^+-ATPase activity in the gills. Nile tilapia, *Oreochromis niloticus*, fed with supplementary NaCl showed increase branchial Na^+, K^+-ATPase activity compared to the control group (Fontainhas-Fernandes *et al.*, 2001).

Gill MR cells, and gill Na^+, K^+-ATPase activities are often investigated when looking at euryhaline species. Na^+, K^+-ATPase α_1 mRNA levels and enzyme activities rise on adaptation of various euryhaline fish species to SW or hypersaline SW, for example trout, *Oncorhynchus mykiss*, (Kisen *et al.*, 1994), *A. anguilla*, (Cutler *et al.*, 1995[a]), chum salmon, *Oncorhynchus keta*, (Uchida *et al.*, 1997), *S. salar*, (Arnesen *et al.*, 1998) and chinook salmon, *Oncorhynchus tshawytscha*, (Ewing *et al.*, 2001). In the pupfish, *Cyprinodon variegates*, branchial Na^+, K^+-ATPase activity increased by 1.6 times after transfer from 50% SW to 100% SW, and then a further 3.9 times after transfer from 100% SW to 200% SW (Karnaky *et al.*, 1976[a]). Increased activity of Na^+, K^+-ATPase can be induced either in the first few hours of acclimation in the case of *F. heteroclitus*, from 2-3 days in the case of many euryhaline fish, such as *A. anguilla*, or even 3-7 days in many anadromous fish, for example *S. salar* (Mancera and McCormick, 2000). In the case of *O. mykiss*, an increase in

branchial Na^+, K^+-ATPase activity was not seen until 10 days after transfer to 80% SW from FW (Richards *et al.*, 2003). However, it is important to note that not all studies conclude a positive correlation between branchial Na^+, K^+-ATPase activity and salinity. A study on Na^+, K^+-ATPase expression and activity in the gills of milkfish, *Chanos chanos*, showed the opposite pattern, with the highest levels in FW-acclimated fish (Lin *et al.*, 2003). The pufferfish, *T. nigroviridis*, exhibits the highest levels of gill Na^+, K^+-ATPase activity and expression when acclimated to brackish water, when compared to FW- or SW-acclimated fish (Lin *et al.*, 2004). Even in *F. heteroclitus*, when transferred from 10% SW to FW, branchial mRNA expression and activity of Na^+, K^+-ATPase both increased to a greater extent than when transferred to 100% SW (Scott *et al.*, 2004; Scott *et al.*, 2005). The sailfin molly, *Poecilia latipinna*, is able to tolerate hyper-saline water of up to nearly 3 times the strength of SW. When exposed to double strength SW, branchial Na^+, K^+-ATPase activity increases 200%, but does not continue to increase with increased salinity suggesting that these fish use a different route of salt excretion when in extremely hyper-saline water (Gonzalez *et al.*, 2005).

The size and location of the MR cells in the gills also plays an important part in salinity tolerance. On acclimation to SW, the number of MR cells and their immunoreactivity for Na^+, K^+-ATPase decreases in the lamellae, however in the filaments, cell number remains the same, but cell size and immunoreactivity increases. Therefore, MR cells in the lamellae may be involved in salt uptake in FW, and MR cells in the filaments are involved with salt secretion in SW (Uchida *et al.*, 1997; Shikano and Fujio, 1998[a]). Newborn *P. reticulata* also display this trend, but their ability to tolerate higher salinities could be altered depending on which environment they were exposed to. Guppies kept in SW were able to tolerate these salinities due to an increase in MR cell size. An interesting find was that young born from FW-acclimated mothers were less able to tolerate higher salinities than those from SW-acclimated mothers. Total cross sectional area of immunoreactive MR cells correlates directly with salinity tolerance (Shikano and Fujio 1998[b]; Shikano and Fujio 1999). In addition to salinity challenge, hormone treatment, or exposure to pollutants can also cause MR cell proliferation. Although this may increase the ion transporting ability of the gills, it also causes the lamellar diffusion barrier to thicken, impairing

gaseous exchange (Perry, 1998).

Salmon species make good test subjects as adults migrate into FW to bear young, and these must then migrate back to the sea. The developmental changes which occur prior to migration from FW to SW are known as smoltification. In the initial stages of migration from FW to SW Na^+, K^+-ATPase specific activity in the gills of juvenile salmon does not rise significantly, although synthesis does increase, as does MR cell proliferation. Only after MR cell proliferation does the enzyme activity increase significantly, reaching its peak some distance before the juvenile enters SW (Ura *et al.*, 1997; Ewing *et al.*, 2001). Both Na^+, K^+-ATPase mRNA expression and activity increased during the later stages of smoltification in *S. salar* (Seidelin *et al.*, 2001). Adults taken from brackish water on their route upstream have already made enough adjustments so that when transferred to SW they cannot survive for more than a few days. In these fish, plasma osmolality increases and Na^+, K^+-ATPase activity decreases. In groups transferred to FW, filament MR cell number decreased, as did Na^+, K^+-ATPase activity, and plasma osmolality was maintained. This decrease in filament MR cells, and subsequent decrease of Na^+, K^+-ATPase activity reduces tolerance to higher salinities (Uchida *et al.*, 1997). This pattern of immunoreactivity in lamellar MR cells in FW, and filament MR cells in SW is also seen in the euryhaline elasmobranch *D. sabina*, (*Figure 1.18*). It is also observed in the teleost *C. chanos* (Lin *et al.*, 2003). It is therefore probable that this pattern occurs in all euryhaline fish whether teleost or elasmobranch. However if total gill Na^+, K^+-ATPase activity in *D. sabina* is considered, enzyme activity is highest in FW specimens.

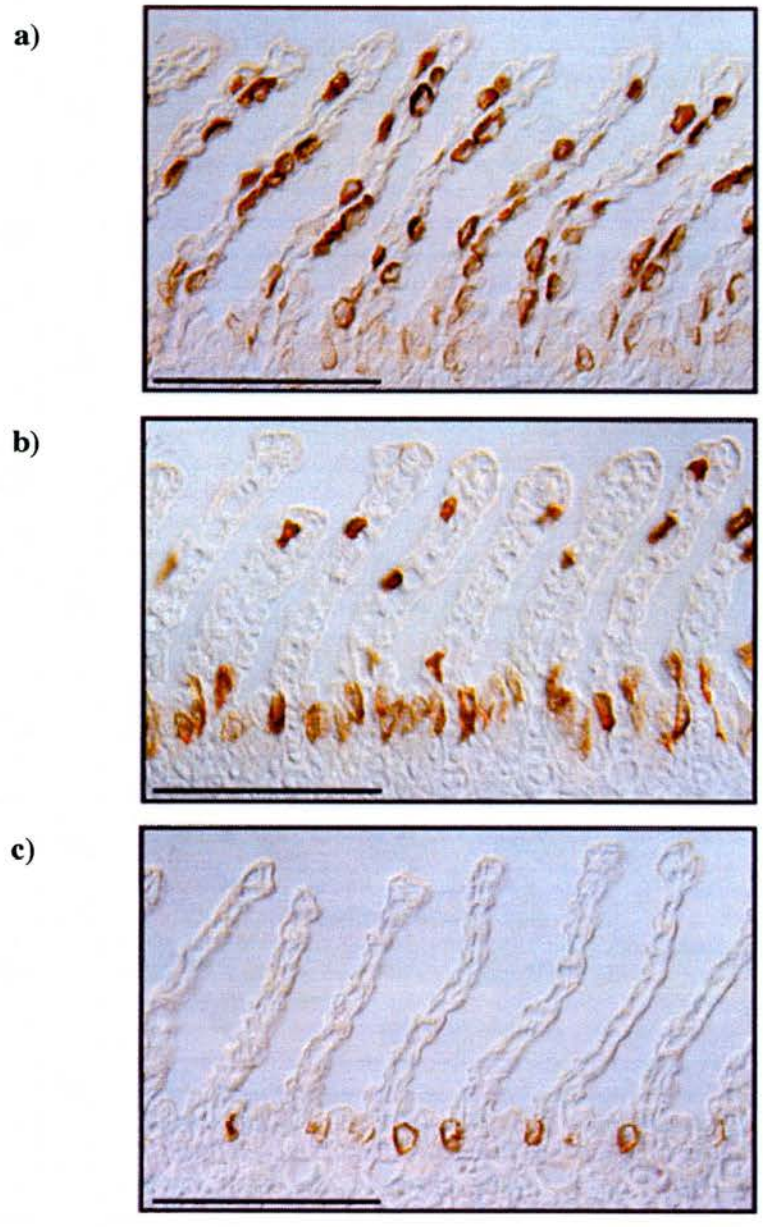

Figure 1.18: Na^+, K^+-ATPase immunostaining in gills from *D. sabina* acclimated to different salinities. Representative immunostaining for Na^+, K^+-ATPase-rich cells in longitudinal sections of gill filaments from FW **a)**, SW-acclimated **b)**, and SW **c)** Atlantic stingrays. Scale bars: 100 μm (Piermarini and Evans, 2000).

In higher salinities, it has been proposed that a decrease in transcription of α subunit Na^+, K^+-ATPase mRNA leads to a decreased activity of the enzyme within the elasmobranch gill in SW (Piermarini and Evans, 2000). Salt and acid-base regulation is closely linked in elasmobranch gills. In the gill of FW and SW *D. sabina*, two types of MR cells have been distinguished by transporter expression. One type expresses large amounts of V-type H^+-ATPase on the basolateral membrane, and the other is rich in Na^+, K^+-ATPase. It is thought that the V-type H^+-ATPase rich cells facilitate Cl^- absorption, and HCO_3^- secretion via an apical Cl^-/HCO_3^- exchanger, and the Na^+, K^+-ATPase rich cells are involved in Na^+ absorption and H^+ secretion via an apical Na^+/H^+ exchanger. The expression of H^+-ATPase, and abundance of cells containing this enzyme is greatest in FW *D. sabina*, compared to SW and SW-acclimated fish, and that in the latter, H^+-ATPase is found in cytoplasmic vesicles rather than located within the basolateral membrane (Piermarini and Evans, 2001). This suggests that osmoregulation in FW is associated with elasmobranch acid-base regulation.

1.4.4. Intestine

The intestine must be considered as an osmoregulatory tissue as all fish ingest water whether in FW or SW, and also take up salts in their food. Marine teleosts must drink to replace the water lost by osmosis (Conley and Mallatt, 1988). Drinking rates are up to 10 times greater in marine teleosts than FW teleosts (Karnaky, 1998). When *P. latipinna* is exposed to hyper-saline water, drinking rate increases significantly (Gonzalez *et al.*, 2005). It was thought that elasmobranchs do not need to drink SW, therefore the gut would be less important in ion regulation (Kormanik, 1993). However, when *S. canicula* was adapted to 120% SW, drinking rate increased, and decreased when adapted to 80% SW (Hazon *et al.*, 1997[a]). Both *S. canicula* and *T. scyllium* adapted to 80% displayed increased drinking rate when transferred to 100% SW (Anderson *et al.*, 2002[b]). Additionally, drinking rate in elasmobranchs can be increased by administering angiotensin I and II (Anderson *et al.*, 2001[b]). These studies provide evidence that elasmobranchs do alter their drinking rate depending on salinity. The intestine almost certainly has a role to play in elasmobranch osmoregulation, since elasmobranchs tend to gorge food intermittently causing a high salt load to be ingested in a short time period, along with a quantity of water.

High Na^+, K^+-ATPase activity has been found in the intestine of teleosts fish such as *S. salar* and *O. mykiss* (Gjevre and Naess, 1996). In *M. macrocephalus*, total intestinal Na^+, K^+-ATPase activity decreases in lower salinities, and enzymatic activities varied along the intestine (Kelly *et al.*, 1999). These differences in Na^+, K^+-ATPase activity along the length of intestine has been further examined in the gilthead sea bream, *Sparus aurata*, and it has been suggested that the differences may be caused by expression of two different Na^+, K^+-ATPase isoforms, since the kinetics properties of the Na^+, K^+-ATPase isolated from the pyloric caeca were different to that of the corresponding enzyme isolated from the anterior intestine (Diaz *et al.*, 1998; Almansa *et al.*, 2001). In double strength SW, intestinal Na^+, K^+-ATPase activity of *P. latipinna* increases by 70% (Gonzalez *et al.*, 2005).

Regulation of salt absorption in the marine teleost intestine is similar to that in other tissues, with hormones such as atrial natriuretic peptide, serotonin and acetylcholine inhibiting absorption, and adrenalin, noradrenaline and dopamine increasing absorption (Ando, 1992). Cortisol increases intestinal Na^+, K^+-ATPase activity in juvenile *O. tshawytscha* and this is thought to aid in smoltification. However, Na^+, K^+-ATPase activity varied throughout the year in these salmon, being significantly higher during summer, and this activity could not be increased by cortisol treatment (Veillette and Young, 2004).

The most important role of the intestine in elasmobranch osmoregulation is possibly the release of hormonal factors, such as Scyliorhinin II in order to regulate the activity of salt secreting cells (Anderson *et al.*, 1995). Intestinal distension after a meal may also trigger rectal gland activity (Hazon *et al.*, 1997[a]).

1.5. Mitochondria Rich Cells

Ion transport in osmoregulatory tissues is carried out largely by mitochondria rich cells (MR cells; *Figures 1.19 and 1.20*). These cells contain an array of ion transporters which work in concert to produce net ion transport. MR cell nomenclature has been a troublesome issue. Cells proposed to be chloride secreting cells were first observed in the gills of SW *A. anguilla* by Keys and Willmer in 1932, and then soon after in SW *F.*

heteroclitus, by Copeland (1948), and Burns and Copeland (1950). These cells were termed 'chloride cells' although their definitive identification as the salt-secretory cells in the SW teleost gill did not occur until much later (Foskett and Scheffey, 1982). Although cells with a similar structure and function to these chloride cells are found in other tissues, such as rectal gland (Bulger, 1963; Valentich *et al.*, 1996), kidney (Hentschel, 1978) and intestine (Noaillac-Depeyre and Gas, 1976), only chloride secreting cells in the gill and opercular epithelium of marine teleosts can be correctly designated as 'chloride cells'. The term 'mitochondria rich cell' was coined to describe any other cell which is actively involved in ion transport in order to maintain plasma osmolality, including rectal gland, intestine, kidney and FW gill. As this name suggests, these cells contain numerous mitochondria, although it is important to note that not all cells rich in mitochondria are involved in osmoregulation. Having spoken to many of the leading researchers in this field (Goss, G., Marshall, WS., Wood, C., and Perry, SF., 2005, pers. comm.), the general consensus is to discontinue the use of the term chloride cell, and replace it completely with MR cell, specifying the tissue of origin, e.g. rectal gland MR cell. In response to this, I shall refer to these cells exclusively as MR cells.

Fish gill epithelia contains large ovoid cells known as MR cells. These cells are dispersed within a layer of pavement cells which can comprise over 95% of the gill surface area (Goss *et al.*, 1998), and are often found adjacent to developing MR cells (Karnaky, 1986). The basolateral membrane has undergone repeated infoldings to create a tubular system which extends into the cytoplasm and associates with mitochondria. This tubular network is the site of Na^+, K^+-ATPase expression in these cells (Philpott, 1980; Evans *et al.*, 2005). In the teleost gill MR cell, the apical membrane bears short microvilli and is concave, often to the extent of forming an apical crypt (Evans *et al.*, 2005). Elasmobranch gill MR cells have long apical microvilli, and usually lack an apical crypt. They also have numerous basolateral invaginations but these are much less extensive than those of teleosts (Evans *et al.*, 1999; Piermarini and Evans, 2000). The lateral membranes between gill MR cells and pavement cells are tightly woven with numerous intercellular junctions. This is in contrast to the borders between gill MR cells and accessory cells (also known as developing MR cells) which are considered to be 'leaky' to

ions (Evans *et al.*, 2005). The basolateral membrane of gill MR cells of *S. acanthias* has been shown to contain a large amount of Na^+, K^+-ATPase, indicated by immunolocalisation (Wilson *et al.*, 2002). Besides the obvious morphological differences from the surrounding pavement cells, MR cells express about 4 times more Na^+, K^+-ATPase (Marshall and Bryson, 1998). The Na^+, K^+-ATPase density is higher closer to the mitochondria, as would be expected for a pump using ATP as its energy source (Eveloff *et al.*, 1979). Cells with similar structure and function to these branchial MR cells can be found in the rectal gland, kidney, intestine and even teleost yolk-sac (Hwang *et al.*, 1999).

The MR cell not only excretes chloride, but also sodium. It was observed that an increase in active gill MR cells is associated with a rise in sodium transport rate (Avella *et al.*, 1987). The mechanisms of salt excretion are shown in *Figure 1.19*. Na^+ is actively pumped out of the cell across the basolateral membrane by the Na^+, K^+-ATPase. This may appear to take Na^+ in the wrong direction (Riordan *et al.*, 1994), but the Na^+ gradient provides the energy required to drive Na^+, Cl^- and K^+, into the cell, across the basolateral NKCC cotransporter (Hannafin *et al.*, 1983; Forbush *et al.*, 1992; Section 1.7.1). K^+ channels of the luminal and basolateral membranes allow exit of K^+ (Evans *et al.*, 1999). Cl^- passively exits via a luminal Cl^- channel, which is the homologue of the mammalian cystic fibrosis transmembrane conductance regulator (CFTR; Section 1.7.2; Silva *et al.*, 1996), creating a trans-epithelial electrochemical potential. This potential forces Na^+ along the cation-selective paracellular pathway which exists within the leaky tight junctions between MR cells and accessory cells (Evans *et al.*, 1999; Bone *et al.*, 1999). Na^+, K^+-ATPase maintains the electrochemical gradient for sodium out of the cells, which in turn drives the mechanism for Cl^- extrusion from the rectal gland (Silva *et al.*, 1977). Na^+, K^+-ATPase activity is a vital component of this system, as ouabain stops secretion (Greger and Schlatter, 1984[b]). This system of salt secretion operates in the gill and rectal gland of fish, but also other vertebrates such as the avian salt gland (Riordan *et al.*, 1994).

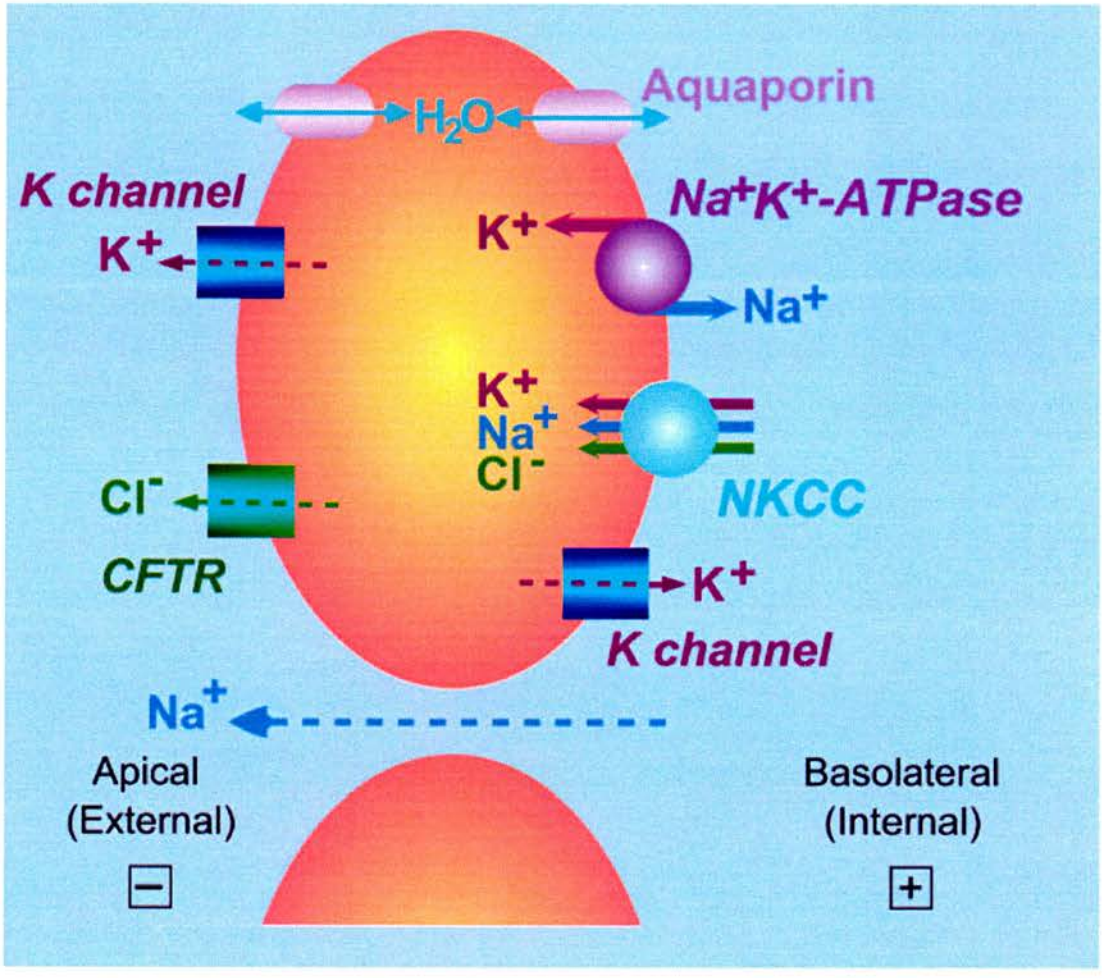

Figure 1.19: Model of ion transport in a seawater fish gill mitochondria rich cell. Cartoon displaying transporter placement in the MR cells of the gill epithelium. The transporters shown are those which are directly involved in osmoregulation. This is an established model of a salt secreting cell. The mechanism of action is described in detail in Section 1.5.

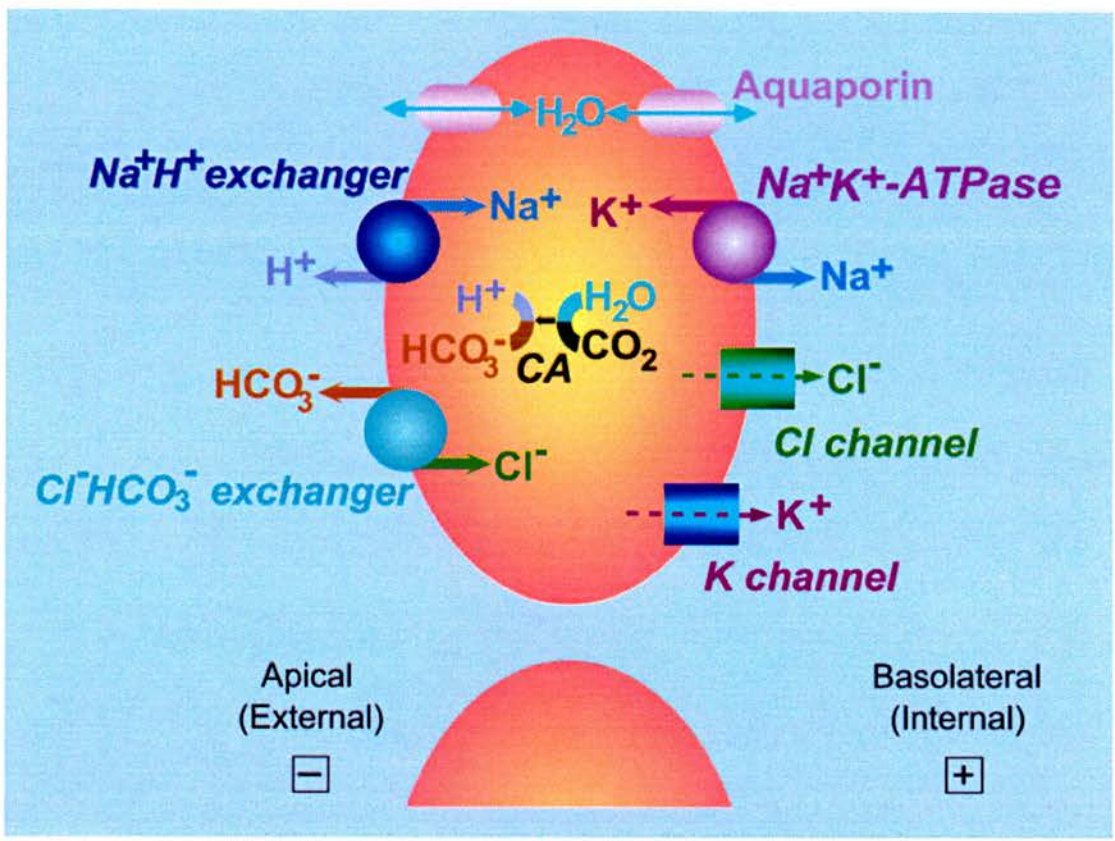

Figure 1.20: Model of ion transport in a freshwater fish gill mitochondria rich cell . Cartoon displaying transporter placement in the MR cells of the gill epithelium. The transporters shown are those which are directly involved in osmoregulation. *CA*, carbonic anhydrase. This is the classic model of transporters proposed for ion uptake when in freshwater. The mechanism of action is described in detail in Section 1.5. Other models have been proposed and are described in Marshall, 2002; Hirose *et al.*, 2003 and Feraille *et al.*, 2003.

Mechanisms of salt absorption in FW fish are still not completed understood, although they may be intrinsically linked to acid-base regulation. The first model proposed involved basolateral Na^+, K^+-ATPase, basolateral K^+ and Cl^- channels, apical Na^+/H^+ and Cl^-/HCO_3^- exchangers (Krogh, 1938; *Figure 1.20*). H_2O and CO_2 enter the cell and are converted into H^+ and HCO_3^- by carbonic anhydrase. The apical exit of hydrogen and bicarbonate ion allows entry of Na^+ and Cl^- into the cell, which then enters the body fluids via the Na^+, K^+-ATPase and a Cl^- channel. It was not until over 50 years later that a different model was proposed, involving a Na^+ channel linked to a H^+-ATPase, rather than a Na^+/H^+ exchanger (Avella and Bornancin, 1989; Piermarini and Evans, 2001). However, Na^+/H^+ exchangers have been immunolocalised in gill cells of agnathans (Edwards *et al.*, 2001; Choe *et al.*, 2002), elasmobranchs (Edwards *et al.*, 2002; Choe *et al.*, 2002), and teleosts (Choe *et al.*, 2002) although it seems likely that these exchangers are more involved with acid-base regulation than with osmoregulation. In some FW fish Na^+ enters the cell through an apical Na^+ channel/transporter, known as the epithelial sodium channel, or ENaC, via the electrochemical potential created by basolateral Na^+, K^+-ATPase and an apical proton pump. Chloride enters the cell from the environment via the chloride bicarbonate exchanger (Marshall, 2002; Pritchard, 2003). A recently proposed model for FW osmoregulation in the teleost gill includes an apical NKCC (Hiroi *et al.*, 2005) similar to the mechanism of NaCl uptake in the thick ascending loop of the mammalian kidney (Knepper *et al.*, 2003). It is noteworthy that MR cells in FW fish often occur singly, and are not associated with accessory cells which would allow for leaky junctions. Instead they integrate tightly with the surrounding pavement cells in order to form a more impermeable barrier to ions (Evans *et al.*, 2005).

The latest model of salt absorption in stenohaline FW and FW-acclimated euryhaline elasmobranchs (*D. sabina*) involves two distinct MR cell types. Type A contains a basolateral Na^+, K^+-ATPase and an apical Na^+/H^+ exchanger, allowing Na^+ uptake. Type B bears a basolateral H^+-ATPase, an unknown basolateral chloride channel, and an apical Cl^-/HCO_3^- exchanger, known as pendrin. The H^+-ATPase would actively pump H^+ across the basolateral membrane, creating a large intracellular HCO_3^- concentration. This would then be secreted via the Cl^-/HCO_3^- exchanger, with the

associated uptake of Cl^- (Piermarini and Evans, 2001; Piermarini *et al.*, 2002). This system has also been proposed in the FW lamprey, *Geotria australis* (Choe *et al.*, 2004)

The mechanism of osmoregulation in the MR cell of SW-acclimated fish is conserved throughout the marine and euryhaline fishes whereas in FW MR cells the process is still not defined fully, and is variable amongst fish. It has been proposed that since FW habitats are more temporary and geographically isolated than SW habitats, it is probable that salt absorption mechanisms in FW fish evolved independently many times in various taxa (Marshall, 2002).

Studies into the gill MR cells of several species of the genus *Fundulus* found that when euryhaline *F. heteroclitus* was adapted to SW, its gill MR cells resembled those found in *F. similis*, a stenohaline SW species. In contrast, the gill MR cells of FW-acclimated *F. heteroclitus* were more similar to those found in *F. chrysotus*, a stenohaline FW species (Philpott and Copeland, 1963). It soon became evident that some osmoregulatory tissues contain more than one MR cell type. In the FW teleost gill, the α MR cells are enlarged cells of the gill which are found at the base of the secondary lamellae, and the β cells are more ovoid shaped cells which are found on the primary filament in the interlamellar region of the gill (Pisam *et al.*, 1987). On adaptation to SW, α MR cells in the gills of the guppy, *Poecilia reticulata*, increased in size and the basolateral tubular network became more developed, resembling those found in SW teleost gills. In contrast, the β MR cells deteriorated and disappeared (Pisam *et al.*, 1987). This pattern was also observed in *S. salar*, during smoltification from FW parr to SW smolt. An additional observation was that most MR cells in SW smolts were associated with accessory cells which were absent from FW fish (Pisam *et al.*, 1988). The β MR cells are only found in FW teleosts (Evans *et al.*, 1999) and these are also associated with accessory cells in some FW fish, e.g. the brown trout, *Salmo trutta* (Pisam *et al.*, 2000). It has been suggested that accessory cells are the precursors of MR cells (Varsamos *et al.*, 2002). Indeed, accessory cells, and α and β MR cells may all simply represent the same cell which changes in morphology and function when the fish is exposed to different environmental salinities (Hirose *et al.*, 2003).

The type of MR cell is a key factor in adaptation to salinity change and the ability of these cells to transform may dictate how well fish can adapt to a wide range of salinities (Shikano and Fujio 1998[c]). The expression and distribution of transporters in the yolk-sac membrane of Mozambique tilapia, *Oreochromis mossambicus*, was determined by immunofluorescence (Hiroi *et al.*, 2005) resulting in the proposal a new classification of MR cells each containing a different set of transporters which are interchangeable with each other (*Figure 1.21*). Type I cells are thought to be immature cells, with Na^+, K^+-ATPase on the basolateral membrane, and are the precursor for transformation into different type MR cells. Type II cells are found in FW-acclimated fish, and have a basolateral Na^+, K^+-ATPase and apical NKCC which is thought to allow for ion absorption. This type can be compared to β MR cells in the former classification system. Type III may be an intermediate stage since it has basolateral Na^+, K^+-ATPase and NKCC, whereas Type IV also has this arrangement, but importantly also supports an apical CFTR, and is associated with an accessory cell. This cell type is found in SW-acclimated fish where this arrangement of transporters would allow for intercellular Cl^- secretion and paracellular Na^+ secretion. This cell type is most similar to the α MR cell as described in former classification. When acclimated to SW, type I and type III cells may transform into secretory type IV cells. In the reverse situation, FW-acclimation causes type IV cells to become inactive type III cells, and type I cells develop into absorptive type II cells. It is clear that the plasticity of these cells would determine the euryhalinity of a given species (Hiroi *et al.*, 2005).

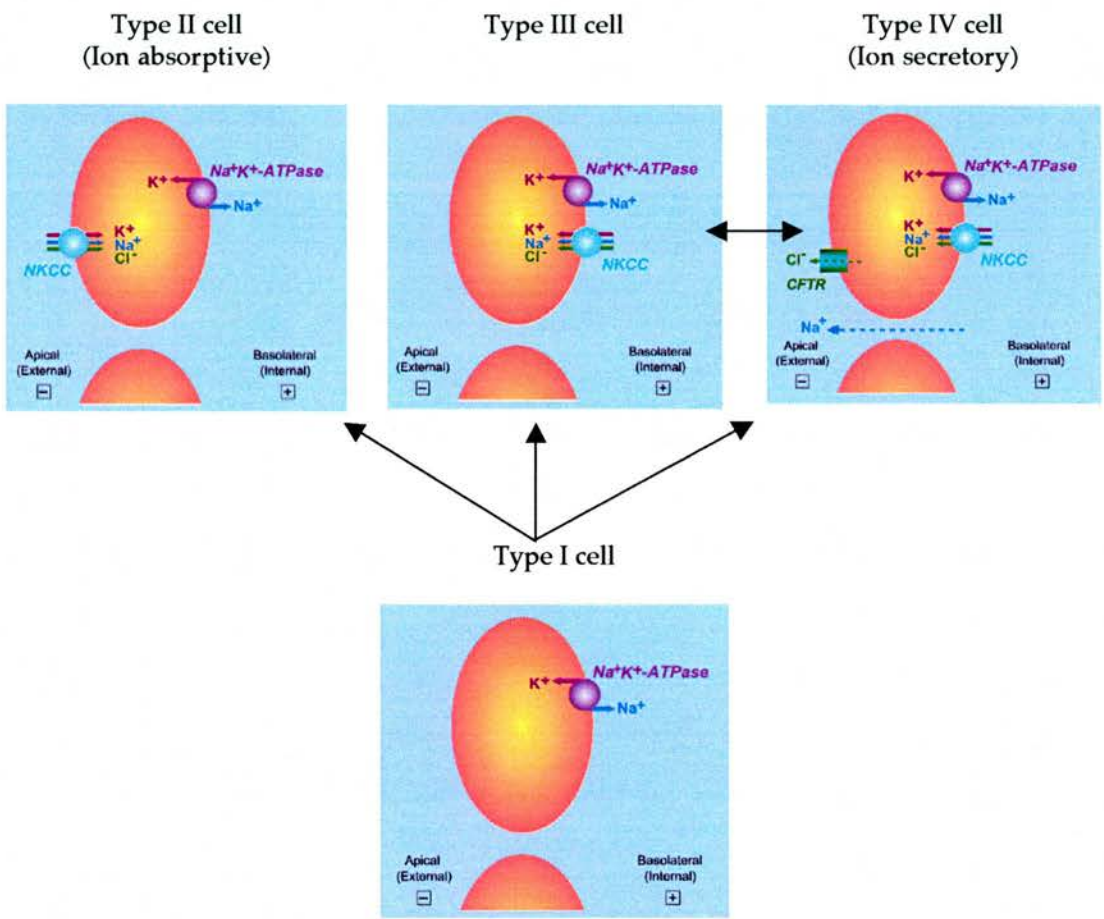

Figure 1.21: Schematic diagram of four proposed mitochondria rich cell types. Transporter placement in the four types of MR cell in the teleost gill epithelium. Only the transporters located by immunofluorescence are shown. The presumed interrelationship among the four cell types are indicated by arrows, and these are described in Section 1.5 (Adapted from Hiroi *et al.*, 2005).

Teleost branchial MR cells exhibit a 'hyperosmotic response' when exposed to increasing salinity or cortisol treatment. The cells generally increase in size and number (Karnaky *et al.*, 1976[b]; Wong and Chan, 1999), the basolateral tubular system becomes more complex (Karnaky *et al.*, 1976[a]; Philpott, 1980), and the cell outline also becomes more angular (Yoshikawa *et al.*, 1993). This is accompanied by an increase in Na^+, K^+-ATPase activity and therefore increased ion transport (Philpott, 1980). An interesting study using confocal laser scanning microscopy showed that the cell number actually decreased when FW *O. mossambicus* were acclimated to SW, however the percentage of cells in contact with the water did increase, as did cell size, showing a 2.5 times increase in cross sectional area. This difference in cell number and size did not apparently cause any alteration to Na^+, K^+-ATPase activity (Heijden *et al.*, 1997). However, Kültz and Jürss (1993) found the specific activity of Na^+, K^+-ATPase and MR cell number to be significantly higher in tilapia acclimated to hypersaline SW than those in FW. Acclimation of SW European seabass, *Dicentrarchus labrax* to FW and doubly concentrated SW produced an increased MR cell number in both cases, and significant development of the MR cell basolateral tubular network in fish acclimated to doubly-concentrated SW. Expression of Na^+, K^+-ATPase was also greatly increased after acclimation to doubly concentrated SW (Varsamos *et al.*, 2002). On acclimation to SW, *S. salar* gills have an increased number and larger size of MR cells on the primary filament, and fewer MR cells on the secondary lamellae (Pelis *et al.*, 2001[a]). These changes are most likely regulated by growth hormone, and cortisol since these hormones have been shown to cause an increase in size and number of MR cells on the primary filament (Pelis *et al.*, 2001[b]).

The function and structure of MR cells can be affected by exposure to certain pollutants, e.g. silver, zinc and copper (Crespo, 1981). The resultant osmotic stress placed on the cells may lead to longer microvilli, and swollen tips (Crespo, 1982), or even the degeneration of the MR cells. However, this may be compensated for by MR cell proliferation when placed under such stresses (Crespo and Sala, 1986). Copper reduces the amount of active MR cells, and therefore Na^+, K^+-ATPase activity in *O. mossambicus* (Dang *et al.*, 2000). Exposure to silver has also been shown to damage the gill epithelia of

S. acanthias, and reduce Na^+, K^+-ATPase activity in both the gill and rectal gland (De Boeck *et al.*, 2001).

1.6. Na^+, K^+-ATPase

Na^+, K^+-ATPase is a major osmoregulatory protein in animal cells. It is an integral membrane transport enzyme, comprising two subunits (α and β), which works as an electrogenic pump. Na^+, K^+-ATPase was determined as a pump by Dean's observation (Dean, 1941) that muscle cells can actively move K^+ and Na^+ against their concentration gradients, this requires work and may be attributable to a membrane bound pump. Jens Skou (1957) later attributed these ion gradients to a Na^+- and K^+-linked ATPase in the peripheral nerves of the shore crab, *Carcinus maenas*. Maintaining and sustaining the Na^+ and K^+ gradients, using ATP, is necessary for the generation of the membrane potential, (depolarisation/repolarisation), cell volume regulation, intra- and extracellular ionic composition regulation, and secondary active transport of other solutes including glucose and amino acids into cells. Therefore, the active transport of Na^+ and K^+ is vital in the transmission of information, regulation of metabolite exchange and in trans-epithelial transport (Skou and Esmann, 1992). It may also assist in transporting ammonia/urea across the gills in marine fishes by substitution of NH_4^+ for K^+ (Wilkie, 1997), and be involved in Na^+-dependent TMAO transport across elasmobranch erythrocyte membranes (Wilson *et al.*, 1999). The action of the sodium pump is the only primary active process present in fish erythrocyte membranes (Thomas and Egee, 1998). This enzyme is found in all animal cells, although it is more prevalent in tissues involved in osmoregulation. It is expressed at variable levels in tissues, from several molecules per square micrometer in erythrocytes to several thousand molecules per square micrometer in the nephron epithelium (Lopina, 2001).

The Na^+, K^+-ATPase is a member of the P-type ATPase superfamily from which many similar transport proteins may be found both in prokaryotic and eukaryotic cells, transporting H^+, Na^+, Mg^{2+}, K^+, Ca^{2+}, Cu^{2+} and Cd^{2+} (Blanco and Mercer, 1998). Members of this enzyme family carry out two functions, that of cation transport and hydrolysis of ATP (Kaplan *et al.*, 2001). The Na^+, K^+-ATPase is found only in animals, and not plants, fungi, or archaea, in which proton pumps are more commonly found (Okamura *et al.*, 2003). It

transports 3 molecules of Na^+ out of the cell in exchange for the influx of 2 molecules of K^+ with the hydrolysis of 1 ATP molecule (Skou and Esmann, 1992). The functional Na^+, K^+-ATPase exists as a heterotetramer, composed of two α and two β subunits ($\alpha_2\beta_2$; *Figure 1.22*), with two conformational states, E_1 and E_2. Na^+ binds to the E_1 conformation which triggers phosphorylation of the enzyme by ATP. This is known as the phosphorylated E_1 state, or E_1P. Phosphorylation causes a conformation transition to the phosphorylated E_2 state (E_2P), which allows Na^+ to exit the cell, and extracellular K^+ to bind to the enzyme. This causes the enzyme to become dephosphorylated (E_2), which in turn causes a conformation transition back to E_1, and the K^+ are released into the cell (Lupfert *et al.*, 2001; *Figure 1.23*). Using cryoelectron microscopy it can be seen that the E_2 Na^+, K^+-ATPase conformation bears a strong resemblance to the E_2 Ca^{2+}-ATPase form, suggesting this E_1- E_2 change is conserved throughout P-type ATPases (Rice *et al.*, 2001). Na^+, K^+-ATPase is also expressed as different combinations of α and β isozymes in different tissues, for example, $\alpha_1\beta_1$ is the predominant form in the mammalian kidney (Blanco and Mercer, 1998).

1.6.1: Na^+, K^+-ATPase α subunit

In vertebrates, the Na^+, K^+-ATPase α subunit is 1009-1029 amino acids long and 110-114 kDa molecular weight. It has ten transmembrane domains, arranged as α helices. Both N- and C- termini are located in the cytosol, and the protein has a large cytoplasmic domain between transmembrane domains 4 and 5 (Lopina, 2001). Several specific sites and amino acids have been identified as necessary for protein function as shown by site-directed mutagenesis (reviewed in Lingrel *et al.*, 1994). The α subunit contains the catalytic unit, containing the binding sites for the cations, ATP, and cardiac glycoside inhibitors such as ouabain. Ouabain binding, and ouabain sensitive oxygen consumption indicate the presence and activity of Na^+, K^+-ATPase in cells (Shuttleworth and Thorndyke, 1984).

There are four known α isoforms in vertebrates, α_1, α_2, α_3 and α_4. The development of isoforms provides the versatility needed by cells, evolving distinct properties to respond to cellular requirements. They are all approximately the same molecular weight, but comprise different sequences which exhibit 80-85% amino acid homology within any one species, the main

sequence differences occurring towards the N-terminal of the proteins (*Figure 1.24*). These differences in amino acid sequence, amongst other things, alter the sensitivity of the isoforms to inhibition by cardiac glycosides and complexes of αβ comprised of different isoforms display markedly different kinetic properties. The α_1 isoform occurs in all cells and the degree of amino acid identity across species is ~92%. The α_2 isoform is the predominant form in skeletal muscle, and is also found the heart and brain and like α_1 shares ~92% identity across species. The α_3 isoform is found in neuronal and cardiac tissue and the degree of identity between species is over 96% (Skou and Esmann 1992; Blanco and Mercer, 1998). The α_4 isoform, which was more recently identified in the human genome and shown to be expressed only in the testes, is the most divergent of the four isoforms, sharing only 78% identity with α_1 (Blanco and Mercer, 1998; Blanco *et al.*, 1999). The isoforms are most divergent at the N-terminus and the extracellular ouabain binding site between transmembrane segments 1 and 2. The isoforms are most homologous in the cytoplasmic middle region, where both ATP binding and phosphorlyation sites are located, the hydrophobic transmembrane regions and the C-terminal region (Blanco and Mercer, 1998). The cytoplasmic region is the site of three structurally and functionally important regions, the A (actuator), P (phosphorylation) and N (nucleotide binding) domains which undergo movement during conformational changes, altering the size of the active site (Jorgensen *et al.*, 2003).

The expression of Na^+, K^+-ATPase α isoforms is tissue-specific, hormonally regulated and often linked to development (Lopez *et al.*, 2002). As discussed previously, Na^+, K^+-ATPase α_1 is expressed in a wide range of tissues, whereas the α_2, α_3, and α_4 are expressed only in particular tissues. It is likely then, that these isoforms are involved in the specialised functions of the tissues they are expressed in (Lingrel *et al.*, 2003). Several neurotransmitters have been found to regulate only certain Na^+, K^+-ATPase isoforms; dopamine increases the endocytosis of Na^+, K^+-ATPase α_2 subunit from the plasma membrane, whereas glutamate inhibits this process, and increases Na^+, K^+-ATPase α_1 subunit recruitment into the membrane (Teixeira *et al.*, 2003). An isoform-specific region has been identified within α isoforms which determines the sensitivity to protein kinase C (PKC) which is known to modulate Na^+, K^+-ATPase activity (Pierre *et al.*, 2003; Section 1.6.4).

1.6.2: Na^+, K^+-ATPase β subunit

The β subunit comprises 300 amino acids, is heavily glycosylated and has a molecular weight of 35-55 kDa. It has one transmembrane segment, a short cytoplasmic N-terminal and a large extracellular C-terminal domain (Geering, 2001). Three isoforms have been discovered in vertebrates. The β_1 isoform is ubiquitously expressed, but predominant in the kidney, β_2 is found largely in neural tissue, and β_3 is expressed in a wide range of tissues, with particularly high levels of expression in testis, liver and lung (Arystarkhova and Sweadner, 1997; Blanco and Mercer, 1998). The β isoforms are much less conserved than the α isoforms; vertebrate β_1 shares 60% amino acid homology with β_2, and 68% with β_3; β_2 shares 61% amino acid homology with β_3 (Blanco and Mercer, 1998). The H^+, K^+-ATPase β subunit is often referred to as the fourth Na^+, K^+-ATPase β isoform, with ~70% homology (depending on species) with the β_1 isoform (Blanco and Mercer, 1998). However, synthetically produced complexes of Na^+, K^+-ATPase α subunit and H^+, K^+-ATPase β subunit are functionally inactive (Kawamura *et al.*, 1994).

The main function of the β subunit is to aid in the transport, and insertion of the α subunit into the correct plasma membrane domain, also providing resistance to cellular degradation. More recently, evidence for a functional role has been suggested, and association with the β subunit may be essential for the transport of K^+ (for review see Geering, 2001). The transport of K^+ is unique to oligomeric P-type ATPases, so it is possible that these enzymes recruited the β subunit to assist in K^+ ion transport (Geering, 2001). Reduction of disulphide bonds in the Na^+, K^+-ATPase β sequence impedes the function of the enzyme (Lutsenko and Kaplan, 1992). These disulphide bonds are essential to the organisation of the extracellular domain of the β subunit, and disruption to these bonds can alter the apparent K^+ affinity of the enzyme (Lutsenko and Kaplan, 1993; Geering, 2001). Further investigation of the disulphide bonds of the extracellular portion of the β subunit revealed that disruption of a single bond resulted in the β subunit lacking the ability to assemble with the α subunit (Kawamura *et al.*, 1994). Disulphide bonding in the β subunit C-terminal domain has more recently been linked not to assembly with the α subunit, but with insertion into the

plasma membrane (Laughery *et al.*, 2003). N-glycosylation of the β subunit is not necessary for assembly, nor it is necessary for transport of assembled sodium pumps into the plasma membrane, and it has little effect on the kinetics of the transport process (Colonna *et al.*, 1997). However, if glycosylation sites are removed from the β subunit, its stability, association efficiency is affected (Beggah *et al.*, 1997). The degree of glycosylation of the β subunit is augmented with an increased period of time within the endoplasmic reticulum (Hasler *et al.*, 2000).

Na^+, K^+-ATPase α and β subunits do assemble, and this occurs rapidly in the endoplasmic reticulum, either during or soon after biosynthesis of the individual subunits (Colonna *et al.*, 1997). Several studies, including some mentioned previously have implicated disulphide bridges in the interaction of the subunits (Kaplan *et al.*, 1994; Lutsenko and Kaplan, 1994). It has also been indicated that a short evolutionarily conserved section of the α subunit, amino acid residues SYGQ (Ser901-Gln904 in the rat; NCBI accession number NM_012504) is vital for interaction with the β subunit (Colonna *et al.*, 1997). Both the transmembrane and extracellular domains of the β subunit must interact with the α subunit to assemble and incorporate into the plasma membrane correctly (Hasler *et al.*, 1998). The β subunit plays a key role in the packing and membrane stabilization of the C-terminal domain of the α subunit therefore enabling the α subunit to function (Beguin *et al.*, 1998). More recent work suggests a greater importance of the N-terminal domain for assembly and recruitment to the plasma membrane (Laughery *et al.*, 2003). A recent study has suggested that β subunits are degraded and removed from the plasma membrane by an unknown protease, leaving functional α subunits in the membrane (Yoshimura and Takeyasu, 2003). This indicates that the β subunit may not be necessary for normal enzymatic activity, although it is possible that these α subunits associate with newly recruited β subunits. By contrast, turnover of α subunits is achieved by lysosomal degradation.

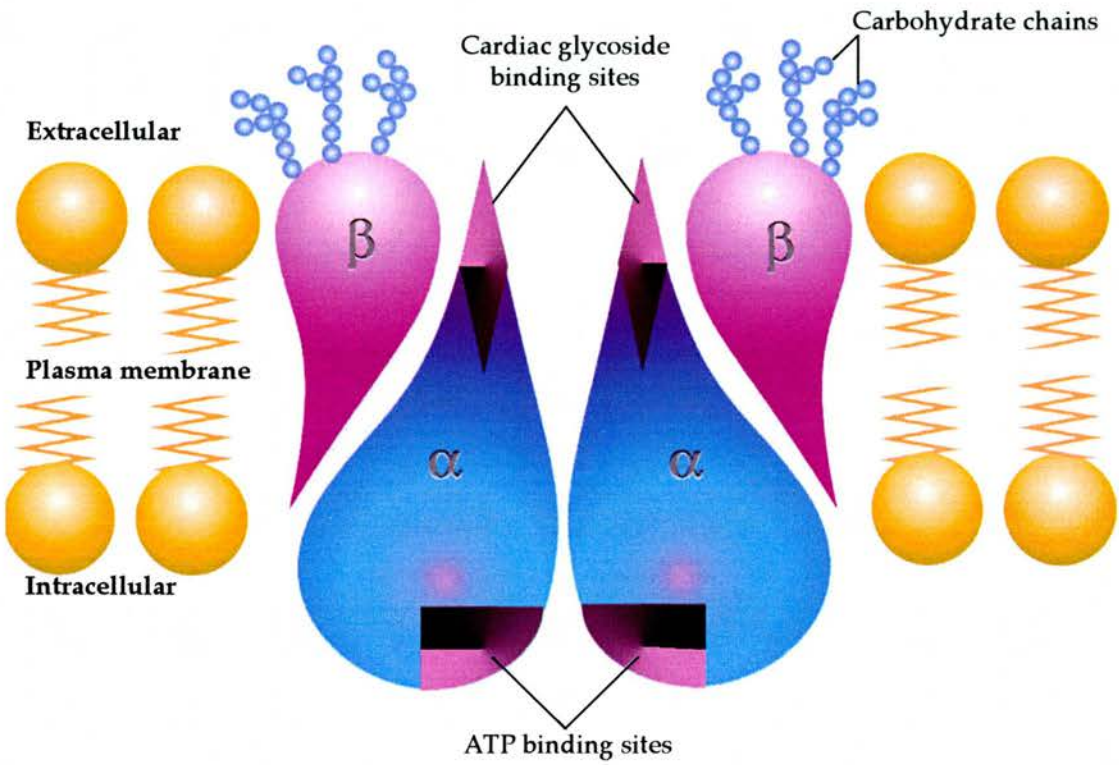

Figure 1.22: Schematic diagram of the Na^+, K^+-ATPase heterodimer in the cell membrane. Two dimensional representation of the Na^+, K^+-ATPase α β complex in the plasma membrane.

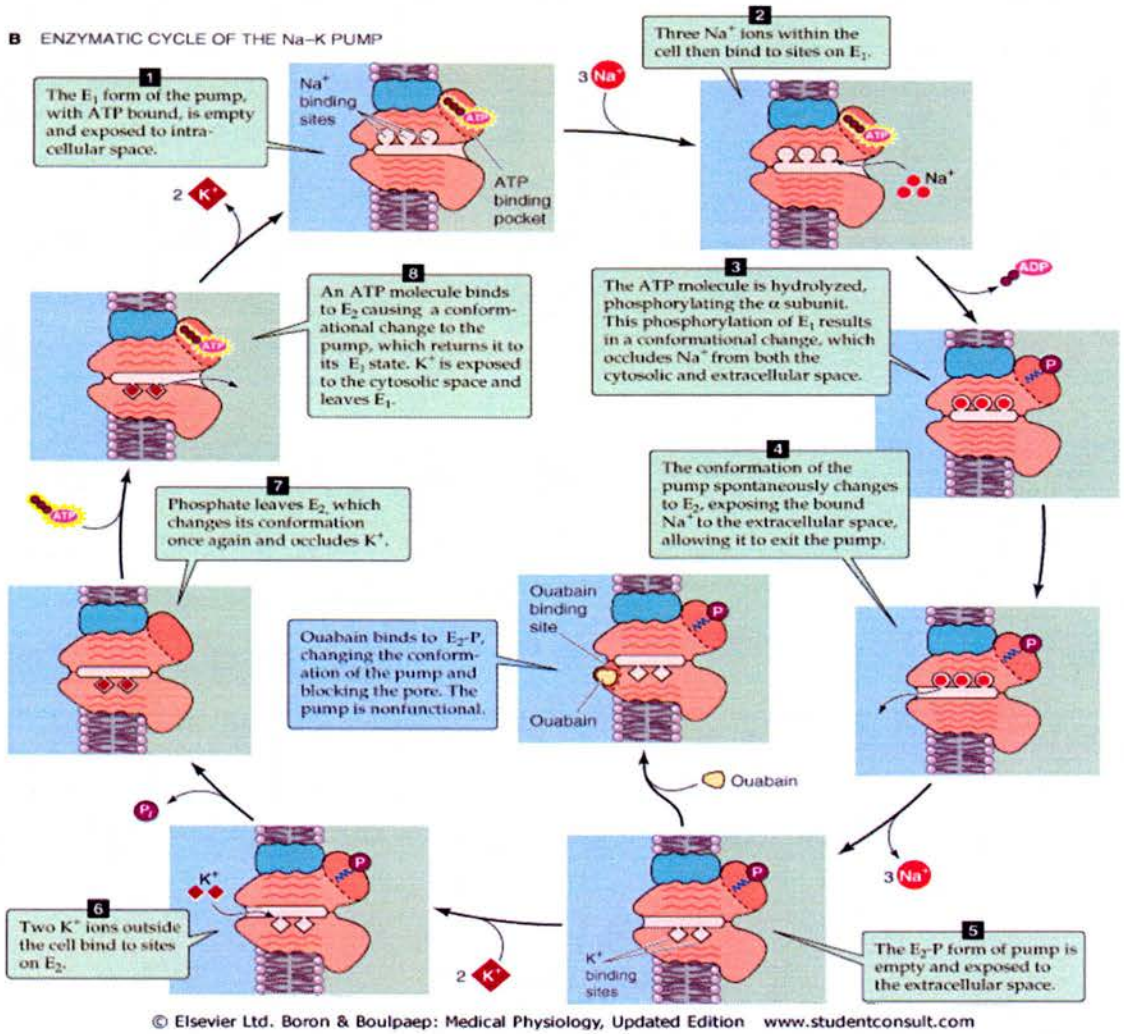

Figure 1.23: Schematic diagram of the Na^+, K^+-ATPase ion transport mechanism. Cartoon representation of the Na^+, K^+-ATPase in action. The various stages of transport of ions and phosphorylation of the enzyme are displayed (Boron and Boulpaep, 2005).

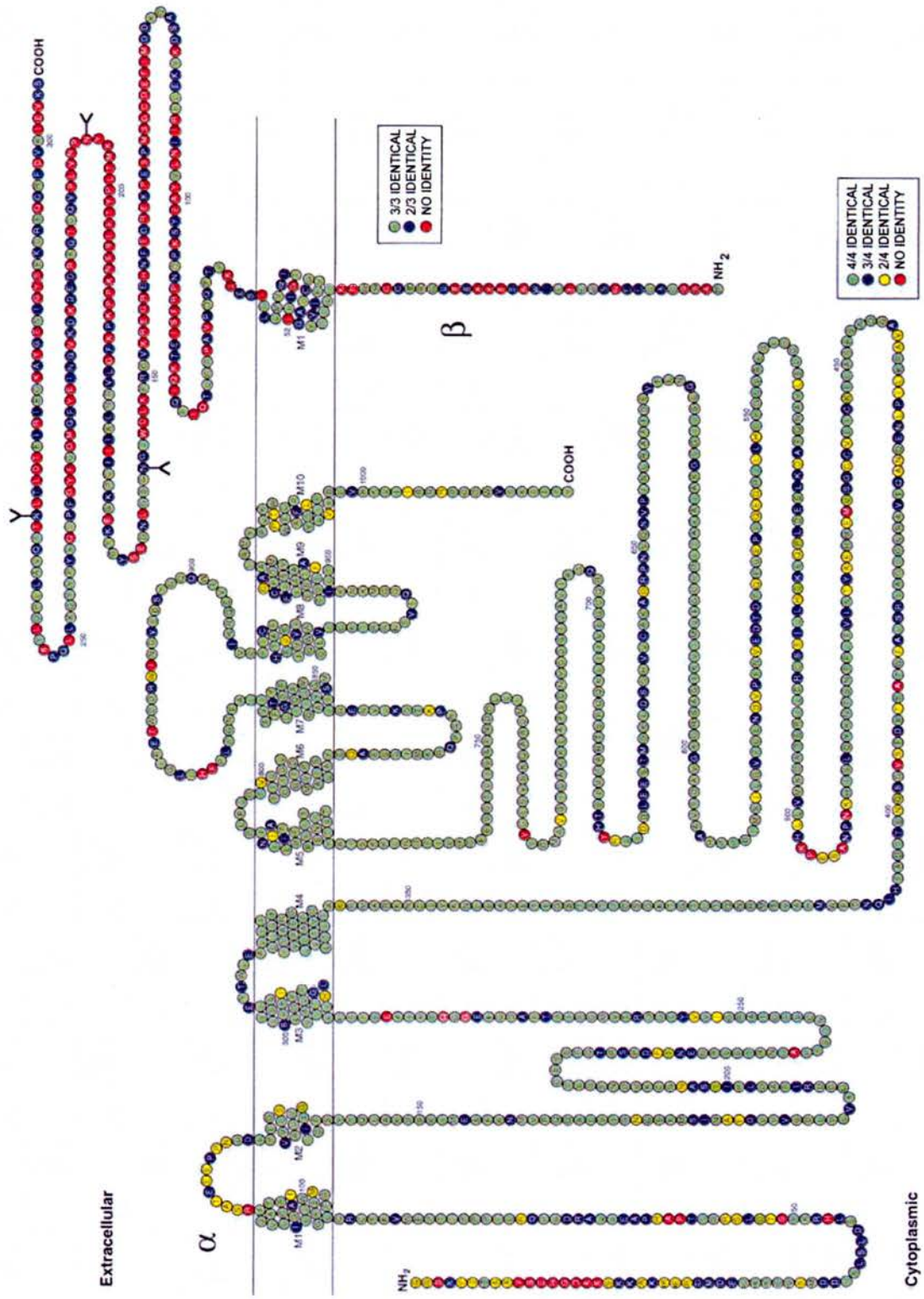

Figure 1.24: Schematic of the membrane topology of Na^+, K^+-ATPase α and β isoforms. Sequences of the rat α_1 and β_1 isoforms are shown. Residues are coloured to indicate the amino acid homology among the different α isoforms (α_1, α_2, α_3 and α_4) or β isoforms (β_1, β_2 and β_3; Blanco and Mercer, 1998).

1.6.3: Na^+, K^+-ATPase gamma subunit and the 'FXYDs'

A 'third subunit' has been found, known as a γ subunit, particularly in those preparations from kidney and rectal gland. The γ subunit is a small 8-15kDa single transmembrane segment polypeptide, belonging to a group of proteins called the FXYD family, including phospholemman, corticosteroid hormone induced factor/channel inducing factor (CHIF), the 8 kDa mammary tumour marker (Mat-8) and RIC (relating to ion channel). These single transmembrane domain proteins exhibit highly variable amino acid sequences, but all share a core motif of 35 conserved amino acids, including the amino acid motif FXYD, from which the family gets it name (Sweadner and Rael, 2000). The FXYD motif is usually found nearer the N-terminal extracellular domain of the proteins. A recent re-classification by Sweadner and Rael (2000) of the FXYD family resulted in the following nomenclature changes with the new name in parentheses: phospholemman (FXYD1); Na^+, K^+-ATPase γ subunit, splice variants γ_a and γ_b (FXYD2); Mat-8 (FXYD3); CHIF (FXYD4); RIC (FXYD5), phosphohippolin (FXYD6), FXYD7, FXYD8, FXYD9 and phosholemman-like protein from shark or PLMS (FXYD10). These are found in a wide range of tissues, with particular prevalence in tissues involved in fluid or solute transport. FXYD 1, 3 and 5 exhibit widespread expression, FXYD2 and 4 are predominant in the kidney and FXYD6 and 7 in nervous tissue (Sweadner and Rael, 2000). All but one of the FXYDs are now known to associate with the α subunit of Na^+, K^+-ATPase and alter the apparent cation affinity the enzyme (Li *et al.*, 2004), or the enzyme activity (Cornelius *et al.*, 2001), similar to the association of phospholamban to Ca^{2+}-ATPase in cardiac sarcoplasmic reticulum (Simmerman and Jones, 1998). It seems likely that different isoforms of Na^+, K^+-ATPase and isoforms from different tissues will be regulated by different FXYDs due to their distinct tissue distributions. Although FXYDs are not necessary for the ion transporting function of Na^+, K^+-ATPase, most FXYDs modulate the functional activity of this enzyme therefore a brief review of their tissue locations and properties will follow.

FXYD1, or phospholemman as it was first named by Palmer *et al.*, (1991), forms anion channels in cell membranes within the heart and muscle, and is involved with cell volume regulation (Moorman *et al.*, 1995; Moorman and Jones, 1998). It is able to associate with six different heterodimer isozymes of

Na^+, K^+-ATPase. Interaction of FXYD1 with either $\alpha_1\beta_1$ or $\alpha_2\beta_1$ induces a small decrease in external K^+ affinity, and a nearly 2-fold decrease in the internal Na^+ affinity (Crambert *et al.*, 2002).

FXYD2 is the formerly termed γ subunit of Na^+, K^+-ATPase (Forbush *et al.*, 1978) since it was found to colocalize (in the kidney) and coimmunoprecipitate with the Na^+, K^+-ATPase α subunit (Mercer *et al.*, 1993). FXYD2 associates with the α subunit and may stabilize conformational changes in the enzyme (Kisen *et al.*, 1994). It is predominantly found in the kidney, and it is not required for Na^+, K^+-ATPase function, but instead associates with Na^+, K^+-ATPase $\alpha\beta$ complexes to regulate the activity of this enzyme (Therien *et al.*, 1997; Beguin *et al.*, 1997; Therien *et al.*, 2001). FXYD2 decreases the Na^+ and K^+ affinities of the Na^+, K^+-ATPase (Arystarkhova *et al.*, 2002). FXYD2 was found to have two splice variants, with differing amino acid sequences at the N-terminal, γ_a and γ_b (Kuster *et al.*, 2000), and further research has suggested the presence of a third variant, γ_c, with each variant displaying distinct mRNA expression patterns in mouse organs (Jones *et al.*, 2001). The γ_a and γ_b variants differ in their location in the kidney nephrons; γ_a is present in the medullary thick ascending loop as well as the macula densa and proximal tubule, and γ_b in both the medullary and cortical thick ascending loop (Pu *et al.*, 2001; Cornelius and Mahmmoud, 2003). The variants both bind to Na^+, K^+-ATPase but the degree to which they affect Na^+ and K^+ affinities of this enzyme differ (Arystarkhova *et al.*, 2002; Arystarkhova and Wetzel, 2003). More recently it has been found that γ associates with β at several sites in the extracellular domain (Fuzesi *et al.*, 2003).

FXYD3, or Mat-8 (Morrison *et al.*, 1995) is found in the stomach, colon, uterus and thymus of mice, and has recently been found to associate with the Na^+, K^+-ATPase where it decreases the apparent affinity for Na^+ and K^+ of this enzyme (Crambert *et al.*, 2005).

FXYD4 was designated as CHIF by Attali *et al.* (1995) and was found in the collecting duct of kidney nephrons and the epithelium of the distal colon (Capurro *et al.*, 1996). It increases the Na^+ affinity and decreases the apparent K^+ affinity of Na^+, K^+-ATPase (Beguin *et al.*, 2001). The increase in Na^+

affinity of Na^+, K^+-ATPase caused by FXYD4 is in direct contrast to the action of FXYD2.

FXYD5, formerly known as RIC for a novel protein 'related to ion channels', was found to be expressed in spleen, lung, skeletal muscle and testis (Fu and Kamps, 1997). It has also been termed dysadherin upon its discovery in human carcinoma cells (Ino *et al.*, 2002) and it has been suggested that this is a more suitable synonym for this FXYD (Sweadner, K., 2005, pers. comm.). More recently, Western blotting revealed abundant expression of FXYD5 in spleen, lung, intestine and kidney (Lubarski *et al.*, 2005). FXYD5 is found in the connecting tubule, collecting tubule and intercalated cells of the collecting duct of the kidney nephron. FXYD5 coimmunoprecipitates with the Na^+, K^+-ATPase α subunit and increases the activity of this subunit when associated with it (Lubarski *et al.*, 2005).

FXYD6, previously termed phosphohippolin (Yamaguchi *et al.*, 2001) is found in most tissues, predominantly skeletal muscle and brain (Saito *et al.*, 2001). The ability of this FXYD to interact with Na^+, K^+-ATPase has yet to be investigated at the time of writing.

FXYD7 (which has no synonyms) is expressed only in the brain and only associates with Na^+, K^+-ATPase $\alpha_1\beta_1$ isozymes despite the fact that all isozymes are present in this tissue. FXYD7 decreases the apparent K^+ affinity of Na^+, K^+-ATPase, but does not alter its Na^+ affinity (Beguin *et al.*, 2002; Crambert *et al.*, 2003).

FXYD8 is a pseudogene of FXYD6 and has thus been disregarded (Sweadner, K., 2006., pers. comm.). FXYD9 was isolated from the zebrafish, *Danio rerio*, and no further research has been carried out on this gene (Sweadner and Rael, 2000).

FXYD10 is a phospholemman-like protein isolated from shark rectal gland, hence the synonym, PLMS, which is homologous to both phospholemman and the γ subunit, and associates with the α subunit (Cornelius *et al.*, 2000). This protein was described independently by another group (Schuurmans Stekhoven *et al.*, 2001), which showed that the protein was highly variable at

the N-terminal portion amongst several elasmobranch orders. Western blot analysis showed expression of PLMS protein in rectal gland, kidney, brain and heart, but not in colon of *S. acanthias* (Schuurmans Stekhoven *et al.*, 2003). Northern blot anaysis demonstrated PLMS mRNA expression in *S. acanthias* rectal gland, kidney, intestine, brain and heart (Mahmmoud *et al.*, 2003). Phosphorylation of PLMS by PKC initiates dissociation of the protein from the α subunit, causing the Na^+, K^+-ATPase to become active (Mahmmoud *et al.*, 2000). More recent work has suggested that PLMS interacts with the N-terminus of Na^+, K^+-ATPase and regulates conformational change (Cornelius *et al.*, 2005).

A combination of FXYDs play an important role in the kidney where they affect the activity of Na^+, K^+-ATPase. The distribution and activity of Na^+, K^+-ATPase varies along the length of the kidney nephron, although only a single isozyme (α_1) is expressed (Cornelius and Mahmmoud, 2003). Since FXYDs (FXYD2, γ, and FXYD4, CHIF) are differentially expressed along the nephron it is thought that they bind to the Na^+, K^+-ATPase, increasing or decreasing its activity (*Figure 1.25*). FXYD4 and the two splice variants of FXYD2 (γ_a and γ_b) are found only in specific portions of the nephron, FXYD4 along the collecting duct, γ_a in the medullary thick ascending loop, and γ_b in the medullary and cortical thick ascending loop (Pu *et al.*, 2001; Farman *et al.*, 2003). FXYD4 increases the cytoplasmic Na^+ affinity of the Na^+, K^+-ATPase, whereas FXYD2 decreases the Na^+ affinity (Cornelius and Mahmmoud, 2003). Immunohistochemical studies have shown that the Na^+, K^+-ATPase α subunit expression along the nephron is always accompanied by expression of either a variant of FXYD2 or FXYD4, except for part of the cortical thick ascending loop region (Wetzel *et al.*, 2001; Garty *et al.*, 2003). This suggests that the FXYDs are associating with the Na^+, K^+-ATPase along the nephron and accommodating for the divergent conditions along the length of the nephron.

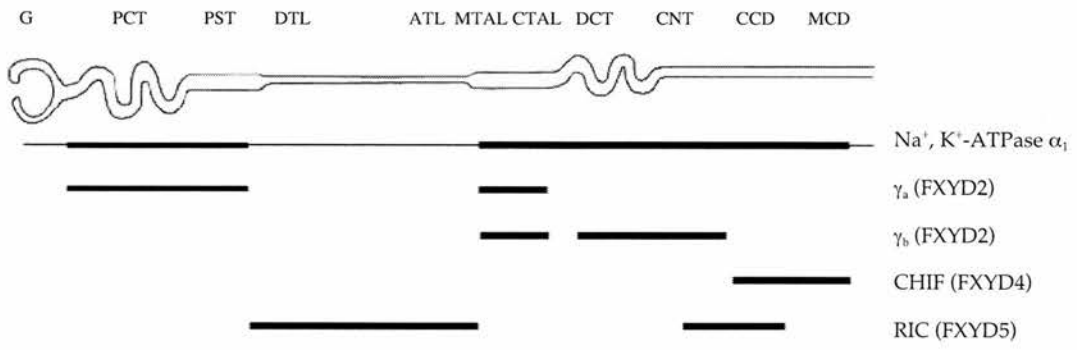

Figure 1.25: Distribution of Na^+, K^+-ATPase α subunit and FXYD proteins along the nephron. Schematic diagram of the mammalian nephron illustrating the expression and distribution of several FXYD proteins. Na^+, K^+-ATPase α_1 is expressed at very low levels in the glomerulus, thin limb of Henle and medullary collecting duct as indicated by a thin line. G, glomerulus; PCT, proximal convoluted tubule; PST, proximal straight tubule; DTL, distal thin limb of Henle; ATL, ascending thin limb of Henle; MTAL, medullary thick ascending limb; CTAL, cortical thick ascending limb; DCT, distal convoluted tubule; CNT, connecting tubules; CCD, cortical collecting duct; MCT, medullary collecting duct (Adapted from Wetzel and Sweadner, 2001; Cornelius and Mahmmoud, 2003; Lubarski *et al.*, 2005).

Recently, FXYD5 has also been revealed as an additional modulator of Na^+, K^+-ATPase in kidney collecting tubules and intercalated cells of collecting ducts (Lubarski *et al.*, 2005). FXYD1 has also been identified by immunohistochemistry in the juxtaglomerular apparaturs of the kidney (Sweadner *et al.*, 2003). Interestingly, no Na^+, K^+-ATPase α_1 subunit is found in this region, however, Na^+, K^+-ATPase α_2 subunit expression was present. FXYDs also regulate Na^+, K^+-ATPase in other tissues such as FXYD1 in the heart and skeletal muscle, FXYD4 in the colon and FXYD7 in the brain where they all decrease the apparent K^+ affinity of the $\alpha_1\beta_1$ isozyme. FXYD1 is primarily involved in increasing muscle contractility, FXYD4 promotes Na^+ conservation, and FXYD7 in the brain promotes neuronal excitability (Geering *et al.*, 2003).

1.6.4. Activity of the Na^+, K^+-ATPase

The increase of biosynthesis of new isoform subunits is a long process requiring several hours or even days (Lopina, 2001). Therefore Na^+, K^+-ATPase enzyme activity is regulated not only by the abundance of the enzyme, but also the modulation of existing functional Na^+, K^+-ATPase subunits within the plasma membrane. Rapid regulation can be achieved by changes in substrate (particularly Na^+) availability and a number of naturally occurring inhibitors and promoters. A high concentration of K^+ inhibits at cytoplasmic sites, and Na^+ and oligomycin at extracellular sites. Oligomycin decreases the rate of hydrolysis, transport and conformational changes (Esmann, 1992). Curcumin, a constituent of the spice turmeric, inhibits Na^+, K^+-ATPase activity by blocking the K^+ occlusion site (Mahmmoud, 2005). Cardiac glycosides such as ouabain and digitoxigenin attach to the enzyme in the E_2P conformation and prevent further K^+ binding and conformational change (Skou and Esmann 1992; Voet and Voet 1990). High extracellular Na^+ promotes the conformational change of Na^+, K^+-ATPase from the E_2 to E_1 state see Section 1.6; Humphrey *et al.*, 2002; Clarke *et al.*, 2003). This transition has been found to be the major rate limiting stage of the Na^+, K^+-ATPase transport cycle (Lupfert *et al.*, 2001). There is also evidence that the enzyme 'autoregulates', whereby the N-terminus interacts with catalytic transmembrane domains of the enzyme to affect conformational change (Segall *et al.*, 2002). As with most enzymes, activity of the pump will also be affected by temperature and pH (Park and Hong, 1976).

As mentioned previously, both the β and γ subunits play an important role in the regulation of Na^+, K^+-ATPase enzyme activity. Besides its main function as a chaperone for the correct insertion of the α subunit into the membrane, the β subunit also affects the affinity of Na^+, K^+-ATPase for K^+ (Lutsenko and Kaplan, 1993; Jaisser *et al.*, 1994; Geering, 2001). The FXYD proteins associate with and affect the activity of Na^+, K^+-ATPase, and these are likely to be vital to the short term rapid changes in activity required when exposed to a new array of conditions, for example when a bull shark encounters sudden salinity challenge. Other proteins may also directly bind to and affect the activity of Na^+, K^+-ATPase, such as ankyrin which may induce oligomerization of the enzyme (Lopina, 2001).

Some observations of increased Na^+, K^+-ATPase activity have been directly linked to increased recruitment of the Na^+, K^+-ATPase subunits into the plasma membrane. Administration of dopamine increases Na^+, K^+-ATPase activity in the lung. This was found to be a result of incorporation of new Na^+, K^+-ATPase molecules into the plasma membrane and therefore increasing total Na^+, K^+-ATPase activity (Bertorello *et al.*, 2003). The amount of cholesterol present in the phospholipid membrane has also been found to influence Na^+, K^+-ATPase activity, with higher levels increasing enzyme activity (Cornelius, 1995).

Hormonal control of Na^+, K^+-ATPase activity can be either long-term, or short-term. Thyroid hormone and aldosterone alter gene expression, and thus can exert long-term control over the amount of Na^+, K^+-ATPase subunits expressed in the plasma membrane (Ewart and Klip, 1995). Catecholamines may control in the short-term by reversible phosphorylation of the catalytic α subunit (Ewart and Klip, 1995). Insulin, aldosterone (in the kidney) and carbachol may act to rapidly alter the subcellular distribution of pump units (Ewart and Klip, 1995). Na^+, K^+-ATPase from intracellular stores can be recruited to the plasma membrane to increase total activity (Blanco and Mercer, 1998). Insulin promotes phosphorylation of skeletal muscle Na^+, K^+-ATPase by an unknown tyrosine kinase, resulting in translocation of Na^+, K^+-ATPase molecules to the plasma membrane and increased Na^+, K^+-ATPase activity (Al-Khalili *et al.*, 2003).

Intracellular second messengers such as cyclic nucleotides can also affect the activity of the pump, possibly by inducing phosphorylation of Na^+, K^+-ATPase. Na^+, K^+-ATPase can be phosphorylated by cyclic adenosine monophosphate (cAMP)-dependent protein kinase A (PKA), cyclic guanosine monophosphate (cGMP)- dependent protein kinase G (PKG), Ca^{2+} and phospholipid-dependent protein kinase C (PKC; Mahmmoud and Cornelius, 2002). Phosphorylation by PKA and PKC were found to decrease Na^+, K^+-ATPase activity in shark rectal gland (Bertorello *et al.*, 1991). Phosphorylation of Na^+, K^+-ATPase may be involved in the regulation of trafficking of the enzyme (Cornelius and Mahmmoud, 2003) by regulating endo- or exocytosis of the Na^+, K^+-ATPase with the result of decreasing or increasing the amount of Na^+, K^+-ATPase in the plasma membrane respectively (Lopina, 2001).

Due to the fact that many cross-salinity migrations undertaken by fish are involved with the reproductive cycle, it is not surprising that many hormones facilitate both the development and salinity tolerance. FW populations of *S. trutta* were treated with various growth hormones, cortisol or transferred to SW, and this significantly increased expression of α subunit Na^+, K^+-ATPase mRNA, and enzyme activity in the gill, but not in the kidney (Madsen *et al.*, 1995).

Na^+, K^+-ATPase activity in fish cells varies with changes in external salinity (Evans *et al.*, 1999). In marine teleosts, with body fluids hyposmotic to SW, cells must excrete Na^+ and Cl^-, and Na^+, K^+-ATPase specific activity tends to be 4-10 times greater in marine teleosts than in FW fish which have body fluids hyperosmotic to the environment (Conley and Mallatt, 1988). When exposed to salinity challenge, levels of transcription and translation of the Na^+, K^+-ATPase α subunit are increased (Hwang *et al.*, 1998), leading to an increase in α subunit synthesis and abundance of Na^+, K^+-ATPase (Cutler *et al.*, 1995[a]; D'Cotta *et al.*, 2000). Na^+, K^+-ATPase was detected by histochemistry in gill MR cells of 6 out of 8 marine teleosts tested, and in the leopard shark (*Triakis semifasciata*) and hagfish (*Myxine glutinosa*), but the technique was not sensitive enough to detect Na^+, K^+-ATPase in FW fish (Conley and Mallatt, 1988). As described previously in Section 1.4.3, Na^+, K^+-ATPase expression and activity in the fish gill is not always maximal in SW.

In *D. labrax* previously acclimated to 15 ppt brackish water, gill Na^+, K^+-ATPase activity doubled when transferred to either FW or hypersaline SW. This increase in activity was preceded by a significant elevation in gill α subunit Na^+, K^+-ATPase mRNA, indicating that an increase in expression of Na^+, K^+-ATPase mRNA is important when transferring to either higher or lower salinities (Jensen *et al.*, 1998). Different isoforms are found in the gills of FW and SW adapted tilapia, *O. mossambicus*, suggesting that teleosts express different isoforms when exposed to different conditions (Lee *et al.*, 1998). Analysis of the Na^+, K^+-ATPase in *D. labrax* indicated that the same isoform is expressed irrespective of salinity (Jensen *et al.*, 1998). In some euryhaline species, Na^+, K^+-ATPase activity is maintained at high levels at all times. The marine longjawed mudsucker, *Gillichthys mirabilis*, must tolerate rapid prolonged changes in salinity in its inter-tidal habitat. Plasma osmolality and chloride concentration in this fish alters during the first 3 days of transfer to either concentrated or dilute SW, although these return to pre-transfer levels after 21 days. Despite this initial variation, neither gill MR cell number nor Na^+, K^+-ATPase activity varied significantly between groups (Yoshikawa *et al.*, 1993).

1.7. Additional Transport Proteins – The sodium, potassium, 2 chloride cotransporter (NKCC), the cystic fibrosis transmembrane conductance regulator (CFTR) and aquaporin (AQP)

Many transport proteins and ion channels are involved in osmoregulation. As shown in *Figure 1.19 and 1.20*, Na^+, K^+-ATPase is just one of a suite of transport proteins involved in the net movement of Na^+ and Cl^- ions across mitochondria rich cells. NKCC and CFTR are also necessary for the coordinated secretion of Na^+ and Cl^- across the gill in SW; NKCC allows Na^+ and Cl^- into the MR cell from the blood, and CFTR allows Cl^- to pass out of the cell into the external medium. This in turn creates an electrochemical potential sufficient for Na^+ to exit the body fluids via the paracellular pathway between MR cells and accessory cells (Section 1.5). AQP plays an important role in maintaining salt and water balance since it allows rapid osmotic water flow, controlling the volume of water contained within the tissues. Proteins such as the V-type ATPases (Piermarini and Evans, 2001; Piermarini *et al.*, 2002), hydrogen and bicarbonate exchangers (Krogh, 1938) and potassium channels (Gogelein *et al.*, 1987[a]; Greger *et al.*, 1996) are equally

important to osmoregulation but have not been studied during the course of this project.

1.7.1. NKCC

The sodium, potassium, 2 chloride cotransporter (NKCC) is one of a class of membrane transport proteins known as the cation-coupled cotransport (CCC) family which transport Na^+ and /or K^+ and Cl^- ions into and out of a wide variety of cells (*Figure 1.26*). This process is almost always electrically neutral, with a stoichiometry of $1Na^+:1K^+:2Cl^-$ (Haas and Forbush, 1998). In all species, NKCC has a molecular weight of 120-130 kDa, and the transcript sizes of the two main isoforms, NKCC1 and NKCC2, are 7.0-7.5 kb and 4.6-5.2 kb respectively. Mammalian NKCC1 is found in both epithelial and non-epithelial cells such as neurons, endothelial cells, and renal mesangial cells and has a 58% amino acid homology with NKCC2 which is found exclusively in the kidney (Haas and Forbush, 2000). Both NKCC species have 12 transmembrane spanning domains and bear extracellular glycoslyation sites (Russell, 2000). NKCC is inhibited by loop diuretics such as bumetanide and furosemide, and also by several environmental pollutants including mercuric chloride (Isenring and Forbush, 2001; Kinne-Saffran and Kinne, 2001). NKCC exhibits species-dependent characteristics; for example, ion affinities of the *S. acanthias* NKCC1 (sNKCC1) are markedly lower than those of human NKCC1 (hNKCC1; Isenring and Forbush, 2001), even though the two forms are 74% identical at the amino acid level (Isenring and Forbush, 1997). Regions involved in ion and inhibitor binding have been indicated using chimaeras of sNKCC1 and hNKCC1; transmembrane domain 2 is involved with cation transport (Isenring *et al.*, 1998[a]), 4 and 7 and involved with anion transport and these, along with transmembrane domains 11 and 12 are involved with bumetanide inhibition (Isenring *et al.*, 1998[b]). It has also been suggested that secretion of nitrate also occurs via this transporter, with the nitrate being substituted for the chloride ion (Silva *et al*, 1993[b]).

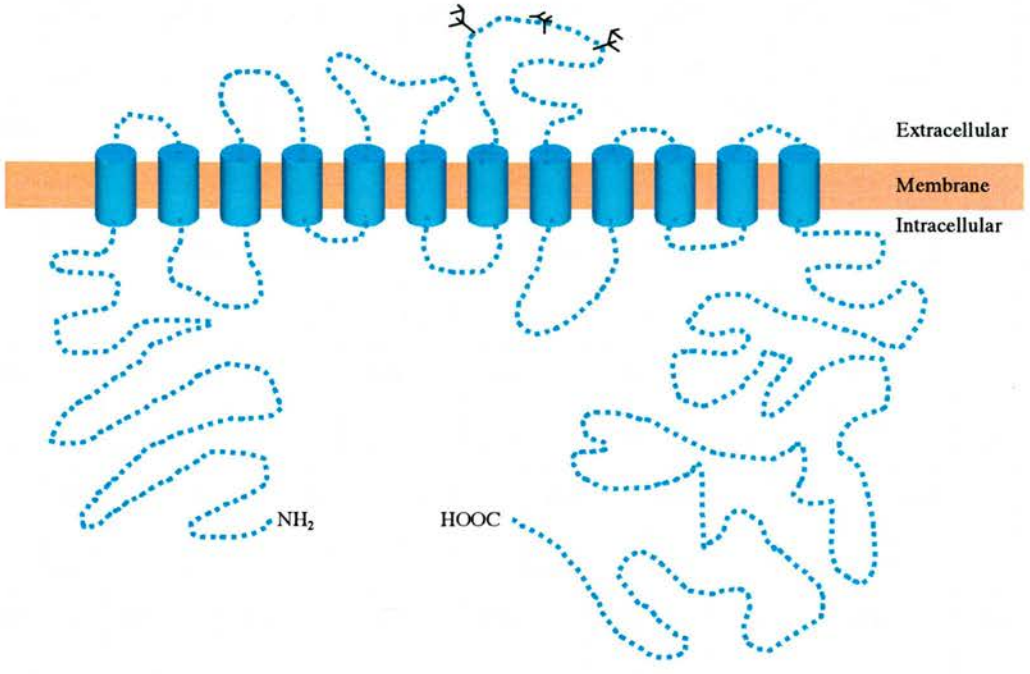

Figure 1.26: Schematic diagram of the NKCC co-transporter. Model of NKCC1 based on cDNA sequence and hydropathy and secondary structural analyses. Branched lines indicate potential glycosylation sites (Adapted from Haas and Forbush, 1998).

NKCC plays a fundamental role in regulating cell volume and ionic composition, particularly in the epithelia of osmoregulatory organs. As shown in *Figure 1.19*, it may be situated on the basolateral membrane and act in conjunction with other transporters resulting in the net NaCl efflux across the epithelial cell layer into the lumen or external environment, or it can be expressed on the apical membrane resulting in net NaCl absorption. In most tissues studied, the NKCC1 "secretory isoform" is found on the basolateral membrane, and the NKCC2 "absorptive isoform" is expressed on the apical membrane (Haas and Forbush, 2000). In the kidney of *S. acanthias*, NKCC is expressed on the apical membranes and to a lesser extent on the basolateral membranes of cells comprising the proximal and distal nephron segments, suggesting that both isoforms are present in the shark kidney (Biemesderfer *et al.*, 1996). In addition, Northern blot analysis using a non-isoform specific NKCC probe identified a 7.4 kb mRNA in rectal gland, brain, gill, intestine, heart, kidney, liver and testis of *S. acanthias*, which may represent NKCC1 in this species, but also a 5.2 kb mRNA in the kidney which may represent the NKCC2 (Xu *et al.*, 1994). Recently, NKCC2 was isolated from *S. acanthias* kidney (sNKCC2), and this isoform is 59% homologous to sNKCC1, and 68% homologous with human NKCC2 (hNKCC2; Gagnon *et al.*, 2002).

NKCC activity in all species is regulated by cell volume, cAMP (Lytle and Forbush, 1992[b]), growth factors, (Jiang *et al.*, 2001), phosphorylation and by intracellular Ca^{2+} (Bleich *et al.*, 2000). A transient decrease in cell volume has been shown to cause activation of NKCC (Bleich *et al.*, 2000). NKCC activity is upregulated when it is phosphorylated by a protein kinase, which is likely to be PKA (Kurihara *et al.*, 2002; Flemmer *et al.*, 2002), and downregulated following dephosphorylation by protein phosphatase 1 (Darman *et al.*, 2001). Intracellular chloride ion concentration can also affect the activity of NKCC, with low intracellular Cl^- concentration activating NKCC, and high concentration inhibiting the activity (Lytle and Forbush, 1996). Low intracellular Cl^- concentration has also been found to increase the activity of sNKCC2 (Gagnon *et al.*, 2002). The presence of a functional apical CFTR has been shown to increase expression of NKCC1 in basolateral membranes of cultured pancreatic duct cells, although this effect is probably caused by a decrease in intracellular Cl^- concentration mediated by the CFTR (Shumaker and Soleimani, 1999).

As a key transporter in epithelial cells of osmoregulatory tissues, it is no surprise that NKCC activity is altered by environmental salinity. On acclimation to SW, or administration of cortisol or growth hormones, *S. salar* gills have increased NKCC abundance (Pelis *et al.*, 2001[a]; Pelis *et al.*, 2001[b]). Developmental stage appears to play a role in these changes, since NKCC expression increases in gills of non-migratory 'yellow' *A. anguilla* on acclimation to SW, whereas no difference in NKCC expression is noted in migratory 'silver' eels (Cutler and Cramb, 2002[a]). In the kidney of the European eel, NKCC1 mRNA expression decreases on acclimation to SW. Expression of NKCC1 mRNA in the eel intestine remains constant regardless of environmental salinity (Cutler and Cramb, 2002[a]). NKCC distribution is also affected by environmental salinity, moving from an uneven cellular location in FW MR cells to a even distribution throughout the MR cells in SW (Marshall *et al.*, 2002[a]; McCormick *et al.*, 2003; Wu *et al.*, 2003) and this pattern could be used to indentify FW and SW MR cell subtypes. It is possible that the change in distribution dependent on salinity as shown by immunolocalisation is in fact expression of the two NKCC isoforms, secretory NKCC1 on the basolateral membrane in SW, and the absorptive NKCC2 on the apical membrane in FW.

1.7.2. CFTR

It has previously been stated that all of the transporters involved in the net movement of ions must be fully functional for the system to operate. The cystic fibrosis transmembrane conductance regulator (CFTR) highlights this fact in humans, where mutations of the CFTR cause the disease cystic fibrosis (CF). Since CF is a life-threatening disease, there has been much study into its cause, resulting in the identification of CFTR mutations as the origin of the disease. Consequently, this has led to CFTR being one of the most intensely investigated membrane transport proteins (Greger *et al.*, 2001).

CFTR has been identified and characterised in a number of vertebrate species. It is expressed as a mRNA transcript of CFTR of ~6.5 kb, encoding a protein of ~1480 amino acids in length, and molecular weight of ~170 kDa (Riordan *et al.*, 1989). CFTR is a member of the ATP-binding cassette transporter family, or ABC transporters (Fuller and Benos, 1992). It has five major domains comprising two nucleotide binding regions, a regulatory

domain and two transmembrane spanning domains (Ko and Pedersen, 1997) each containing six membrane spanning segments (Morales *et al.*, 1999; *Figure 1.27*). CFTR is expressed at high levels in epithelial cells, where it is found predominantly on the apical membrane where it operates as a gated anion (Cl^-) channel (Kleizen *et al.*, 2000). CFTR also modifies the activity of many other ion channels such as those for Na^+ (ENaC; Greger *et al.*, 1996) and K^+ (ROMK; Greger *et al.*, 1996) and has been implicated in the upregulation of expression of NKCC (Shumaker and Soleimani, 1999). CFTR can be regulated by phosphorylation by PKA and PKC (Darman *et al.*, 2001). Using mutated forms of CFTR, it is possible to identify residues which are potential phosphorylation sites, and examine whether phosphorylation at these residues cause an increase or decrease in channel activity (Dahan *et al.*, 2001). CFTR has also been reported to be stimulated by C-type natriuretic peptide (CNP) dependent increase in intracellular cGMP concentrations (Aller *et al.*, 1999).

CF is an autosomal recessive genetic disorder caused by mutations in the CFTR gene, particularly when the mutation occurs in a site vital to the correct intracellular trafficking of the protein to the apical membrane or to the functioning of the protein when inserted into the correct membrane domain. Symptoms of CF include, but are not limited to, elevated sweat NaCl concentration in sweat, pulmonary disease, pancreatic insufficiency, bile duct and intestinal obstruction, nasal polyp formation, chronic sinusitis, secretion of dehydrated mucus from respiratory epithelia and male infertility (Morales *et al.*, 1999; Kleizen *et al.*, 2000). For those with a good understanding of osmoregulation, these symptoms would be expected since the affected epithelial cells are unable to sustain normal ion transport. Mucus becomes dehydrated after secretion in the lungs which commonly leads to bacterial lung infections responsible for 90% of the mortality of CF patients (Morales *et al.*, 1999). Prospective parents may be screened in order to assess the likelihood of having a child with CF, in addition to testing the unborn fetus for CFTR mutations as was suggested upon the discovery of CFTR (Kerem *et al.*, 1989). It is hoped that further investigation into the mutations and activity of CFTR may lead to advances in CF therapy.

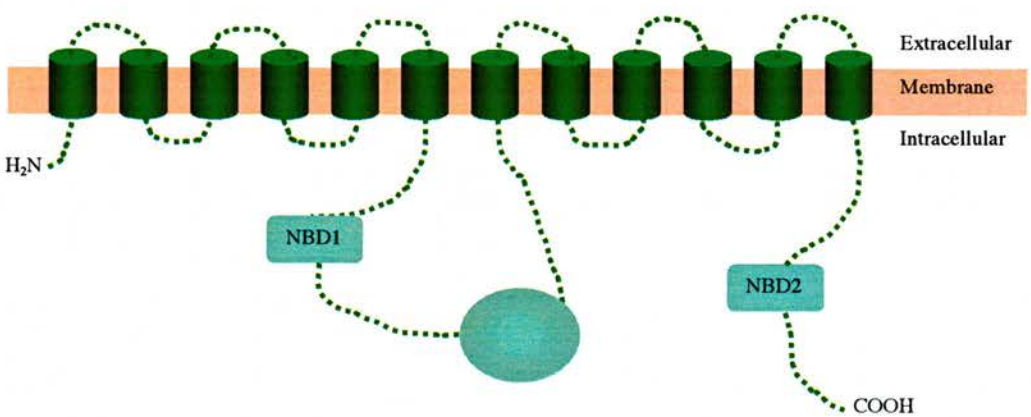

Figure 1.27: Schematic diagram of the CFTR. Structure of CFTR; NBD1 and NBD2, nucleotide binding domains 1 and 2; R domain, regulatory domain (Adapted from Devidas and Guggino, 1997).

CFTR has been characterised in the epithelia of several fish species, including in the apical membrane of the cells lining the lumen of the *S. acanthias* rectal gland, where the CFTR amino acid sequence shares 72% amino acid identity with the human protein (Marshall *et al.*, 1991). Particular emphasis has been placed on CFTR in euryhaline fish. In *F. heteroclitus*, CFTR is expressed in the intestine, gill and opercular epithelium, and to a lesser extent, the brain. Expression of CFTR in these tissues increased several fold when FW-adapted *F. heteroclitus* were acclimated to SW (Singer *et al.*, 1998). This increase in CFTR expression in gill epithelia of fish adapted to SW has also been observed in the Hawaiian goby, *Stenogobius hawaiiensis* (McCormick *et al.*, 2003). Cellular distribution of CFTR is also altered depending on environmental salinity, since it is found exclusively in the apical crypt region in SW gill cells, but is located on the apical membrane and throughout the cytoplasm in FW *F. heteroclitus* (Marshall *et al.*, 2002[a]) and *S. hawaiiensis* (McCormick *et al.*, 2003). The apical location in SW is concurrent with the proposed model of chloride transport by MR cells in SW-adapted fish gills (Marshall and Singer, 2002). Further evidence to the model has been shown in *S. hawaiiensis*, where CFTR co-localises with Na^+, K^+ -ATPase in MR cells (McCormick *et al.*, 2003). CFTR is found in both the basolateral and apical membranes of cells in the intestine, where it is thought they perform uptake and secretion of Cl^- respectively (Marshall *et al.*, 2002[b]).

1.7.3. Aquaporins (AQPs)

Most cell membranes have a high water permeability; water movement in and out of the cell occuring by simple diffusion. Cell membranes with unusually high water permeabilities were found to contain water channel proteins, or aquaporins (AQPs; van Os *et al.*, 1994). AQPs are members of a larger family of channel-forming proteins, the major intrinsic protein (MIP) family (Deen and van Os, 1998). All AQPs are able to transport water, but AQP_3, AQP_7 and AQP_9 can also transport glycerol and are known as aquaglyceroporins. AQPs comprise homotetramers, where each monomer is 26-34 kDa in size and has six transmembrane α helical domains (Verkman and Mitra, 2000). AQP protein sequences contain two highly conserved 'NPA' motifs (asparagine: N; proline: P; alanine: A), which are thought to fold back into the membrane and help form the water channel (Deen and van Os, 1998; *Figure 1.28*).

In a review by Deen and van Os in 1998, 10 AQPs had been identified in a wide range of secretory and absorptive tissues, AQP_0 – AQP_9. In mammals these AQPs share amino acid identities ranging from 19 to 52% (Verkman and Mitra, 2000). AQP_0, also known as MIP26, is expressed only in lens fibre cells (Mulders at el., 1995). AQP_1 is found in a wide range of tissues, including the proximal tubules and thin descending limbs of Henle's loop in the kidney, and also the eye, lung and erythrocytes (King and Agre, 1996). Expression of AQP_1, and therefore water transport, can be upregulated by glucocorticoids (Lee *et al.*, 1997). AQP_2, also known as the vasopressin-regulated water channel, is found only in the collecting duct of the kidney (Sabolic *et al.*, 1995). Similarly, AQP_3 is also expressed in the kidney collecting duct, and also in the intestinal and respiratory epithelia. AQP_4 is found primarily in the brain, and AQP_5 in salivary gland and respiratory tissue (Lee *et al.*, 1997). Therefore, AQP_0, AQP_1, AQP_3, AQP_4 and AQP_5 are all found in different parts of the respiratory system (Nielsen *et al.*, 1997; Liu *et al.*, 2003) and the eye (Hamann *et al.*, 1998) where they work in combination to regulate the water balance. Likewise, AQP_2, AQP_3 and AQP_4 also work together to allow resorption of water in the collecting duct of the kidney (Deen and van Os, 1998). AQP_6 is found only in the kidney (Ma *et al.*, 1996), AQP_7 is expressed primarily in spermatids and AQP_8 in hepatocytes and testis (Ishibashi *et al.*, 1997). AQP_9 is primarily found in adipocytes (Kuriyama *et al.*, 1997). An additional three AQPs have been discovered since the review by Deen and van Os (1998), and these are AQP_{10}, AQP_{11} and AQP_{12} (Deen, P., 2005, pers. comm.). More than 200 members of this family have now been identified in a wide range of species (Agre *et al.*, 2002).

The first AQP to be discovered in fish was a homologue of AQP_3 which was cloned from the gill of FW-acclimated *A. anguilla* (Cutler and Cramb, 2000), and expression was shown to be down-regulated when fish were transferred to SW (Lignot *et al.*, 2002; Cutler and Cramb, 2002[b]). An AQP_1 homologue was subsequently discovered in many tissues from *A. anguilla*, and expression of this AQP in the intestine was found to increase on transfer of fish from FW to SW (Martinez *et al.*, 2005[a]), however the expression of this isoform in the kidney was decreased after SW transfer (Martinez *et al.*, 2005[b]). A third AQP which exhibited high amino acid homology to eel AQP_1 and

hence called eel AQP_1 duplicate was isolated from *A. anguilla* kidney and was found to be down-regulated on transfer of eels from FW to SW (Martinez *et al.*, 2005[b]). It was also discovered that cortisol, at concentrations similar to that found during FW-SW acclimation, increases expression of AQP_1 in the intestine (Martinez *et al.*, 2005[a]) and oesophagus (Martinez *et al.*, 2005[c]), but significantly decreases AQP_1 expression in the kidney (Martinez *et al.*, 2005[b]).

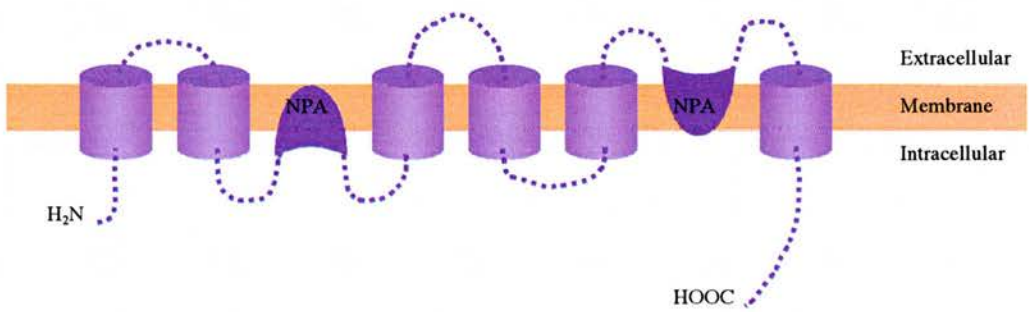

Figure 1.28: Schematic diagram of an Aquaporin. Membrane spanning model of one subunit of AQP1, showing arrangement of transmembrane domains and position of conserved NPA motifs (Adapted from Agre *et al.*, 2002).

1.8: Research Aims and Hypotheses

This study represents the first investigation of the molecular mechanisms of osmoregulation in the euryhaline bull shark. The aims of the study were:

- To clone, sequence and examine the expression and distribution of Na^+, K^+-ATPase subunit isoforms in *C. leucas*.

- To examine whether the expression and distribution of one or more of these isoforms is altered in the osmoregulatory tissues (rectal gland, kidney, gill and intestine) when fish move from FW to SW.

- To attempt to clone and sequence other transporters (NKCC, CFTR, AQP) which are also known to be involved in osmoregulation in teleost fish.

Since Na^+, K^+-ATPase is expressed abundantly in vertebrate osmoregulatory tissues it was expected that the full length sequences of *C. leucas* α and β subunits of Na^+, K^+-ATPase would be straightforward to identify. It was expected that the expression of Na^+, K^+-ATPase in osmoregulatory tissues would be similar to the reported activity of this enzyme, as revealed by Pillans *et al.* (2005). The highest levels of Na^+, K^+-ATPase mRNA and protein expression were expected in the rectal gland and kidney, with lower levels expressed in the gill and intestine. It was also predicted that the expression of Na^+, K^+-ATPase may increase in the rectal gland, and decrease in the kidney, following transfer to SW in accordance with the reported levels of Na^+, K^+-ATPase in these tissues (Pillans *et al.*, 2005).

2

Materials and Methods

General Chemicals and Reagents

Unless otherwise stated all chemicals were Analar® grade supplied by Sigma Aldrich Ltd., or from VWR Laboratory Supplies. Addresses for suppliers of materials and equipment can be found in Appendix 2. Sequences of the synthetic oligonucleotides (MWG Biotech) and those supplied with commercial kits are listed in Appendix 3.

2.1: Fish collection, transport and holding conditions

Juvenile *C. leucas* of 60-90 cm total length (TL) were captured via hook and line from the Karana Downs area of the Brisbane River, Queensland, Australia, over 50 km inland, in freshwater (FW) of <5 $mOsm.kg^{-1}$ (Pillans & Franklin, 2004; *Figures 2.1 - 2.4*). Immediately after capture, sharks were carefully placed into a 400 l plastic container of water collected from the capture site in the fishing boat and transported back to the bank. At the bank, the fish was transferred to a second 400 l container of water and then transported to a purpose built re-circulating aquarium at the University of Queensland (*Figures 2.5 and 2.6*).

Up to six fish were simultaneously held in each of the three 10,000 l plastic tanks. One tank held FW, from the Brisbane River, 3 $mOsm.kg^{-1}$; Na^+: 0.5 $mmol.l^{-1}$, Cl^-: 0.1 $mmol.l^{-1}$. Two tanks held seawater (SW) from Moreton Bay diluted with water from the Brisbane River to the desired concentration of 400 $mOsm.kg^{-1}$. Tank water was tested daily for temperature, and dissolved oxygen, nitrites, nitrates and ammonia levels, and was filtered through a 200 l submerged coral rubble filter, a 200 l trickle BioBall filter (Polytech) and a venturi action foam fractionator (Aquasonic) powered by LZS4-6 pumps (Aquasonic) at a rate of 1,800-2,000 $l.h^{-1}$ (*Figure 2.6*).

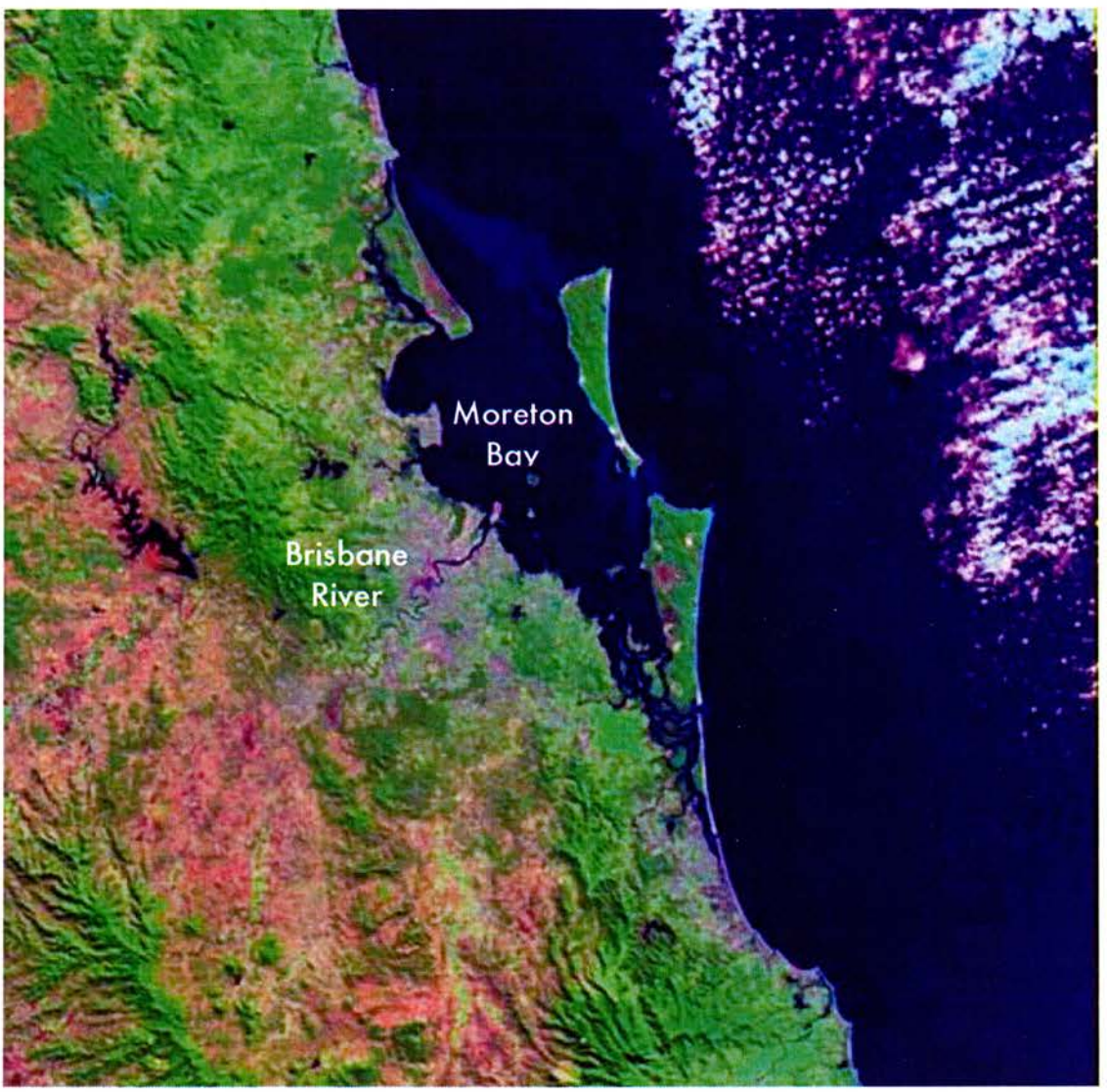

Figure 2.1: Satellite image of Brisbane, Queensland. (Courtesy of http://www.wildhorizons.com.au/city2city/city4.html)

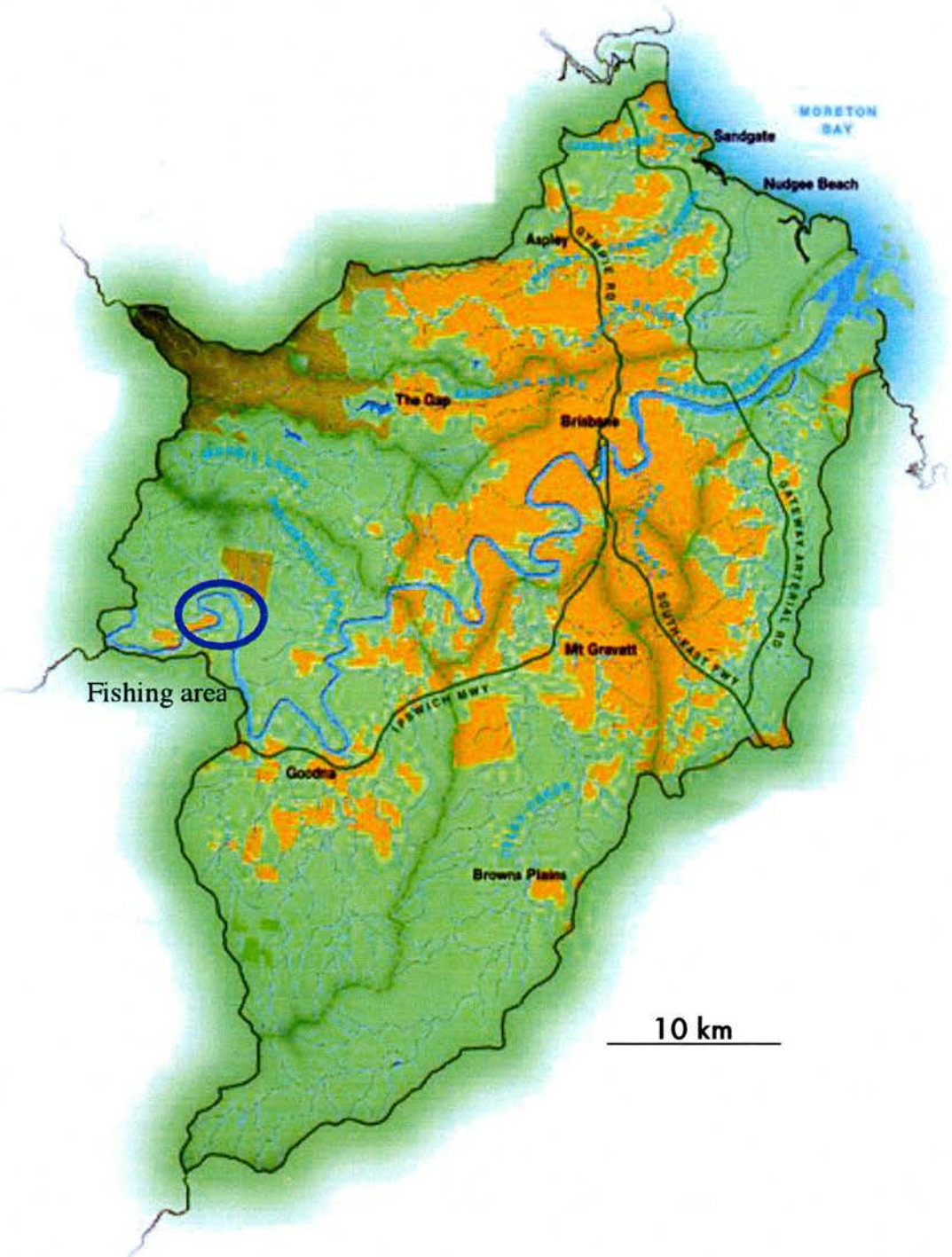

Figure 2.2: Map of Brisbane, Queensland, indicating the fishing area. All juvenile bull sharks were collected via hook and line from this area. (Courtesy of http://www.coastal.crc.org.au/)

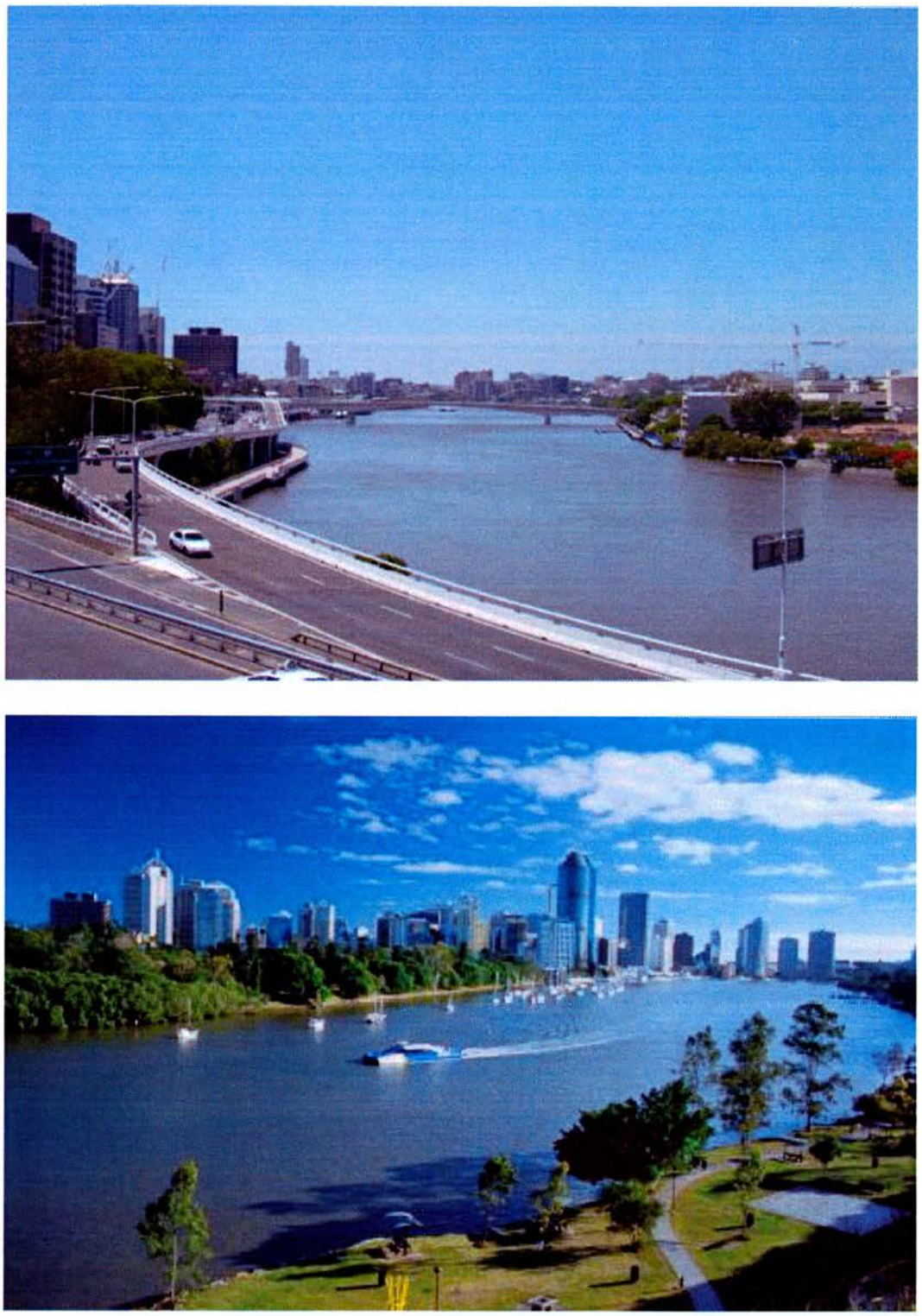

Figure 2.3: Photographs of Central Brisbane. The Brisbane River runs through the centre of Brisbane. Juvenile bull sharks swim up this city centre section of the river to get further inland. (Top: Photograph courtesy of http://www.innerbrisbane.com/218/images/still-31521-large.jpg Bottom: Courtesy of http://www.usasa.unisa.edu.au/sport_rec/river-city.jpg)

Figure 2.4: Photographs of the fishing area. The Karana Downs region of the Brisbane River was the location of fishing. These photographs are of this region as highlighted in Figure 2.2.

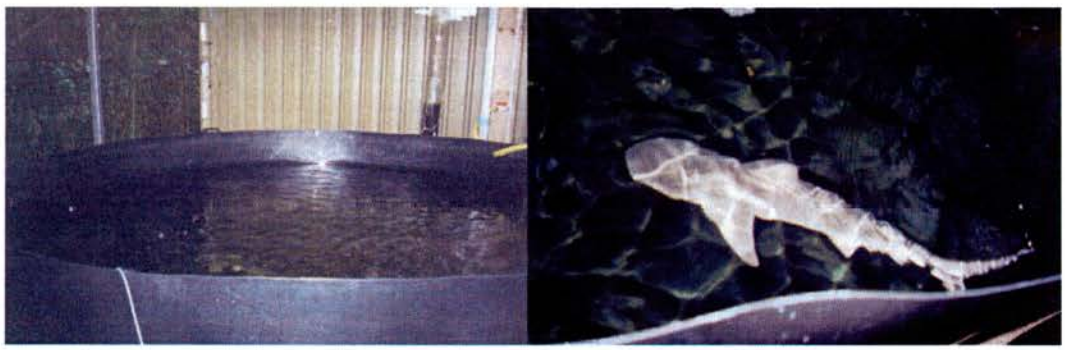

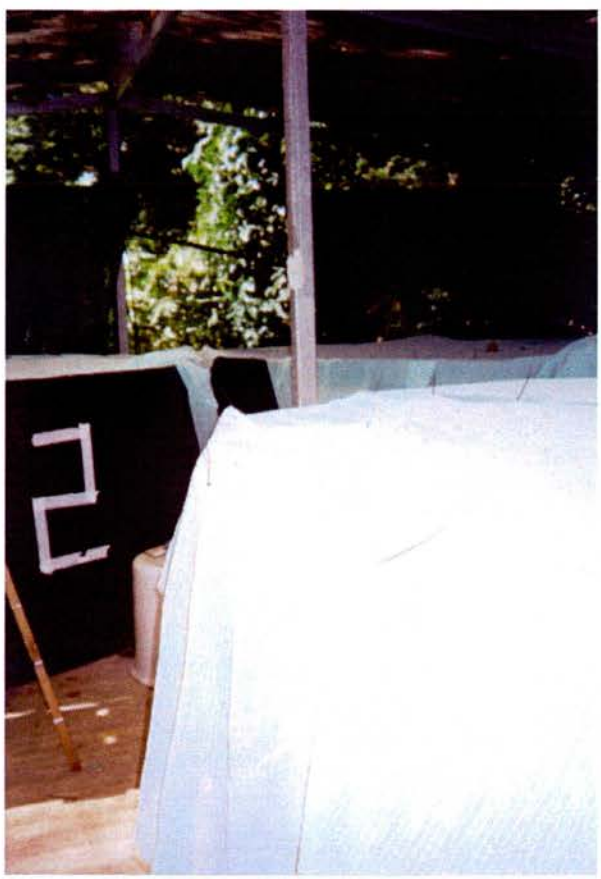

Figure 2.5: Aquarium tanks. Each of the three plastic tanks held 10,000 l of water, and up to 6 juvenile bull sharks. The mesh sheeting covering the tanks prevented sharks from jumping out of the tanks.

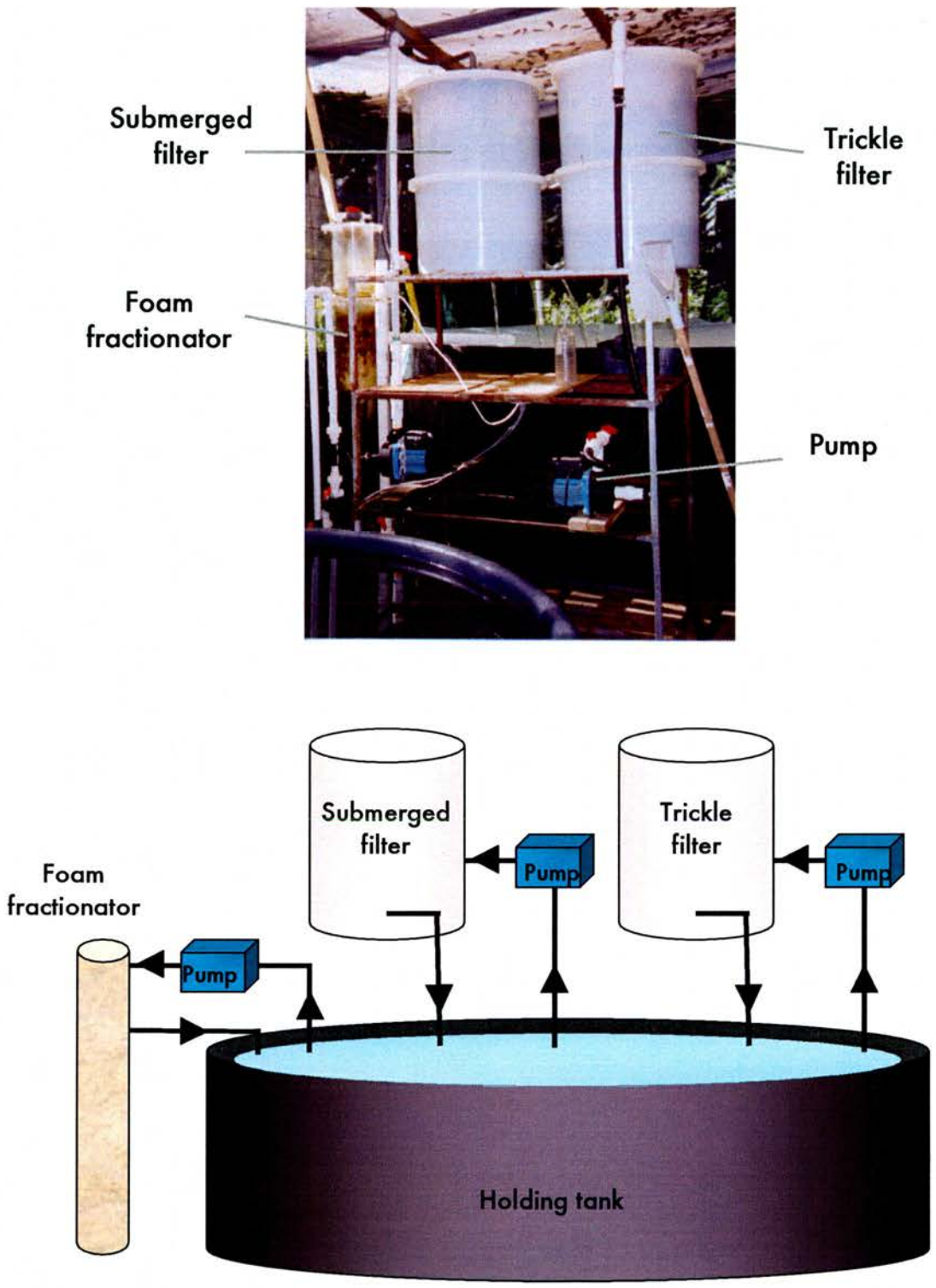

Figure 2.6: Aquarium filtration system. Photograph and diagram to illustrate recirculating tank filtration mechanisms.

After a 48-72 h acclimation period in the FW tank, fish were transferred into diluted SW (400 $mOsm.kg^{-1}$) and then subject to a series of increases in osmolality until full strength SW (~1000 $mOsm.kg^{-1}$) was reached. The osmolality was first increased to 600 $mOsm.kg^{-1}$ (at 100 $mOsm.kg^{-1}$ per 24 h) over 48 h by addition of SW, then to 800 $mOsm.kg^{-1}$ (at 50 $mOsm.kg^{-1}$ per 24 h) over 96 h, and finally to ~1000 $mOsm.kg^{-1}$ (at 100 $mOsm.kg^{-1}$ per 24 h) over 48 h. Sharks were left to acclimate for a period of 7 days prior to sampling. The composition of the tank water for the SW-acclimated group was 980–1,000 $mOsm.kg^{-1}$, Na^+: 410-440 $mmol.l^{-1}$, Cl^-: 540-560 $mmol.l^{-1}$, K^+: 7.4 $mmol.l^{-1}$. FW-acclimated sharks were maintained in FW for the same period as the SW-acclimated sharks prior to sampling (Anderson *et al.*, 2005).

All sharks were fed regularly with small live bait fish (striped mullet, *Mugil cephalus* and bony bream, *Nematalosa erebi*) during acclimation and holding. This occasionally caused the sharks to jump out of the tanks in a burst of speed. In the second and third sampling seasons, strong nets were used to cover the tanks to prevent this.

2.2: Collection of tissues

Fish were killed in accordance with University of Queensland animal ethics guidelines; permit number ZOO/ENT/144/04/URG/PHD. Tissue samples were quickly collected and either immediately homogenised using a Polytron PT 10 homogeniser (Kinematica Ltd.) in 1:10 (w/v) Solution D (4 M guanidinium isothiocyanate, 25 mM sodium citrate, 0.5% (v/v) sarkosyl and 50 mM 2-mercaptoethanol) for RNA extraction (Section 2.3), or wrapped in aluminium foil and placed into liquid nitrogen for protein extraction (Section 2.18), or placed into 4% paraformaldehyde in phosphate buffered saline (PBS) to fix the tissues for immunohistochemistry (Section 2.24). Tissues were collected as follows: gill, pancreas, spleen, liver, rectal gland, intestine, oesophagus, ventricle, atrium, kidney, inter-renal gland, brain, muscle and eye. All tissues were collected for RNA extraction, but only gill, intestine, rectal gland and kidney for protein extraction and immunohistochemistry. In all cases tissues were excised and divided into small pieces, except the brain which was collected intact for RNA extraction, and the gill and intestinal epithelium, which were scraped with a scalpel blade for RNA extraction (*Figure 2.7*). Homogenates for RNA and protein

extraction were stored at –80°C until use, and those for immunohistochemistry were stored in 4% paraformaldehyde in PBS for no longer than 2 days at 4°C until processing.

The limitations of tissue collection were soon apparent. Since this project was a collaboration with other investigators, tissue had to be divided. Tissues such as the kidney and gut were plentiful, but the rectal gland of these juvenile FW sharks was much smaller with an average total weight of 0.2 g, of which only a small proportion was allocated to RNA extraction (and therefore subsequent RT-PCR and Northern blotting), protein extraction (for Western blotting) and immunohistochemistry. Some individual projects required the perfusion of whole organs, such as the rectal gland or kidney, which also restricted the number of tissues available. Difficulties with processing and transportation from Brisbane, Australia to St Andrews, UK also led to the loss of viability of a number of samples. This has in all cases, reduced the total number of samples available for each experiment, and in some cases there were no available samples, for example no frozen intact rectal glands were available from SW-acclimated fish and only three rectal glands were available from FW-acclimated fish for protein extraction.

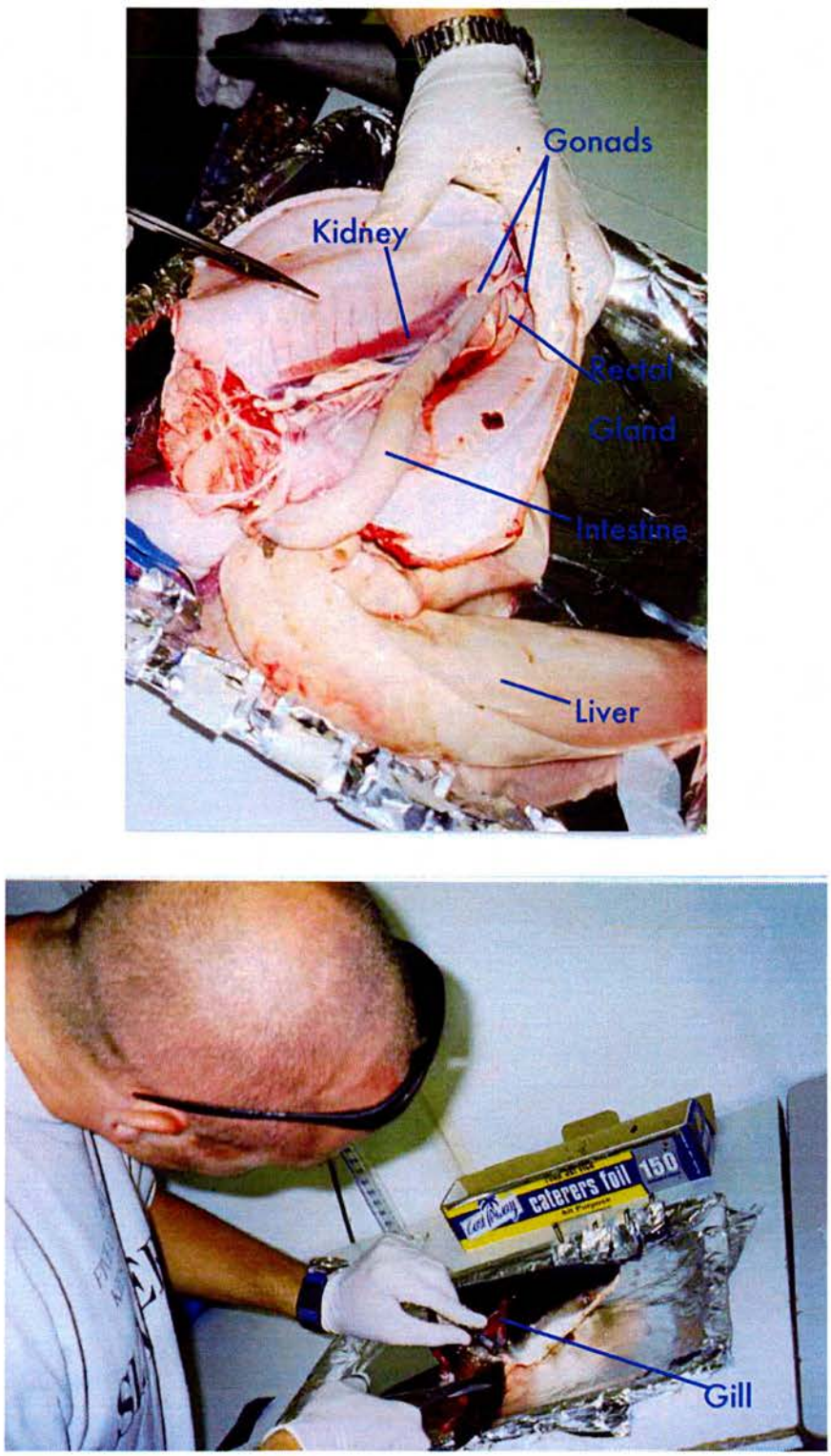

Figure 2.7: Dissection of juvenile bull sharks. Photographs taken during dissection of a juvenile bull shark showing the organs of the body cavity (top) and gill (bottom).

2.3: RNA extraction

Total RNA was isolated from tissues using the guanidinium isothiocyanate method (Chomczynski and Sacchi, 1987), as modified in Cutler *et al.*, 2000. Tissues previously homogenised in Solution D were stored at -80°C. Samples were allowed to thaw on ice and the following reagents added sequentially, vortexing between each addition: 0.1 vol. 2 M sodium acetate (pH 4.0), 0.5 vol. water saturated phenol and 0.2 vol. of 1-bromo-3-chloropropane (Chomczynski and Mackey, 1995). The tubes were then centrifuged in a Beckman J6-MC centrifuge, rotor JS-4.2 (Beckman Instruments Inc.), at 4,200 rpm (3,640 g_{ave}), set to 4°C for 30 minutes. The upper aqueous supernatant was transferred to a new centrifuge tube, taking care not to dislodge the white protein-laden interphase. To the supernatant was added 0.2 vol. of propan-2-ol and 0.2 vol. of high salt buffer (1.2 M NaCl, 0.8 M sodium citrate, pH 7.0), vortexing between additions, before incubating at room temperature (RT) for 10 minutes. Samples were centrifuged as above at 4,200 rpm (3,640 g_{ave}), at RT for 30 minutes, after which the supernatant was poured off. The pellet was washed twice in 80% ethanol and centrifuged as above at RT for 10 minutes, before inverting the tube over paper tissue allowing the pellet to dry at RT. The pellet was re-suspended in MilliQ®H_2O (20 – 30 µl/g tissue; Millipore), with the tubes briefly heated to 65°C to aid solubility. To determine the RNA concentration, the absorbance of diluted samples (1:200) was measured at 260 nm (Phillips PU 8620 UV/VIS/NIR spectrophotometer) where 1 A_{260} unit = 40 ng RNA/µl, and concentrations calculated taking into account the dilution factor. Viability and degradation of the RNA was assessed by ethidium bromide staining following formaldehyde denaturing gel electrophoresis (Sambrook *et al.*, 1989).

2.4: RNA denaturing gel electrophoresis

RNA denaturing gel electrophoresis was used to separate molecules by size. Total RNA (5 – 10 µg) previously quantified using a spectrophotometer was added to 23 µl sample denaturing buffer; 1 x MOPS (20 mM 3-[N-Morpholino]-propanesulphonic acid, 8 mM sodium acetate, and 1mM EDTA pH 7.8), 50% (v/v) formamide and 6.7% (v/v) formaldehyde. The tubes were mixed and heated at 65°C for 15 minutesto denature the RNA, and then

snap-cooled on ice. Where the size of RNA species were to be estimated an RNA ladder (500 μg/ml, NEB) was also prepared, using 1-3 μg of the ladder, diluted to 20 μl with sample denaturing buffer. This was heated at 65°C for 15 minutes to denature. Loading dye (0.1 volume of 0.025% bromophenol blue, 0.025% xylene cyanol and 50% glycerol, all w/v) was added to all samples and marker. To prepare a 1.2% (w/v) agarose/formaldehyde gel, 1.2 g agarose (Biogene Ltd.), 10 ml 10 x MOPS buffer (200 mM 3-[N-Morpholino]-propanesulphonic acid, 80 mM sodium acetate, and 10 mM EDTA pH 7.8) and 72 ml of MilliQ®H_2O were boiled in a conical flask until dissolved. After cooling to approximately 55°C, 18 ml of a 37 % (v/v) formaldehyde solution was added (final concentration 6.7% (v/v) formaldehyde). After swirling to mix, this was poured into a gel mould (Scotlab) and a comb with the desired number of wells was placed into position before leaving to set for at least 20 minutes. The gel was cooled for 10 minutes in a refrigerator then placed into a horizontal electrophoresis tank (Scotlab) containing 1 x MOPS. Denatured RNA samples were loaded onto the gel, and power switched on at 10 V/cm until the samples have run into the gel and then 5 V/cm applied for approximately 1 h. After electrophoresis, the gel was removed from the tank and placed in a tray of MilliQ®H_2O and set on a horizontal shaker for 1 h, replacing with fresh MilliQ®H_2O twice. An ethidium bromide solution (1 μg/ml) was then added to the tray to stain for 30 minutes, and then the gel was de-stained in Milli-Q® H_2O for 1 h as before. The RNA samples could then be visualised on an UV transilluminator (UVT-20M Trans-luminator, Herolab), and further analysed using Gene Snap and Gene Tools computer software (Syngene). Sample viability was assessed by noting the relative band intensity levels of the 28S and 18S ribosomal RNA, where the ratio should be approximately 2:1 (28S : 18S). In order to calibrate the amount of RNA in each sample, both 28S and 18S band intensities were quantified and standardised (Mahmmoud *et al.*, 2003).

2.5: Conversion of mRNA to cDNA

Total RNA from various bull shark tissues (2.5 μg) and 1 μl 10 μM oligo dT primer (Pharmacia Ltd.) were mixed together and made up to a total volume of 5 μl using MilliQ®H_2O. The tube was then heated for 10 minutes at 70°C on a thermal cycler (Techne Progene, Techne Ltd.), and then snap cooled on

ice for 2 minutes. Single-strand complementary DNA (cDNA) was synthesised from mRNA by reverse transcription. The following reagents were then added to the RNA/oligo dT mixture: 2 μl 5x reaction buffer (250 mM Tris-HCl, 375 mM KCl, 15 mM $MgCl_2$ and 50 mM DTT, pH 8.3; Promega), 1 μl 0.1M dithiothreitol (DTT; Gibco), and 1 μl 10 mM deoxyribonucleotide triphosphates (dNTPs - 10 mM each of, dATP, dTTP, dCTP and dGTP; Promega); the contents of the tube were then mixed and preheated to 45°C for 2 minutes. To initiate the reverse transcription reaction, 1μl of Moloney-Murine Leukaemia Virus reverse transcriptase (M-MLV RT, 200 U/μl; Promega) was added and mixed gently, then incubated at 45°C for 2-5 h (Cutler *et al.*, 2000). The cDNA samples were stored at –20°C until required.

2.6: Marathon™ cDNA synthesis

Marathon™ cDNA was synthesised according to the protocol included with Clontech's Marathon™ cDNA amplification kit; any differences in protocol will be outlined below (*Figure 2.8*). Total RNA was used as a template for first strand cDNA synthesis. An amount up to 5 μg of total RNA was added to 1 μl of BD Smart II™ A Oligo (12 μM; BD Biosciences, Clontech; Appendix 3), and 1 μl of cDNA synthesis primer (10 μM; Clontech; Appendix 3), and made up to a total volume of 5 μl with water. After mixing, the tube was incubated at 70°C for 10 minutes then snap cooled on ice for 2 minutes. After cooling, 2 μl 5x first strand buffer (250 mM Tris pH 8.5, 40 mM $MgCl_2$ and 150 mM KCl; Clontech) and 1 μl 10 mM dNTPs were added, mixed and preheated to 45°C for 3 minutes. Keeping the tube at 45°C, 1 μl of reverse transcriptase (either M-MLV reverse transcriptase, 200 U/μl; Promega, or Superscript II RNase H^- reverse transcriptase, 200 U/μl; Gibco BRL) was added and incubated at 45°C for 2 hours. The 'cap' structure at the 5'end of full length mRNA is composed of a 7-methylguanosine residue linked to a triphosphate (Alberts *et al.*, 1994). When reverse transcriptase reaches the cap structure, several deoxycytidine residues are attached to the 3′ end of the cDNA. The BD Smart II™ A Oligo which has several guanine residues at its 3′ end, base pairs with the cytidine residues on the cDNA binding to the 5′ end of the mRNA to serve as an extended template for reverse transcription

of full length cDNAs. To terminate the first strand synthesis, the tube was placed on ice after incubation.

Second strand cDNA was then synthesised from the first strand. The following reagents were added to the first strand cDNA: 48.8 µl MilliQ®H_2O, 16 µl of 5x second strand buffer (500 mM KCl, 50 mM $(NH_4)_2SO_4$, 25 mM $MgCl_2$, 0.75 mM β-NAD, 100 mM Tris pH 7.5 and 0.25 mg/ml BSA; Clontech), 1.6 µl 10 mM dNTPs and 4 µl second strand enzyme cocktail (compromising DNA Polymerase I, 6 U/µl, *E. coli* DNA ligase, 1.2 U/µl and RNase H 0.25 U/µl; Clontech). The enzyme cocktail contains reagents which hydrolyse the RNA (RNase) and allow building of the second strand (DNA polymerase and DNA ligase) from the BD Smart II™ A Oligo. The tube contents were mixed and then incubated at 16°C overnight. Leaving the tube at 16°C, 2 µl of T4 DNA ligase (5 U/µl) was added to create blunt ends on the now double stranded cDNA, and then incubated for a further 45 minutes at 16°C. After incubation, 4 µl 0.2 M EDTA/2 mg/ml glycogen mix was added and mixed, to terminate the second strand synthesis.

Double stranded cDNA was extracted by adding 100 µl phenol: chloroform: isoamyl alcohol (25:24:1, v/v/v, pH 7.5, prepared according to Clontech's Marathon™ cDNA amplification kit user manual), and centrifugation at 20,000 g for 10 minutes to separate phases. The upper aqueous phase was carefully removed and transferred to fresh tube to which 0.5 vol. of 4 M ammonium acetate (pH 4.6) and 2.5 vol. of 95% ethanol at RT were added. The tube was vortexed and centrifuged at 20,000 g for 10 minutes and the supernatant was removed and discarded. The pellet was washed at RT by adding 300 µl 80% ethanol and centrifugation at 20,000 g for 10 minutes, after which the supernatant was removed and discarded. The pellet was air dried, and dissolved in 5 µl MilliQ®H_2O.

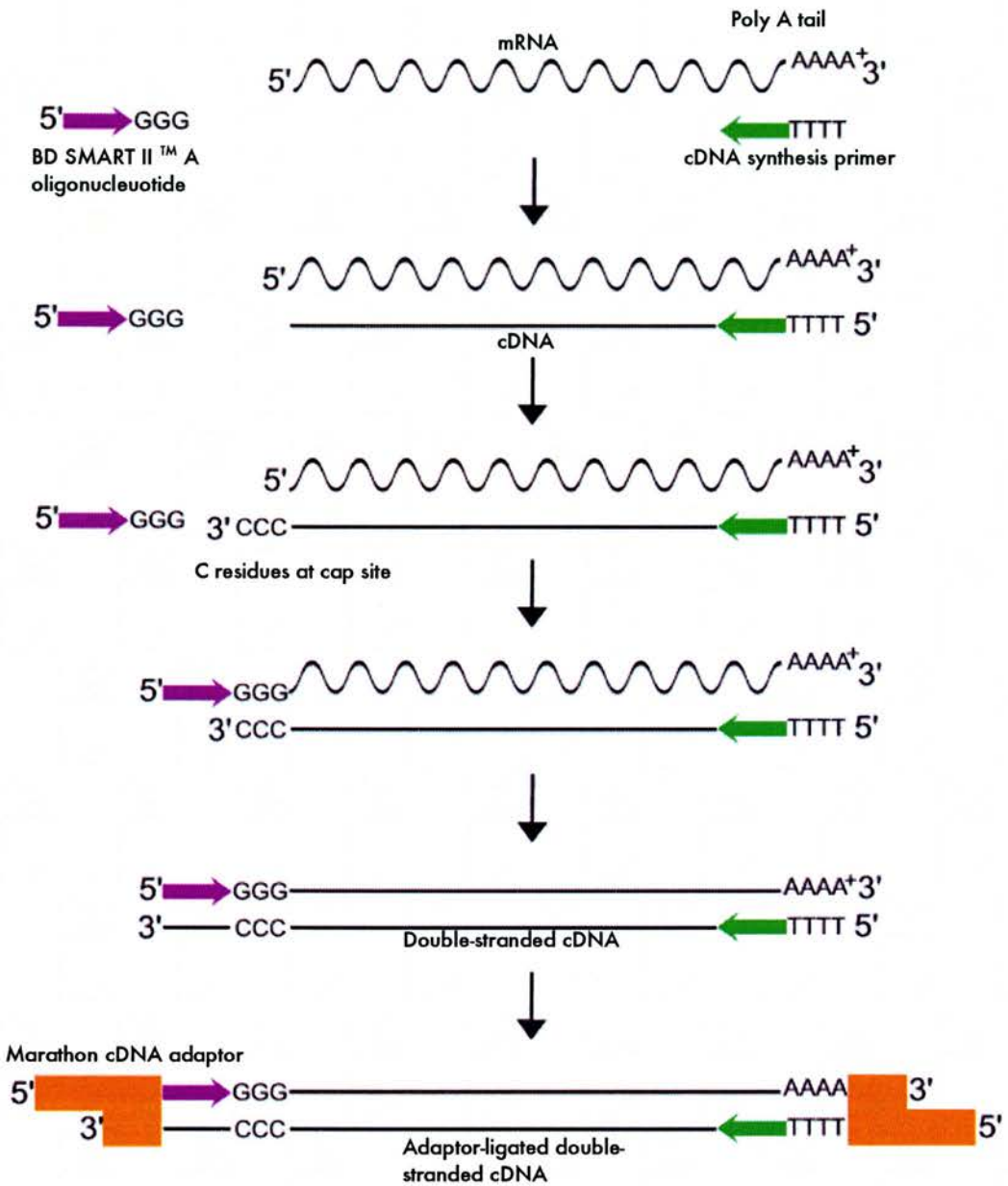

Figure 2.8: Marathon cDNA synthesis. Flow chart explaining the steps of Marathon cDNA synthesis (adapted from Marathon cDNA amplification kit user manual, Clontech and BD SMART ™ PCR cDNA synthesis kit user manual, BD Biosciences, Clontech).

The Marathon™ cDNA adaptor was then ligated to the blunt ended double stranded cDNA. To 5 µl of the previously purified cDNA, was added 2 µl Marathon™ cDNA adapter (10 µM; Clontech), 2 µl 5x DNA ligation buffer (250 mM Tris-HCl pH 7.8, 50 mM $MgCl_2$, 5 mM DTT, 5 mM ATP and 25 % (w/v) polyethylene glycol; Clontech) and 1 µl T4 DNA ligase (400 U/µl; Clontech). Components were mixed and incubated at 16°C overnight. After incubation, the tube was heated to 70°C for 5 minutes to inactivate the ligase. The complete Marathon™ cDNA reaction mix was then diluted 1:50 in Tricine-EDTA buffer (10 mM Tricine-KOH pH 8.5 and 0.1 mM EDTA; Clontech) to a concentration suitable for use in subsequent RACE PCR (Section 2.8).

2.7: Amplification of specific cDNA fragments using Reverse Transcriptase Polymerase Chain Reaction (RT-PCR)

The Polymerase Chain Reaction (PCR; *Figure 2.9*) was used to amplify specific fragments of DNA by adding template cDNA to primers, nucleotides, and a thermostable DNA polymerase and subjecting the mix to a sequence of temperature cycling. This leads to an exponential amplification of the desired DNA fragment (Burke, 1996). Primers were synthetic oligonucleotides designed to align to upstream and downstream extremes of the target DNA region. During this study, many degenerate and specific primers were used for amplification, and these are detailed in Appendix 3. All primers were synthesised by MWG Biotech. Degenerate primers were designed from known amino acid sequences in other vertebrates (Genbank®, NCBI) which exhibited high amino acid conservation between species and incorporating inosine bases (a neutral purine analogue) or inosine/cytidine nucleotide wobbles at positions of nucleotide uncertainty (Cutler *et al.*, 1995[a]). Degenerate primers were used in the first instance, whereas specific primers were designed to overlap parts of the sequence which were already known in the bull shark. The first strand cDNA template used for each amplification dependent on the gene to be amplified as many genes were known to be differentially expressed throughout the tissues. For this study, cDNA from the rectal gland of SW-acclimated sharks was mainly used, but cDNAs from gill, intestine, kidney and brain were also used.

For PCR, 0.5 µl cDNA template (prepared by reverse transcription of mRNA), 1 µl sense primer and 1 µl antisense primer (4 µM specific primers or 100 µM degenerate primers) were added to a 0.2 ml PCR tube taking care not to mix at this stage. The following reagents were mixed together to form a stock to be added to the tube just prior to initialisation of the reaction: 2 µl 10x Taq DNA polymerase buffer (500 mM KCl, 100 mM Tris-HCl, pH 9.0, 15 mM $MgCl_2$; Amersham Pharmacia Biotech Ltd.), 0.4 µl 10 mM dNTPs, 15 µl Milli-Q® H_2O and 0.25 µl of Taq DNA polymerase (5 U/µl; Biogene). The contents of the tube were mixed and the tube placed in a preheated (92°C) PCR thermal cycler (Techne Progene, Techne Ltd.) for 2 minutes. PCR reaction cycle parameters were optimised within the following ranges: DNA denaturation at 94 °C for 5-15 seconds to separate double stranded DNA into two strands to provide templates for DNA synthesis, primer annealing at 50-60°C for 10-20 seconds to allow sense and antisense primers to anneal to the separated DNA strands, and DNA polymerase extension at 72°C for 30-120 seconds allowing the Taq DNA polymerase to extend the sequence from each primer site by adding free nucleotides corresponding to the template, resulting in a reverse copy of each single stranded template. The extension time was dependent on the length of the fragment to be amplified as estimated by the position of the sense and antisense primers; in general 1 minute of extension time was allowed for a 1 kb DNA fragment. Reactions were conducted for 40 cycles and finally incubated at 72°C for 15 minutes to ensure full length extension of fragments. A simplified guide for programming the thermal cycler is outlined below: -

Program	Cycles	Temperature (°C)	Time
1	1	92	2 minutes
2	40	94	5-15 seconds
		50 – 60	10-20 seconds
		72	30-120 seconds
3	1	72	15 minutes

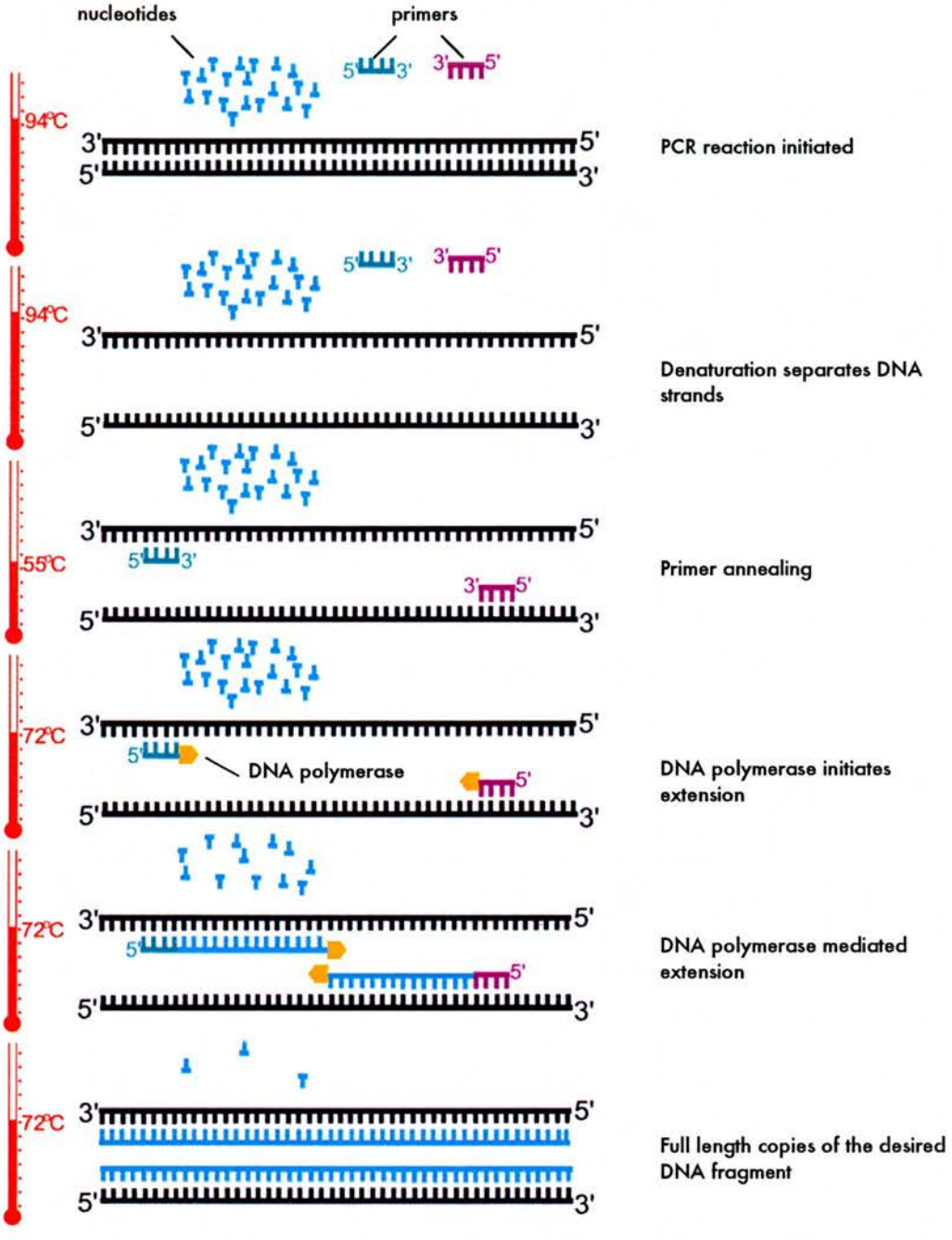

Figure 2.9: Polymerase chain reaction (PCR). Diagram illustrating the steps of the PCR. Denaturation of the DNA occurs at 94°C, followed by primer annealing at between 50-60°C. At 72°C, DNA polymerase extends the complimentary sequence from each primer site by adding nucleotides resulting in a full length copy of the desired DNA fragment.

When the PCR programme was complete, samples were either stored at -20 °C or used directly in non-denaturing agarose gel electrophoresis (Section 2.9).

2.8: Rapid amplification of cDNA ends (RACE)

Rapid amplification of cDNA ends (RACE; *Figure 2.10*) is a specialised type of RT-PCR where the known fragment can be extended towards the 5′ and 3′ ends. Using the sequence of the known fragments, primers were designed to extend the sequence on both sides of the original fragment, and these were used with the ligator adaptor AP1 and AP2 primers (from Clontech's Marathon™ cDNA amplification kit; Appendix 3) with Marathon™ cDNA as the template. Two RACE primers are designed from known sequences at both 5′ and 3′ ends, one nested inside the other. In the first PCR, 0.5 μl of Marathon™ cDNA (diluted 1:50), 1 μl of AP1 primer (4 μM) and 1 μl of the relevant specific 5′or 3′ RACE 1 primer (4 μM) were used with the standard PCR reagents (2 μl 10x PCR Taq DNA polymerase buffer, 0.4 μl dNTPs (10 mM), 15 μl Milli-Q® H_2O and 0.25 μl of the enzyme Taq DNA polymerase (5 U/μl)), and this mixture was then placed in a PCR thermal cycler and subject to conditions outlined previously (Section 2.7). This product amplified by AP1 primer and the specific RACE 1 primer was then used as a template for the second PCR, known as a nested reaction. In the second PCR, 0.5 μl of the product of the first reaction (template) was mixed with 1 μl of the corresponding specific 5′ or 3′ RACE 2 primer (4 μM), 1 μl of AP2 primer (4 μM) and standard PCR reagents (see above), and tubes were then placed in a PCR thermal cycler set as for the first reaction. An aliquot from the first and second reactions were electrophoresed on a 1% agarose non-denaturing gel (Section 2.9). If the correct fragments have been amplified, then the fragment produced by the second RACE reaction, using AP2 and RACE 2 will be smaller in size than the initial fragment amplified by the first RACE reaction using AP1 and RACE 1. The AP2 and RACE 2 sites are within the AP1 and RACE 1 sites so the difference in fragment size will correspond to the difference in lengths of the expected AP1/RACE 1 fragment and AP2/RACE 2 fragment (Cutler *et al.*, 2000).

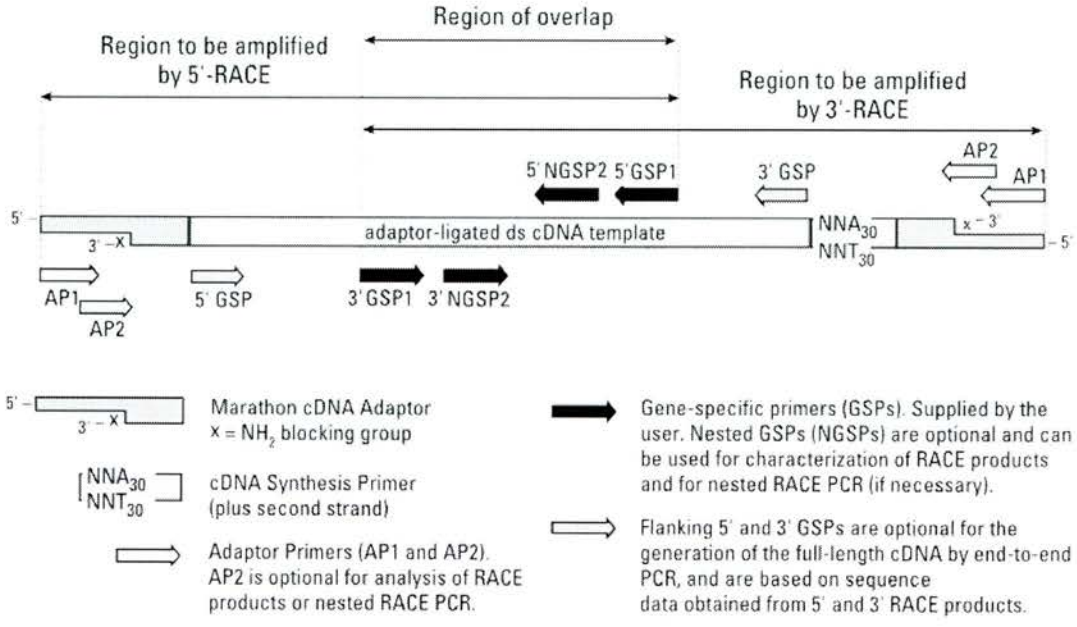

Figure 2.10: RACE PCR. Components needed to carry out Rapid Amplification of cDNA Ends and locations of primer sites. (Marathon cDNA amplification kit user manual, Clontech)

2.9: Non-denaturing agarose gel electrophoresis

As with RNA denaturing gel electrophoresis, this technique is used to size separate DNA rather than RNA (Davis *et al.*, 1986). To prepare a 1% agarose gel, agarose was added to a conical flask with 1 x TAE (40 mM Tris acetate and 10 mM EDTA, pH 8.0 at 1:100 (w/v) and boiled in a microwave oven until completely dissolved. When the mixture had cooled to ~50°C, ethidium bromide (10 mg/ml) was added and mixed by gently swirling to give a final concentration of 0.5 μg/ml. The gel mixture was poured into a gel mould of required size (Scotlab/Scie-Plas) and a comb with the desired number of wells was placed into position before leaving to set for at least 20 minutes. Where required, a 100 base pair (bp) DNA ladder marker (500 μg/ml; NEB) was prepared using 1 μl marker diluted to 20 μl with 1 x TAE. Samples and markers were prepared for non-denaturing agarose gel electrophoresis by adding 0.1 volumes of sample preparation solution (50% glycerol, 0.025% bromophenol blue and 0.025% xylene cyanol; all w/v). The gel was placed into a horizontal electrophoresis tank (Scotlab/Scie-Plas) containing 1 x TAE. Samples were carefully added to the wells and electrophoresis was carried out at 5 V/cm for 20 – 30 min. Following electrophoresis the gel was viewed on an UV transilluminator and an image captured either using a Quickshooter Photosystem (Polaroid) or the Gene Genius Gel Documentation and Analysis package via a charge-coupled device (CCD) camera using Gene Snap software (Syngene). Fragments of the correct size were excised from the gel using a scalpel, purified, cloned and sequenced as described in Sections 2.10, 2.11, 2.12 and 2.14 respectively.

2.10: Purification of DNA fragments

When a fragment of the correct size had been identified, a single reaction seldom provided enough material for successful cloning, therefore duplicate PCR samples were produced. Once sufficient DNA fragments had been amplified and gel fragments collected together, they were purified using the Geneclean Spin kit (Bio 101, Anachem Ltd). The gel slices (up to 300 mg max) were collected together in a 1.5 ml Eppendorf tube, to which 400 μl Glassmilk (suspension of glass beads; Geneclean Spin kit, Bio 101, Anachem Ltd.) was added and the tube heated at 55°C for 5 minutes, inverting the tube each minute to mix and ensure uniform melting of the agarose gel pieces.

The tube was then put directly on ice for 5 minutes in order to optimise DNA binding to the glass beads after which tubes were centrifuged at 14, 000 rpm (20,000 g) for 30 seconds (Eppendorf centrifuge 5417C, Helena Biosciences Europe) and the supernatant discarded. The pellet containing glass beads and recovered DNA fragments was washed twice in 0.5 ml New Wash (Geneclean Spin kit, Anachem Ltd.) at RT, re-suspending the pellet and centrifuging for 30 seconds at 14, 000 rpm each time. The pellet was then re-suspended in 15 µl of Milli-Q®H_2O, which had been preheated to 55°C, and then the tube was heated to 55°C for 2 minutes. During this stage DNA fragments dissociate from the glass beads and are solubilized in the water. The tube was centrifuged at 14, 000 rpm for 1 minute, leaving a pellet of glass beads and supernatant of water and DNA fragments. The supernatant was transferred to a filter tube which was then centrifuged at 14, 000 rpm for 2 minutes. The remaining pellet was again re-suspended in 5 – 10 µl of preheated water, heated at 55°C for 2 minutes, and centrifuged once more, so that the supernatant may be added to the filter tube which was also centrifuged. In order to precipitate the DNA, 2.5 vol of 100% ethanol and 0.1 vol 3 M Na acetate pH 4.2 were added and mixed with the filtered DNA, and the tube placed at –80°C overnight. A Beckman J2-MC centrifuge, 18.1 rotor (Beckman Instruments Inc.) was pre-cooled to 4°C and the tubes centrifuged for 1 hour at 16, 000 rpm (30, 000 g_{ave}). The supernatant was removed and discarded, and the pellets washed with 400 µl 70% ethanol at 4°C. The tube was re-centrifuged at 20,000 g for 20 minutes, after which the supernatant was discarded leaving the pellet to air dry at RT.

2.11: Preparation of agar plates

Bacterial culture plates (10 cm; two per cloned fragment) were prepared by addition of 20 ml of liquid Ezmix™ LB agar (35.6 g/l; Sigma) which had been autoclaved at 110°C for 20 min. The agar contains nutrients providing a substrate conducive to bacterial growth. After cooling the agar to ~55°C, stock antibiotic solution was added to give a final concentration of 50 µg/ml and plates were poured and left to set in a laminar flow cabinet with the lids ajar. Kanamycin antibiotic solution was used to select for transformed cells, since the pCR® 4-TOPO® vector (TOPO® PCR cloning kit; Invitrogen; *Figure 2.11*) contained the kanamycin resistant gene. By adding kanamycin to the

agar used to make the culture plates, those cells that have taken up the vector will be able to grow by virtue of the kanamycin resistance gene found within the vector. The vector offers a second control measure, ensuring only cells containing the vector with a DNA insert are able to grow. Within the pCR® 4-TOPO® vector is a ccdB gene which attaches to the C-terminus of the Lac Z fragment, becoming lethal to the One Shot® TOP10 chemically competent *E.coli* cells if transcribed. If the vector takes up a DNA fragment, the ccdB is not synthesised or synthesis is disrupted, therefore it does not attach to the Lac Zα fragment. Cells transformed with vector without an inserted DNA fragment are therefore unable to grow, since the ccdB gene remains functional, whereas cells transformed with vector that contains a DNA fragment will be able to grow since the ccdB gene has been disrupted and inactivated by the insertion of the DNA fragment. This ensured that only cells transformed with a vector containing the DNA fragment of interest, would grow on the bacterial culture plates.

2.12: Cloning reaction

The DNA fragment purified using the Geneclean® process (Section 2.10), once dried, was re-suspended in 4μl Milli-Q® H_2O. In order for the DNA to be incorporated into the vector, 1 μl Salt Solution (1.2 M NaCl, 0.06 M $MgCl_2$; TOPO® PCR cloning kit, Invitrogen) and 1 μl TOPO® PCR 4 vector (10 ng/μl plasmid DNA; *Figure 2.11*) were added to the re-suspended DNA, mixed and incubated for 30 minutes at RT. After incubation, the tube contents were added to 25μl of One Shot® TOP10 chemically competent *E.coli* bacterial cells (Invitrogen), gently mixed and placed on ice for 30 minutes. Successful cloning is highly dependent on careful treatment of the cells, including the use of cut pipette tips when dispensing competent cells, and gentle mixing. The tube was heated at 42°C for 30 seconds to heat shock the bacterial cells and immediately returned to the ice for 2 minutes. In order for the bacteria to recover from the heat shock, 200 μl of SOC medium (2% tryptone, 0.5% yeast extract, 10 mM NaCl, 2.5 mM KCl, 10 mM $MgCl_2$, 10 mM $MgSO_4$, 20 mM glucose) was added, and the tube place on an orbital mixer (Baird and Tatlock) at 37°C for 1 hour. The contents of the tube were divided between the two culture plates, therefore approximately 100 μl of the cell suspension were spread onto each plate using a sterilised glass spreader. Plates were

placed into a 37°C incubator (MkII Proportional Temperature Controller, Leec Ltd.) overnight allowing bacterial colony growth (*Figure 2.12*).

Individual colonies were selected using sterilised wooden cocktail sticks and transferred to 2 ml tubes containing 1 ml of a mixture containing Terrific Broth (47.6 g/l; Sigma), 0.8% glycerol (v/v) and 50 μg/ml kanamycin antibiotic solution. Approximately twelve colonies were selected for each DNA fragment of interest. Tubes were placed on an orbital mixer and incubated for 6-24 hours. The level of bacterial growth was estimated by visually examining the opacity of the sample. This step aims to further amplify cells containing the DNA fragment of interest by providing the required nutrients for optimal growth (Terrific broth and glycerol), but also selecting for cells containing the vector and therefore kanamycin resistance, by the addition of kanamycin antibiotic. After sufficient growth, the colonies could be used as templates for colony PCR. To prepare colonies for use in colony PCR, a 50 μl sample of the colony was transferred to a fresh tube and centrifuged at 20,000 g (Eppendorf centrifuge 5417C, Helena Biosciences Europe) for 1 minute to obtain a condensed pellet of cells which was then re-suspended with 200-500μl Milli-Q®H_2O.

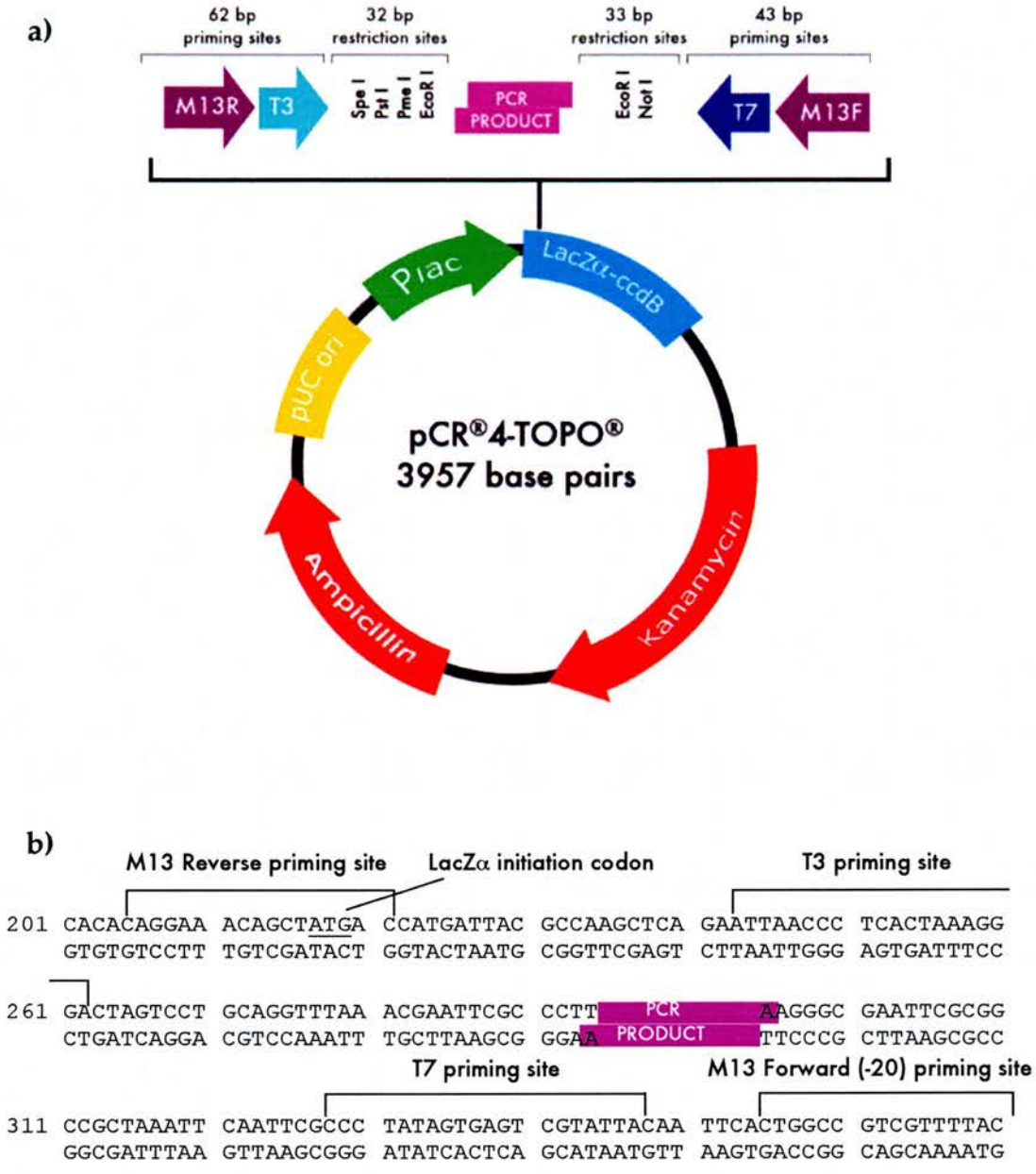

Figure 2.11: Vector map of pCR®4-TOPO® **a)** Simplified map showing main features of pCR®4-TOPO® **b)** Nucleotide sequence of the TOPO® cloning site indicating priming sites. (Figures adapted from the TOPO TA Cloning® Kit for Sequencing Instruction Manual, Version J, 2000-2002, Invitrogen Corporation.)

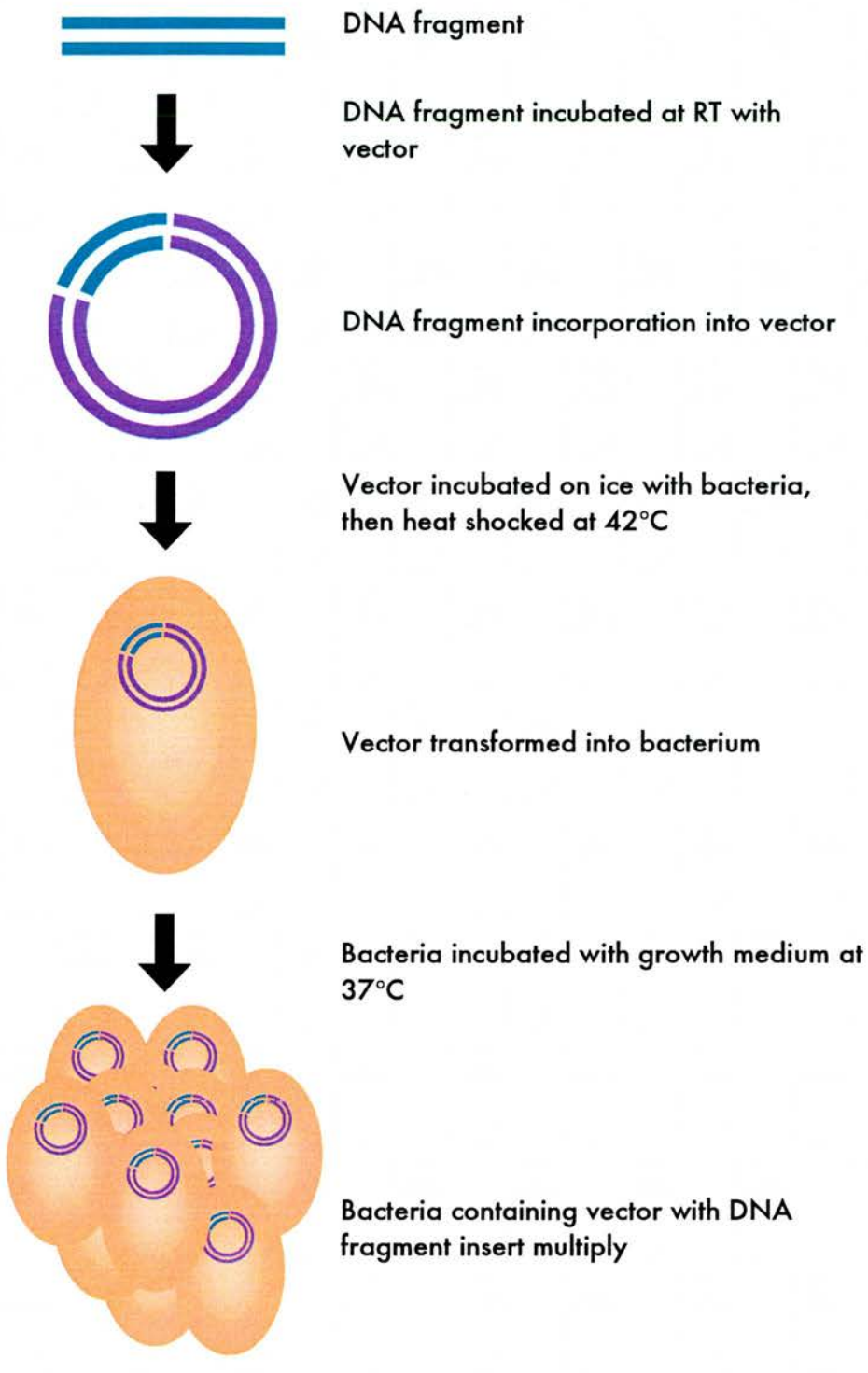

Figure 2.12: Cloning reaction. DNA fragments are incorporated into the vector which is then inserted into bacterial cells. The bacterial cells are then allowed to recover from the transformation process in the absence of antibiotic before spreading onto an agar plate for further multiplication. Colonies grown on the agar will contain the DNA fragment, and can be used to further amplify the DNA fragment by colony PCR.

2.13: Colony PCR – amplification of cloned DNA inserts

In order to further amplify and purify a specific fragment of cloned DNA, an additional PCR was carried out subsequent to cloning. Using the colony as the template, 1µl M13 forward primer (4 µM) and 1 µl M13 reverse primer (4 µM; Appendix 3) were used to amplify the fragment since the M13 forward and reverse sites are located within the pCR® 4-TOPO® vector immediately upstream and downstream of the cloning site. The standard PCR reagents were added to the template and primers (Section 2.7), mixed and then placed on the thermal cycler, (Techne Progene, Techne Ltd), programmed as follows, with the extension time corresponding to the expected size of the fragment (as detailed in Section 2.7):

Program	Cycles	Temperature (°C)	Time
1	1	92	2 minutes
2	40	94	5 seconds
		58	20 seconds
		72	0.5-2 minutes
3	1	72	15 minutes

To detect positive colonies, all samples were electrophoresed on a non-denaturing agarose gel (Section 2.9). Colonies displaying a fragment of the expected size were selected and colony PCR repeated to provide enough DNA for purification prior to sequencing or use as a probe. Products of the repeated PCR were purified using the Quickstep™ 2 PCR purification kit (Edge Biosystems). This kit uses a solid phase oligo/protein elimination (SOPE™) resin which as the name suggests binds non incorporated nucleotides, oligonucleotides, and single stranded DNA, and also any proteins, including the Taq polymerase, but does not bind to the double stranded DNA fragments produced in by PCR. Spin columns to separate the PCR product from other nucleotides and reagents attached to the SOPE™ resin were prepared by adding a 200 µl of a slurry of Sephacryl S-400 to a spin module (Qbiogene Inc.). Sephacryl S-400 beads were swollen overnight in water and stored at 4°C in 0.1% NaN_3 as a preservative. The swollen bead volume was approximately 80% of the slurry volume. The Sephacryl spin columns were centrifuged at 800 g for 3 minutes (Eppendorf centrifuge

5417C) to remove the liquid from the suspension leaving only the Sephacryl beads within the spin column. Each 20 µl of colony PCR product was mixed gently with 4 µl of SOPE™ resin, and then added to the top of the Sephacryl column which was then again centrifuged at 800 g for 3 minutes. The resulting filtrate is a highly purified solution containing the DNA fragment of interest.

2.14: Quantification of DNA fragment

DNA fragments were quantified before using in downstream applications. For quantification, 2µl of the purified DNA sample was diluted in 18 µl 1 X TAE and 3 µl of sample preparation solution (50% glycerol, 0.025% bromophenol blue and 0.025% xylene cyanol; all w/v) added, and then loaded onto a 1% non denaturing agarose gel. A 100 bp DNA ladder (NEB; 1 µl diluted in 19 µl 1 x TAE) was also used for assessment of fragment size and amount. Using the NEB standard, the 1000 bp fragment of this marker contained 94 ng DNA per µl, and the 500 bp fragment contained 97 ng/µl. These two DNA fragments were used to compare the signal strength of the unknown DNA fragment and estimate the concentration. For accurate quantification, it is important to stop the power supply to the electrophoresis tank before the sample runs out of the area of the gel containing ethidium bromide. Gels were then viewed on a UV transilluminator (Gene Genius Gel Documentation and Analysis, Syngene) and using the analytical software packages, Gene Tools and Gene Snap (Syngene) the relative intensity of the bands was recorded. The integrated peak area value obtained from the absorption of each fragment equates to the amount of DNA in the sample. Since standard markers were included, the average signal intensity per ng DNA can be calculated and the DNA concentration (ng/µl) of the unknowns were determined.

2.15: DNA sequencing

Vector inserts were sequenced using an ABI Prism Big Dye™ Terminator Cycle Sequencing Ready Reaction kit (Applied Biosystems). Vector DNA is combined with Taq polymerase, dNTPs, dideoxyribonucleotides (ddNTPs), and specific vector primers. The ddNTPs are present at a limiting concentration, and are each labelled with a fluorescent tag (A: dichloro

[R6G], C: dichloro [TAMRA], G: dichloro [R110], and T: dichloro [ROX]; ABI Prism Big Dye™ Terminator Cycle Sequencing Ready Reaction kit, Applied Biosystems). The DNA is denatured by heating, then cooled to allow primer annealing. The Taq polymerase then extends the primer sequence by adding dNTPs and ddNTPs that are complementary to the template. If a ddNTP is incorporated into the sequence being extended, this terminates extension since ddNTPs lack a 3′ OH group for the next nucleotide in the sequence to attach, preventing the addition of further nucleotides and extension of the oligonucleotides chain. This reaction is also described as the chain termination method (Sanger *et al.*, 1977). Some strands will extend to several hundred bases because the concentration of ddNTPs is less than the concentration of dNTPs. The resulting sequence reaction contains fragments of different length, each ended by one of the four fluorescent-tagged nucleotides. The fragments are size-separated on a polyacrylamide gel with such resolution that fragments varying in length by only one nucleotide can be distinguished from each other. The gel is then processed by a fluorescence analyser and because the four nucleotides each display different emission spectra, each fragment can be detected and represented as a coloured chromatographic peak corresponding to the wavelength of fluorescence from the fragment, which in turn corresponds to one of the four nucleotide bases. The fluorescent analyser produces an electrophoretogram which indicates the wavelength of the fluorescence at each nucleotide position, and from this electrophoretogram, the DNA sequence can be inferred (*Figure 2.13*).

The cycle sequencing reaction was carried out in house, whereas the electrophoresis and subsequent electrophoretogram generation was carried out by the Protein and Nucleic Acid Chemistry Laboratory (PNACL, University of Leicester). The sequencing reaction required 30-100 ng of DNA depending on the size of the fragment to be sequenced. The required amount of DNA was added to a tube and made up to 7 µl with Milli-Q® H_2O. To this tube was added 1 µl of 4 µM specific vector primer (T7, T3, or specific sequencing primer; Appendix 3), and 2 µl of the Big Dye™ terminator ready reaction mix (Version 3.1). This solution contains all the reagents necessary for the sequencing reaction: AmpliTaq DNA polymerase, $MgCl_2$ and Tris-

HCl buffer pH 9.0, deoxyribonucleotide triphosphates, and fluorescent dye coupled nucleotides (A: dichloro [R6G], C: dichloro [TAMRA], G: dichloro [R110], and T: dichloro [ROX]) (ABI Prism, PE Biosystems). The tube was then placed in a preheated thermal cycler and programmed as follows (N.B. The rate of change of temperature was set to 1°C/s):

Program	Cycles	Temperature (°C)	Time
1	25	96	10 seconds
		50 - 58	5 seconds
		60	4 minutes
2	1	4	15 minutes – 24 hours

DNA produced in the sequencing reaction was precipitated by addition of 0.625 µl 0.5 M EDTA (pH 8.0) and 26 µl 100% ethanol. The precipitated DNA solution was mixed and transferred to a larger 0.5 ml Eppendorf tube to facilitate washing. The tube was incubated at RT for 20 minutes for the DNA to precipitate. Precipitates were centrifuged 20,000g for 20 minutes (Eppendorf centrifuge 5417C), and the supernatant carefully removed and discarded. The remaining (invisible) pellet was washed once with 400 µl 70% ethanol, centrifuging as before and discarding the supernatant. After washing, the pellet was left to air dry at RT and was then sent to the Protein and Nucleic Acid Chemistry Laboratory (PNACL, University of Leicester). At PNACL, the pellet was re-suspended and electrophoresed on a polyacrylamide gel and the resultant bands recorded by a fluorescence analyser and associated software. An ABI prism electrophoretogram was created for each DNA fragment being sequenced, and sent back to the University of St Andrews where it could be read using ABI Prism software (EditView 1.0, Applied Biosystems), and analysed using GeneJockey II software (Biosoft). Using this software, nucleotide and derived amino acid sequences could be aligned and compared. Unknown sequences were entered into the Genbank® NCBI nucleotide sequence database to find closest matches and identify the sequence.

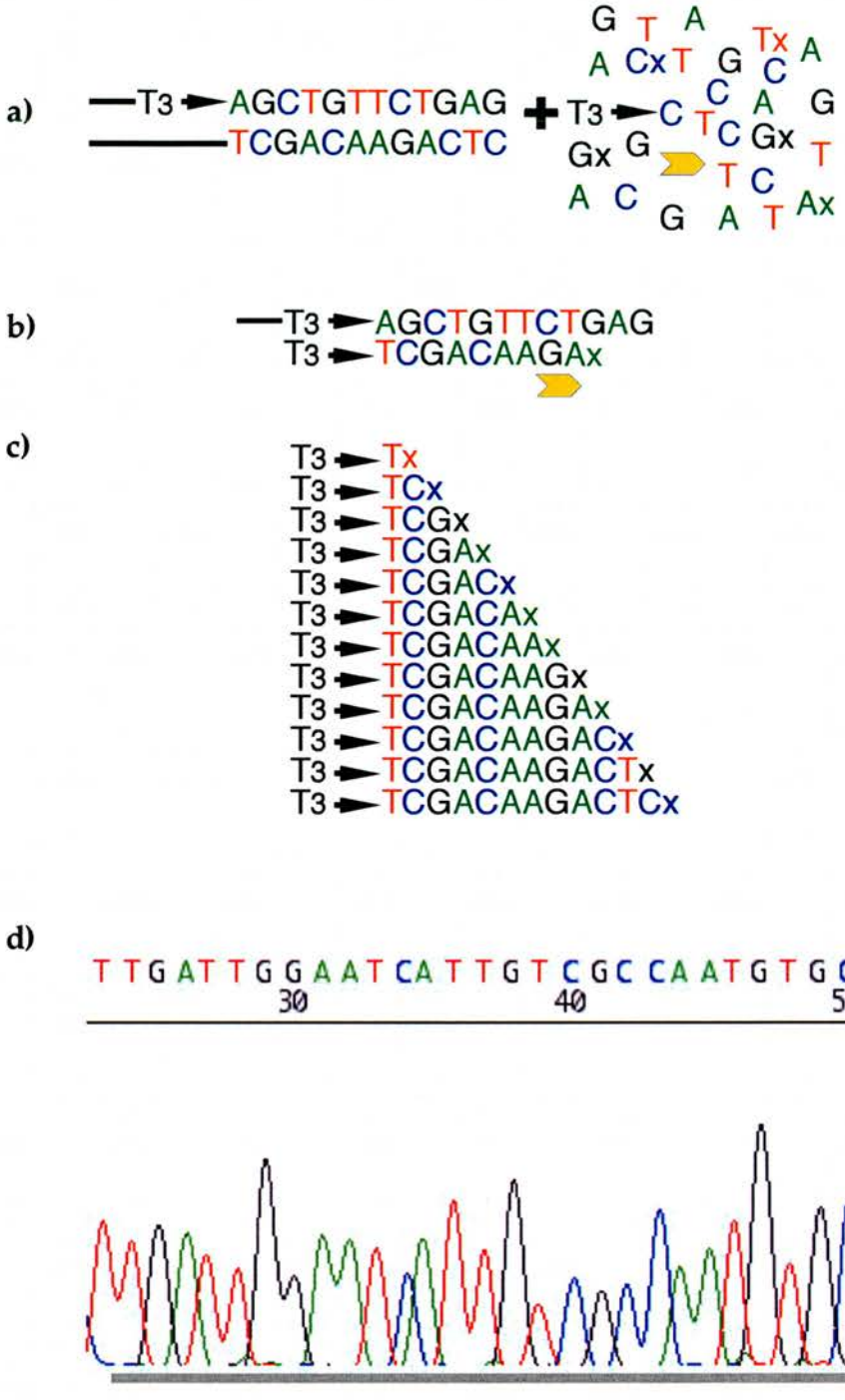

Figure 2.13: DNA sequencing. **a)** Purified DNA is combined with a sequencing primer (T3), deoxynucleotides (A, G, C, T) and dideoxynucleotides (Ax, Gx, Cx, Tx) and a Taq polymerase (yellow chevron). **b)** Primer annealing and extension; extension halted when dideoxynucleotide attaches. **c)** Series of possible dideoxynucleotide positions. All of these products will be made in the sequencing reaction. **d)** Example electrophoretogram representing a typical DNA sequence.

2.16: Northern blotting

Quantitative expression of genes at the mRNA level were assessed by Northern blotting. Total RNA was size separated using denaturing agarose gel electrophoresis (Section 2.4) and transferred by electroblotting onto a nylon membrane. The cloned DNA fragment of interest was radiolabelled and used as a probe to hybridise gene-specific mRNA transcripts bound to the membrane (Davis *et al.*, 1986). The amount and distribution of the radioactive probe bound to the membrane could then be used to show the distribution of mRNA expression in specific tissues and to quantify this expression. In this way, Na^+, K^+-ATPase subunit mRNA expression was identified in bull shark tissues, and mRNA expression in tissues from sharks acclimated to SW could be compared with tissues from sharks held in FW.

When comparing the levels of expression between any conditions, it was essential that RNA samples are calibrated against each other so that an equal amount of total RNA is loaded for each sample. As explained in Section 2.4, total RNA samples were initially quantified using a spectrophotometer and the quality assessed by denaturing gel electrophoresis. RNA samples which did not display discrete 28S and 18S bands had been degraded and were not used for Northern blotting. Similarly, RNA samples that contained a large amount of contaminating DNA and/or protein as indicated by a portion of the sample remaining in the sample well were not used for Northern blotting since the concentration of RNA loaded onto the gel was not consistent. Samples displaying a 28S:18S ratio closest to 2:1 were chosen for Northern blotting. For each group of samples a denaturing agarose gel was run using 5 - 10 μg total RNA loaded for each sample, using the concentrations estimated from spectrophotometer readings. This gel was subsequently stained with ethidium bromide as described in Section 2.4 and then analysed using Gene Snap and Gene Tools (Syngene) software packages (Section 2.4). The raw values representing the intensity of the 28S and 18S bands were recorded for each RNA sample. These values were added together and compared to the other samples in order to assess the total RNA loading for all of the samples. The RNA concentrations were normalised to the 28S:18S absorption and volumes adjusted accordingly so that when a second gel is loaded, all samples contained approximately the same amount of RNA.

Selected total RNA samples (5 - 10 μg, calibrated as described above) were denatured, and a denaturing agarose gel prepared as described in Section 2.4. Electrophoresis was carried out, and RNA stained with ethidium bromide also as described in Section 2.4. Although the samples have previously been calibrated, 28S and 18S bands were again viewed using a UV transilluminator, and the raw values given for intensity according to the Gene Tools program (Syngene) were recorded. This reading was used as a final measure of the RNA concentration loaded onto each well, and subsequently used to adjust the specific activity of hybridised probe to counts per minute per μg RNA.

After RNA transcripts had been size-separated by denaturing agarose gel electrophoresis, they were subsequently electroblotted onto a nylon membrane. A transfer cassette was prepared and assembled in ice cold 1 X TAE (*Figure 2.14*). The cassette was loaded onto the 'white' side (anode), adding a pre-soaked Scotbrite™ pad, Whatman® 3MM filter paper, and Zetaprobe™ membrane (Bio-Rad Laboratories), taking care to press down each layer firmly to remove any air bubbles. The de-stained RNA gel was placed, well side up, onto the membrane, and covered with a second piece of Whatman® 3MM filter paper, and a pre-soaked Scotbrite™ pad. The cassette was then locked shut and loaded into a plate electrode transfer tank containing ice cold 1x TAE ensuring the cassette was loaded such that the current direction allows migration of RNA from the gel onto the membrane (black side of the cassette facing the cathode). The transfer current was set at 0.25 amps, and left to transfer overnight and cooled by a re-circulating water system cooler. When transfer was complete, the cassette was removed from the tank and opened so that the gel is above the membrane. Using a pencil, the position of the corners and wells of the gel were marked on the membrane, before placing between two sheets of Whatman® 3MM filter paper and vacuum dried for 10 minutes at room temperature. The membrane was then transferred to a UV-crosslinker (L 1500 UV Crosslinker, Spectronics Corporation) in order to covalently link the RNA strands to the Zetaprobe™ membrane by irradiating with ultra violet light. Membranes were then either immediately used for Northern blotting, or stored at –20°C until required.

Figure 2.14: Northern blotting transfer cassette assembly. Cassette assembled as shown and placed into transfer tank.

To prepare the radioactive DNA probe, 30 ng of purified, cloned DNA fragment (prepared as detailed in Section 2.13) was made up to a volume of 24.5 µl with Milli-Q® H_2O before addition of 10 µl 5x labelling buffer (250 mM Tris-HCl, pH 8.0, 25 mM $MgCl_2$, 10 mM DTT, and 26 A_{260}u/ml random nonamer nucleotides; Megaprime DNA labelling system, Amersham Biosciences). After mixing, tubes were boiled for 5 minutes to denature the DNA strands and then snap-cooled on ice. When the sample had cooled, the following reagents from the DNA labelling kit were added: 5 µl 200 µM dNTPs minus dCTP (mixture of dATP, dGTP and dTTP), 5 µl 0.4 mg/ml BSA, 0.5 µl Klenow enzyme (5000 U/ml). The tube was mixed gently and placed behind a Perspex screen before addition of 5 µl $\gamma[^{32}P]$ dCTP (6000 Ci/µmol; Amersham Pharmacia Biotech). The solution was mixed and incubated at 37°C for 30 minutes. The incubation period allowed the nonamer primers to bind to the single stranded DNA and extend the sequence in the presence of the Klenow enzyme, incorporating the $\gamma[^{32}P]$ dCTP molecules into specific complementary probes of varying lengths.

Size exclusion column chromatography was used to separate the synthesised radiolabelled DNA probe from smaller non-radiolabelled primers and free nucleotides. A 2 ml siliconised glass column was prepared by adding glass wool and glass beads to the bottom of the column to form a plug and fixing this column upright using a clamp and stand. A bottle of pre-swollen Sephadex G-50 suspension in Milli-Q® H_2O was placed in a vacuum oven (Weiss-Gallenkamp) for 15 minutes to de-gas. Using a long tube affixed to a syringe, the Sephadex G-50 slurry was added to the column and the beads left to settle leaving ~5 cm at the top of the column. Milli-Q® H_2O was continually added to the top of the column using a glass pipette to prevent the Sephadex G-50 from drying out. The column was placed behind Perspex and covered with Nescofilm until required. The reaction mixture from the Megaprime DNA labelling system (Amersham Biosciences) was added to the column using a glass syringe and the column eluted with water. A Geiger counter was positioned at the bottom of the column, and 16 x 1.5 ml Eppendorf tubes were labelled and placed in a Perspex rack. When the Geiger counter detected counts of radioactivity above 10 cpm, serial fractions of 4 drops per tube were collected in the prepared tubes. Milli-Q® H_2O was

added throughout the collection to ensure a steady flow of material through the column.

The radioactivity contained in each sample was measured by transferring a 1 µl sample from each fraction into a 6 ml polyethylene pony scintillation vial (Packard Instruments) and diluting this with 4.5 ml Milli-Q®H_2O. The pony vials were loaded into a scintillation counter (Packard TRI-CARB 1600TR counter, Packard Instruments) which was programmed to detect $\gamma[^{32}P]$ by Cerenkov counting, enabling the radioactivity in each sample could be determined. The 16 fractions usually contain 2 independent peaks in radioactivity. The fractionation through the column separates out DNA fragments by size with the first radioactive peak being excluded from the beads and eluted in the column void volume (the DNA probe). The second radioactive peak is caused by the non-incorporated $\gamma[^{32}P]$ dCTP which is retained for longer elution times due to equilibration within the water spaces of the beads. The fractions containing the radiolabelled probe were required, so the 5 fractions containing the highest radioactive concentration from the leading peak were retained, and the others were disposed of. To estimate the amount of radioactivity incorporated into the DNA probe, the total counts per minutes from the 4-5 tubes selected were divided by the total counts per minutes summed for all 16 fractions, and then multiplied by 100 to obtain the percentage incorporation. Probes with less than 20% incorporation of $\gamma[^{32}P]$ dCTP were usually discarded and a new cDNA probe prepared.

To prepare the membrane for Northern blotting, a glass hybridisation bottle containing 5 – 10 ml Milli-Q®H_2O was pre-warmed to 47°C in a hybridisation oven (Techne Hybridiser HB-1D, Techne Ltd.) and constantly rotated. Previously frozen membranes were allowed to thaw at RT before use. The membrane was carefully inserted into the glass cylinder so that any pencil marks made on the membrane faced away from the glass surface. The bottle was placed in the hybridisation oven briefly to wet the membrane and equilibrate it to the hybridisation temperature (47°C). The water was poured off the membrane, and 15 ml preheated Ultrahyb™ buffer (hybridisation solution; Ambion Inc.) was added to the cylinder. The cylinder was then

replaced into the hybridisation oven and prehybridisation continued for at least 4 hours at 47°C in order to block non-specific binding sites.

The fractions collected for use as the DNA probe were boiled for 5 minutes, and snap cooled on ice for 2 minutes to ensure the radiolabelled DNA probe was single-stranded therefore optimising the subsequent hybridisation to the homologous mRNA crosslinked to the membrane. The radiolabelled fractions were combined and added to the solution in the hybridisation bottle. The bottle was replaced into the hybridisation oven and the membrane incubated with the radiolabelled DNA probe at 47°C overnight. Following incubation, the Ultrahyb™ buffer containing the non-hybridised radiolabelled DNA probe was disposed of into a designated waste sink. The membrane was then washed with a series of 30 ml washes. Wash 1 consisted of 1% sodium dodecyl sulphate (SDS) and 1 x standard saline citrate solution (SSC; 0.15 M NaCl and 15 mM sodium citrate, pH 7.0), which was added to the bottle and incubated at 47°C for 20 minutes. This was then poured off and preheated Wash 2 (0.1% SDS, 0.2 x SSC) added and membrane was incubated further at 47°C for 20 minutes. Wash 2 was discarded and Wash 3 (0.1% SDS, 0.1x SSC) added to the hybridisation bottle and the membrane washed for an additional 30 minutes. Each wash was disposed of into a designated radioactive sink.

After washing, membranes were carefully removed from the cylinder, sealed in polythene using a bag sealer (Calor), and positioned in an Instant Imager (Canberra Packard). The Instant Imager builds up an image over time by quantifying the radioactivity associated with the hybridised DNA probe on the membrane resulting in an image of high signal intensity bands representing the abundance of mRNA expression within the RNA samples. The radioactive counts for each RNA sample were recorded and adjusted according to the amount of total RNA loaded onto the gel estimated by band intensity as indicated by the ethidium bromide-stained 28S and 18S RNA bands. This allows for calculation of the radioactive counts per μg RNA. Blots were also captured using autoradiographic film. The blot was secured in an X-ray cassette (Kodak Biomax™, Eastman Kodak Co.), and a sheet of autoradiographic film (Kodak Biomax™ film, Eastman Kodak Co.) placed

within intensifying screens under a red safe light. The cassette was locked and placed in a –80°C freezer for a period of time depending on the radioactive intensity on the blot as indicated by the Instant Imager. The cassette was then removed from the freezer and left to equilibrate to RT, and the autoradiographic film developed by placing into Kodak GBX Developer solution (Eastman Kodak Co.) until the image appeared (30-60 seconds), then rinsed in water and placed into Kodak GBX Fixer solution (Eastman Kodak Co.) for approximately twice the developing time. The film was then rinsed in water, and suspended in a drying cabinet.

If the blot was required for additional radioactive probing, the radioactive DNA was removed by repeated boiling of the membrane for 10 minutes in 0.1% SDS. After each boiling a Geiger counter was used to initially assess whether the radioactive probe had been successfully removed, after which the blot was placed in the Instant Imager to ensure that the blot was free of any radioactive probe. Further boiling was carried out if radioactive signals were still detected from the blot.

2.17: Membrane protein preparation

Tissues were collected as detailed in Section 2.2, and immediately frozen in liquid nitrogen, and stored at -80°C. Intestine, kidney and rectal gland samples were thawed on ice and then cut into small pieces, before homogenisation. Whole gills were taken from the shark, and gill filaments were cut from the gill arch and then transferred to a tube on ice. Homogenisation buffer (25 mM Tris, 0.25 M sucrose, 0.5 mM DTT, and 0.18 mg/ml phenyl methyl sulfonyl fluoride (PMSF) was prepared and placed on ice. Each sample of 0.1 – 1 g in weight was homogenised in 10 ml of ice cold homogenisation buffer using a Polytron PT 3100 homogeniser (Kinematica Ltd.) at approximately 10,000 rpm for 10 seconds, then 20,000 rpm for 5 seconds or more until a homogenous sample was obtained. The homogenate was poured into a centrifuge tube through four layers of muslin gauze. The homogenisation tube was then rinsed using 20 ml of ice cold homogenisation buffer, and this was then poured through the gauze, and repeated. The tubes were then balanced and centrifuged (Beckman J2-MC centrifuge, JA-20 rotor, Beckman Instruments Inc.) at 20,000 rpm (48,400 g_{max}) for 1 hour at 4°C. The supernatant was carefully discarded so as not to dislodge the loose pellet.

Re-suspension buffer (25 mM Tris, 0.25 M sucrose, and 0.5 mM DDT, at 4°C) was used to re-suspend the pellets (0.5 – 1.5 ml per sample), using a syringe and needle where necessary. The protein concentration of re-suspended samples was determined using the Bradford protein assay, after which samples were divided into aliquots and stored at –20°C.

The Bradford protein assay was used in conjunction with an ELISA plate reader to determine protein concentration. This required a set of bovine serum albumin (BSA) standards which were prepared from a 2 mg/ml BSA stock (20, 34, 56, 93, 155, 259, 432, 720, 1200 and 2000 μg/ml). Unknown protein samples were prepared over a range of dilutions from 1:4 to 1:100. Using a 96 well micro titre flat bottomed plate, BSA standards were loaded in duplicate, and protein samples in triplicate (20 μl/well). Bradford's reagent (100 mg/l Coomassie Brilliant Blue G, 110 ml/l orthophosphoric acid and 55 ml/l 96% ethanol) was added to the plate (200 μl/well). The plate was then placed into an ELISA plate reader and absorbance read at 650 nm and then optical density values were compared to the standard concentrations to calculate the protein concentration of each sample.

2.18: Sodium dodecyl sulphate polyacrylamide gel electrophoresis (SDS-PAGE)

SDS PAGE was used to size separate proteins according to their molecular weights. An SDS PAGE gel mould was prepared by cleaning two glass plates with 100% ethanol, before laying two grease-covered spacers along the sides of the first glass plate, then placing the second glass plate carefully on top. This glass gel mould was then clamped together, and placed upright in a mount, after greasing the contact points (*Figure 2.15*). The mould was locked into place, and MilliQ®H_2O was added to check that the mould did not leak. A 10% polyacrylamide separating gel (total volume 30 ml) was prepared by combining 10 ml 37.5:1 acrylamide/bisacrylamide solution (v/v; Sigma Aldrich Ltd.), 11.9 ml MilliQ®H_2O, 7.5 ml 1.5 M Tris pH 8.8, 0.3 ml 10% SDS (v/v), 0.3 ml 10% $NH_4S_20_4$ (w/v) and 24 μl TEMED (N,N,N,N tetramethylethylenediamine; Sigma Aldrich Ltd.) in a flask, adding the TEMED immediately prior to pouring the gel. TEMED initialises the polymerisation reaction which is required for the setting of the gel. The

MilliQ®H_2O was discarded from the mould, and the 10% polyacrylamide gel mixture was added to the mould using a syringe and needle, taking care not to introduce air bubbles into the mixture. The mould was filled to approximately 1 cm below the bottom of the comb which will be inserted. In order to level the gel and remove any bubbles that may have formed, the gel mixture was overlaid with a 1 cm layer of water-saturated butanol, before leaving to set for 10 minutes. A 4% polyacrylamide stacking gel was prepared by combining 1.34 ml 37.5:1 acrylamide/ bisacrylamide solution (v/v), 7.21 ml MilliQ®H_2O, 0.83 ml 1.5 M Tris pH 6.8, 0.1 ml 10% SDS (v/v), 0.1 ml 10% $NH_4S_20_4$ (w/v) and 10 µl TEMED, again adding the TEMED immediately prior to pouring the gel. When the separating gel had set, the butanol was carefully poured off, and the gel surface was rinsed with MilliQ®H_2O before adding the stacking gel using a syringe and needle. A suitable comb was inserted and the stacking gel added up the level of the top of the glass. The stacking gel was left to polymerise for 15 – 20 minutes.

To prepare protein samples for electrophoresis, protein aliquots of 5 – 100 µg were diluted in an equal volume of 2 x gel loading buffer (62.5 mM Tris HCl pH 6.8, 2 % (w/v) SDS, 10 % (v/v) glycerol, 0.005 % (w/v) bromophenol blue and 5 % (v/v) β mercaptoethanol) and were either left at RT or heated to 85 or 100°C for 10 minutes. The gel loading buffer contains both SDS which masks any charges of the proteins and disrupts hydrophobic bonds, and β mercaptoethanol which reduces any intra or inter molecular disulphide bonds leading to the unfolding of the proteins. These denaturing properties ensure that the proteins separate according to their molecular weight. Samples were then cooled to RT and centrifuged at 20,000 g for 2 minutes (Eppendorf centrifuge 5417C). Samples were prepared in excess to the volume required, so that when centrifuged, any particulate material will settle into a pellet, and only the volume of supernatant required to achieve the amount to be loaded onto the gel was taken. The comb was removed from the fully set stacking gel, and wells filled with 1 x running buffer (25 mM Tris, 200 mM glycine and 0.1% (w/v) SDS, pH 8.3). Centrifuged samples (5 – 50 µl) and 18 µl of SeeBlue® Plus2 pre-stained molecular weight standards (Invitrogen) were carefully loaded into the wells.

The gel was positioned into a vertical gel electrophoresis tank, the upper and lower chambers of which were filled with 1 x running buffer, circulated with a magnetic stirrer and cooled by continuously flowing tap water (*Figure 2.16*). A constant current of 25 mAmp/gel was set for electrophoresis, for 3 – 5 hours. The proteins initially migrate from the well into the stacking gel where they are 'stacked' together according to their molecular weight at the boundary between the stacking and separating gels. Low molecular weight proteins are at the bottom of the stack and high molecular weight protein at the top of the stack. The stack then migrates into the separating gel where the concentrated stack of protein will be able to unstack and spread along the gel, according to the size of the protein. Normal electrophoresis principles apply whereby low molecular weight proteins are smaller and are therefore more able to migrate more quickly through the gel matrix towards the bottom, leaving the slower migrating, higher molecular weight proteins nearer to the top of the separating gel. The electrophoresed proteins were either stained with Coomassie Blue (Section 2.19) or transferred to a PVDF membrane (Section 2.20) in preparation for Western blotting.

2.19: Coomassie blue staining of SDS-PAGE gels

In order to visualise the protein composition of the samples, the gel was stained with Coomassie Blue. After electrophoresis, the gel was placed in a tray and rinsed with MilliQ®H_2O. A sufficient quantify of Coomassie Blue staining solution (0.1% Coomassie Brilliant Blue R-250, 50% methanol and 10% glacial acetic acid) to cover the gel was poured onto the gel. The tray was then placed on a shaker (Gyro Rocker STR9, Bibby Stuart) for 1 hour. The Coomassie Blue solution was poured off and de-stain I solution (50% methanol and 10% glacial acetic acid) was used to wash the gel under shaking, with four changes over 2 hours. It is important not to keep the gel in de-stain I solution for any longer than this as the high methanol concentration causes shrinkage of the gel. Sufficient de-stain II solution (10% methanol and 10% glacial acetic acid) was added to cover the gel, and left overnight at RT. Protein bands were visualised by placing the gel on a white light box and images captured using Gene Snap software (Syngene).

2.20: Transfer of proteins to PVDF membrane

Proteins were transferred from SDS PAGE gels onto polyvinylidene difluoride membranes (Hybond – P, PVDF membrane, Amersham Pharmacia Biotech; *Figure 2.17*). When proteins were transferred to membranes, proteins of interest could then be identified using specific antibodies raised against the peptide sequences within these proteins. In this way, protein expression could be assessed by Western blotting. A sheet of PVDF membrane corresponding to the size of the gel was added to a tray containing methanol for 5 minutes, after which the methanol was poured off and replaced by MilliQ®H_2O for 5 minutes. The water was poured off and the gel was equilibrated in 1 x transfer buffer (48 mM Tris, 1 M glycine, pH 9.2) for 10 minutes. A transfer cassette with two Scotbrite™ pads and two sheets of Whatman® 3MM paper was prepared as described in Section 2.16, with the assembly of the cassette carried out in 1 x transfer buffer. The PVDF membrane was placed onto the Whatman® 3MM paper with the smooth side facing upwards, and the gel placed on top of the membrane, before completing assembly and locking the cassette. It is important to be precise when placing and positioning the gel onto the membrane since some transfer may occur on contact. The cassette was positioned in a transfer tank containing circulating 1 x transfer buffer and cooled by continuously flowing tap water. The power supply to the tank was set at 30 V and proteins were left to transfer from the gel to the membrane overnight. After transfer, the cassette was opened and the position of the gel corners marked onto the membrane using a pencil. The membrane was then either used immediately in immunostaining techniques, or placed between two sheets of Whatman® 3MM paper, vacuum dried, and stored at –20°C until required.

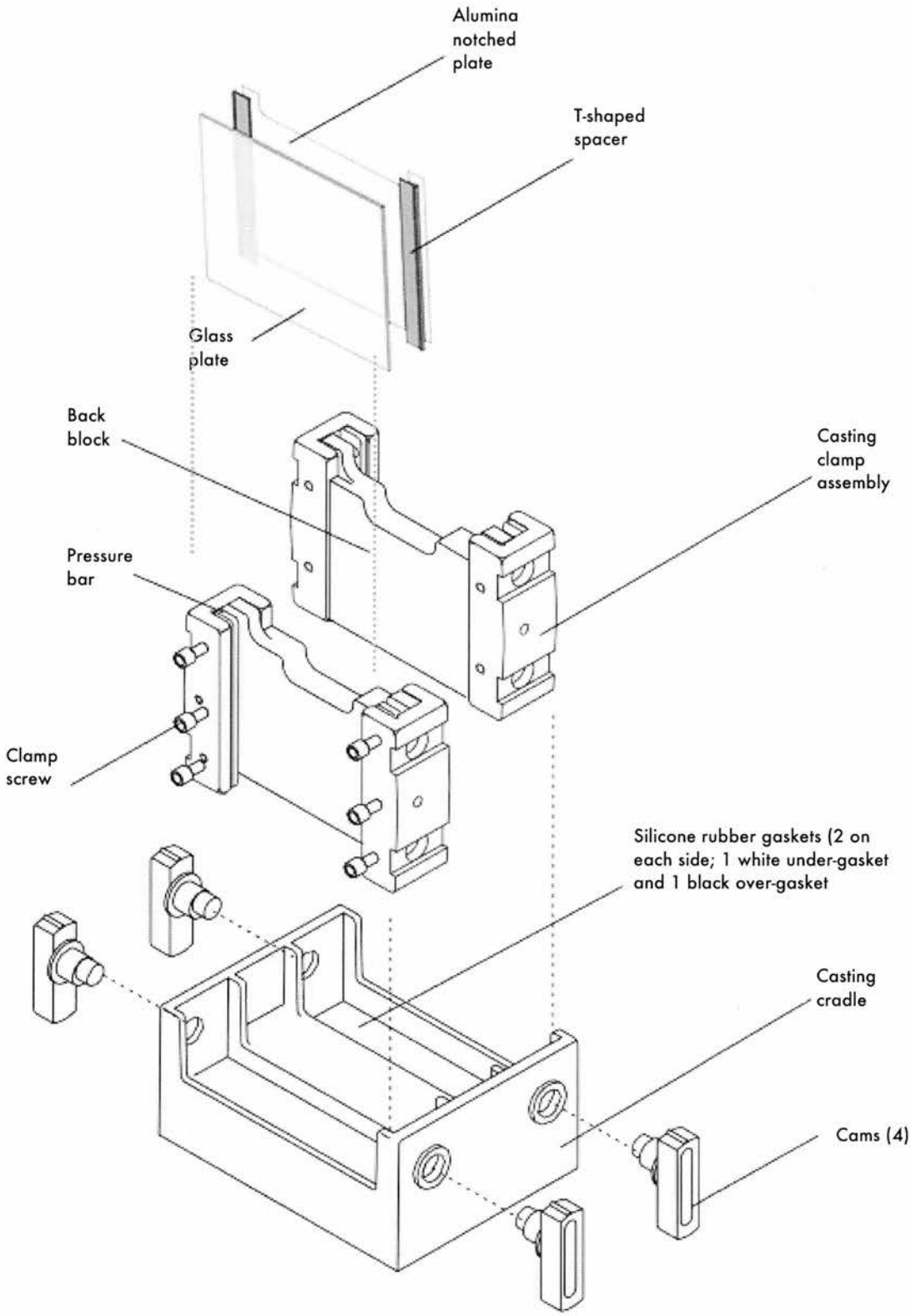

Figure 2.15: Gel casting assembly. The glass/alumina gel sandwich stack is placed into the caster and clamped into place. The caster is then positioned into the casting cradle and locked into place with cams. Gel mixture is then poured into the glass/alumina gel sandwich stack. Figure adapted from Hoefer SE 245 Dual Gel Caster User Manual, Amersham Biosciences, 2002.

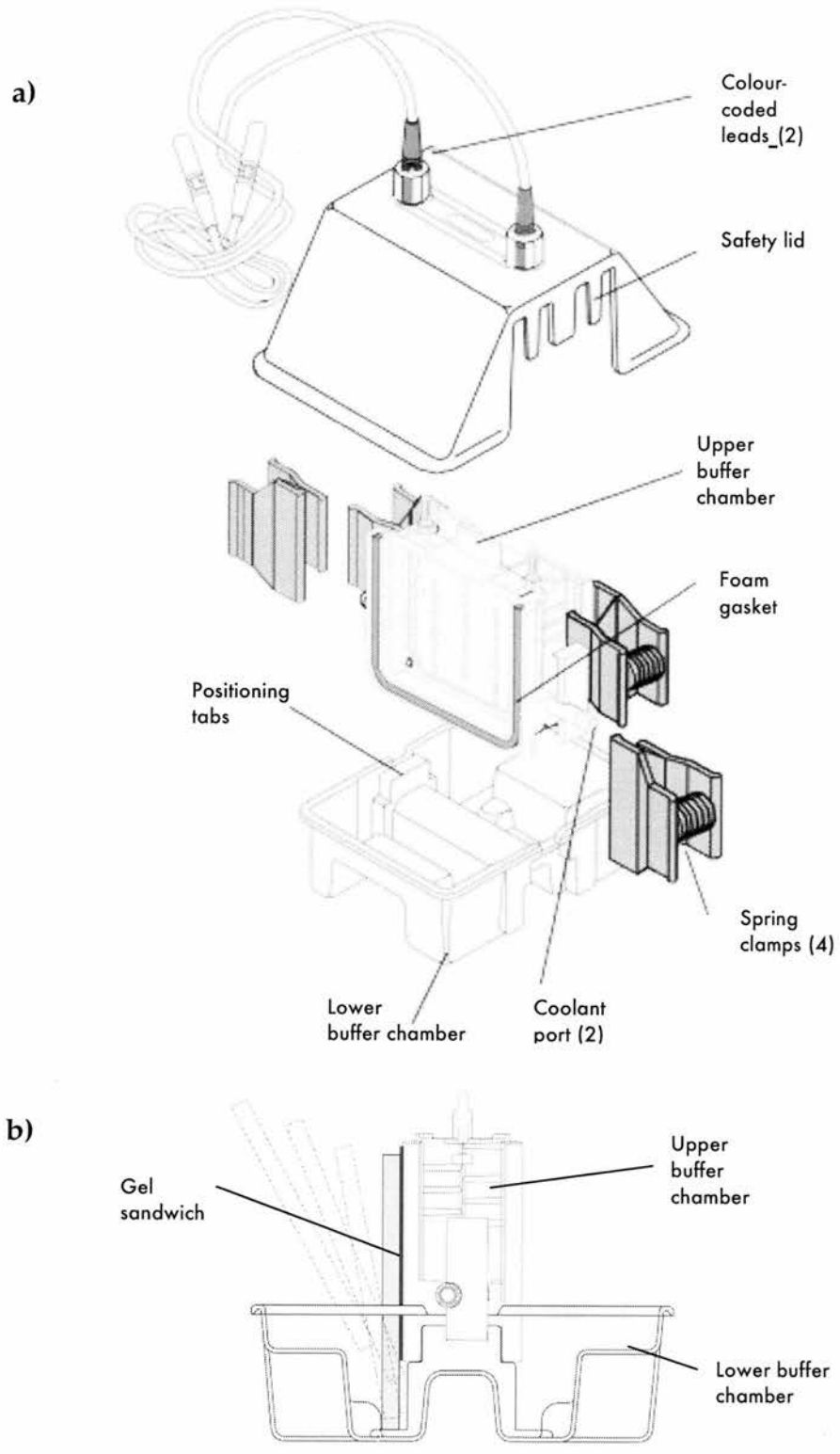

Figure 2.16: SDS PAGE unit assembly. **a)** Electrophoresis unit. **b)** Gel sandwich installation. The polymerized gel is positioned into the electrophoresis unit and loaded before completing assembly and electrophoresis. Figure adapted from Hoefer SE 260 Mini-Vertical Gel Electrophoresis Unit User Manual, Amersham Biosciences, 2002.

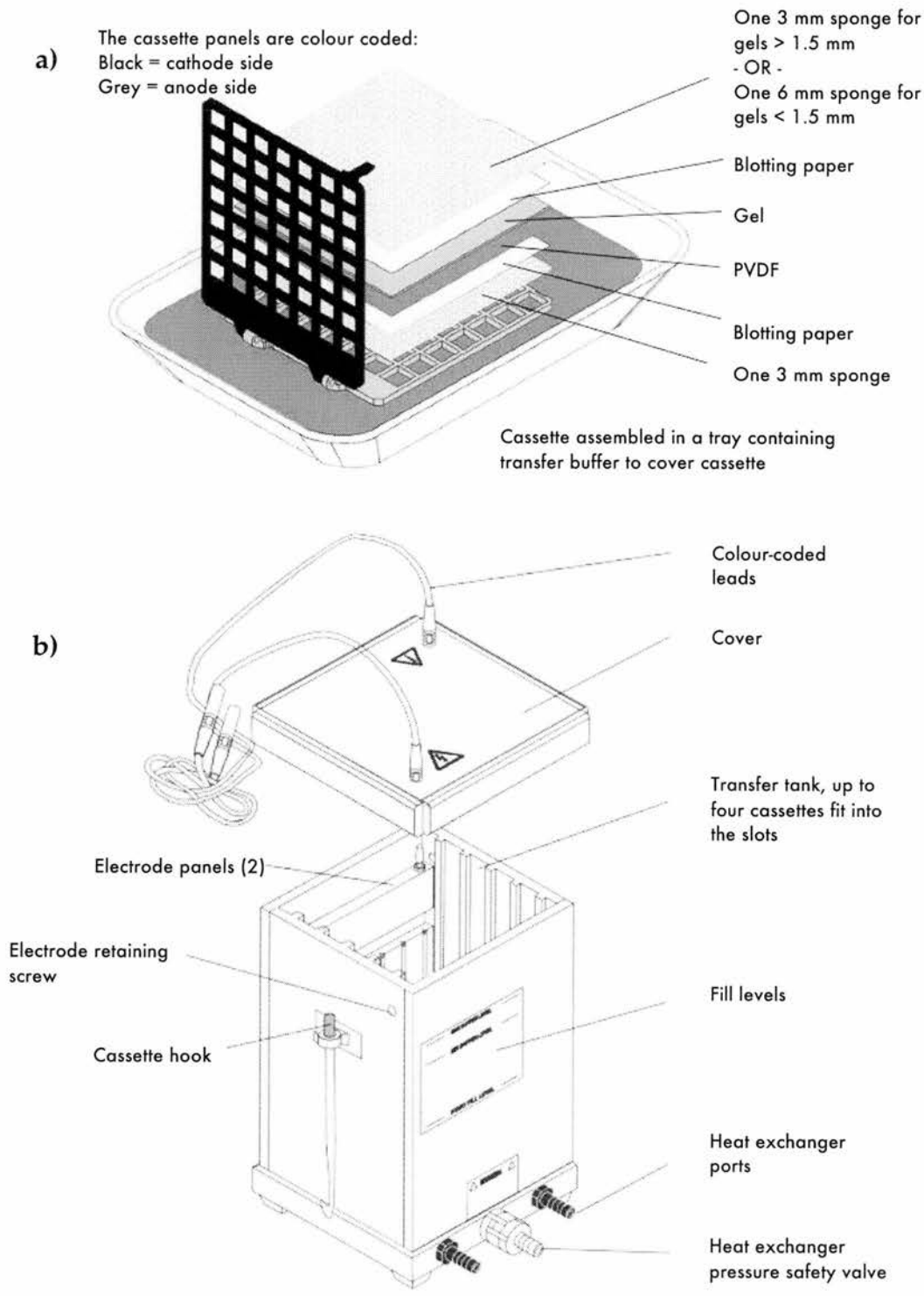

Figure 2.17: Transfer tank assembly. **a)** Transfer stack cassette assembly. After electrophoresis, the gel is placed into a cassette against PVDF membrane in order for the proteins to be transferred into the membrane. **b)** Transfer tank unit. Cassettes are orientated in the tank according to colour coding allowing negatively charged molecules to migrate towards the anode. Figure adapted from Hoefer TE 22 Tank Transfer Unit User Manual, Amersham Biosciences, 2002.

2.21: Synthesis and purification of antibodies

Expression and tissue distribution studies required the use of specific polyclonal antibodies to the proteins of interest. A section near the N-terminal end of the Na^+, K^+-ATPase α subunit and a sequence at the extracellular C-terminal of the Na^+, K^+-ATPase β subunit were chosen for antibody production (*Figure 2.18*), and these sequences were sent to Sigma Genosys, where the synthetic peptides were produced, cross-linked to keyhole limpet haemocyanin (KLH) and used to raise a polyclonal antibodies in rabbits.

The peptides were synthesised and purified by High-Performance Liquid Chromatography (HPLC), and a 2 – 3 mg aliquot of the peptide was conjugated to the carrier protein, keyhole limpet haemocyanin (KLH) using sulphydryl crosslinking with m-maleimidobenzoyl-N-hydroxysuccinimide (MBS), to create a specific antigen. Pre-immune serum (5 ml per each rabbit) was collected prior to immunisation and these sera were used as negative controls for immunohistochemistry (Section 2.24). Antibodies were raised in two rabbits for each peptide with six immunisations and five bleeds taken per animal over a 77-day period. The rabbits were initially immunised with antigen mixed in complete Freunds adjuvant with additional peptide injections prepared in incomplete Freunds adjuvant, at bi-weekly intervals as follows:

Antigen Injection	Bleed
Day 0	-
Day 14	-
Day 28	Day 35
Day 42	Day 49
Day 56	Day 63
Day 70	Day 77

Antisera were purified by affinity chromatography in order to reduce background from the host serum proteins which bound non-specifically to the samples. The specific synthetic peptide antigen was covalently bound by

a glutathione spacer arm to thiol groups on the Sepharose™ 4B as detailed by the manufacturer (Activated Thiol Sepharose™ 4B; Amersham Biosciences). Elution buffer (50 mM Tris, 0.5 M NaCl and 1 mM EDTA, pH 7.5) was prepared and 200 ml was added to 1 g of activated thiol Sepharose™ 4B (ATS4B) for 15 minutes at RT. After collecting the now swollen ATS4B on a sintered glass filter, it was washed with 100 ml of elution buffer. The washed ATS4B was added to 2.5 mg of the synthetic peptide of interest dissolved in 5 ml elution buffer and placed on a mixer at RT for 2 hours, followed by an overnight incubation at 4°C. The ATS4B/peptide complex was washed three times in 50 ml elution buffer, by adding the elution buffer, mixing briefly, allowing to settle, and then decanting off the buffer. Ensuring that the correct antiserum is used, 5 – 20 ml of the antiserum corresponding to the peptide was added to the ATS4B/peptide complex and incubated at RT with continuous rotation for 1 hour. A column was prepared by inserting glass wool into the tip of a 5 ml syringe to form a plug, and the syringe (without plunger) was positioned in a clamp stand. A section of thin tubing was attached to the syringe, along with a clamp to enable or prevent flow. The antiserum/ATS4B/peptide mixture was gradually poured into the column, and the eluate collected in a tube. The incubation tube was fully rinsed with elution buffer and added to the column. The column was then washed with 10 column volumes of elution buffer in order to wash out any remaining unbound material. Bound antibodies were eluted from the column by addition of 0.1 M glycine pH 2.5 and collected in 1 ml fractions in tubes containing 0.3 ml 1 M Tris HCl pH 8.0. The low pH of the glycine elutes the antibody from the resin/peptide complex, and the Tris buffer neutralises the pH limiting the denaturing effects of the acidic glycine solution. The column was then washed with 10 ml elution buffer before the syringe was covered with Nescofilm and stored at 4°C and used to purify additional antibody if required. Samples, (10 µl) from each of the 10 fractions containing the purified antibody were loaded onto an SDS PAGE gel (Section 2.18), and the amount of antibody contained in each fraction was visually estimated by Coomassie blue staining (Section 2.19). Those fractions containing the highest amount of antibody were retained and combined, before dividing into aliquots and storing at -20°C (Martinez *et al.*, 2005).

a)

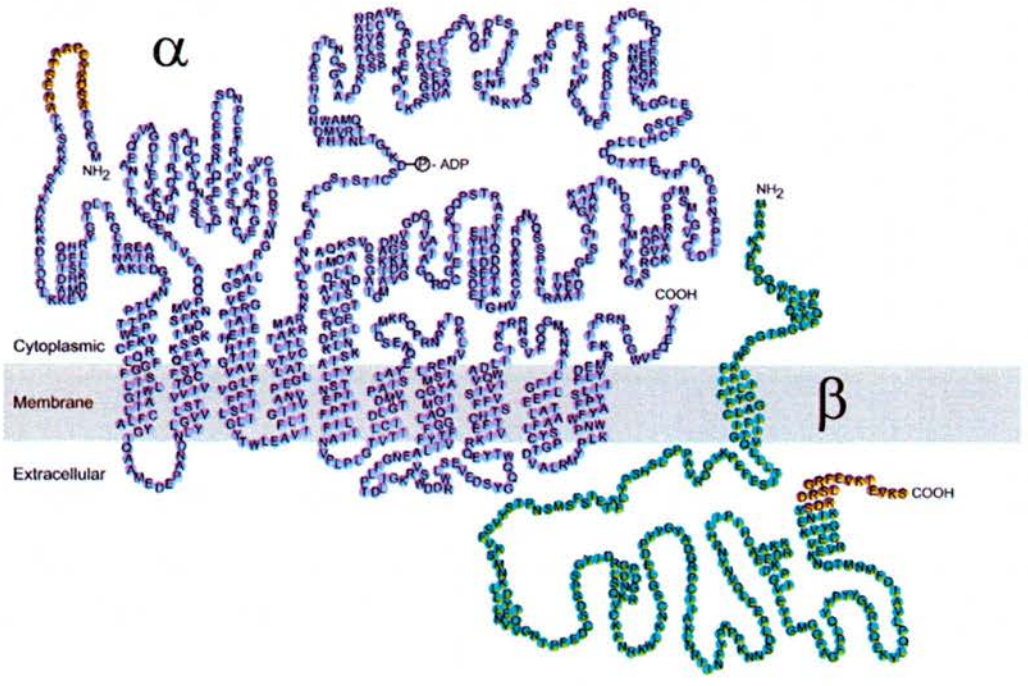

b)

Bull shark Na^+, K^+-ATPase alpha 1 subunit antibody raised to

ASD KYE PAA TSE NA(C)

Bull shark Na^+, K^+-ATPase beta subunit antibody raised to

(C)SD KDR LSG RFE VKI EVK S

c)

```
          10        20
           |         |
α1    ASDKYEPAAT-SENA
α2    GRD-YTPTDT-SENA
α3    -SDSYRVATTQGDKD
```

Figure 2.18: Na^+, K^+-ATPase sequences used to raise antibodies. **a)** Two dimensional model of Na^+, K^+-ATPase α and β subunits positioned in the membrane. The sequences used for antibody synthesis are highlighted in orange. Adapted from Vilsen *et al.*, 1997. **b)** Amino acid sequences used to synthesise antibodies. The cysteine residues incorporated for cross-linking to KLH are shown in parentheses. **c)** Sequence selected for synthesis of α 1 antibody aligned with α 2 and α 3 sequences to indicate antibody specificity. Purple denotes total homology between all isoforms, orange denotes close similarity and black denotes low similarity.

2.22: Western blotting

Proteins were bound to PVDF membranes as in Section 2.20 and were either used directly for Western blotting or stored at –20°C. In preparation for Western blotting, membranes were rinsed at room temperature in methanol for 5 minutes after which they were rinsed in MilliQ®H_2O for 5 minutes. Solutions for immunostaining were prepared while washing membranes. A sufficient amount of Phosphate Buffered Saline (PBS) was prepared by adding 1 PBS tablet (Dulbecco A, Oxoid) for every 100 ml MilliQ®H_2O. All incubations are carried out at RT. Solution 1 (5% non-fat milk in PBS) was added to cover the membrane and left to incubate with shaking (Gyro Rocker STR9, Bibby Stuart) for 1 hour in order to block non-specific binding sites. The purified primary antibody was added to Solution 2 (1% non-fat milk and 0.5% Tween 20 in PBS) at a dilution of 1:50 – 1:5000. Solution 1 was discarded and Solution 2 containing the primary antibody was added to cover the membrane and incubated for 90 minutes allowing the primary antibody to bind to the specific proteins on the membrane. The membrane was then washed three times in Solution 3 (0.2% Tween 20 in PBS) for 15 minutes each time to remove any non-bound primary antibody. An alkaline phosphatase conjugated secondary antibody (Anti-Rabbit IgG, alkaline phosphatase conjugate, developed in goat and adsorbed with human IgG, Sigma) was diluted 1:10,000 in Solution 4 (5% non fat milk, 0.5% Tween 20 in PBS) and added to the membrane and incubated for 90 minutes. A further three 15 minute washes in Solution 3 rinsed any non-bound secondary antibody from the membrane. This was followed by two 30 minute washes in PBS, followed by a 5 minute rinse in MilliQ®H_2O. Western Blue® stabilised substrate (Promega) was used to stain the membrane for 3 – 10 minutes. This solution contains a substrate for the bound secondary antibody-enzyme conjugate and produces a coloured product to visually indicate where the primary and secondary antibodies have bound and thus the protein of interest is located on the membrane. The membrane was finally rinsed in water to prevent over-staining by the Western Blue® stabilised substrate. The intensity of immunopositive bands was determined using a CCD camera attached a computer running the analytical software packages Gene Tools and Gene Snap (Syngene). The raw value of band intensity was used and compared against other samples with all comparisons made on the same blot.

2.23: Collection and preparation of samples for immunolabelling and immunofluorescent light microscopy

Specific antibodies were used to determine the location and distribution of the protein of interest in fixed tissue using immunofluorescent light microscopy. Small pieces (from 0.5 – 2 cm in length/width) of rectal gland, kidney, gill and intestine were collected and immediately placed in 4% paraformaldehyde fixative (4% paraformaldehyde in PBS, pH 7.4) at 4°C. The fixative is able to penetrate the whole tissue if the pieces taken for fixing are small. Slightly larger pieces may be taken from the gill since its structure has a high surface area allowing for greater fixative penetration. The tissue pieces were fixed in 10 ml 4% paraformaldehyde per piece for 24-48 h at 4°C before rinsing twice in PBS over 24 hours at 4°C, and then storing the tissue pieces in 70% ethanol at 4°C until further processing. The samples were then dehydrated and embedded in wax according to the following schedule:

Solution	Time
96% ethanol	1 hour
96% ethanol	1 hour
100% ethanol	1 hour
100% ethanol	1 hour
50% ethanol, 50% chloroform	2 hours
100% chloroform	2-3 hours
100% chloroform	Overnight
Paraffin wax	1 hour
Paraffin wax	1 hour
Paraffin wax	1 hour

A small amount of hot wax was added to a sufficient number of metal moulds and placed on ice, and the samples transferred to these moulds. A plastic mount was then pressed into the wax and topped up with hot wax. Samples were cooled at 4°C until they had set. Embedded sample blocks were stored at RT until required. Blocks were positioned on a Leitz Wetzlar microtome, and used to cut 3 – 5 μm sections which were collected on poly-L-lysine coated slides. Prior to immunostaining, tissues were de-waxed and re-hydrated according to the following schedule, where slides were placed

into slide baths containing the stated solutions: Histochoice clearing agent (Sigma) was used to dissolve the wax and a series of graded ethanol washes applied to re-hydrate the tissues.

Solution	Time
Histochoice clearing agent (Sigma)	5 minutes
Histochoice clearing agent (Sigma)	5 minutes
100% ethanol	5 minutes
95% ethanol	5 minutes
90% ethanol	5 minutes
70% ethanol	5 minutes
50% ethanol	5 minutes
PBS	5 minutes

2.24: Immunolabelling and immunofluorescent light microscopy

Prepared slides (Section 2.23) were transferred to a slide bath containing chilled Solution A (0.01% Tween 20, 150 mM NaCl in 10 mM phosphate buffer pH 7.3) for 10 minutes to permeabilise the tissues. Slides were then transferred to Solution B (50 mM NH_4Cl in PBS pH 7.3) for 5 minutes to mask any free aldehyde groups on the fixative and thus reduce associated background. Finally slides were transferred to Solution C, also referred to as blocking solution (1% BSA, 0.1% gelatin in PBS pH 7.3) for 10 minutes to block non-specific binding sites. Slides were removed from the slide bath and the back and sides of the slides cleaned and dried with paper towel, then placed in a wet slide chamber. A solution containing 1% BSA in PBS was prepared and used to dilute the primary antibody to 1:10 to 1:100, of which 100 µl was spread onto each slide. The lid of the wet chamber was lined with paper towel so that any condensation formed on the lid did not drop onto the slides. The slide chamber was kept at 4°C overnight. Slides were then washed for three x 15 minutes in blocking solution (1% BSA, 0.1% gelatin in PBS pH 7.3) to remove any unbound primary antibody, dried as before and placed in a wet slide chamber. Fluorescein Isothiocyanate (FITC)-conjugated secondary antibody (Fluorescein (FITC)-conjugated affinipure donkey anti-rabbit IgG; Jackson ImmunoResearch) was diluted to 1:200 in 1% BSA in PBS

pH 7.3, and 100 µl spread onto each of the slides and left to incubate for 1 h at RT, and covered with a dark sheet to reduce light degradation of the fluorescent FITC conjugate. After incubation, slides were again washed with three 15 minutes washes with blocking solution, dried and then 12 µl of anti-bleaching mounting medium (Sigma) was dropped onto the slides and sections covered with a cover slip. The sections were immediately examined with a Zeiss Axioplan fluorescent microscope system, including a Zeiss Super Pressure Mercury Lamp (HBO 50 W AC, Zeiss) and a filter set of the correct wavelength band pass excitation filter (450-490 nm, with emission filters of filter type 510 nm, and long pass of 520 nm) to detect FITC immunostaining. Microscopy was also carried out using phase contrast. Fluorescent staining images were captured using a Zeiss Axiophot microscope camera and controller.

2.25: Statistical analyses

To compare Na^+, K^+-ATPase mRNA expression by Northern blotting and Na^+, K^+-ATPase protein expression by Western blotting in FW- and SW-acclimated samples, a two-way analysis of variance (ANOVA) was performed followed by Fisher's PLSD post analysis of significance where differences were considered significant if $P<0.05$. These tests were performed using Statview (SAS Institute Inc.).

3

Amplification, cloning and sequencing of Na^+, K^+-ATPase α and β subunit isoforms from the bull shark

Results

3.1: Amplification, cloning and sequencing of Na^+, K^+-ATPase α subunit

It is known from experiments in various species, that the Na^+, K^+-ATPase α subunit mRNA is approximately 3 kb, and as such the homologue in *C. leucas* required more than one set of degenerate primers to amplify the whole sequence. In the first instance, a degenerate primer pair, homologous to all P-type ATPases (P-type, Appendix 3) was used along with bull shark rectal gland and gill cDNA to amplify by RT-PCR (Section 2.7) a 1049 base pair (bp) central fragment encoding amino acid positions 388 to 723 of the final sequence (*Figures 3.1a and 3.2*). A second pair of degenerate primers homologous to all Na^+, K^+-ATPase α subunit isoforms (All Na^+, K^+-ATPase α, Appendix 3) was then used to amplify a 896 bp fragment encoding amino acid positions 123 to 383 (*Figure 3.1a*) in *C. leucas* and a number of other species (*Figure 3.1b*). Amplified products were purified, cloned and sequenced as detailed in Sections 2.10 – 2.15. At least three positive clones were used to deduce the sequence for each fragment. The fragment amplified by the P-type ATPase primers yielded clones containing not only a Na^+, K^+-ATPase fragment, but also fragment of a Ca^{2+}-ATPase. Only the α_1 isoform was initially amplified and cloned from *C. leucas* gill cDNA using the degenerate Na^+, K^+-ATPase α primers. Specific primers were then designed (α mid, Appendix 3) to amplify a fragment in between these sections; a fragment of 434 bp, encoding amino acid positions 353 to 453 of the final sequence. Specific RACE (Section 2.8) primers (*C. leucas* α_1 3′ RACE 1 & 2 and *C. leucas* α_1 5′ RACE 1 & 2, Appendix 3) were also designed to known sequences of the Na^+, K^+-ATPase α_1 subunit. These primers were used in conjunction with the RACE, AP1 and AP2 primers (Appendix 3) to successfully amplify a 1354 bp fragment at the 3′ end, encoding amino acid positions 677 to 1025 plus a 204 bp 3′ untranslated region (UTR), and a 689 bp fragment at the 5′ end, encoding amino acid positions 1 to 135 plus a 247 bp 5′ UTR. The entire bull shark Na^+, K^+-ATPase α_1 subunit nucleotide sequence comprised 3530 bp which translates to a protein of 1025 amino acids. The interleaved nucleotide and putative amino acid sequence is shown in *Figure 3.2*. The bull shark Na^+, K^+-ATPase α_1 subunit isoform amino acid sequence shares high identities with Na^+, K^+-ATPase α_1 isoforms

from other vertebrates, as shown in *Figure 3.3*, and with the α subunits cloned so far for other elasmobranchs (*S. acanthias*: 91%; *T. californica*: 88%). Compared to the human Na^+, K^+-ATPase α subunit isoforms, the *C. leucas* sequence is most homologous to human Na^+, K^+-ATPase α_1 isoform (87%), but exhibits almost equivalent homology with human α_2 (86%) and α_3 (84%).

3.2: Cloning of additional Na^+, K^+-ATPase α subunit isoforms from *C. leucas*

To determine whether fragments of other isoforms were also amplified in low concentrations, restriction enzymes were used to cleave the known α_1 DNA fragments amplified with either the All Na^+, K^+-ATPase or P-type primers. The restriction enzymes were selected to cut at specific sites in the DNA sequence of the α_1 isoform. Any cloned DNA fragments not cleaved at the expected sites were sequenced (*Figure 3.4*). This method resulted in the detection of both α_2 and α_3 cDNA fragments. These were subsequently extended using 3′ and 5′ RACE primers as for the α_1 subunit. The combined fragments for Na^+, K^+-ATPase α_2 isoform comprised 3453 bp and the open reading frame encoded a protein of 1018 amino acids with 271 bp of 3′ and 124 bp of 5′ UTR (*Figure 3.5*). The combined fragments of the Na^+, K^+-ATPase α_3 isoform comprised 3309 bp which encoded a protein of 1025 amino acids with 103 bp of 3′ and 127 bp of 5′ UTR (*Figure 3.6*). Sequencing of the α_3 3′ UTR was incomplete. The bull shark Na^+, K^+-ATPase α_2 amino acid sequence is 89% homologous to *C. leucas* α_1, and 88% homologous to *C. leucas* α_3, with the Na^+, K^+-ATPase α_3 isoform amino acid sequence being 86% homologous to the α_1 sequence (*Figure 3.7*). *C. leucas* Na^+, K^+-ATPase α_1, α_2 and α_3 isoforms share highest homology with the α_1, α_2 and α_3 paralogues in humans. Amino acid homologies to other vertebrate Na^+, K^+-ATPase α subunit isoforms is shown in *Figures 3.8 and 3.9*. The isoform-specific region is highly variable between the α isoforms of *C. leucas*, as is shown in *Figure 3.10a*.

3.3: Amplification, cloning and sequencing of Na^+, K^+-ATPase β subunit

The Na^+, K^+-ATPase β subunit mRNA is shorter than the α subunit, at only 2 kb. In order to amplify the full Na^+, K^+-ATPase β subunit sequence from *C. leucas*, a degenerate primer pair, designed to be homologous to all known Na^+, K^+-ATPase β subunit isoforms (All Na^+, K^+-ATPase β, Appendix 3) was used in RT-PCR (Section 2.7) to amplify a 632 bp cDNA fragment from *C. leucas* intestine encoding amino acid positions 43 to 252 of the final sequence (*Figure 3.11*). The amplified product was purified, cloned and sequenced as detailed in Sections 2.10 – 2.15. At least three positive clones were sequenced in forward and reverse directions and used to deduce the sequence for each fragment. Specific nested 5′ and 3′ RACE primer pairs were also designed to extend the known sections of the Na^+, K^+-ATPase β subunit as described for the α_1 subunit, and used to amplify a 1108 bp 3′ end fragment, encoding amino acid positions 235 to 305 plus a 888 bp 3′ UTR, and a 625 bp fragment at the 5′ end, encoding amino acid positions 1 to 100 plus a 322 bp 5′ UTR. The entire cloned bull shark Na^+, K^+-ATPase β nucleotide sequence comprised 2129 bp with a reading frame which translates into a 305 amino acid protein (*Figure 3.12*). The bull shark Na^+, K^+-ATPase β subunit amino acid sequence is almost certainly a β_1 isoform, since it shares 61% identity with human β_1 isoform, but only 38% and 37% with β_2 and β_3, respectively. The amino acid homologies of the bull shark sequence with those of other vertebrates is shown in Figure *3.13*. Although attempts were made to isolate additional Na^+, K^+-ATPase β isoforms from fragments amplified from bull shark brain cDNA, these were unsuccessful.

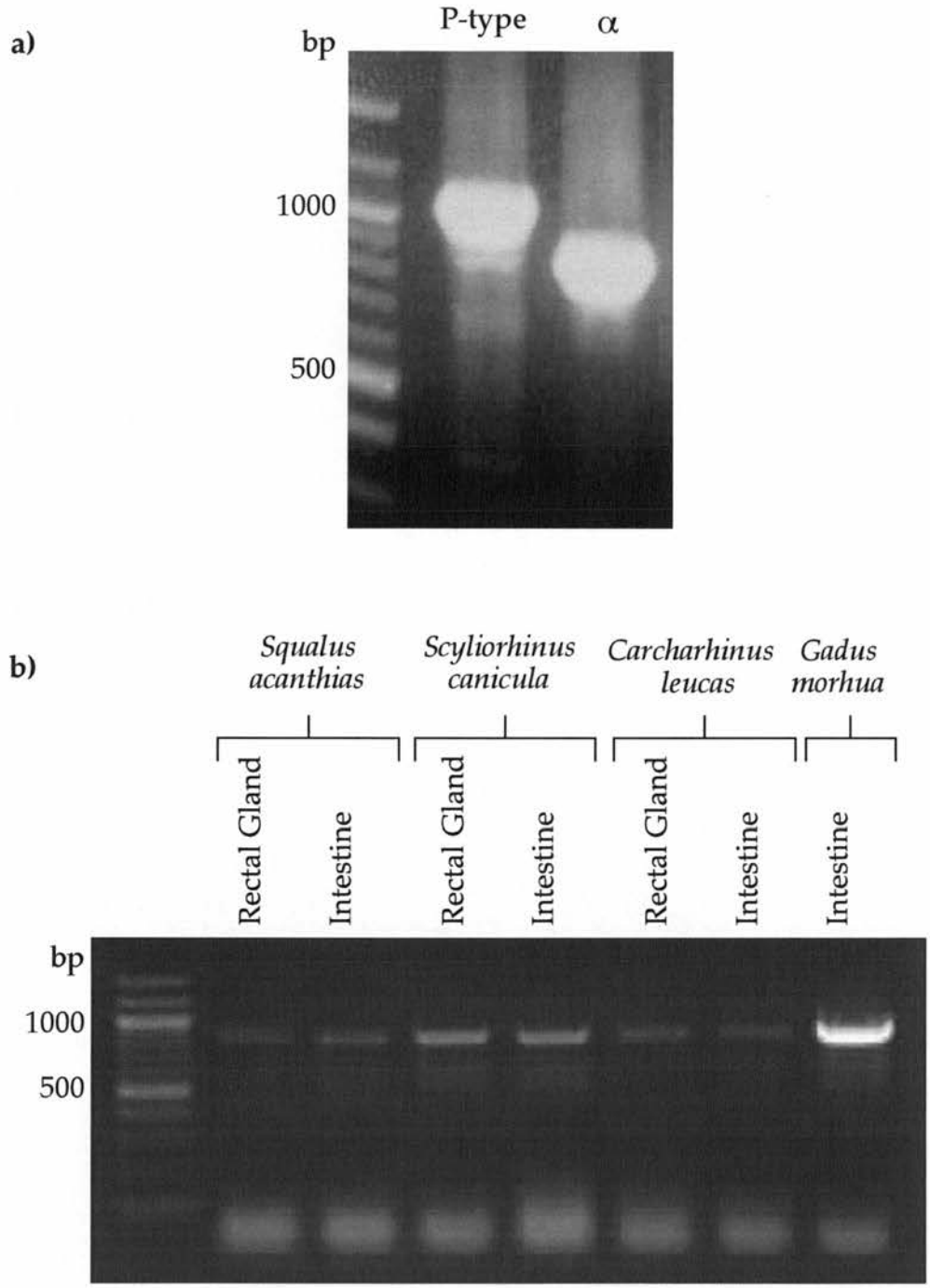

Figure 3.1: RT-PCR amplificiation of Na^+, K^+-ATPase α subunit using P-type and all α primers (Appendix 3). a) Fragments of Na^+, K^+-ATPase α subunit from *C. leucas* gill cDNA template, 1049 bp for the P-type primers, 896 bp for all α. **b)** Fragments of Na^+, K^+-ATPase α subunit of 896 bp amplified using all α primers with cDNA templates from different tissues and species.

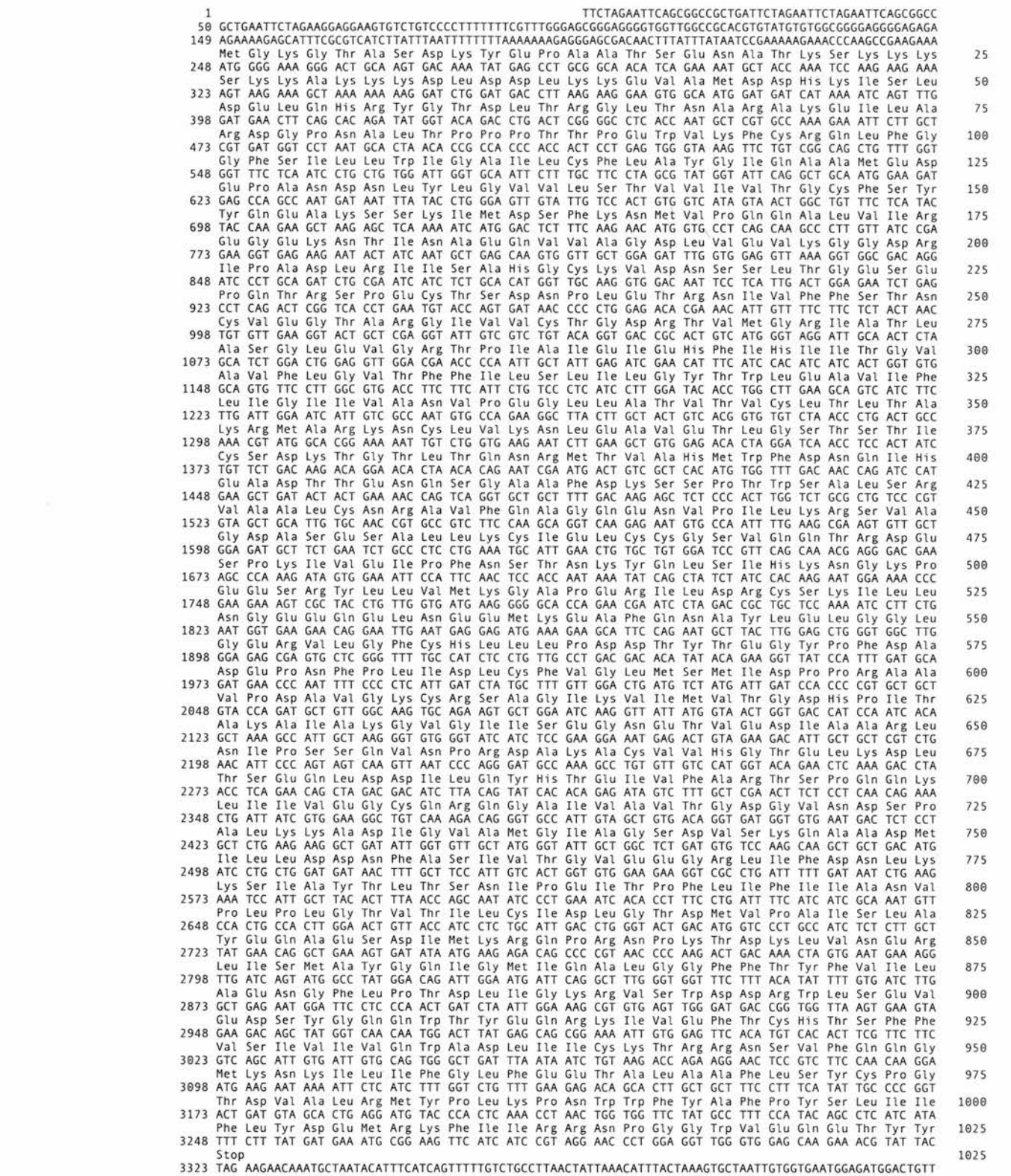

Figure 3.2: Interleaved sequence of Na^+, K^+-ATPase α_1 subunit: Nucleotide and amino acid sequences of the Na^+, K^+-ATPase α_1 subunit from *C. leucas*.

Species	Isoform	Identity with *C. leucas* Na^+, K^+-ATPase α_1 amino acid sequence (%)	NCBI accession number
Squalus acanthias (spiny Dogfish)	α	91	AJ781093
Torpedo californica (Pacific electric ray)	α	88	X02810
Anas platyrhynchos salt secreting gland (mallard duck)	α_1	88	AY206681
Xenopus laevis (African clawed frog)	α_1	88	U10108
Homo sapiens (modern human)	α_1	87	AL136376
Rattus norvegicus (brown rat)	α_1	87	P06685
Gallus gallus (domestic chicken)	α_1	87	P09572
Homo sapiens (modern human)	α_3	86	BC015566
Fundulus heteroclitus (killifish)	α_1	85	AY057072
Danio rerio (zebrafish)	α_1	85	BC085663
Anguilla anguilla (European eel)	α_1	85	X76108
Homo sapiens (modern human)	α_2	84	BC052271

Figure 3.3: Homology of *C. leucas* Na^+, K^+-ATPase α_1 subunit amino acid sequence with a range of vertebrates: Percentage identity of Na^+, K^+-ATPase α_1 subunit sequence amino acid sequence with representative vertebrates, including elasmobranchs, birds, amphibians, mammals, and teleost fish. Human α_2 and α_3 are also included for comparison. Sequences were compared using NCBI Blast. NCBI accession numbers for the nucleotide sequences encoding these proteins are listed.

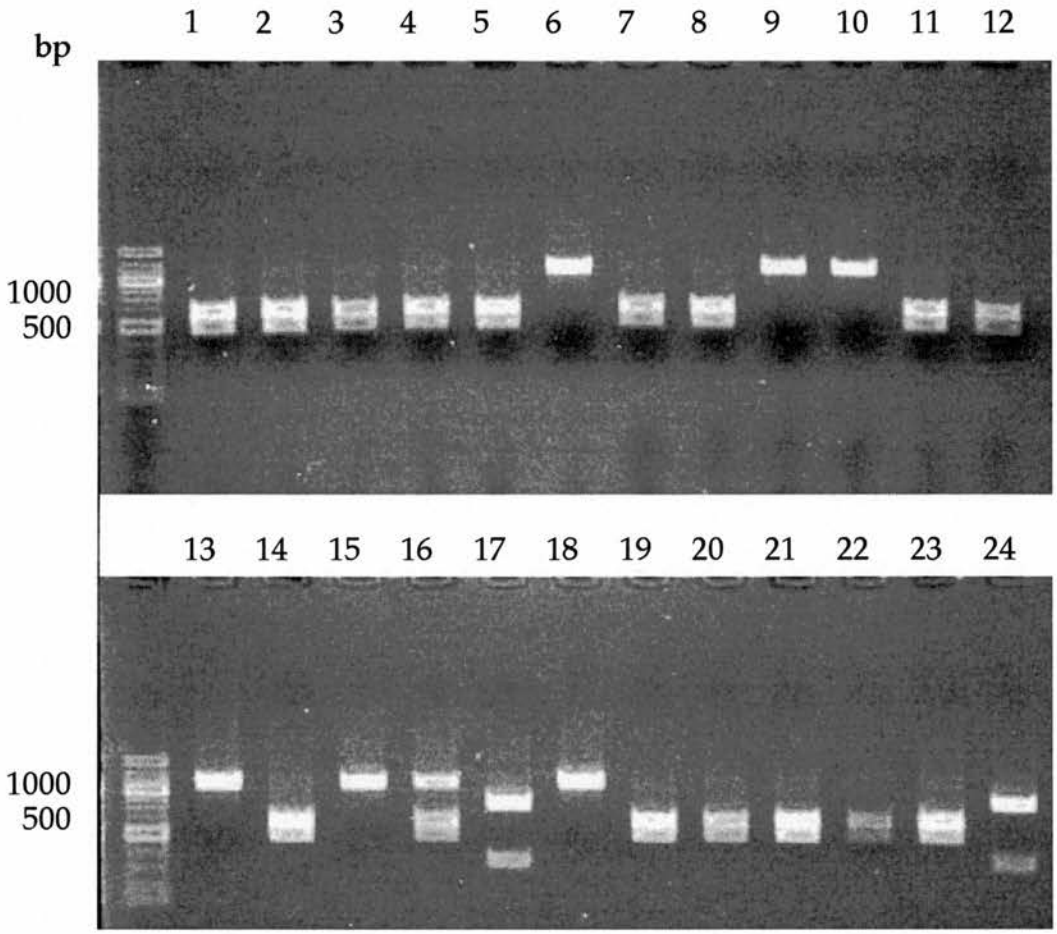

Figure 3.4: RT-PCR amplification of isoforms of Na^+, K^+-ATPase α subunit. A fragment of Na^+, K^+-ATPase α subunit using P-type primers (Appendix 3) with *C. leucas* brain cDNA template was cloned into a vector, and positive colonies were cut with the restriction enzyme XhoI. The restriction patterns reveal 3 different cut patterns, indicating the possibility of 3 different isoforms. After sequencing, colonies 1-5, 7, 8, 11, 12, 14, and 19-23 were found to be the α_1 isoform, colonies 15 and 18 were found to be α_2, and colonies 6, 9, 10, 13, 17 and 20 were α_3. (Additional α_2 colonies not shown.)

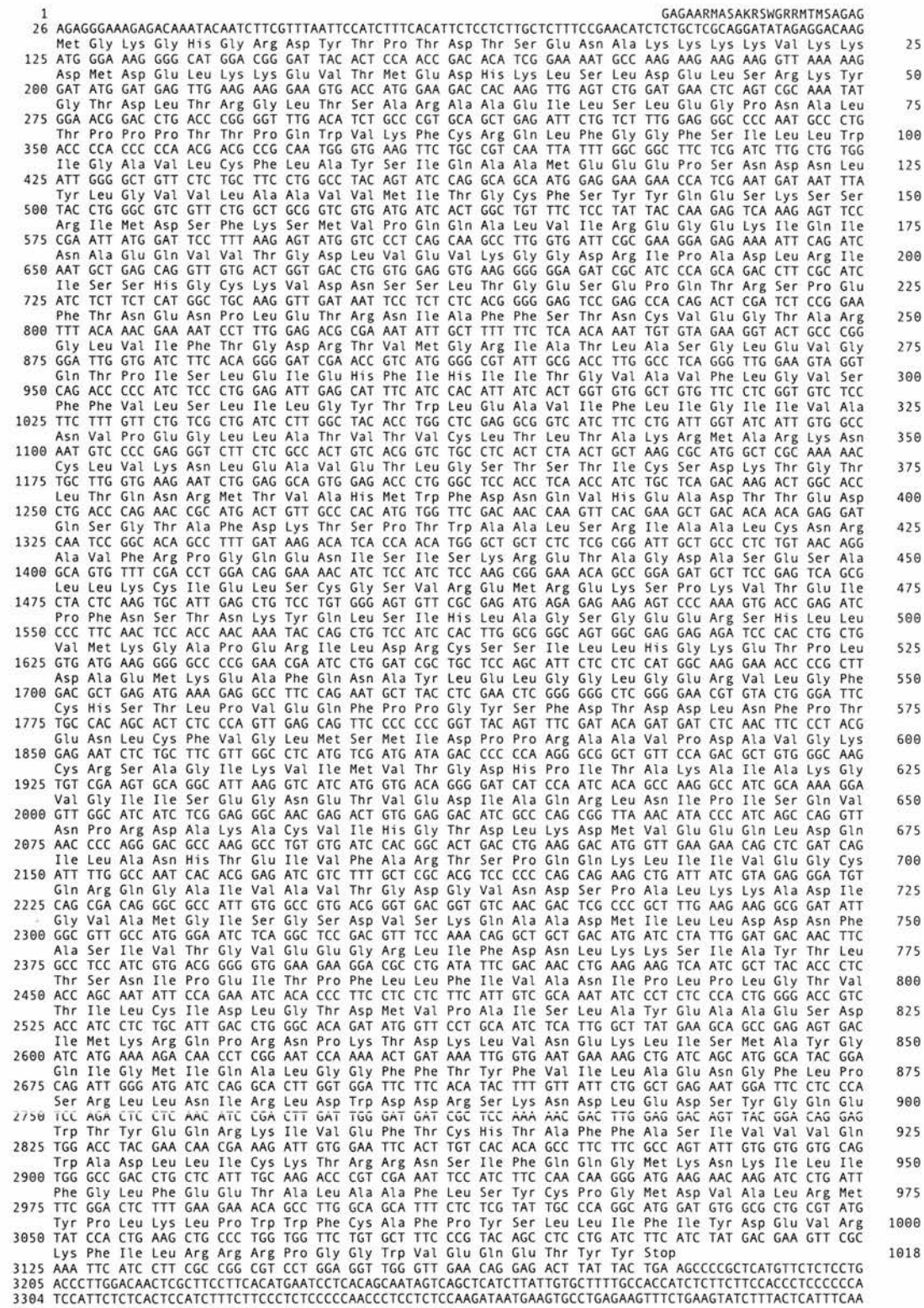

Figure 3.5: Interleaved sequence of Na^+, K^+-ATPase α_2 subunit: Nucleotide and amino acid sequences of the Na^+, K^+-ATPase α_2 subunit from *C. leucas*.

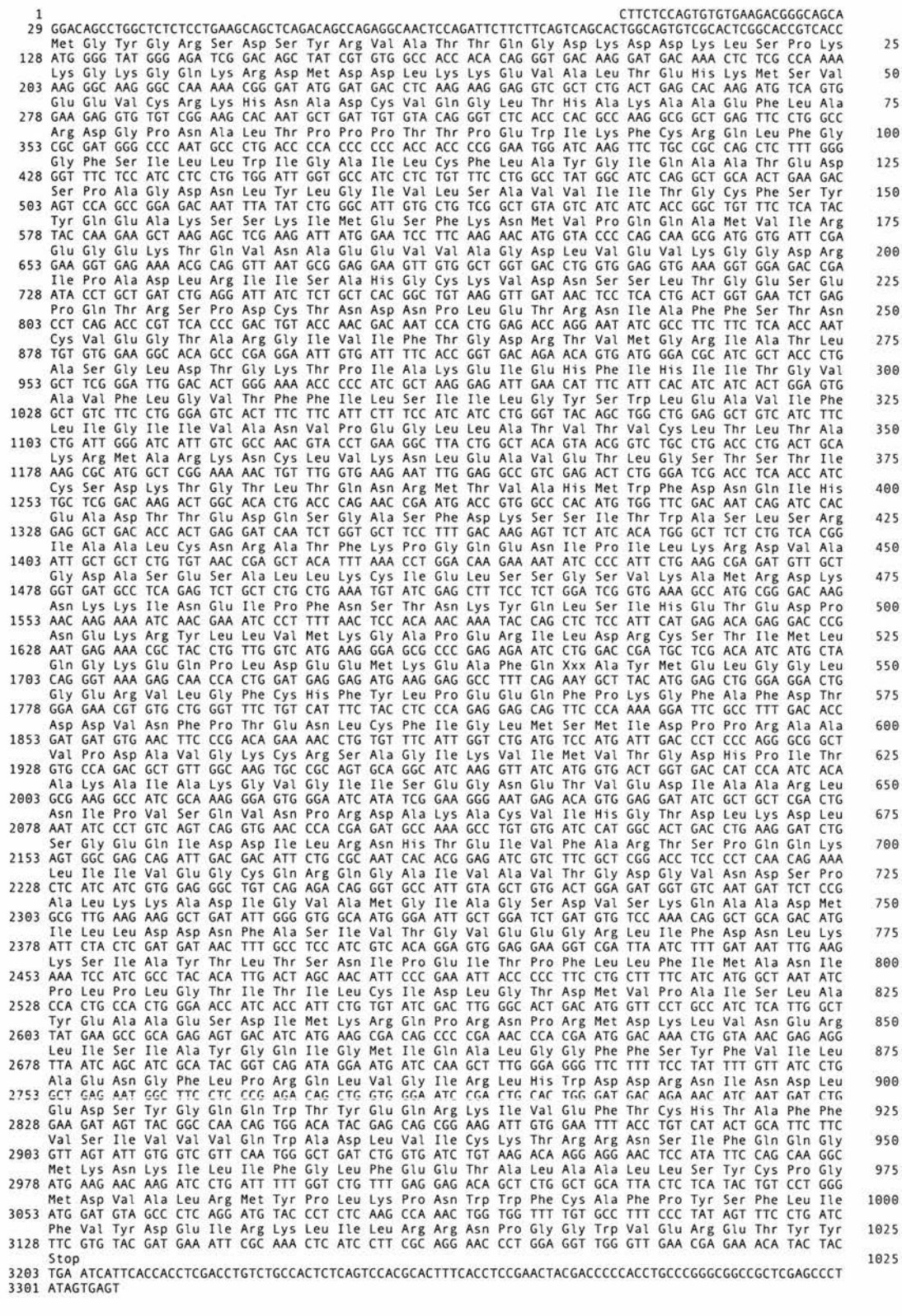

Figure 3.6: Interleaved sequence of Na^+, K^+-ATPase α_3 subunit: Nucleotide and amino acid sequences of the Na^+, K^+-ATPase α_3 subunit from *C. leucas*.

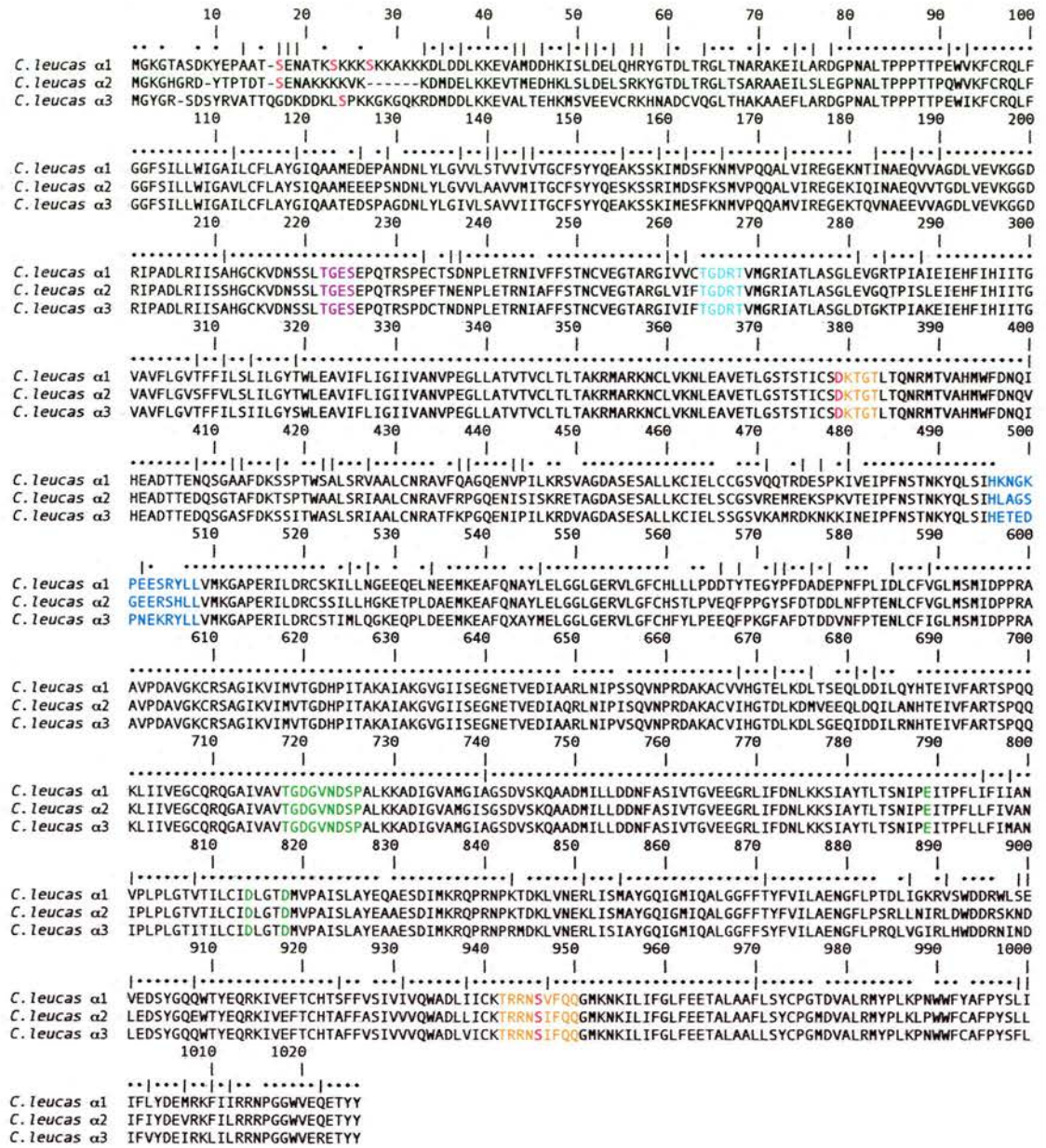

Figure 3.7: Amino acid sequence alignment of the isoforms of Na^+, K^+-ATPase α subunit. *C. leucas* Na^+, K^+-ATPase α_1, α_2 and α_3 subunit isoforms amino acid sequences were aligned using GeneJockey II software (Biosoft). Residues highlighted in orange represent potential phosphorylation sites, with the phosphorylated residue highlighted in red; purple highlights residues which may be involved in conformational change; turquoise residues comprise the ATP binding site; blue highlights the isoform-specific region; green indicates potential ion binding sites. Amino acid residue numbers differ from those of the individual sequences (*Figures 3.2, 3.5* and *3.6*) since gaps have been taken into account in this alignment.

Species	Isoform	Identity with *C. leucas* Na^+, K^+-ATPase α_2 amino acid sequence (%)	NCBI accession number
Homo sapiens (modern human)	α_2	87	BC052271
Rattus norvegicus (brown rat)	α_2	87	P06686
Gallus gallus (domestic chicken)	α_2	87	P24797
Homo sapiens (modern human)	α_1	86	AL136376
Anas platyrhynchos salt secreting gland (mallard duck)	α_1	86	AY206681
Xenopus laevis (African clawed frog)	α_2	86	BC060332
Homo sapiens (modern human)	α_3	86	BC015566
Squalus acanthias (spiny Dogfish)	α	84	AJ781093
Fundulus heteroclitus (killifish)	α_2	84	AY057073
Danio rerio (zebrafish)	α_2	84	AF286373
Torpedo californica (Pacific electric ray)	α	83	X02810

Figure 3.8: Homology of *C. leucas* Na^+, K^+-ATPase α_2 subunit amino acid sequence with a range of vertebrates: Percentage identity of Na^+, K^+-ATPase α_2 subunit sequence amino acid sequence with representative vertebrates, including elasmobranchs, birds, amphibians, mammals, and teleost fish. Human α_1 and α_3 sequences are also included for comparison. Sequences were compared using NCBI Blast. NCBI accession numbers for the nucleotide sequences encoding these proteins are listed.

Species	Isoform	Identity with *C. leucas* Na^+, K^+-ATPase α_3 amino acid sequence (%)	NCBI accession number
Homo sapiens (modern human)	α_3	92	BC015566
Rattus norvegicus (brown rat)	α_3	92	P06687
Gallus gallus (domestic chicken)	α_3	92	P24798
Danio rerio (zebrafish)	α_3	91	BC064703
Xenopus laevis (African clawed frog)	α_3	90	BC043743
Homo sapiens (modern human)	α_1	87	AL136376
Homo sapiens (modern human)	α_2	86	BC052271
Anas platyrhynchos salt secreting gland (mallard duck)	α_1	85	AY206681

Figure 3.9: Homology of *C. leucas* Na^+, K^+-ATPase α_3 subunit amino acid sequence with a range of vertebrates: Percentage identity of Na^+, K^+-ATPase α_3 subunit sequence amino acid sequence with representative vertebrates, including elasmobranchs, birds, amphibians, mammals, and teleost fish. Human α_1 and α_2 are also included for comparison. Sequences were compared using NCBI Blast. NCBI accession numbers for the nucleotide sequences encoding these proteins are listed.

a)

Species	Isoform	Amino acid sequence	NCBI accession number
		493 506	
Rat (*Rattus norvegicus*)	α_1	HKNPNASEPKHLL	P06685
Chicken (*Gallus gallus*)	α_1	HKNANAGESRHLL	P09572
Frog (*Xenopus laevis*)	α_1	HKNANPSESRYIL	U10108
Rockcod (*Trematomus bernacchi*)	α_1	HKNATPGESKQLL	AY081863
Bull shark (*Carcharhinus leucas*)	α_1	HKNGKPEESRYLL	
Rat (*Rattus norvegicus*)	α_2	HEREDSPQSHVLV	P06686
Chicken (*Gallus gallus*)	α_2	HEREEDPQGHILV	P24797
Frog (*Xenopus laevis*)	α_2	HEREDSPEGHLLV	BC060332
Rockcod (*Trematomus bernacchi*)	α_2	HEAEDNPSGHILV	AY081864
Bull shark (*Carcharhinus leucas*)	α_2	HLAGSGEERSHLL	
Rat (*Rattus norvegicus*)	α_3	HETEDPNDNRYLL	P06687
Chicken (*Gallus gallus*)	α_3	HETEDPNDNRYLL	P24798
Frog (*Xenopus laevis*)	α_3	HETEDPNDNRYLL	BC043743
Rockcod (*Trematomus bernacchi*)	α_3	HETEDTNDNRYLL	AY081865
Bull shark (*Carcharhinus leucas*)	α_3	HETEDPNEKRYLL	

b)

Species	Amino acid sequence	Homology of *S. acanthias* α_1 to rat sequences
	498 510	
S. acanthias α_1	HENEKSSESRYLL	
Rat α_1	HKNPNASEPKHLL	6/13
Rat α_2	HEREDSPQSHVLV	6/13
Rat α_3	HETEDPNDNRYLL	7/13
	124 136	
S. acanthias α_1 alternative region	AATEDPANDNLYL	10/13 (gapped homology with rat α_3 antibody)

Figure 3.10: Isoform-specific region of the Na^+, K^+-ATPase α subunit amino acid sequence for a range of vertebrates. **a)** Amino acid sequences from the isoform-specific regions of the Na^+, K^+-ATPase α_1, α_2 and α_3 subunit isoforms of a mammal, a bird, an amphibian, a teleost fish and *C. leucas*. The location of the isoform-specific region in the amino acid sequence is indicated for the rat (^{493}His-^{506}Leu). NCBI accession numbers for the nucleotide sequences encoding these proteins are listed. **b)** Comparison of the *S. acanthias* Na^+, K^+-ATPase α_1 amino acid sequence (NCBI accession number AJ781093) with the isoform-specific regions of the Na^+, K^+-ATPase α_1, α_2 and α_3 subunit isoforms of the rat. An alternative region within the *S. acanthias* α sequence showing high gapped homology to the rat α_3 isoform-specific region has also been shown.

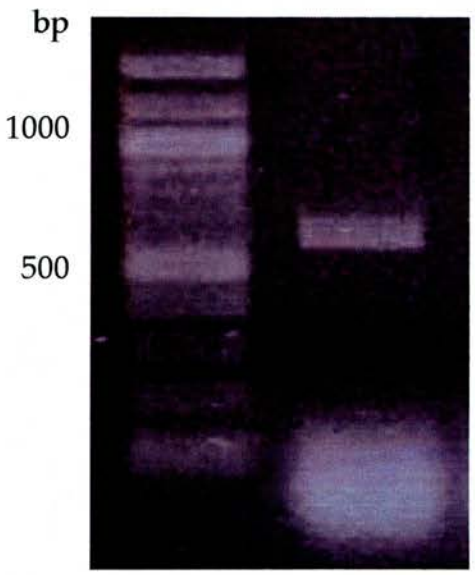

Figure 3.11: RT-PCR amplification of Na^+, K^+-ATPase β_1 subunit using all Na^+, K^+-ATPase β primers (Appendix 3). A fragment of Na^+, K^+-ATPase β_1 subunit from a *C. leucas* intestine cDNA template was 632 bp in length.

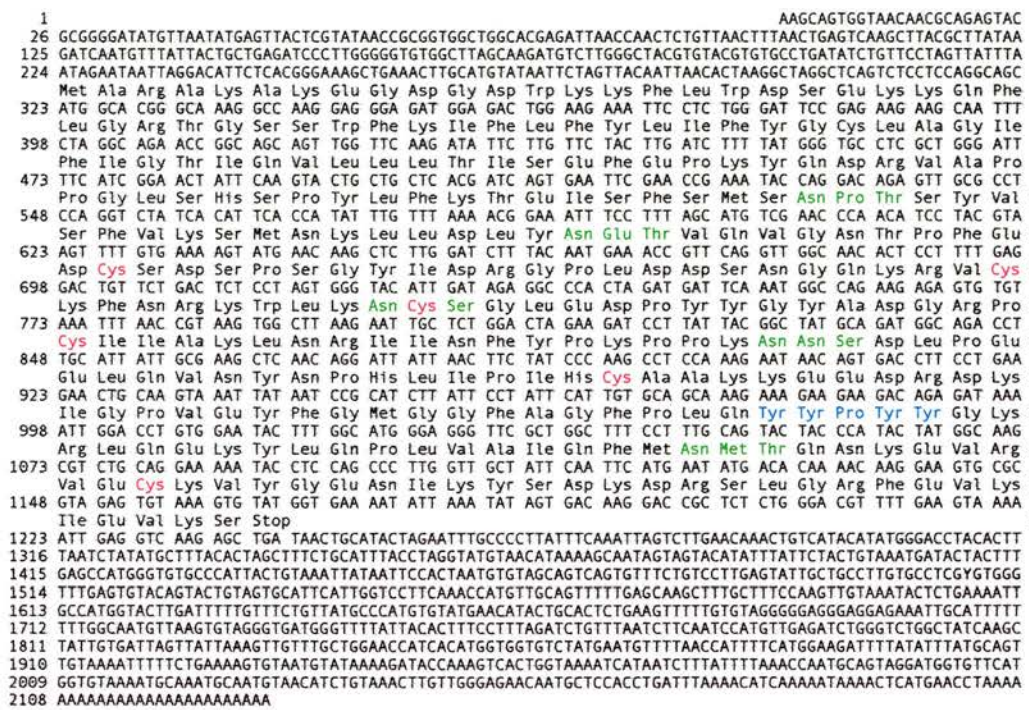

Figure 3.12: Interleaved sequence of Na^+, K^+-ATPase β_1 subunit: Nucleotide and amino acid sequences of the Na^+, K^+-ATPase β_1 subunit from *C. leucas*. Residues highlighted in green represent potential glycosylation sites, cysteine residues highlighted in red form disulphide bonds, and the motif highlighted in blue is a highly conserved site thought to be involved in interaction with the α subunit.

Species	Isoform	Identity with *C. leucas* Na^+, K^+-ATPase β amino acid sequence (%)	NCBI accession number
Torpedo californica (Pacific electric ray)	β	74	X03471
Xenopus laevis (African clawed frog)	β_1	66	U17061
Anas platyrhynchos salt secreting gland (mallard duck)	β_1	65	AY422199
Gallus gallus (domestic chicken)	β_1	65	P08251
Homo sapiens (modern human)	β_1	61	BT009787
Rattus norvegicus (brown rat)	β_1	61	BC078902
Danio rerio (zebrafish)	β_1	61	AF308597
Anguilla anguilla (European eel)	β_1	58	X76109
Homo sapiens (modern human)	β_2	38	AF007876
Homo sapiens (modern human)	β_3	37	BC011835

Figure 3.13: Homology of *C. leucas* Na^+, K^+-ATPase β_1 subunit amino acid sequence with a range of vertebrates: Percentage identity of Na^+, K^+-ATPase β_1 subunit sequence amino acid sequence with representative vertebrates, including elasmobranchs, birds, amphibians, mammals, and teleost fish. Human β_1, β_2 and β_3 are also included for comparison. Sequences were compared using NCBI Blast. NCBI accession numbers for the nucleotide sequences encoding these proteins are listed.

3.4: Amplification, cloning and sequencing of Na^+, K^+-ATPase α subunit isoforms.

Three isoforms of the Na^+, K^+-ATPase α subunit have been identified in the bull shark (*C. leucas*). The cDNA sequence of Na^+, K^+-ATPase α_1 subunit isoform is 3.53 kb long and encodes a 1025 amino acid protein. This isoform is 91% homologous to the amino acid sequence of *S. acanthias*, 88% homologous to *T. californica* and 87% homologous to the sequence of the human Na^+, K^+-ATPase α_1 subunit isoform. Amino acid homologies with several other vertebrates are shown in *Figure 3.3*. The additional Na^+, K^+-ATPase α_2 and α_3 subunit isoforms were discovered using restriction digest pattern analysis. The full length *C. leucas* Na^+, K^+-ATPase α_2 subunit isoform cDNA sequence is 3.453 kb in length and encodes for 1018 amino acids. The incomplete cDNA of Na^+, K^+-ATPase α_3 subunit isoform cDNA sequence is 3.309 kb in length and encodes a protein of 1025 amino acids. A summary of the homologies of α_2 and α_3 to other vertebrate α subunit amino acid sequences is given in *Figures 3.8 and 3.9*. *C. leucas* Na^+, K^+-ATPase α_2 amino acid sequence is 87% homologous to the human α_2 sequence, and the amino acid sequence of *C. leucas* Na^+, K^+-ATPase α_3 is 92% homologous to the human α_3 sequence. Additional isoforms such as the human Na^+, K^+-ATPase α_4 isoform were not identified in *C. leucas*. However, the α_4 isoform is specific to the testes, which were not examined in this species.

Benz *et al.*, (1992) and Hansen (1999) have both reported that the major Na^+, K^+-ATPase α isoform expressed in the rectal gland of *S. acanthias* is the α_3 isoform. Indeed both authors suggested that only one isoform (the α_3) existed in elasmobranchs and therefore the elasmobranch α_3 may have been the evolutionary ancestor of all isoforms (α_1, α_2, α_3 and α_4) found in mammals. However, MacKenzie (Ph. D. thesis, 1996) found that a Na^+, K^+-ATPase α_1 subunit isoform was expressed in the rectal gland of *S. canicula*. The full length Na^+, K^+-ATPase α subunit sequence from the rectal gland of *S. acanthias* (NCBI accession number AJ781093) has recently been sequenced, and this sequence shares greatest amino acid sequence homology with the α_1 sequences of other vertebrates. By comparing the *S. acanthias* sequence to the

mammalian α isoform sequences, it is now clear why Benz (1992) and Hansen (1999) inaccurately concluded that only the α_3 isoform was present in the elasmobranch rectal gland. Isoform-specific antibodies raised to mammalian Na^+, K^+-ATPase α isoform sequences were used to determine which isoform was expressed in the dogfish rectal gland. The isoform-specific region runs from ^{498}His-^{510}Leu in *S. acanthias* (*Figure 3.10b*), and shares the highest amino acid homology with the α_3 isoform of the rat. The isoform-specific antibody for α_3 recognises the HTEDP sequence, which is not present in *S. acanthias*. However, there is an alternative region on the α_1 sequence of *S. acanthias* (^{124}Ala-^{136}Leu) which is more homologous to the α_3 isoform of the rat. Therefore it is likely that the antibody raised to the mammalian α_3 isoform has cross-reacted with this non-isoform specific region within the *S. acanthias* α_1 sequence. The authors' conclusions that the predominant Na^+, K^+-ATPase α subunit isoform in *S. acanthias* rectal gland was α_3 is incorrect.

Since the Na^+, K^+-ATPase α subunit is the functional catalytic unit, it is not surprising that it is so well conserved throughout the vertebrates. Several regions are conserved throughout all P-type ATPases and as would be expected, they are conserved in the three *C. leucas* α isoforms. With reference to *Figure 3.7*, these include the phosphorylation site, ^{379}Asp-^{383}Thr (^{379}Asp is phosphorylated); a motif involved with conformational change, ^{222}Thr-^{225}Ser; a putative ATP-binding domain motif, ^{264}Thr-^{267}Arg; and an ion binding and translocation region, ^{718}Thr-^{726}Pro (Lutsenko and Kaplan, 1995). The conserved transmembrane residue ^{789}Glu is an essential part of the cation binding site (Kaplan *et al.*, 1994). In the subsequent transmembrane span, conserved residues ^{814}Asp and ^{818}Asp have also been implicated in cation binding (Lingrel *et al.*, 1997). A putative protein kinase A (PKA) phosphorylation motif located on the rat Na^+, K^+-ATPase α_1 subunit isoform sequence (Feschenko *et al.*, 1997) is also found in the *C. leucas* α_1 sequence (^{943}Arg-^{950}Gln; ^{946}Ser being phosphorylated). Interestingly, although the Ser residue is conserved throughout all isoforms, the surrounding sequence is slightly altered in *C. leucas* α_2 and α_3 where an Ile residue replaces Val in both. There is also evidence that either ^{18}Ser or ^{23}Ser are involved in phosphorylation by protein kinase C (PKC; Feschenko *et al.*, 1997) and equivalents of these are both present in the *C. leucas* α_1 isoform sequence,

however only the equivalent ^{17}Ser is present in the *C. leucas* α_2 subunit, whereas ^{24}Ser is found in *C. leucas* α_3 (*Figure 3.7*). PKC may also phosphorylate ^{942}Thr (Mahmmoud and Cornelius, 2000) which is conserved in all three *C. leucas* α isoforms (*Figure 3.7*). The Na^+, K^+-ATPase isoform-specific regions in *C. leucas* α isoforms (^{496}His-^{508}Leu) were compared to other vertebrates (*Figure 3.10a*), and this region shows the most variance between the central segment of the three isoforms (*Figure 3.7*; Pierre *et al.*, 2002).

3.5: Amplification, cloning and sequencing of Na^+, K^+-ATPase β subunit isoforms.

A single Na^+, K^+-ATPase β subunit isoform was identified in *C. leucas*. The full length cDNA sequence was 2.129 kb in length encoding a 305 amino acid protein. The amino acid sequence shares 74% homology with the β sequence of the electric ray, *T. californica*, 61% homology with human β_1 and represents the first Na^+, K^+-ATPase β subunit sequence cloned from a shark. Amino acid sequence homologies with various vertebrates are shown in *Figure 3.12*. No additional β isoforms were discovered in *C. leucas*. It is unlikely that this will be the only β isoform expressed in *C. leucas* since all other vertebrates have at least two Na^+, K^+-ATPase β subunit isoforms.

Although the Na^+, K^+-ATPase β subunit is not as highly conserved throughout vertebrates as the α subunit, there are some highly invariant motifs which may be involved in folding, interaction with the α subunit and insertion of the α/β complex into the plasma membrane. The six invariant cysteine residues which form three extracellular structural disulphide bonds are located at positions ^{127}Cys-^{150}Cys, ^{160}Cys-^{176}Cys and ^{215}Cys-^{278}Cys in the *T. californica* sequence (Kawamura *et al.*, 1994), and these positions are identical in the *C. leucas* β_1 sequence (*Figure 3.12*). The extracellular domain of the *C. leucas* Na^+, K^+-ATPase β_1 subunit has five consensus glycosylation sites (^{95}Asn-^{97}Thr; ^{114}Asn-^{116}Thr; ^{159}Asn-^{161}Ser; ^{194}Asn-^{196}Ser; ^{267}Asn-^{269}Thr). The Tyr-Tyr/Phe-Pro-Tyr-Tyr motif of the β subunit may be involved in interactions with α subunit (Geering, 2001) and this is located at ^{244}Tyr-^{248}Tyr on the *C. leucas* β_1 sequence (*Figure 3.12*).

4

Expression of Na^+, K^+-ATPase α and β subunit isoform mRNAs in the osmoregulatory tissues of FW- and SW-acclimated bull sharks

Results

4.1: Evaluation of Na^+, K^+-ATPase subunit mRNA expression

A two-way approach was taken to investigating mRNA expression in the osmoregulatory tissues of the bull shark. Initially, Northern blotting (Section 2.16) was used to determine the mRNA expression. Due to the low levels of expression and low abundance of mRNAs of α_2 and α_3 isoforms, RT-PCR (Section 2.7) was also used in a semi-quantitative procedure to assess levels of expression of all three isoforms. Both methods were used to examine changes in Na^+, K^+-ATPase mRNA expression in the osmoregulatory tissues and the brain of bull sharks acclimated to FW or SW.

4.2: Determination of Na^+, K^+-ATPase α subunit mRNA expression by Northern blotting

Denaturing agarose gels supporting rectal gland, kidney, gill, intestine, liver, interrenal gland, muscle, pancreas, atrium, ventricle and brain total RNA samples were made accordingly to the method detailed in Section 2.4. The amount of total RNA loaded for rectal gland and brain was 5 μg due to the low sample abundance, whereas 20 μg of the other RNAs were loaded. After electrophoresis, the RNA was transferred by electroblotting to a membrane, and used with a gene specific DNA probe for Northern blotting (Section 2.16). These tissue blots were probed with isoform-specific DNA produced by colony PCR (Section 2.13). Three different DNA fragments were amplified from variable 5′ ends of the Na^+, K^+-ATPase α subunits, each of which was isoform-specific (primers listed in Appendix 3). The Na^+, K^+-ATPase α_1 cDNA fragment encompassed nucleotides 1-333 (*Figure 3.2*), the α_2 comprised nucleotides 1-193 (*Figure 3.5*), and the α_3 comprised nucleotides 1-317 (*Figure 3.6*) of the full cDNA sequences. *Figure 4.1* shows expression of the three Na^+, K^+-ATPase α isoforms in the tissues listed above. Each of the α isoforms has an mRNA transcript of ~3.8 kb. The Na^+, K^+-ATPase α_2 and α_3 isoforms were only detected in the brain using Northern blotting, with no visible transcripts in the rectal gland, kidney, gill or gut. Although we have confirmed that these isoforms are present in other tissues by using RT-PCR, Northern blotting was not sensitive enough to observe and quantify expression in these tissues. Na^+, K^+-ATPase α_1 mRNA is highly expressed in

the osmoregulatory tissues, the rectal gland, kidney, gill and intestine, and is also expressed in the atrium, ventricle and brain. Na^+, K^+-ATPase α_1 mRNA is likely to be expressed in all tissues, although levels were below the detectable levels in some tissues, including the liver and interrenal gland. For these tissue distribution blots, RNA from both FW- and SW-acclimated sharks were used, but only the results from the FW RNAs are shown. The same tissue distribution of Na^+, K^+-ATPase mRNA expression was observed in tissues from sharks acclimated to SW.

To compare Na^+, K^+-ATPase mRNA expression in FW- and SW- acclimated fish, a number of RNA samples from tissues from individual sharks acclimated to each salinity were used to prepare quantitative Northern blots. For each tissue to be examined, six RNA samples from FW-acclimated fish and six RNA samples from SW-acclimated were loaded into wells on the same denaturing agarose gel to produce an RNA blot as described in Sections 2.4 and 2.16. These blots were hybridised with DNA probes which were specific to the Na^+, K^+-ATPase α_1 subunit. Quantitative analysis of the radioactive probe hybridised to these blots was carried out using an Instant Imager (Section 2.16) which determined the radioactivity, in counts per minute per unit area, bound to the membrane. Bound radioactivity was corrected for total RNA levels as detailed in Section 2.16. This represents the relative expression of Na^+, K^+-ATPase mRNA in tissues from FW- and SW-acclimated sharks. *Figure 4.2a* shows expression of the ~3.8 kb Na^+, K^+-ATPase α_1 subunit mRNA transcript in 5 μg RNA samples isolated from rectal gland, kidney, gill and intestine from six FW-acclimated and six SW-acclimated sharks. These blots also illustrate the high variability in α_1 expression between fish within the same group. *Figure 4.2b* shows the radioactive intensity in counts per min per μg RNA in the rectal gland, kidney, gill and intestinal samples. Values shown are the mean values and associated standard errors for each tissue in sharks acclimated to each salinity, where n = 6. SW- acclimation had no significant effect on the expression of the Na^+, K^+-ATPase α_1 subunit mRNA in any tissue.

4.3: Determination of Na^+, K^+-ATPase α isoform subunit expression by semi-quantitative RT-PCR

When the full length sequences of all three isoforms were obtained, isoform-specific primers were designed (Appendix 3) to amplify fragments within the 3′ untranslated region of the three isoforms. This region was the most variable between the 3 isoforms. The primers for the α_1, α_2 and α_3 isoforms amplify fragments of 301, 188 and 257 bp respectively. In order to use semi-quantitative RT-PCR technique to compare DNA in samples from different fish, a fragment from a control gene was also amplified. The control gene chosen was β-actin, since the expression of this so called 'housekeeping gene' is unlikely to be dependent on environmental conditions such as salinity and has been used by others as an invariant control. Degenerate primers for β-actin were used to amplify a fragment from *C. leucas* brain cDNA, which was subsequently cloned and sequenced (see Section 7.5 for sequence). Specific primers were then designed in order to amplify a fragment of β-actin of 425 bp. All four sense and antisense primer sets (Na^+, K^+-ATPase α subunit isoforms 1, 2 and 3, and β-actin; Appendix 3) were added to each PCR tube. A master mix was prepared for six reactions, including primers and template cDNA, and then aliquoted into six separate tubes to be removed from the PCR machine at the intervals required. Reaction parameters for standard RT-PCR were set (Section 2.7). For verification of the technique, *Figure 4.3* shows the products of semi quantitative RT-PCR at the completion of 15, 20, 25, 30, 35 and 40 cycles using all four primer sets with *C. leucas* cDNA. Band intensity measured by image analysis (Gene Snap and Gene Tools, Sygene) was representative of the quantity of DNA at each cycle, and this increases with increasing cycle number. As illustrated in *Figure 4.3*, this technique clearly showed that within all tissues, expression of α_1 was highest, with much less expression of α_2, and very low levels of expression of α_3.

This semi-quantitative RT-PCR technique was used to compare expression of each isoform in tissues from sharks acclimated to FW and SW. For each of the four tissues, rectal gland, kidney, gill and intestine, three separate cDNAs were prepared from RNAs extracted from both FW- and SW-acclimated sharks. These cDNAs were used as templates for semi-quantitative RT-PCR as described above, with individual tubes removed at the completion of 16,

18, 20, 22, 24, 26, 28, 30, 35 and 40 cycles. This resulted in ten reaction products per cDNA. Since there were a total of six cDNAs from each tissue (three FW and three SW) there was a total of sixty reaction products per tissue. A 5ul aliquot of each product was loaded onto a non denaturing agarose gel (Section 2.9); all of the products from one tissue were loaded onto the same gel to allow direct comparison. The band intensities of each product were recorded and analysed using Gene Snap and Gene Tools software (Section 2.14). For each cycle number recorded, the band intensity of each α isoform was expressed as a percentage of the band intensity found for β-actin (Tolentino *et al.*, 2002). To compare FW and SW expression of α isoforms, the mean and standard error for FW and SW samples from each tissue at each cycle number were calculated and plotted (*Figures 4.4 - 4.7*). A two way ANOVA was performed followed by Fisher's PLSD post analysis of significance for FW and SW data at each cycle number. Asterisks indicate a significant difference in the level of expression of Na^+, K^+-ATPase α isoform cDNA at $p < 0.05$ between FW- and SW-acclimated sharks. Only α_1 and α_2 are plotted for the intestine, since the amount of α_3 amplified from the tissue was only detectable at cycle numbers 35 and 40. These figures show no significant differences in expression of Na^+, K^+-ATPase α isoforms in tissues of FW- and SW-acclimated sharks. In some samples there were significant differences in α/β-actin ratios between FW and SW kidney and gill (*Figures 4.5 and 4.6*) samples but these were not consistently found after all cycles so overall there was no significant difference in Na^+, K^+-ATPase expression.

4.4: Determination of Na^+, K^+-ATPase β_1 subunit mRNA expression by Northern blotting

Expression of the Na^+, K^+-ATPase β_1 subunit in tissues of *C. leucas* was performed as described in Section 4.2. A single fragment of probe DNA was amplified for the Na^+, K^+-ATPase β_1 subunit, from nucleotide positions 449-1080 of the full length cDNA sequence (*Figure 3.12;* All Na^+, K^+-ATPase β primers, Appendix 3). *Figure 4.8* shows the Na^+, K^+-ATPase β_1 subunit distribution. The β_1 subunit mRNA transcript is ~2.2 kb and was expressed in all tissues examined. Expression of the Na^+, K^+-ATPase β_1 subunit mRNA transcript in 5 μg RNA samples isolated from rectal gland, kidney, gill and intestine from six FW-acclimated and six SW-acclimated sharks is shown in *Figure 4.9a*. Northern blots revealed two or in some fish three different sized

Na^+, K^+-ATPase β_1 subunit mRNA transcripts in rectal gland and in some cases also in the kidney and gill. Again, high variability in expression between fish was observed. *Figure 4.9b* shows the counts per minute per μg RNA resulting from the probe hybridised to rectal gland, kidney, gill and intestinal samples. Values shown are the mean values and associated standard errors for each tissue in each salinity where n = 6. There was no significant difference in β_1 subunit mRNA expression between tissues from FW- and SW-acclimated fish.

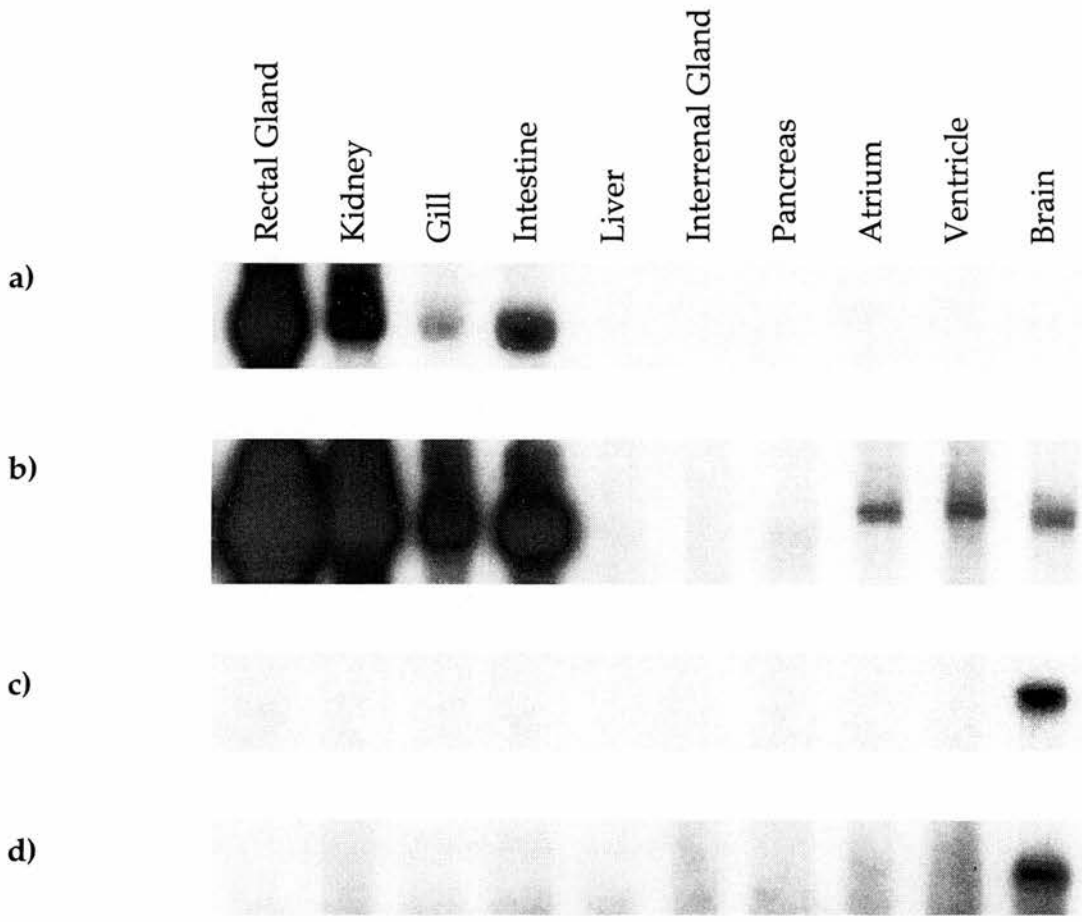

Figure 4.1: Expression of Na^+, K^+-ATPase α subunit isoform mRNA in bull shark tissues determined by Northern blotting. Autoradiographs indicating the levels of expression in various bull shark tissues. All mRNA transcripts are ~3.8 kb in size. **a)** α_1 expression autoradiograph after 5 hour exposure to the blot at –80°C; **b)** α_1 expression after 18 hour exposure; **c)** α_2 expression after 5 hour exposure; **d)** α_3 expression after 5 hour exposure. Na^+, K^+-ATPase α_1 isoform mRNA is highly expressed in rectal gland, kidney, gill and intestine, and is also expressed at lower levels in the atrium, ventricle and brain. Na^+, K^+-ATPase α_2 and α_3 isoforms are expressed primarily in the brain.

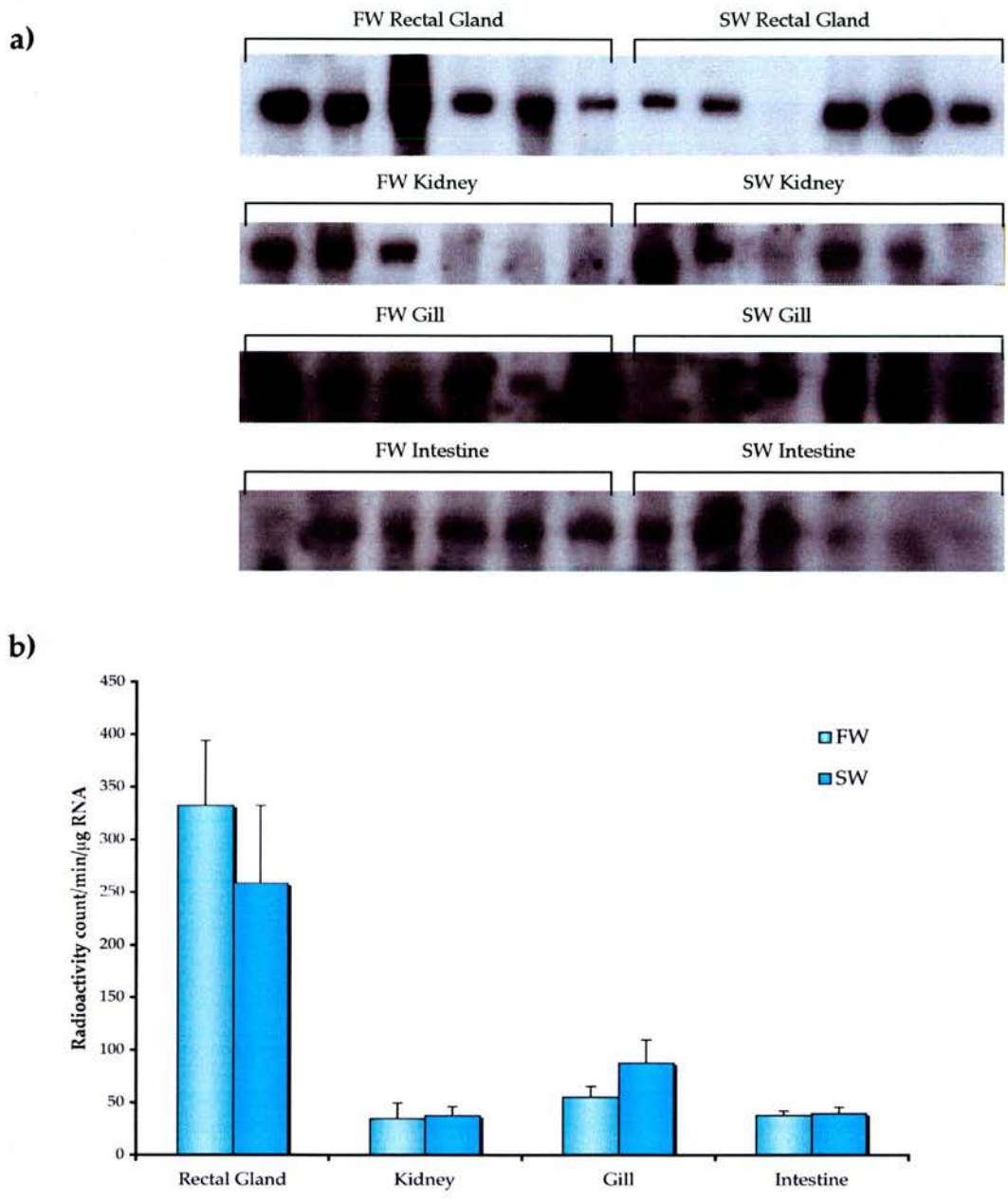

Figure 4.2: Expression of Na^+, K^+-ATPase α_1 subunit mRNA in tissues from FW- and SW-acclimated fish determined by Northern blotting. **a)** Autoradiographs indicating the levels of expression in FW- and SW-acclimated bull shark rectal gland (after 5 hour exposure to the blot at –80°C), kidney, gill and intestine (all after 18 hour exposure). For each sample, 5 µg of RNA was used. **b)** Average radioactivity counts per µg of RNA per minute representing the amount of Na^+, K^+-ATPase α_1 subunit mRNA expression in rectal gland, kidney, gill and intestine from FW- or SW-acclimated sharks, using data obtained from *Fig. 4.2a* (mean ± s.e.). For all tissues, n=6, and data were analysed using two way ANOVA and Fisher's PLSD test which indicated no significant difference in expression of Na^+, K^+-ATPase α_1 subunit mRNA between tissues from FW- and SW-acclimated fish.

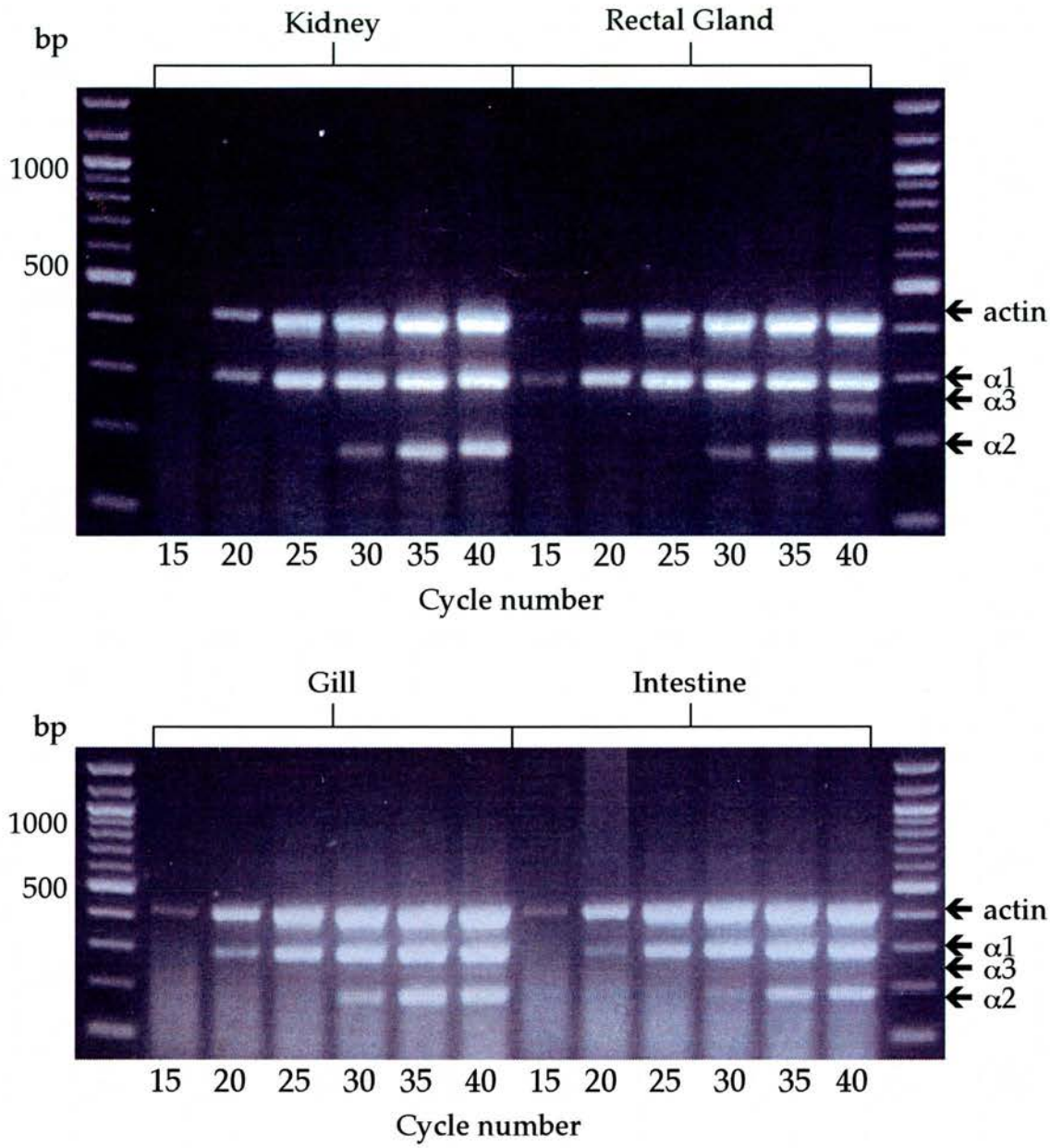

Figure 4.3: RT-PCR amplification of Na^+, K^+-ATPase α subunit isoforms and β-actin. Fragments of Na^+, K^+-ATPase α subunit isoforms and actin from *C. leucas* kidney, rectal gland, gill and intestine cDNA templates. The size of each fragment (in bp) is as follows: α_1, 301; α_2, 188; α_3, 257; actin, 425. DNA concentration represented by band intensity increases with increasing cycle number. Of the three α isoforms, α_1 is expressed in the greatest quantity, followed by α_2, and α_3 displays very low abundance.

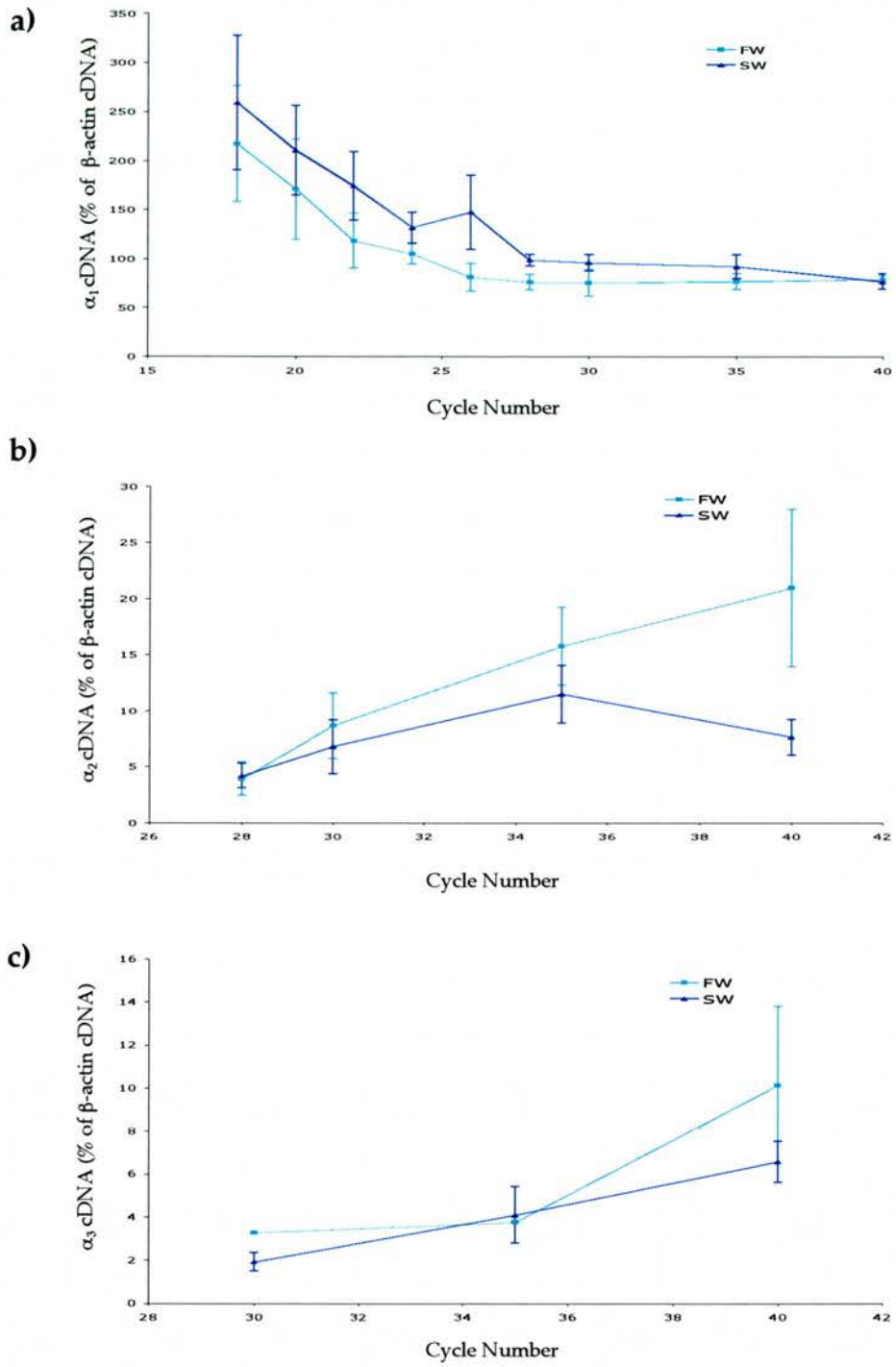

Figure 4.4: Semi-quantitative analysis of RT-PCR amplifications of Na^+, K^+-ATPase α subunit isoforms in the rectal gland. Abundance of Na^+, K^+-ATPase α subunit isoform cDNA relative to β-actin cDNA amplified from rectal gland cDNA templates from FW- or SW-acclimated *C. leucas* (means and s.e.). n = 3; data were analysed using two way ANOVA and Fisher's PLSD test, which indicated no significant difference in the level of expression of Na^+, K^+-ATPase α isoform cDNA between FW- and SW-acclimated sharks. **a)** α_1, **b)** α_2, **c)** α_3. RT-PCR gels not shown.

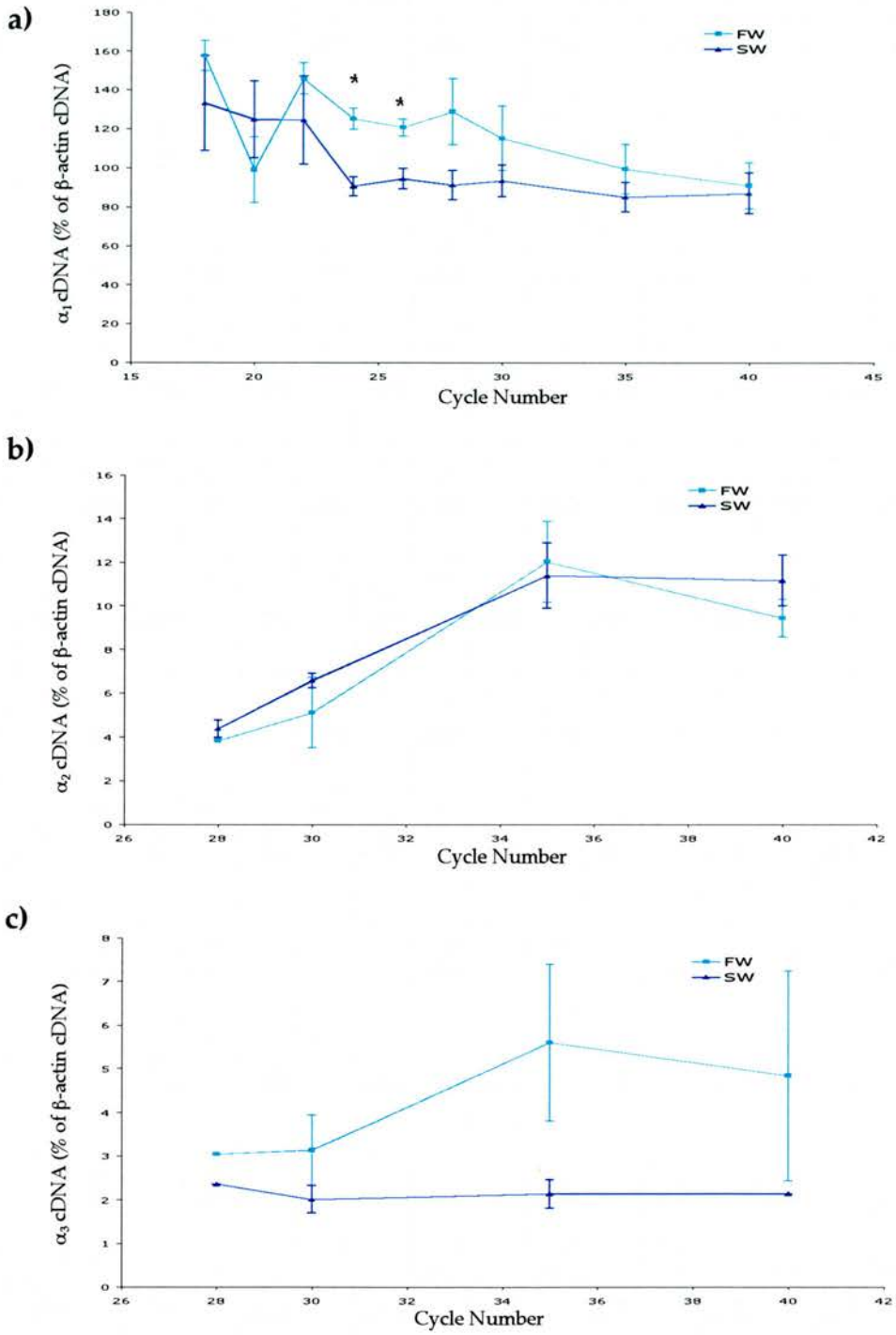

Figure 4.5: Semi-quantitative analysis of RT-PCR amplification of Na^+, K^+-ATPase α subunit isoforms in the kidney. Each graph shows the abundance of Na^+, K^+-ATPase α subunit isoform cDNA relative to β-actin cDNA amplified from kidney cDNA templates from FW- or SW-acclimated *C. leucas* (means and s.e.). n = 3; data were analysed using to way ANOVA and Fisher's PLSD test, asterisks indicate a significant difference in the level of expression of Na^+, K^+-ATPase α isoform cDNA at $p < 0.05$ between FW- and SW-acclimated sharks. **a)** α_1, **b)** α_2, **c)** α_3. RT-PCR gels not shown.

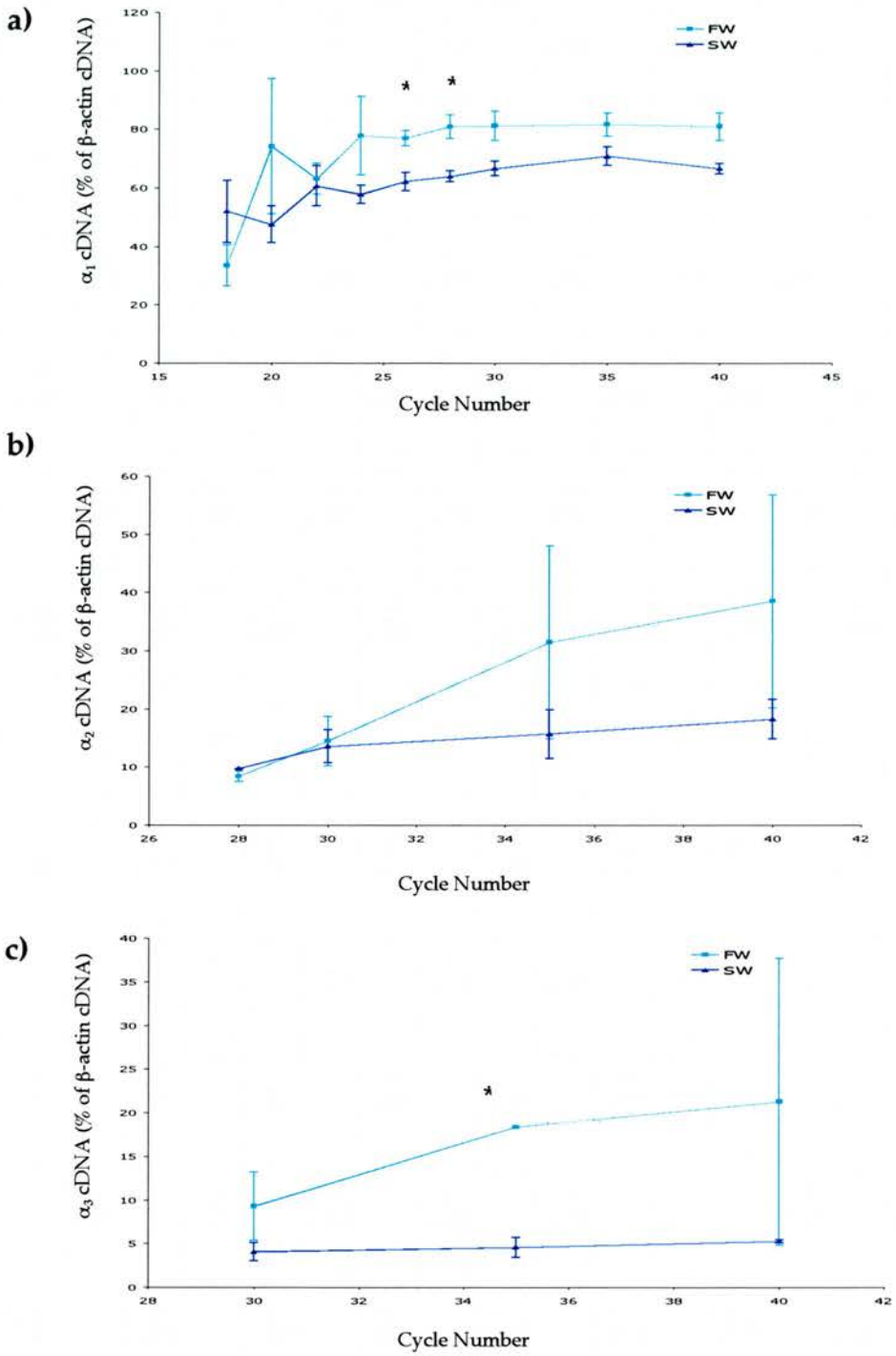

Figure 4.6: Semi-quantitative analysis of RT-PCR amplification of Na^+, K^+-ATPase α subunit isoforms in the gill. Each graph shows the abundance of Na^+, K^+-ATPase α subunit isoform cDNA relative to β-actin cDNA amplified from gill cDNA templates from FW- or SW-acclimated *C. leucas* (means and s.e.). n = 3; data were analysed using to way ANOVA and Fisher's PLSD test, asterisks indicate a significant difference in the level of expression of Na^+, K^+-ATPase α isoform cDNA at $p < 0.05$ between FW- and SW-acclimated sharks. **a)** α_1, **b)** α_2, **c)** α_3. RT-PCR gels not shown.

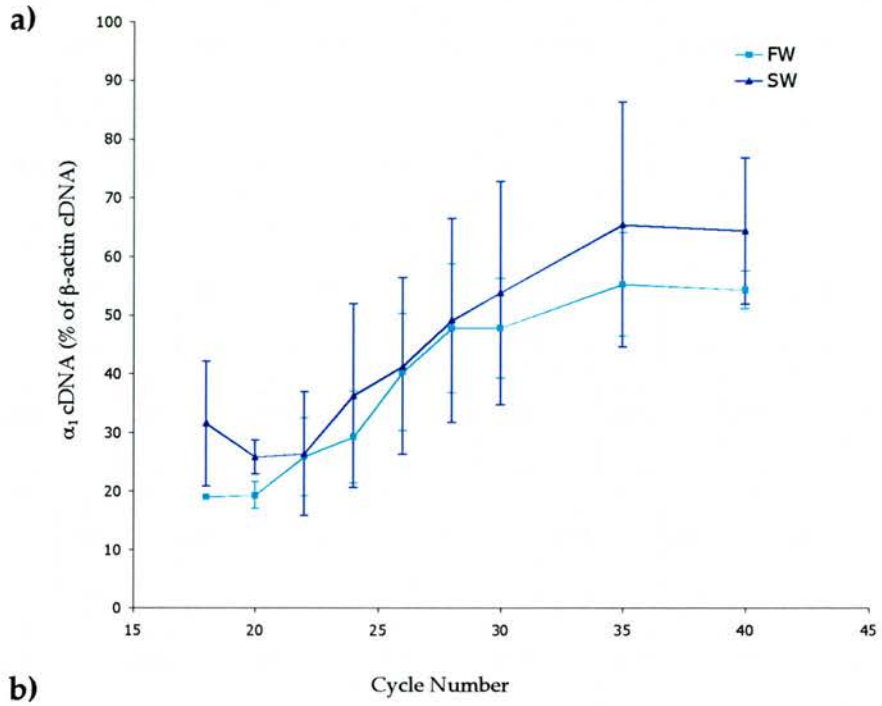

Figure 4.7: Semi-quantitative analysis of RT-PCR amplification of Na^+, K^+-ATPase α subunit isoforms in the intestine. Each graph shows the abundance of Na^+, K^+-ATPase α subunit isoform cDNA relative to β-actin cDNA amplified from intestine cDNA templates from FW- or SW-acclimated *C. leucas* (means and s.e.). n = 3; data were analysed using to way ANOVA and Fisher's PLSD test, which indicated no significant difference in the level of expression of Na^+, K^+-ATPase α isoform cDNA between FW- and SW-acclimated sharks. **a)** α_1, **b)** α_2. RT-PCR gels not shown.

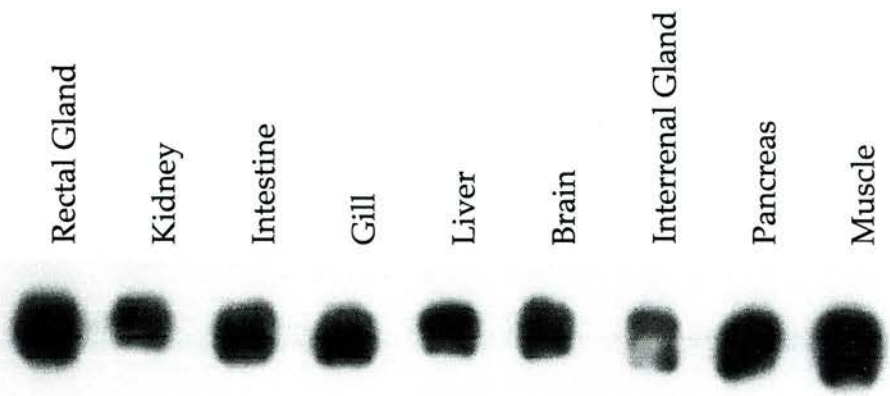

Figure 4.8: Expression of Na^+, K^+-ATPase β_1 subunit mRNA in bull shark tissues determined by Northern blotting. Autoradiograph indicating the levels of expression in various bull shark tissues. The mRNA transcripts are ~2.2 kb in size. Na^+, K^+-ATPase β_1 subunit expression autoradiograph after 8 hour exposure to the blot at –80°C. Na^+, K^+-ATPase β_1 subunit mRNA is expressed in rectal gland, kidney, intestine, gill, liver, brain, interrenal gland, pancreas and skeletal muscle.

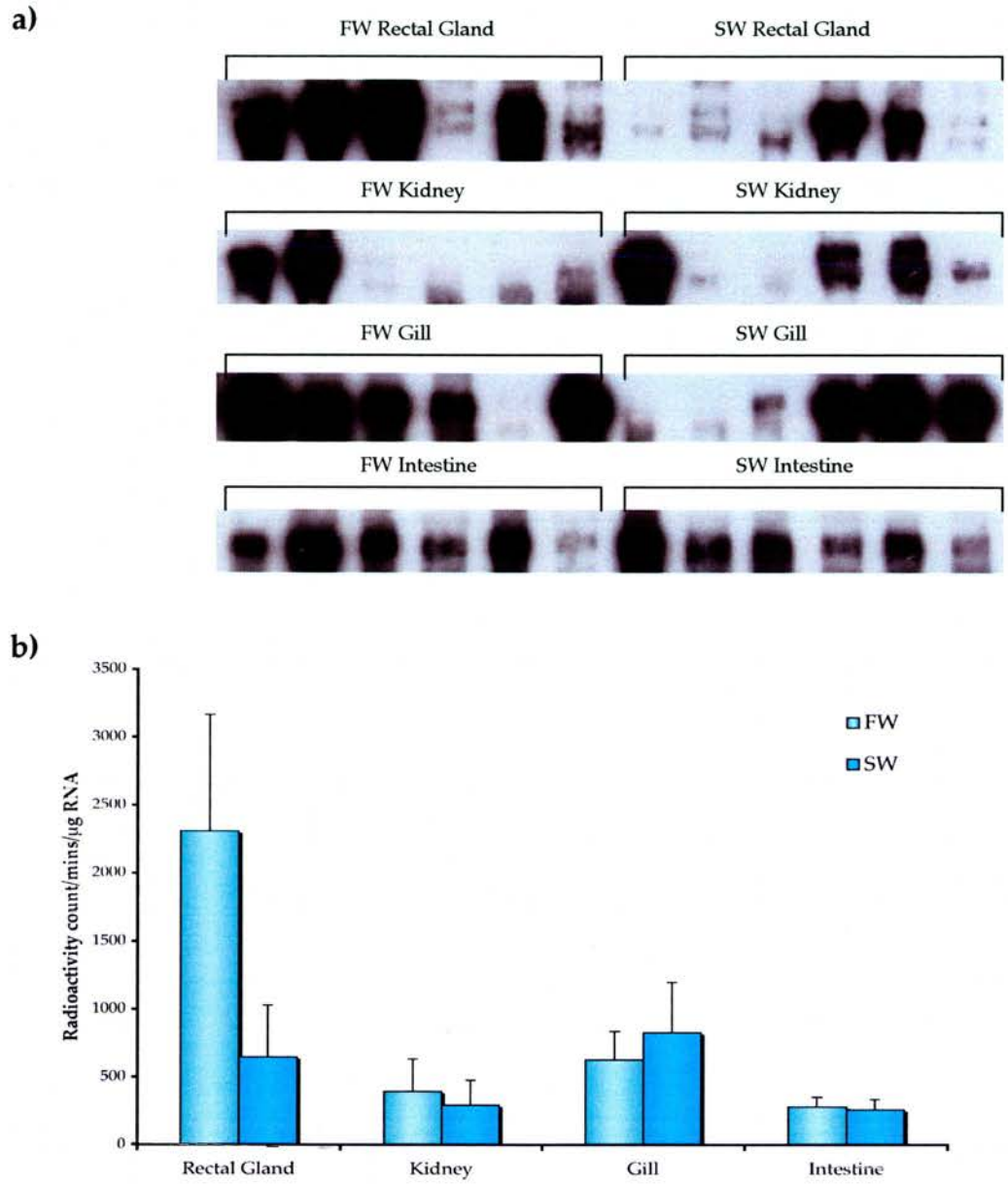

Figure 4.9: Expression of Na^+, K^+-ATPase β_1 subunit mRNA in tissues from FW- and SW-acclimated fish determined by Northern blotting. **a)** Autoradiographs indicating the levels of expression in FW- and SW-acclimated bull shark rectal gland (after 8 hour exposure to the blot at –80°C), kidney, gill and intestine (all after 18 hour exposure. For each sample, 5 µg of RNA was used. **b)** Average radioactivity counts per µg of RNA per minute representing the amount of Na^+, K^+-ATPase β_1 subunit mRNA expression in rectal gland, kidney, gill and intestine from FW- or SW-acclimated sharks, using data obtained from *Fig. 4.9a* (mean ± s.e.). For all tissues, n=6, and data were analysed using two way ANOVA and Fisher's PLSD test which indicated no significant difference in expression of Na^+, K^+-ATPase β_1 subunit mRNA between tissues from FW- and SW-acclimated fish.

4.5: Expression of Na^+, K^+-ATPase α and β subunit mRNAs in the osmoregulatory tissues of bull sharks acclimated to FW and SW

Northern blots supporting RNA isolated from various tissues from FW- and SW- acclimated *C. leucas* were used to determine the tissue-specific expression of the Na^+, K^+-ATPase α subunit isoforms in *C. leucas*. Since this enzyme is vital for cell homeostatis, Na^+, K^+-ATPase expression should be ubiquitous in all tissues. The mRNA transcripts of ~3.8 kb in size representing Na^+, K^+-ATPase α_1 subunit isoform were expressed predominantly in the osmoregulatory tissues, with the highest levels of expression in the rectal gland. High levels of α_1 subunit mRNA were also present in the kidney, intestine and gill with lower levels in the heart (atrium and ventricle), and the brain. Na^+, K^+-ATPase α_1 subunit isoform mRNA was not detected in the liver, interrenal gland or pancreas using this technique, although cDNA fragments could be amplified from these tissues using Na^+, K^+-ATPase primers and RT-PCR (results not shown). Na^+, K^+-ATPase α_2 and α_3 subunit isoform mRNA transcripts of ~3.8 kb were only detected in Northern blots supporting samples from the brain. In other vertebrates, the Na^+, K^+-ATPase α_2 subunit isoform is predominantly expressed in muscle tissue, and at a lesser extent in the brain. In mammals, the Na^+, K^+-ATPase α_3 subunit isoform is the principle isoform expressed in nervous tissue, but is also found in cardiac tissue during development (Blanco and Mercer, 1998). Neither α_2 or α_3 were expressed at detectable levels on Northern blots of RNA from the atrium or ventricle of *C. leucas*.

The size of the Na^+, K^+-ATPase α_1 subunit isoform mRNA transcript is similar to those found in other elasmobranchs and teleost fish. A mRNA transcript of 3.6 kb was identified in the rectal gland of *S. canicula* (Mackenzie *et al.*, 2002), and ~4.0 kb in the electric organ of *T. californica* (Kawakami *et al.*, 1985). In *A. anguilla*, a Na^+, K^+-ATPase α_1 subunit isoform mRNA transcript of 3.5 kb was expressed primarily in the intestine, but also in the kidney, brain and gill, with much lower levels in the eye, oesophagus, pancreas, liver and spleen. Na^+, K^+-ATPase α_1 subunit isoform was not present at detectable levels in cardiac or skeletal muscle (Cutler *et al.*, 1995[a]).

This is in contrast to *C. leucas* where Na^+, K^+-ATPase α_1 subunit isoform was detected in the heart, but not in the liver or pancreas.

In adult rat tissues, the isoforms of the Na^+, K^+-ATPase α subunit were found to be differentially expressed (Schneider *et al.*, 1988). Like in *C. leucas*, all three isoforms are highly expressed in the rat brain. Na^+, K^+-ATPase α_1 subunit isoform was expressed throughout the tissues examined (brain, diaphragm, intestine, heart, kidney, spinal cord), whereas the Na^+, K^+-ATPase α_2 subunit isoform was found in the brain and diaphragm, and at low levels in the heart, but was not expressed at detectable levels in the intestine or kidney. Na^+, K^+-ATPase α_3 subunit isoform was only expressed in the brain and in the spinal cord (Schneider *et al.*, 1988). This pattern of expression is similar to that found in *C. leucas*.

Expression of Na^+, K^+-ATPase α_1 subunit mRNA in the osmoregulatory tissues of the FW juvenile bull shark was not altered followng a 7-day acclimation to SW. Northern blotting techniques did not indicate any significant differences in Na^+, K^+-ATPase α_1 subunit mRNA expression in rectal gland, kidney, gill or intestine RNA from *C. leucas* acclimated to FW or SW for 7-days. For further validation of the results from the Northern blotting technique, semi-quantitative RT-PCR analysis of Na^+, K^+-ATPase α_1 subunit isoform expression also indicated that mRNA abundance was unchanged in the rectal gland, kidney, gill and intestine of FW- and SW-acclimated *C. leucas*. Data from all tissues from *C. leucas* were compared at each RT-PCR cycle number interval as described in Section 4.3. The results from all cycle numbers are equivalent and only two out of nine assay points showed any significant signs of differential expression. Signs of upregulation or downregulation were not consistently found at all points, therefore overall, no significant difference was found.

Since RT-PCR is a more sensitive technique than Northern blotting, it was also used to examine the expression of Na^+, K^+-ATPase α_2 and α_3 subunit isoforms in the rectal gland, kidney, gill and intestine of *C. leucas*. RT-PCR has previously been used to demonstrate expression of all three Na^+, K^+-ATPase α subunit isoform cDNAs from the brain, gill, heart, kidney and

skeletal muscle of *T. bernacchii* (Guynn *et al.*, 2002). Expression of these Na^+, K^+-ATPase α_2 and α_3 subunit isoforms in *C. leucas* tissues is much less than that of the Na^+, K^+-ATPase α_1 subunit isoform. This would be expected since these isoforms were not expressed at detectable levels on Northern blots. Expression of Na^+, K^+-ATPase α_3 subunit isoform was only detectable in the intestine of FW- and SW-acclimated *C. leucas* after 35 and 40 cycles, therefore a graph for these data could not be plotted. There was no significant difference in expression of Na^+, K^+-ATPase α_2 or α_3 subunit isoforms in any of the tissues examined from FW- and SW-acclimated *C. leucas*.

Northern blots supporting RNA isolated from various tissues from *C. leucas* acclimated to FW and SW were used to determine the tissue-specific expression of the Na^+, K^+-ATPase β_1 subunit in *C. leucas*. The ~2.2 kb Na^+, K^+-ATPase β_1 subunit mRNA transcripts were ubiquitously expressed throughout the tissues analysed. The size of this transcript is the same as that reported for the Na^+, K^+-ATPase β_1 subunit mRNA in the rectal gland of *S. canicula* (Mackenzie *et al.*, 2002). In *A. anguilla*, the size of the Na^+, K^+-ATPase β_1 subunit isoform mRNA transcript was reported as 2.35 kb and was found to be expressed at high levels in the intestine, ovary, kidney, marginally lower levels in the brain, spleen, oesophagus, eye and pancreas, intermediate levels in the gill, and low levels in skeletal muscle. In *A. anguilla*, the Na^+, K^+-ATPase β_1 subunit isoform mRNA expression was below detectable levels in the heart and liver (Cutler *et al.*, 1995[b]).

Upon examination of the literature, the effect of salinity on the levels of expression of Na^+, K^+-ATPase mRNA is not consistent amongst fish. Any observed changes in the expression of Na^+, K^+-ATPase after transfer between salinities may be affected by many variables, for example, the salinity of the water in which the fish was collected, the salinity transfer process, the time left to acclimate prior to sampling and the number of time points examined. Where possible it is preferable to collect a series of time points after transfer in order to carefully determine temporal changes in expression following transfer. The ability to do this depends on the availability of the model species being studied, and in the case of *C. leucas*, it was only possible to examine a single time point.

In many teleosts studied, branchial Na^+, K^+-ATPase α and β subunit mRNA expression is increased after transfer from FW to SW. There was a significant increase in Na^+, K^+-ATPase α_1 subunit isoform mRNA expression in the gills of *A. anguilla* transferred from FW to SW (Cutler *et al.*, 1995[a]). The Na^+, K^+-ATPase β_1 subunit mRNA abundance was also greater in *A. anguilla* transferred to SW and 200% SW, compared to the control FW group (Cutler *et al.*, 1995[b]). After 3 weeks of adaptation from FW to SW, Na^+, K^+-ATPase α_1 mRNA expression in the gills and also the gut of *O. mykiss* were increased (Kisen *et al.*, 1994). In *O. mossambicus*, branchial Na^+, K^+-ATPase α_1 subunit mRNA expression increased parallel to an increase in environmental salinity. Fish transferred from FW to 10 ppt, 20 ppt and 30 ppt exhibited a greater increase in Na^+, K^+-ATPase mRNA expression with the maximum Na^+, K^+-ATPase α_1 mRNA expression levels observed at 30 ppt (Hwang *et al.*, 1998).

In some species, Na^+, K^+-ATPase mRNA expression in osmoregulatory tissues is not always altered by salinity change. In *S. trutta*, renal Na^+, K^+-ATPase α_1 subunit mRNA expression and activity were unchanged after transfer from FW to 25 ppt SW (Madsen *et al.*, 1995). There was no significant difference in *S. sarba* branchial Na^+, K^+-ATPase α or β subunit mRNA expression between the control SW group (33 ppt) and a group acclimated to 6 ppt for 3 weeks (Deane *et al.*, 1999).

Increases in Na^+, K^+-ATPase mRNA expression are usually (but not always) coupled to an increase in Na^+, K^+-ATPase activity. In *S. trutta*, branchial Na^+, K^+-ATPase α_1 subunit isoform mRNA expression increased within 1 day of transfer from FW to 25 ppt SW, which was followed 24 hours later by an increase in Na^+, K^+-ATPase activity (Madsen *et al.*, 1995). In *D. labrax*, branchial Na^+, K^+-ATPase subunit mRNA expression increased 5 fold ten days after transfer from 15 ppt to 50 ppt. Expression was also increased following transfer of fish from 15 ppt to FW compared to the 15 ppt control group (Jensen *et al.*, 1998). It is perhaps not surprising that Na^+, K^+-ATPase mRNA expression levels rise in both FW and SW conditions, since the control group was exposed to 15 ppt, which would be much closer to the plasma osmolality of *D. labrax*. For fish transferred to either 50 ppt or FW, external conditions would be very different from the internal plasma

composition and therefore expression of osmoregulatory proteins would be increased. Importantly, a rise in the expression of Na^+, K^+-ATPase mRNA was observed several days prior to a rise in Na^+, K^+-ATPase activity (Jensen *et al.*, 1998). This implicates other regulatory mechanisms in controlling Na^+, K^+-ATPase activity, such as recruitment to the plasma membrane. A similar lag in Na^+, K^+-ATPase activity following an increase in Na^+, K^+-ATPase α subunit mRNA expression was observed in *S. salar* smolts (D'Cotta *et al.*, 2000).

There was no significant difference in the Na^+, K^+-ATPase activity in the gill or intestine of *C. leucas* after 7-day acclimation to SW (Pillans *et al.*, 2005), and consequently a change in branchial or intestinal mRNA expression would not be expected. However, a significant difference in Na^+, K^+-ATPase activities in *C. leucas* rectal gland and kidney were reported following FW-SW transfer (Pillans *et al.*, 2005). The present study found no significant difference in the expression of Na^+, K^+-ATPase α or β subunit mRNA transcripts in these tissues from 7-day FW- and SW-acclimated *C. leucas*. This indicates that the reported change in Na^+, K^+-ATPase activity must be independent of Na^+, K^+-ATPase α or β subunit mRNA abundance. Na^+, K^+-ATPase activity may be altered by the regulation of protein translation, the activation and recruitment of preformed protein subunits into the plasma membrane, phosphorylation of the enzyme, and/or the actions of associated proteins. These mechanisms of regulation have been discussed previously in Section 1.6.4.

A study of Na^+, K^+-ATPase expression and activity in *S. canicula* after a feeding event provides an example for the current study since both feeding and transfer to increased salinity will have the effect of increasing the salt load on the fish. Nine hours after a feeding event, Na^+, K^+-ATPase activity increased markedly in the rectal gland of *S. canicula*, and this returned to control levels after 24 hours (MacKenzie *et al.*, 2002). The increase in activity was not caused by any increase in Na^+, K^+-ATPase mRNA expression. This suggests that the acute and transient upregulation of the Na^+, K^+-ATPase activity may be occurring in the rectal gland of S. *canicula* at some point downstream of transcriptional regulation. Levels of Na^+, K^+-ATPase α and β

subunit mRNAs did rise 2 days after a feeding event, but returned to control levels by the third day. Again on day 5, mRNA expression of both subunits increased. There was a decrease to control levels of the β subunit mRNA expression by day 7, however expression levels of α subunit mRNA were maintained throughout the experimental period (10 days). These increases may be in response to dietary input, since elasmobranchs are thought to feed intermittently, and therefore the slow release of salt in the intestine after feeding may be responsible for this increase in Na^+, K^+-ATPase mRNA expression (MacKenzie *et al.*, 2002). This study supports the proposal that changes in Na^+, K^+-ATPase activity in the elasmobranch are not fully dependent on the expression of Na^+, K^+-ATPase mRNA transcripts, and that other mechanisms of regulation are in action.

Expression of Na^+, K^+-ATPase α subunit isoforms was investigated in *O. mykiss* by RT-PCR (Richards *et al.*, 2003). This study found three duplicates of Na^+, K^+-ATPase α_1, and found that these were differentially expressed in the tissues. Na^+, K^+-ATPase α_{1a} expression in the gill of *O. mykiss* decreased after transfer from FW to 40% SW and 80% SW. However, Na^+, K^+-ATPase α_{1b} expression decreased after transfer to 40% SW, but increased again after transfer to 80% SW. Expression of the third α_1 duplicate (α_{1c}) and also the α_3 isoform was unchanged after transfer (Richards *et al.*, 2003).

In *F. heteroclitus*, a similar method was employed to monitor Na^+, K^+-ATPase α_1 subunit isoform expression at various time points before, during and after transfer from brackish water (BW; 10 ppt) to FW, BW, or SW. There is a significant initial increase in Na^+, K^+-ATPase α_1 subunit isoform mRNA expression in the gills of *F. heteroclitus* transferred to SW, but this had returned to pre-transfer levels within four days. The initial increase of Na^+, K^+-ATPase α_1 subunit isoform mRNA expression in the gills of FW-transferred *F. heteroclitus* is less than that of SW-transferred animals, but it continues to increase for four days, after which it returns to pre-transfer levels. If the Na^+, K^+-ATPase mRNA expression levels of only pre-transfer and 7-day transfer animals were compared, there would be no significant different in expression, despite there being a large increase in expression of this enzyme for both FW- and SW-transferred fish earlier in the time course

(Scott *et al.*, 2004). This finding has significant implications to the present study in which animals were only sampled after a 7-day period.

The data presented in Sections 4.1-4.4 suggest that Na^+, K^+-ATPase α and β subunit mRNA expression is unchanged in *C. leucas* rectal gland, kidney, gill and intestine after transfer of fish from FW to SW, and that the changes in Na^+, K^+-ATPase activity previously reported in the rectal gland and kidney (Pillans *et al.*, 2005) must occur downstream of transcriptional regulation.

5

Expression and distribution of Na^+, K^+-ATPase α and β subunit proteins in osmoregulatory tissues of FW- and SW-acclimated bull sharks

Results

5.1: Evaluation of Na^+, K^+-ATPase α_1 subunit protein expression by Western blotting.

Using SDS polyacrylamide gel electrophoresis (PAGE; Section 2.18), proteins contained in tissue homogenates (as prepared in Section 2.17) from bull shark rectal gland, kidney, gill and intestine were size separated and transferred to a PVDF membrane (Section 2.20). Purified Na^+, K^+-ATPase α_1 subunit antibodies were used in conjunction with Western blotting techniques (Section 2.22), to detect and quantify the Na^+, K^+-ATPase α_1 subunit protein.

The N-terminal epitope sequence recognised by the Na^+, K^+-ATPase α_1 subunit antibody is indicated in *Figure 2.18*. Due to the high levels of sequence heterology at the N-terminal, the antibody is likely to be highly specific for the Na^+, K^+-ATPase α_1 isoform. The optimal antibody dilution was determined by using a range of dilutions of the affinity purified antibody and by observing the signal strength on the PVDF membranes. Membranes supporting all four of the osmoregulatory tissues, the rectal gland, kidney, gill and intestine were used for determining the optimal antibody dilution. The primary Na^+, K^+-ATPase α_1 isoform-specific antibody was purified as in Section 2.21, and the optimal dilution was found to be 1 in 5000. It was found that optimal immunoreactive signals were obtained if the protein samples loaded onto the SDS PAGE gel were not boiled prior to loading but instead were incubated at room temperature for 15 minutes with sample preparation solution (Section 2.18). Protein samples of 100 μg were prepared as in Section 2.18 and loaded in the first instance to compare expression between tissues. *Figure 5.1a* shows Na^+, K^+-ATPase α_1 subunit expression in representative tissue samples from both FW- and SW-acclimated fish. A single strong immunoreactive band with a molecular weight of approximately 95 kDa was present in all tissues. *Figure 5.1b* shows a control Western blot, loaded with 100 μg tissue protein as for the previous blot, but probed with pre-immune serum, also diluted 1:5000. Although this is not directly comparable with the affinity purified antibody, no protein

eluted from the affinity column with acid wash when pre-immune serum is applied. No immunopositive bands were visible on this blot.

To compare Na^+, K^+-ATPase α_1 subunit protein expression in individual tissues from FW- and SW- acclimated fish, a number of samples from different fish were separated on the same blot. It was necessary to reduce the protein concentration used for tissues with high Na^+, K^+-ATPase α_1 subunit protein expression in order not to saturate the binding signal response and therefore to reliably examine potential differences in expression between FW- and SW- acclimated fish. *Figure 5.2a* shows ~95 kDa immunopositive bands representing expression of the Na^+, K^+-ATPase α subunit protein present in kidney (5 μg) or gill and intestinal (25 μg) samples prepared from FW- and SW- acclimated fish. Regrettably, no rectal gland tissue from SW-acclimated sharks was collected for protein extraction, therefore Na^+, K^+-ATPase protein expression in rectal glands from FW- and SW-acclimated fish could not be compared. As described in Section 2.22, the intensity of immunopositive bands was determined using a CCD camera and analytical software packages Gene Tools and Gene Snap (Syngene). The raw values of the immunopositive band intensities were noted and analysed. *Figure 5.2b* shows the relative intensities of immunopositive bands in the kidney, gill and intestine. Values shown are the mean raw values and associated standard errors for each tissue at each salinity (N = 4 for kidney, and N = 5 for gill and intestine). Data were analysed using two way ANOVA and Fisher's PLSD test, which confirmed no significant difference in expression of Na^+, K^+-ATPase α subunit protein in any tissue between FW- and SW-acclimated fish. Analysis of results clearly indicated that SW acclimation has no effect on the expression of Na^+, K^+-ATPase α_1 subunit protein in kidney, gill or intestine.

5.2: Evaluation of Na^+, K^+-ATPase β_1 subunit protein expression by Western blotting.

The methods for studying the expression of Na^+, K^+-ATPase β_1 subunit protein were as described for the α_1 subunit. As shown in *Figure 2.18*, the Na^+, K^+-ATPase β_1 subunit antibody recognises an epitope sequence located within the extracellular domain of the protein. The optimal antibody dilution for the purified Na^+, K^+-ATPase β_1 subunit antibody was found to be

1 in 60. When optimising immunoreactive signals with the Na^+, K^+-ATPase β_1 subunit antibody, there was no difference in signal strength of bands on Western blots if the proteins were boiled or incubated at RT in sample preparation solution prior to loading onto the SDS PAGE gel as described for α_1. *Figure 5.3a* shows Na^+, K^+-ATPase β_1 subunit expression in representative tissue samples from both FW- and SW- acclimated fish. Protein samples from tissues from individual fish were not boiled and 100 μg of protein was loaded into each well. The primary antibody used was affinity purified as in Section 2.21, and used at a dilution of 1:60 for Western blotting. A series of bands ranging from 45-55 kDa were present in all tissues. A control Western blot was also performed, loaded with 100 μg protein samples from each tissue but probed with pre-immune serum, also diluted 1:60. Although this is not equivalent to the affinity purified antibody, *Figure 5.3b* shows that no bands of the same size as those found with the Na^+, K^+-ATPase β_1 subunit antibody were seen with the diluted pre-immune serum.

The comparison of Na^+, K^+-ATPase β_1 subunit protein expression in tissues from FW- and SW- acclimated fish was performed as described for the Na^+, K^+-ATPase α_1 subunit. Since the β_1 subunit protein immunopositive band was not as intense as the α_1 subunit band, 100 μg protein samples were loaded for all tissues to optimise signal strength. *Figure 5.4a* shows the series of bands from ~45-55 kDa representing the levels of β_1 subunit protein expression in kidney samples taken from four FW- and four SW- acclimated fish, and in gill and intestine samples taken from five FW- and five SW-acclimated fish. *Figure 5.4b* shows the relative intensity of immunopositive bands for the Na^+, K^+-ATPase β_1 subunit in the kidney, gill and intestine. Values shown are the raw value means and associated standard errors for each tissue in each salinity (N = 4 for kidney, and N = 5 for gill and intestine). Data were analysed using two way ANOVA and Fisher's PLSD test, which indicated no significant difference in expression of Na^+, K^+-ATPase β_1 subunit protein between FW- and SW- acclimated tissues. Although the bands were very diffuse, image analysis was still possible and this revealed no significant difference in expression of Na^+, K^+-ATPase β_1 subunit protein in any tissue between FW- and SW- acclimated fish.

5.3: Immunolocalisation of Na^+, K^+-ATPase α_1 subunit protein in bull shark tissues

Gill, intestine, kidney and rectal gland samples from FW- and SW-acclimated bull shark were collected and processed for microscopy as described in Section 2.23. Purified primary antibody raised against the bull shark Na^+, K^+-ATPase α_1 subunit protein (*Figure 2.18*) was used for immunolabelling and immunofluorescent light microscopy as described in Section 2.24. For all tissues, the primary antibody was applied to tissue sections at a 1:10 dilution and incubated overnight at 4°C. The secondary FITC-conjugated antibody was applied at a dilution of 1:200, incubated for 1 hour, and covered to protect the fluorescent label antibody from light degradation. Duplicate and sequential sections were treated as above, but with pre-immune serum at 1:10 dilution. These sections were used as comparable controls to gauge the level of autofluorescence in the tissues and are shown alongside the positively stained sections in all figures. These controls showed no positive immunoreactivity with non-specific auto fluorescence being mainly restricted to red blood cells. Additional sections were stained with several different dilutions of the purified primary antibody raised against the bull shark Na^+, K^+-ATPase β_1 subunit protein (*Figure 2.18*), but no specific immunofluorescence was observed (results not shown).

5.4: Distribution of Na^+, K^+-ATPase α_1 subunit protein in the gill

Immunofluorescent staining of sagittal gill sections from FW- and SW-acclimated bull sharks are shown in *Figures 5.5* and *5.6*. *Figure 5.5a* shows representative gill sections taken from bull sharks acclimated to FW, where there is immunopositive staining in mitochondria rich cells (MRCs) along both the primary gill filament (PGF) and the secondary lamellae (SL). A non-specific autofluorescence was observed in the red blood cells (RBC) in all sections. Marginal capillaries (MC) are also identified at the terminal end of each secondary lamellae. In all sections from SW-acclimated sharks, immunopositive staining is restricted to MRCs within the interlamellar regions along the primary gill filament (*Figure 5.6a*). The blood channels, marginal capillaries and autofluorescent red blood cells are again clearly identified. The distribution of Na^+, K^+-ATPase α_1 subunit is markedly

different between sections from FW- and SW- acclimated sharks; in gill sections from FW-acclimated sharks, Na^+, K^+-ATPase is found on both the filament and lamellae, whereas in SW-acclimated sharks it is found primarily along the filament.

5.5: Distribution of Na^+, K^+-ATPase α_1 subunit protein in the intestine

Immunofluorescent staining in sections of the intestine from FW- and SW-acclimated bull sharks is shown in *Figures 5.7a* and *5.8a*. In both salinities, immunopositive staining was seen in the epithelial layer (E) of the villi (V), but not in the lamina propria (LP). These contrast with the pre-immune serum treated sections (*Figures 5.7b* and *5.8b*) where there was only weak background autofluorescence. There were no observable differences in location or abundance of immunofluorescent staining between intestine sections from FW- and SW-acclimated bull sharks.

5.6: Distribution of Na^+, K^+-ATPase α_1 subunit protein in the kidney

Kidney sections from FW-acclimated bull sharks *(Figures 5.9 – 5.11)*, and SW-acclimated bull sharks (*Figure 5.12*) exhibit distinct patterns of immunofluorescent staining. Due to the complex arrangement of the renal tubules in elasmobranchs, kidney sections are challenging to interpret. The tubules types within the kidney are difficult to identify in these sections since the distinguishing characteristics of the tubules are their microanatomy, most of which cannot be observed in fluorescent images. In order to examine cellular detail, adjacent sections would have to be stained with specific histological stains. For example, a periodic acid-Schiff (PAS) stain would reveal the brush border of proximal tubule cells (Lacy and Reale, 1985[a]; Lacy and Reale, 1985[b]). All definitive sub-segment identifications (Proximal I, II or III) are made by the examination of subcellular microanatomical features. Unfortunately, histological staining was not carried out on these sections. Tubules may also be identified by their position in a particular zone of the kidney, and without accompanying low magnification microscopy sections, it is difficult to establish whether the section are from the bundle zone or sinus zone of the kidney. However, after consultation with Dr. E. Lacy (Medical University of South Carolina), the sections shown appeared to be from the sinus zone. Mainly proximal and intermediate tubules are found in

the sinus zone, with the occasional distal or collecting duct. With the assistance of Dr. E. Lacy, identification of the tubules has been attempted.

Immunofluorescent staining in kidney sections from FW-acclimated bull sharks is shown in *Figures 5.9, 5.10* and *5.11*. In these sections, both proximal (Px) and intermediate (Int) tubules have been identified. Cells of the proximal tubules often bear large flagella (F), which are highly fluorescent in these sections. Strong cell fluorescence was seen in only selected proximal tubule cells, with many of these coinciding with the presence of flagella. Flagella are absent from intermediate tubule cells, which display strong basal immunofluorescence. The renal corpuscle (RC) is devoid of fluorescence, and its presence indicates a section taken from the border between the sinus and bundle zones (*Figure 5.9*). These sections also show autofluorescent red blood cells (RBC). In sections of the kidney of a bull shark acclimated to SW, (*Figure 5.12*), fluorescence is associated with the tubules is similar to that seen in the sections from FW-acclimated bull sharks. Certain proximal tubule cells again bear fluorescent flagella, but in these sections, these cells are not fluorescent. However fluorescence is seen again on the basolateral membrane of the intermediate tubule cells. A renal corpuscle is again observed in *Figure 5.12b*.

The intensity of the fluorescence observed from kidney sections taken from SW-acclimated bull sharks was generally weaker than that observed in sections from FW-acclimated bull sharks, although no quantitative measures were taken. In addition, in kidney sections from FW-acclimated sharks, both flagella and the cells bearing the flagella were immunofluorescent, whereas in sections from SW-acclimated sharks, only the flagella were fluorescent. In all cases, the control sections treated with pre-immune serum (*Figures 5.9b – 5.12b*) showed only weak background fluorescence.

5.7: Distribution of Na^+, K^+-ATPase α_1 subunit protein in the rectal gland

Immunofluorescent staining in sections of the rectal glands from FW- and SW-acclimated bull sharks is shown in *Figures 5.13 - 5.16*. Secretory tubules in the rectal gland are composed of a single columnar epithelium. Expression of Na^+, K^+-ATPase α_1 was most abundant in the secretory tubules (ST) in the sub-capsular region of rectal glands from both FW- (*Figure 5.13*)

and SW-acclimated sharks (*Figure 5.15*). There was a gradual decrease in immunostaining towards the central tubular region (*Figures 5.14* and *5.16*) where low levels of expression were observed. This pattern was particularly evident in the rectal glands of SW-acclimated sharks. In the sub-capsular region of rectal glands from FW-acclimated *C. leucas* (*Figure 5.13*), immunostaining was restricted to the basolateral membrane of tubule cells. However in rectal glands from SW-acclimated sharks (*Figure 5.15*), immunostaining was more extensive in the cells of this region. No immunofluorescence was observed in the rectal gland capsule (C) of either FW- or SW-acclimated sharks.

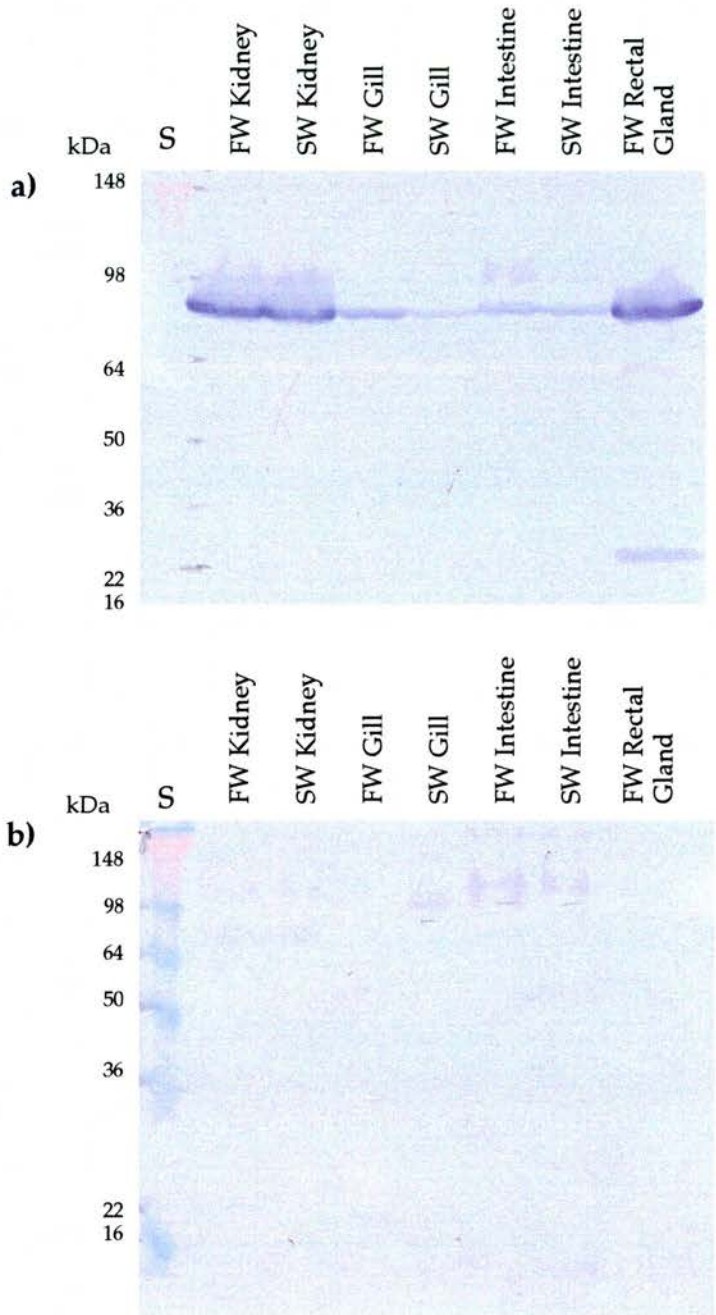

Figure 5.1. Representative Western blot of bull shark tissues probed with a Na^+, K^+-ATPase α_1 subunit-specific antibody. a) 100 μg protein from different tissue homogenates probed with purified Na^+, K^+-ATPase α_1 subunit antiserum, diluted 1:5000. **b)** Control Western blot with 100 μg of protein from tissue homogenates probed with pre-immune serum, diluted 1:5000. S: SeeBlue® Plus2 pre-stained molecular weight standard (Invitrogen).

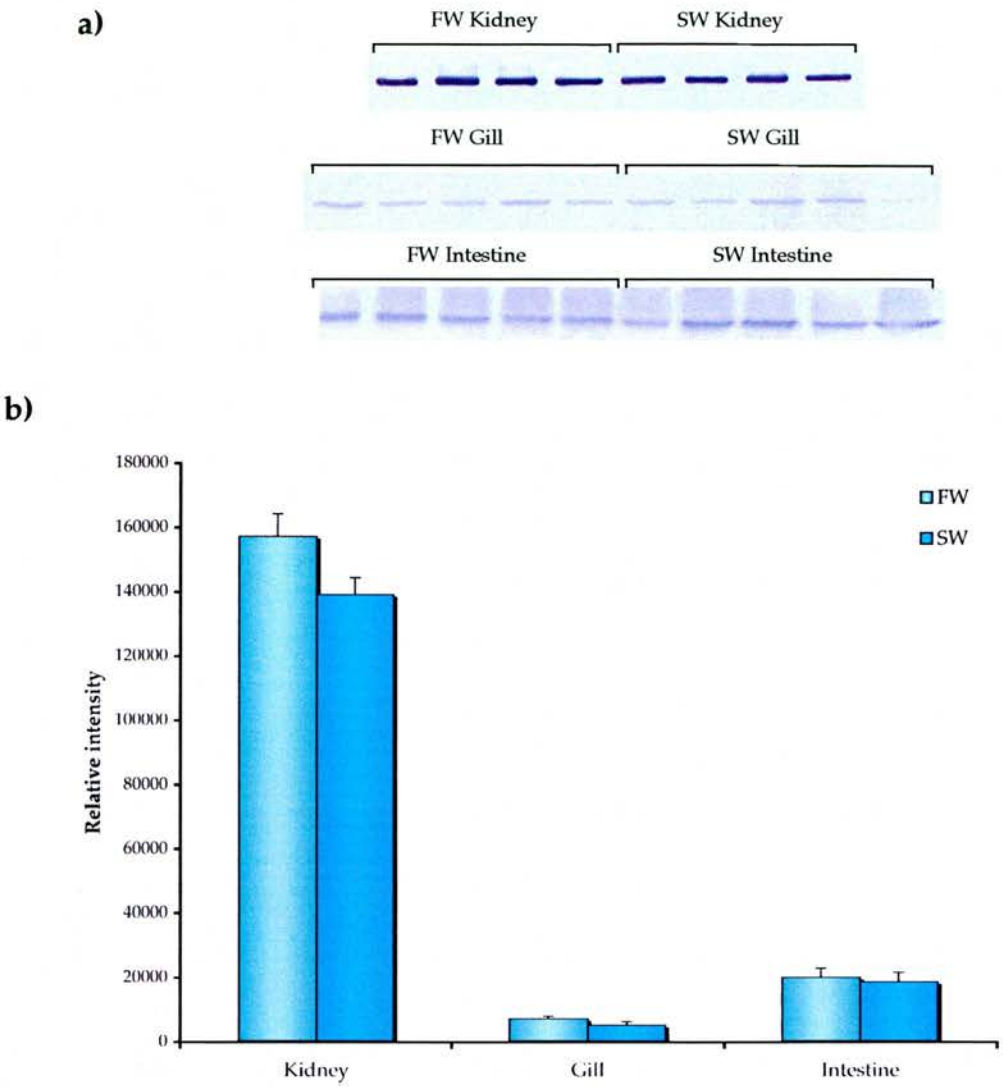

Figure 5.2: Expression of Na^+, K^+-ATPase α_1 subunit protein in different tissues from FW- and SW- acclimated fish. a) Western blots showing Na^+, K^+-ATPase α_1 subunit protein expression in kidney, gill and intestine from FW- or SW- acclimated bull sharks. The purified Na^+, K^+-ATPase α_1 subunit antibody was diluted 1:5000. The amount of tissue protein used was 5 μg for kidney and 25 μg for gill and intestine. **b)** Relative intensity of immunopositive bands measured by image analysis representing Na^+, K^+-ATPase α_1 subunit protein in kidney, gill and intestine from FW- or SW-acclimated bull sharks, using data obtained from *Fig. 5.2a* (mean ± s.e). For kidney n=4, and for gill and intestine n=5, and data were analysed using two way ANOVA and Fisher's PLSD test, which indicated no significant difference in expression of Na^+, K^+-ATPase α_1 subunit protein between tissues from FW- and SW-acclimated fish.

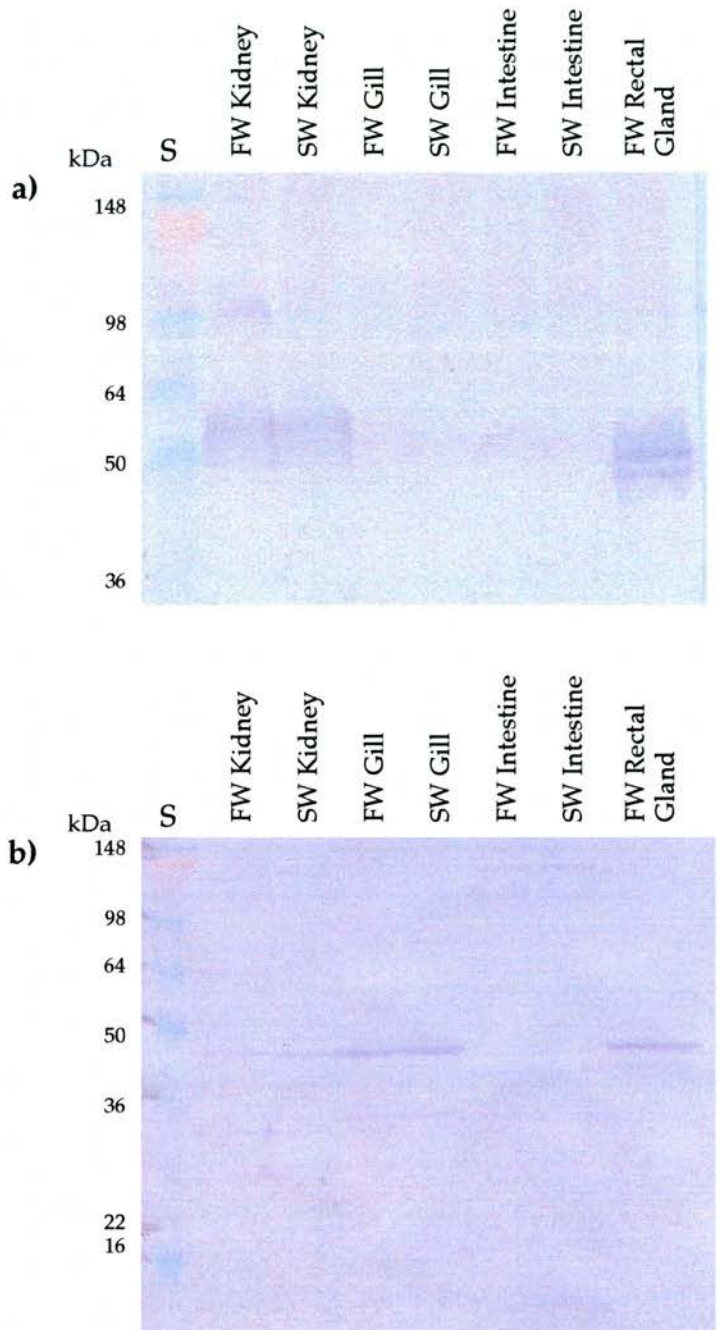

Figure 5.3. Representative Western blot of bull shark tissues probed with a Na^+, K^+-ATPase β_1 subunit-specific antibody. a) 100 μg protein from different tissue homogenates probed with purified Na^+, K^+-ATPase β_1 subunit antiserum, diluted 1:60. **b)** Control Western blot with 100 μg protein from tissue homogenates probed with pre-immune serum, diluted 1:60. S: SeeBlue® Plus2 pre-stained molecular weight standard (Invitrogen).

a)

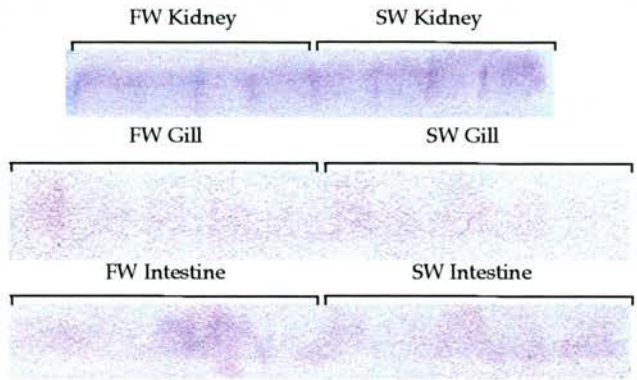

b)

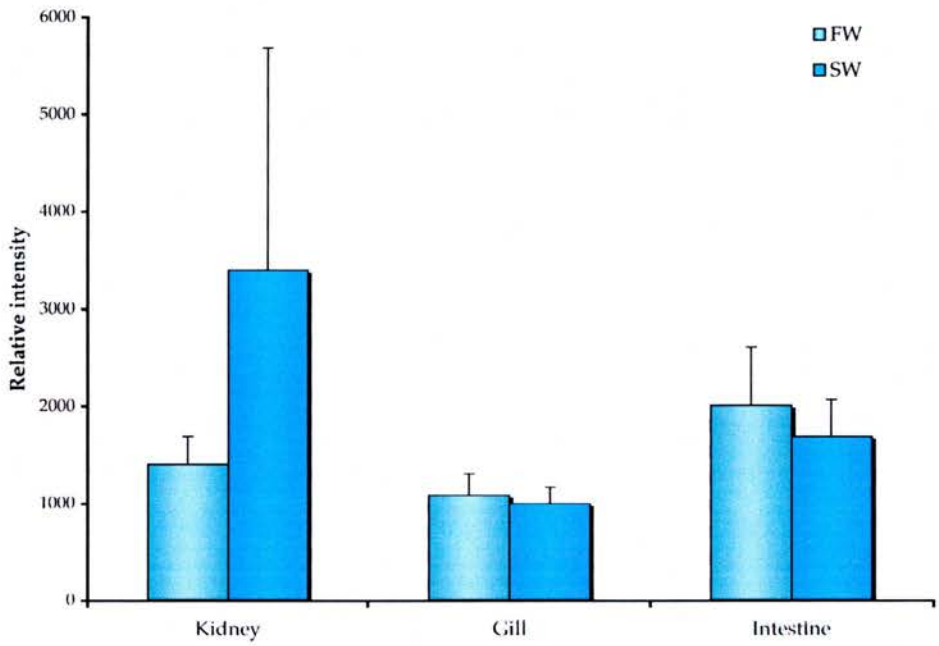

Figure 5.4. Expression of Na^+, K^+-ATPase β_1 subunit protein in different tissues from FW- and SW- acclimated fish. a) Western blots showing Na^+, K^+-ATPase β_1 subunit protein expression in kidney, gill and intestine from FW- or SW- acclimated bull sharks. The purified Na^+, K^+-ATPase β_1 subunit antibody was diluted 1:60. The amount of tissue protein used was 100 μg for kidney, gill and intestine. **b)** Relative intensity of immunopositive bands measured by image analysis representing Na^+, K^+-ATPase β_1 subunit protein in kidney, gill and intestine from FW- or SW-acclimated bull sharks, using data obtained from *Fig. 5.4a* (mean ± s.e). For kidney n=4, and for gill and intestine n=5, and data were analysed using two way ANOVA and Fisher's PLSD test, which indicated no significant difference in expression of Na^+, K^+-ATPase β_1 subunit protein between FW- and SW-acclimated tissues.

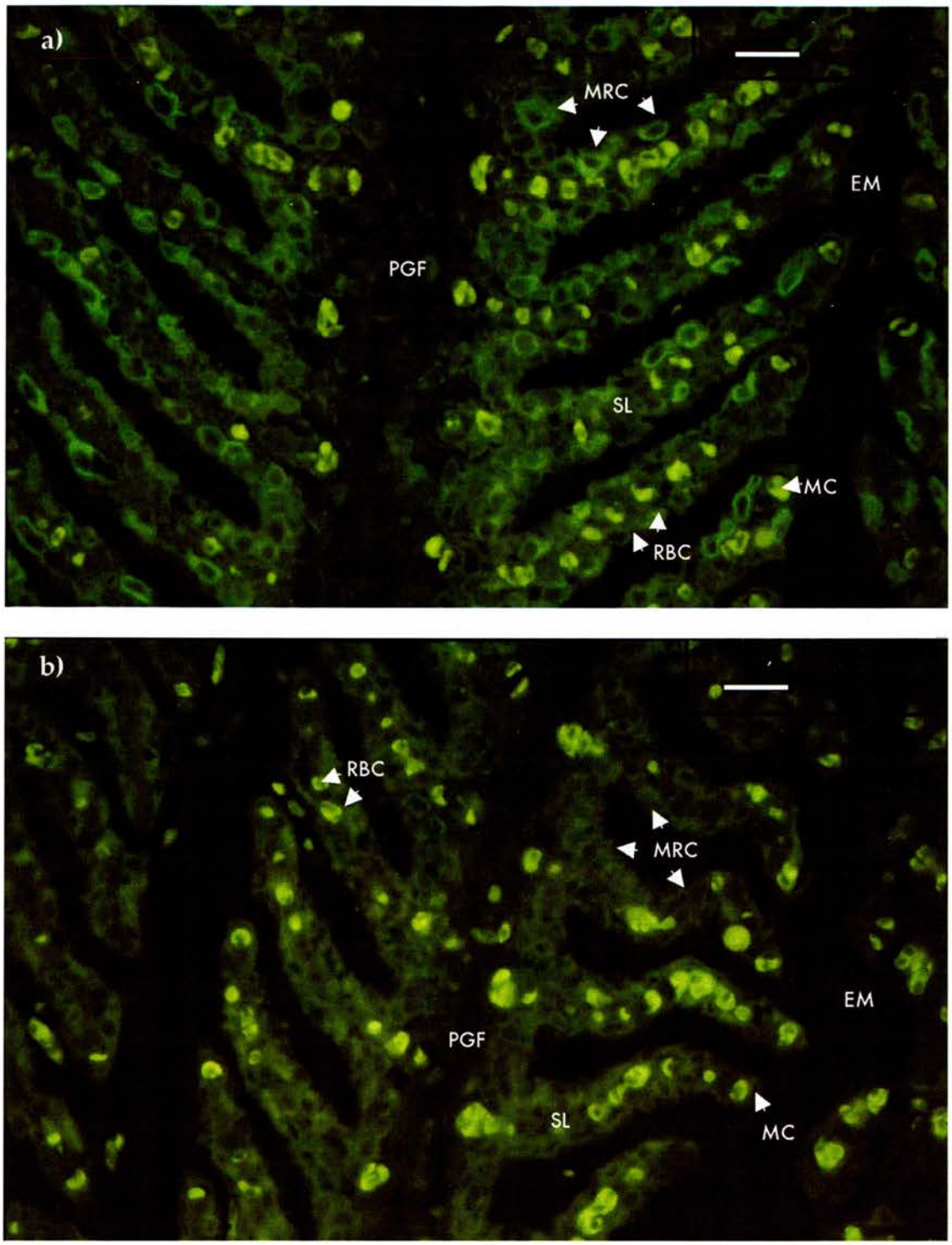

Figure 5.5: Gill sections from bull sharks acclimated to FW. a) Incubated with Na^+, K^+-ATPase α_1 subunit antibody diluted 1:10. **b)** Incubated with pre-immune serum diluted 1:10. PGF, primary gill filament; SL, secondary lamella; EM, external medium; MC, marginal capillary; RBC, red blood cell; MRC, mitochondria rich cell. Bars 25 μm.

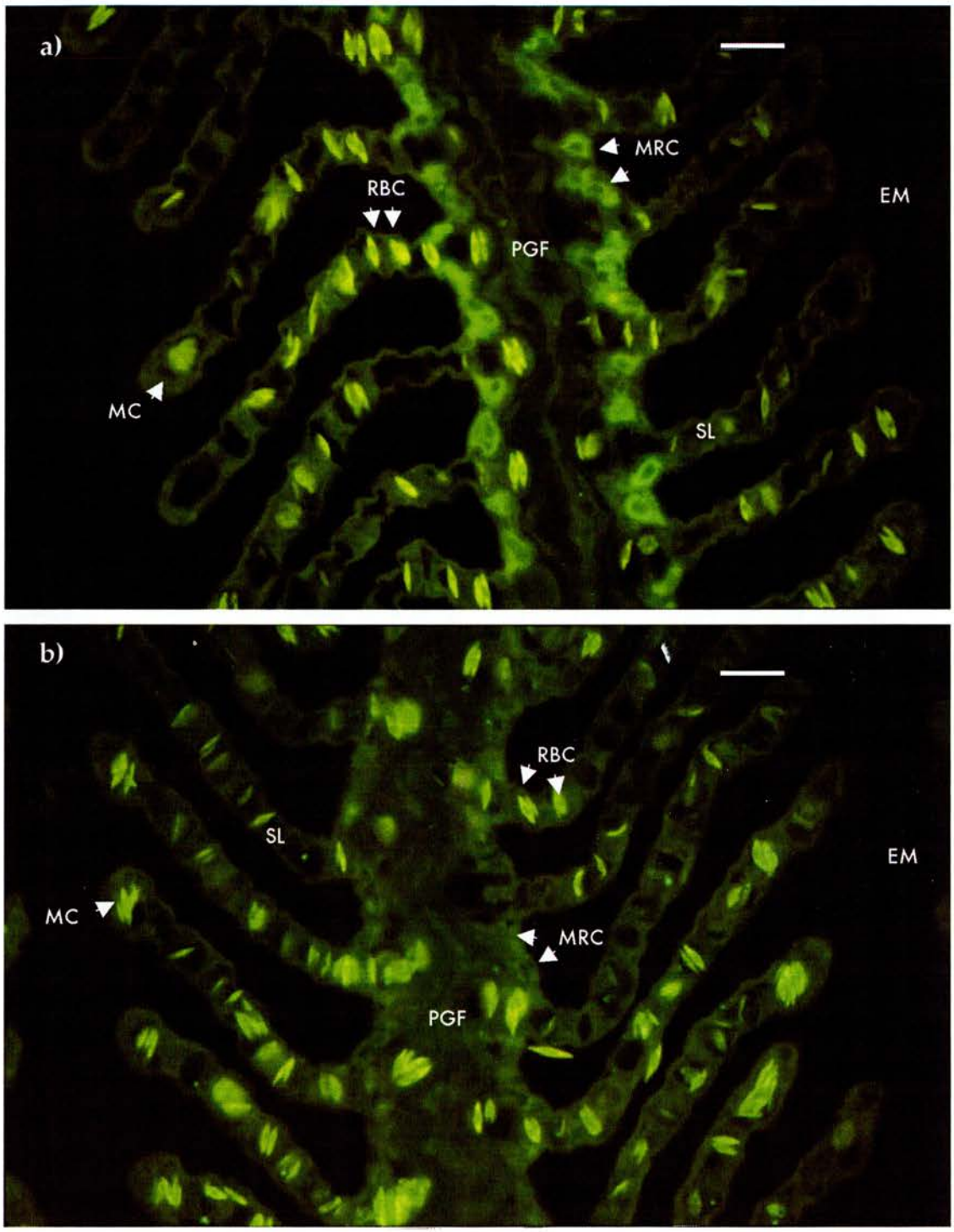

Figure 5.6: Gill sections from bull sharks acclimated to SW. a) Incubated with Na^+, K^+-ATPase α_1 subunit antibody diluted 1:10. **b)** Incubated with pre-immune serum diluted 1:10. PGF, primary gill filament; SL, secondary lamella; EM, external medium; MC, marginal capillary; RBC, red blood cell; MRC, mitochondria rich cell. Bars 25 μm.

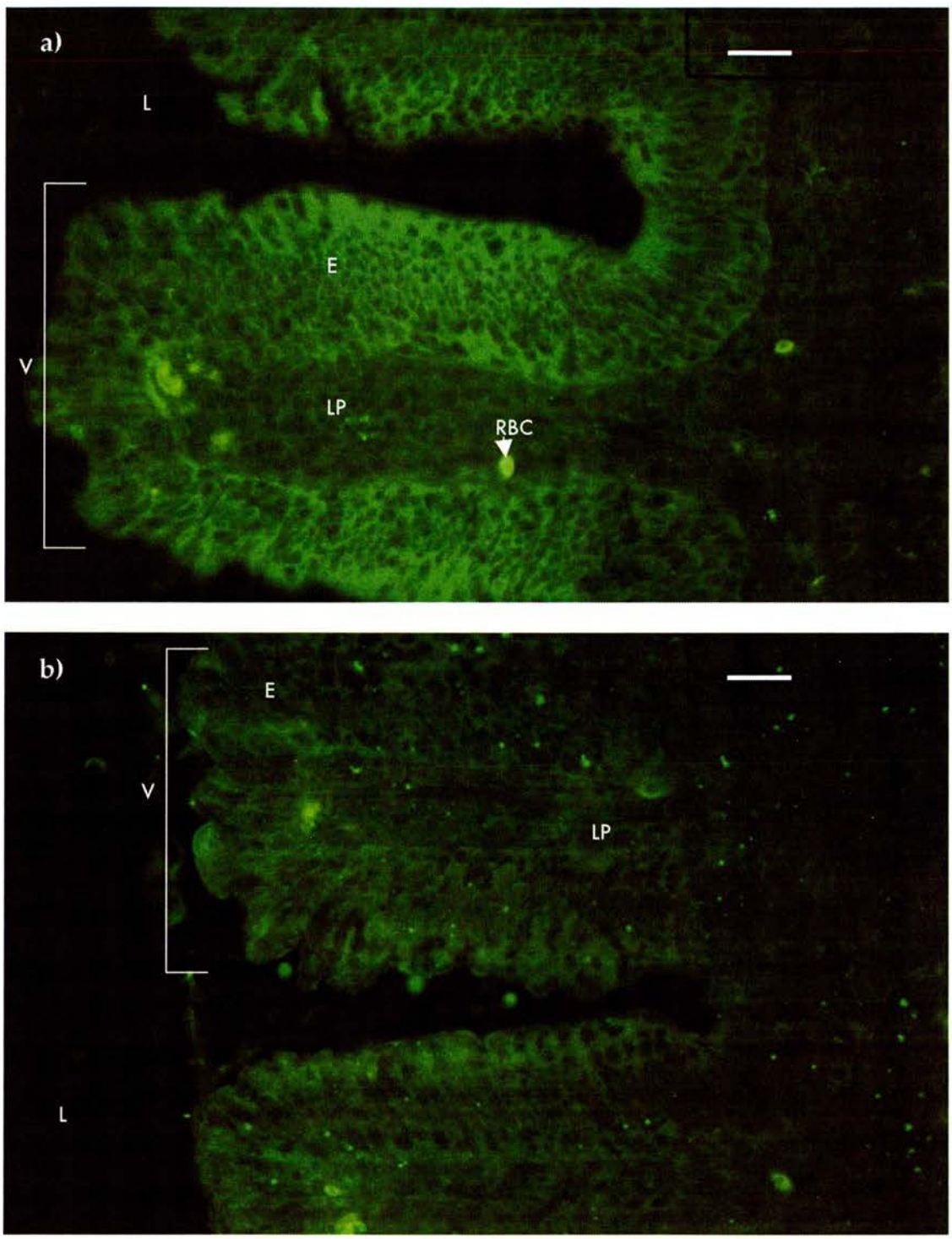

Figure 5.7: Intestine sections from bull sharks acclimated to FW. a) Incubated with Na^+, K^+-ATPase α_1 subunit antibody diluted 1:10. **b)** Incubated with pre-immune serum diluted 1:10. V, villus; E, epithelium; LP, lamina propria; L, lumen; RBC, red blood cell. Bars 25 μm.

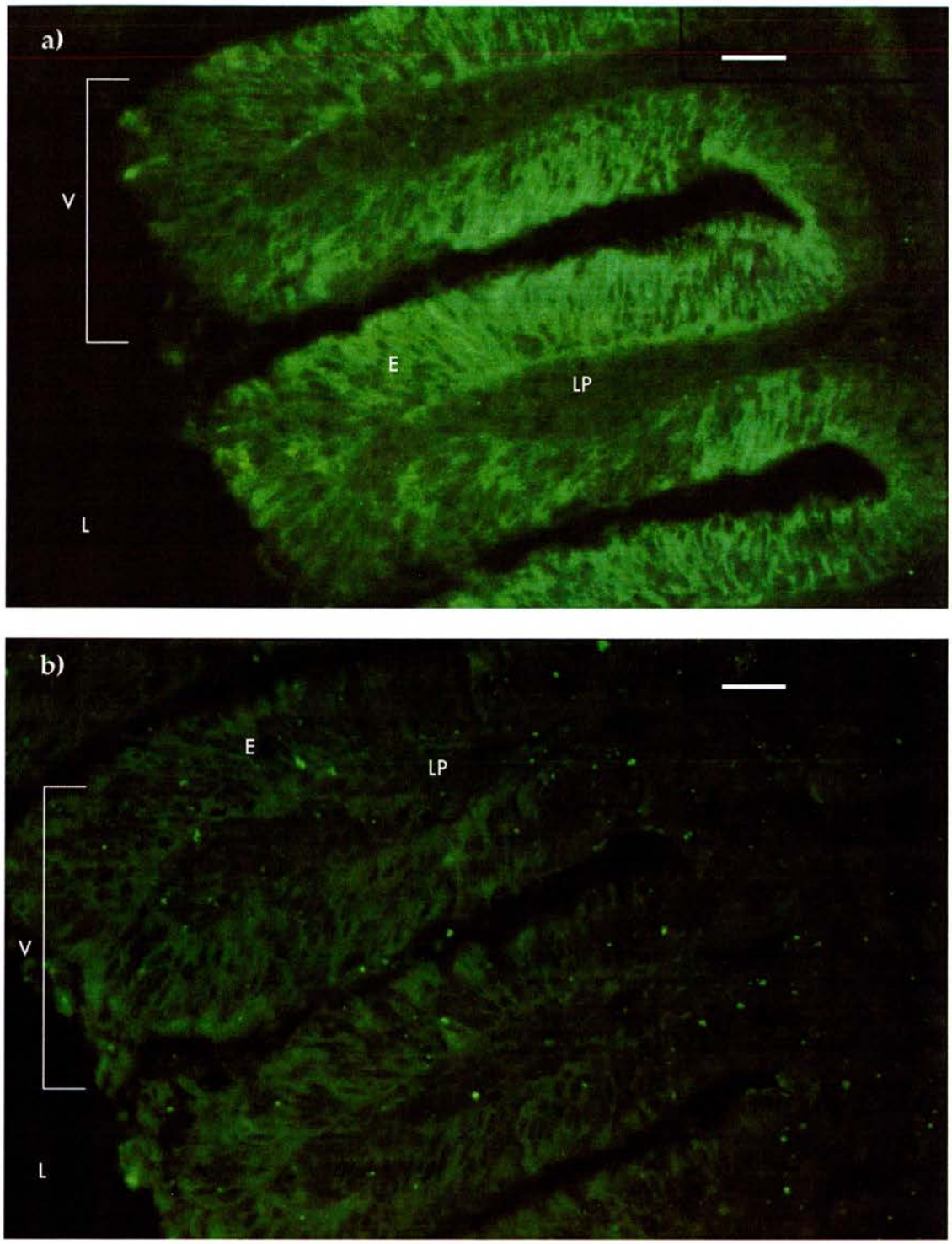

Figure 5.8: Intestine sections from bull sharks acclimated to SW. a) Incubated with Na^+, K^+-ATPase α_1 subunit antibody diluted 1:10. **b)** Incubated with pre-immune serum diluted 1:10. V, villus; E, epithelium; LP, lamina propria; L, lumen. Bars 25 μm.

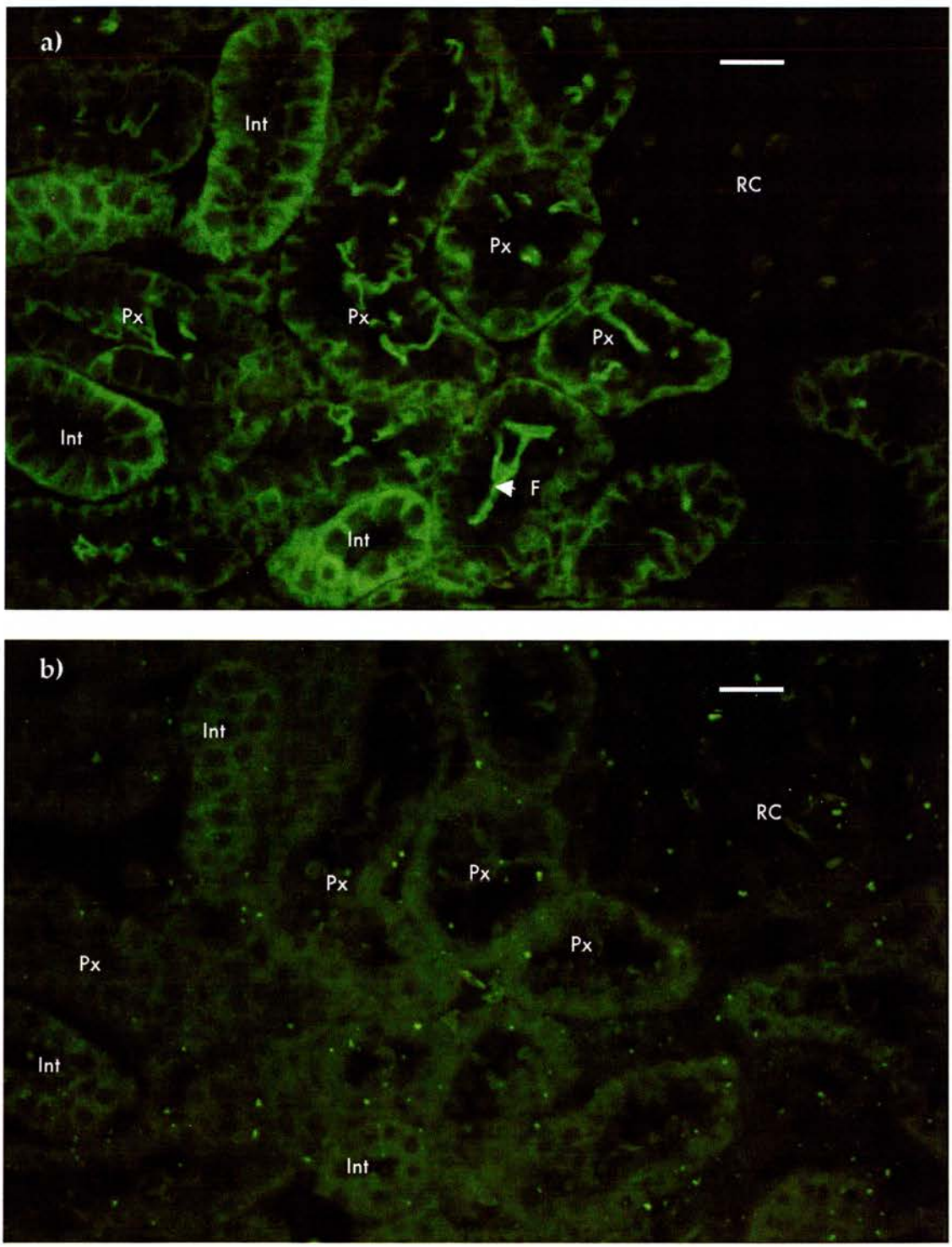

Figure 5.9: Kidney sections from bull sharks acclimated to FW. a) Incubated with Na^+, K^+-ATPase α_1 subunit antibody diluted 1:10. **b)** Incubated with pre-immune serum diluted 1:10. Px, promixal tubule; Int, intermediate tubule; RC, renal corpuscle; F, flagellum. Bars 25 μm.

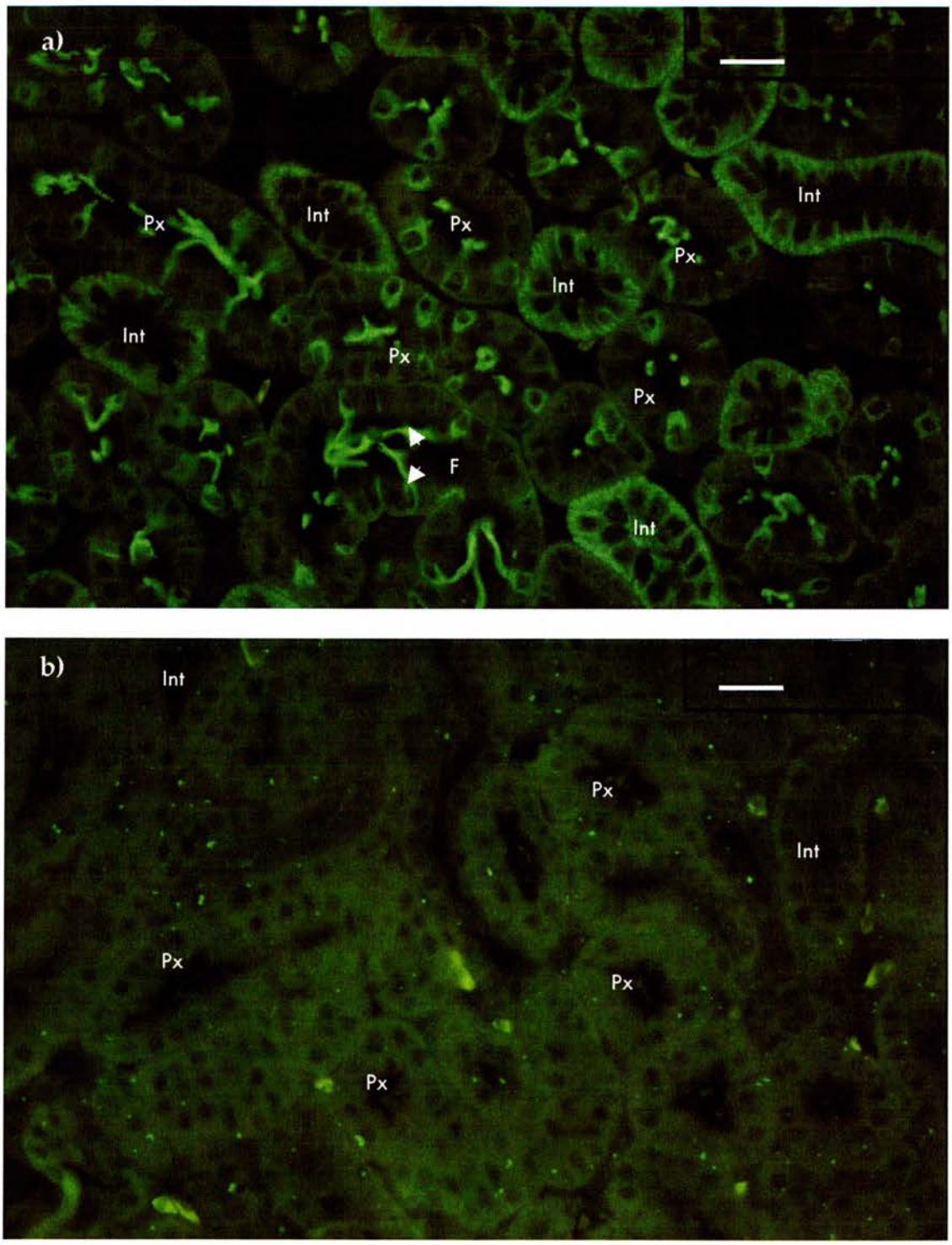

Figure 5.10: Kidney sections from bull sharks acclimated to FW. a) Incubated with Na^+, K^+-ATPase α_1 subunit antibody diluted 1:10. **b)** Incubated with pre-immune serum diluted 1:10. Px, promixal tubule; Int, intermediate tubule; F, flagellum. Bars 25 μm.

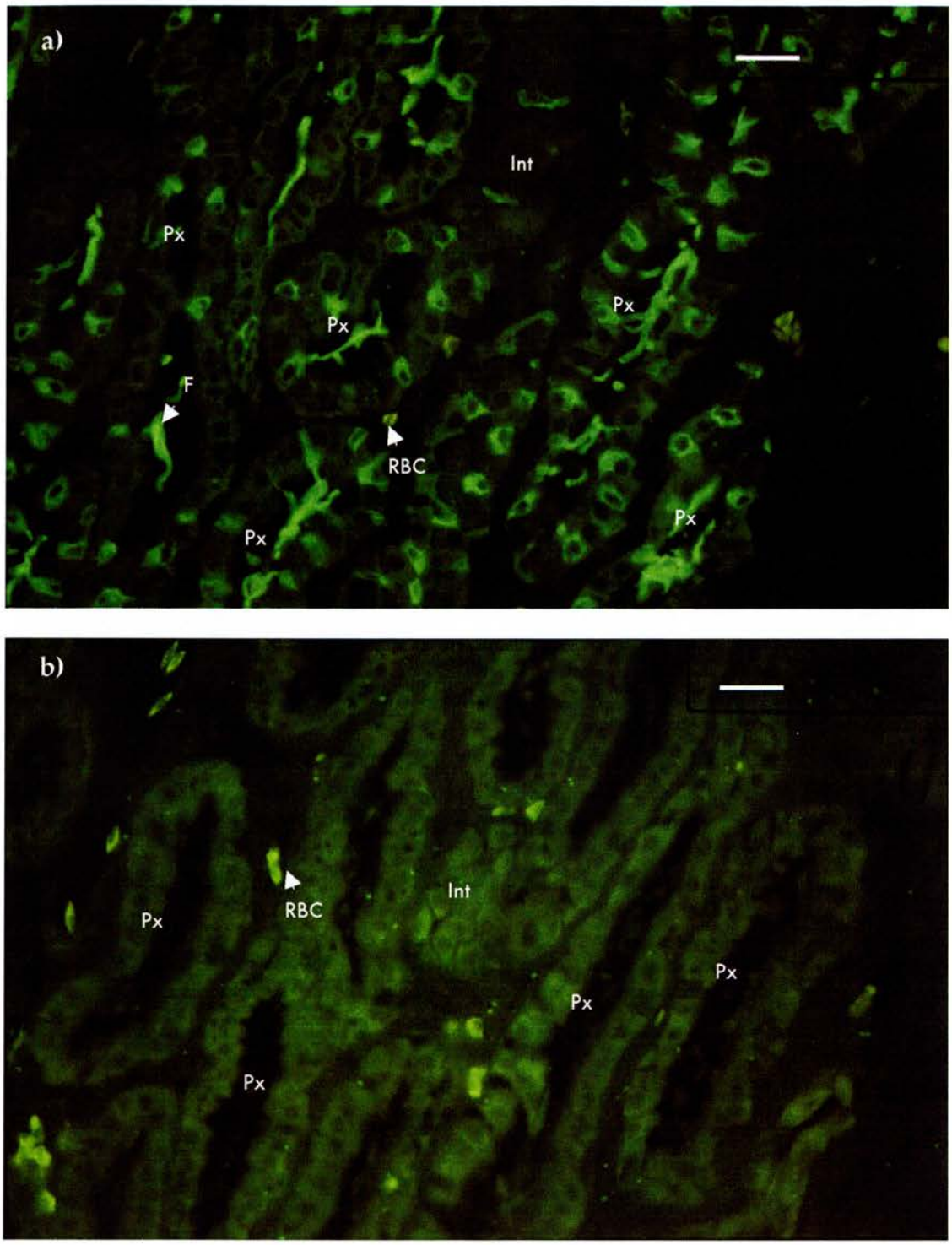

Figure 5.11: Kidney sections from bull sharks acclimated to FW. **a)** Incubated with Na^+, K^+-ATPase α_1 subunit antibody diluted 1:10. **b)** Incubated with pre-immune serum diluted 1:10. Px, promixal tubule; Int, intermediate tubule; F, flagellum; RBC, red blood cell. Bars 25 μm.

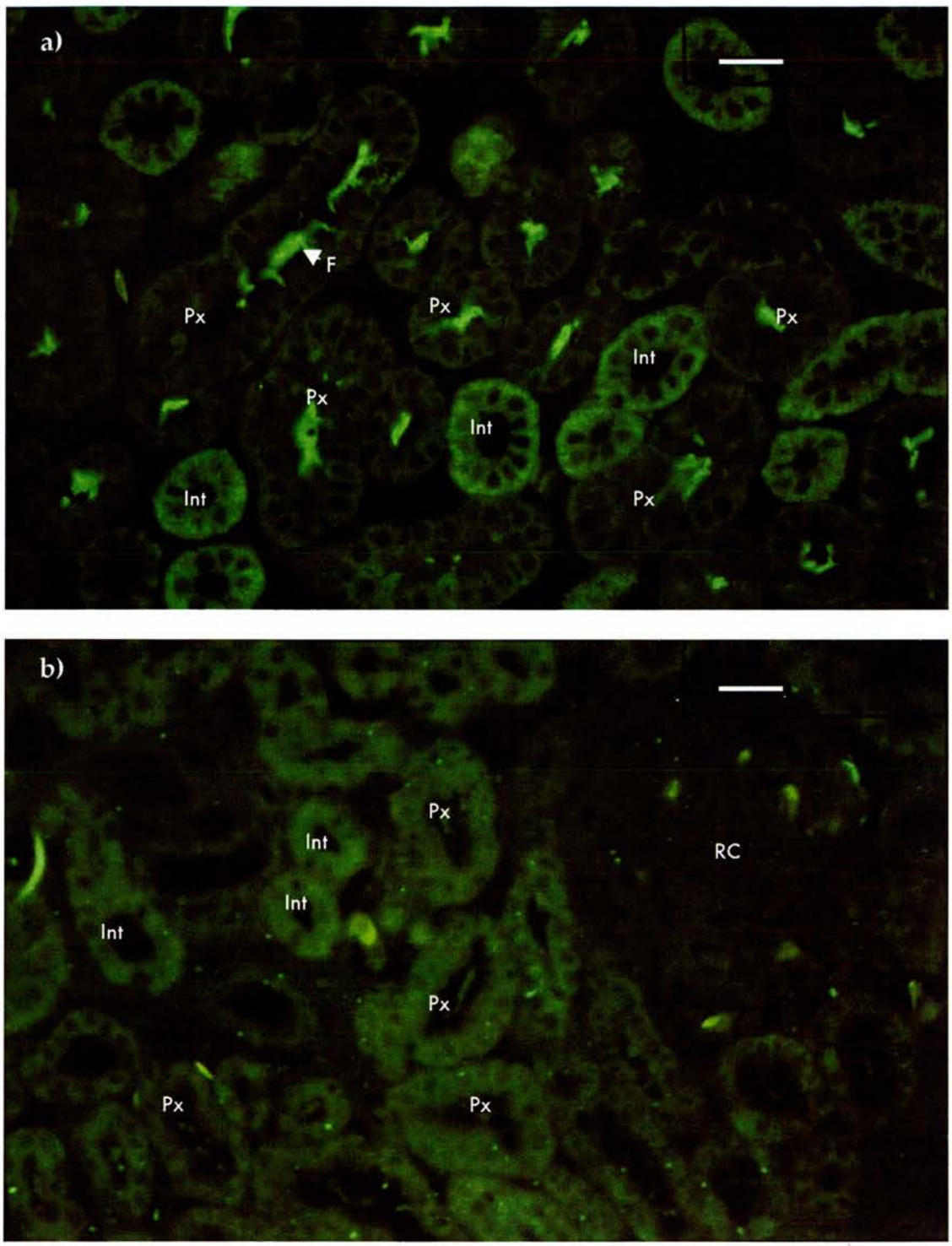

Figure 5.12: Kidney sections from bull sharks acclimated to SW. **a)** Incubated with Na^+, K^+-ATPase α_1 subunit antibody diluted 1:10. **b)** Incubated with pre-immune serum diluted 1:10. Px, promixal tubule; Int, intermediate tubule; F, flagellum; RC, renal corpuscle. Bars 25 μm.

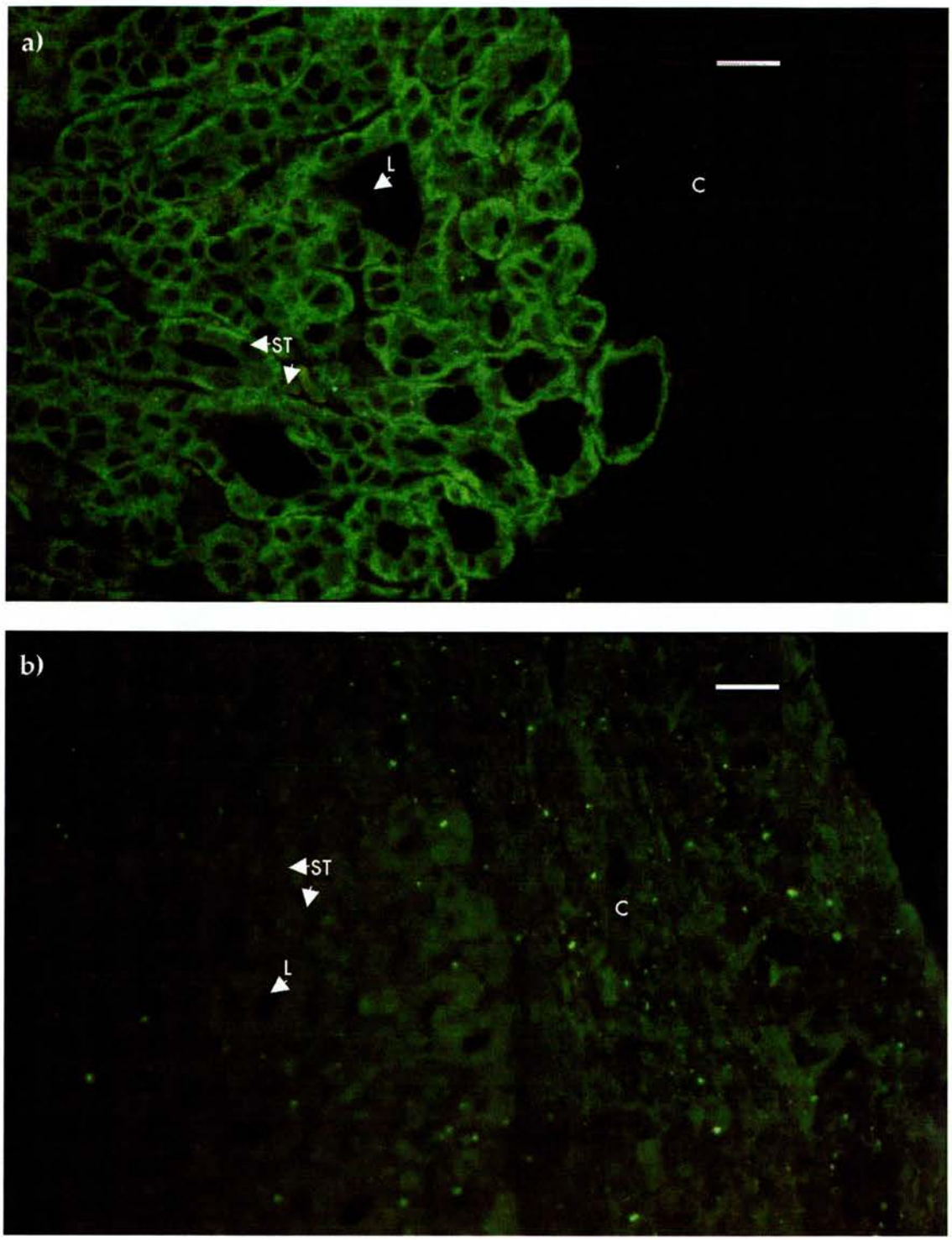

Figure 5.13: Sub-capsular rectal gland sections from bull sharks acclimated to FW. a) Incubated with Na^+, K^+-ATPase α_1 subunit antibody diluted 1:10. **b)** Incubated with pre-immune serum diluted 1:10. ST, secretory tubule; L, tubule lumen; C, capsule. Bars 25 μm.

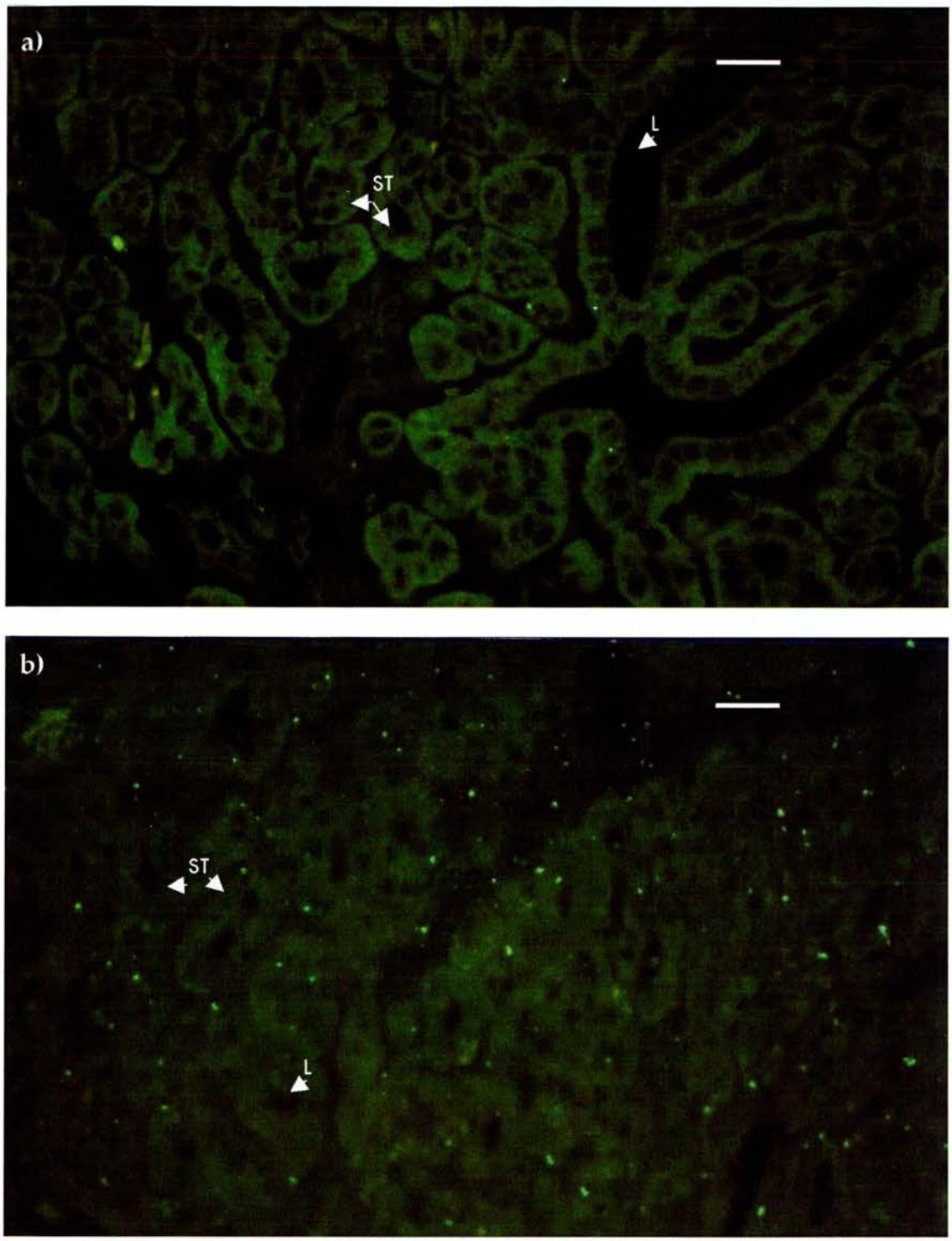

Figure 5.14: Central tubular region rectal gland sections from bull sharks acclimated to FW. **a)** Incubated with Na^+, K^+-ATPase α_1 subunit antibody diluted 1:10. **b)** Incubated with pre-immune serum diluted 1:10. ST, secretory tubule; L, tubule lumen. Bars 25 μm.

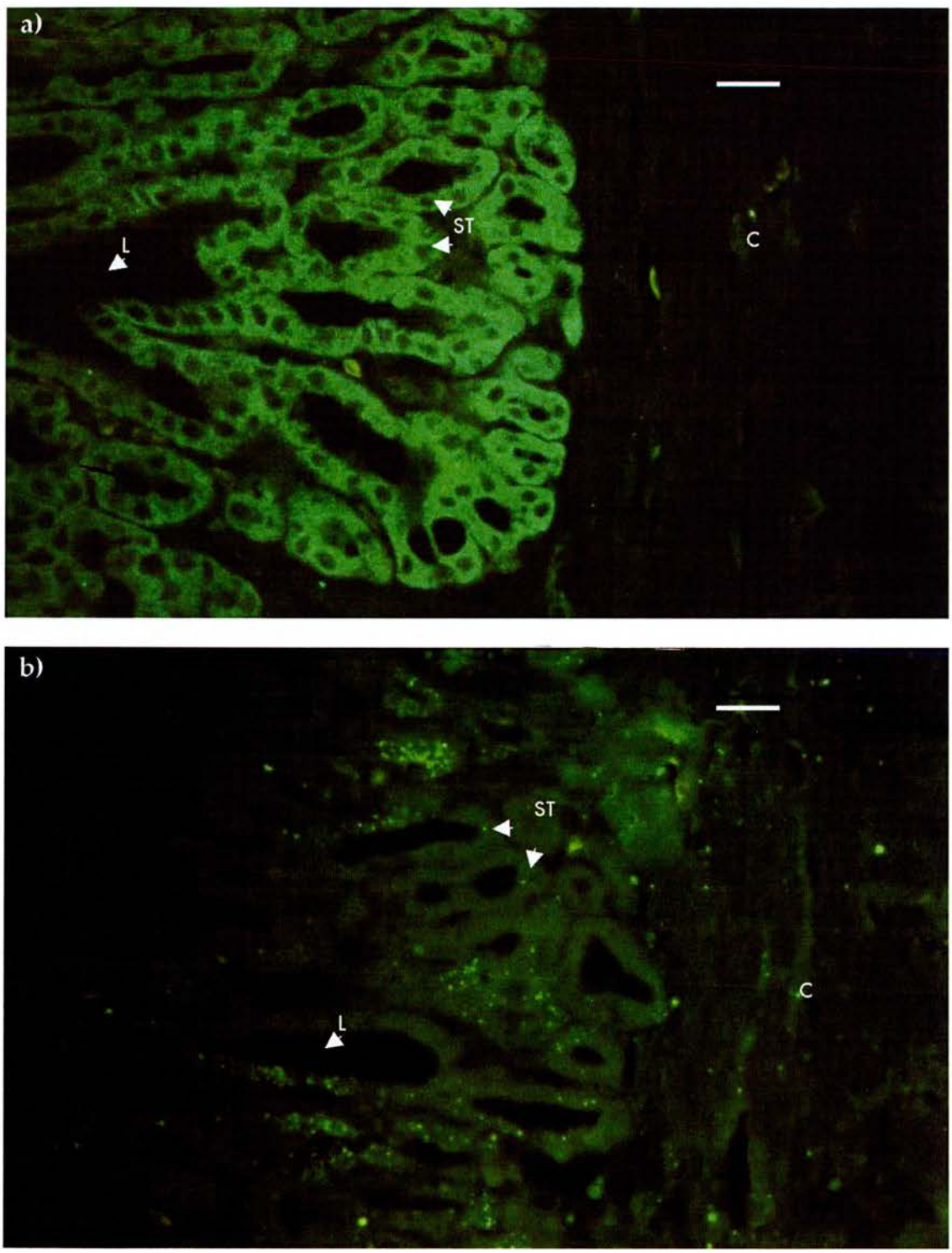

Figure 5.15: Sub-capsular rectal gland sections from bull sharks acclimated to SW. a) Incubated with Na^+, K^+-ATPase α_1 subunit antibody diluted 1:10. **b)** Incubated with pre-immune serum diluted 1:10. ST, secretory tubule; L, tubule lumen; C, capsule. Bars 25 μm.

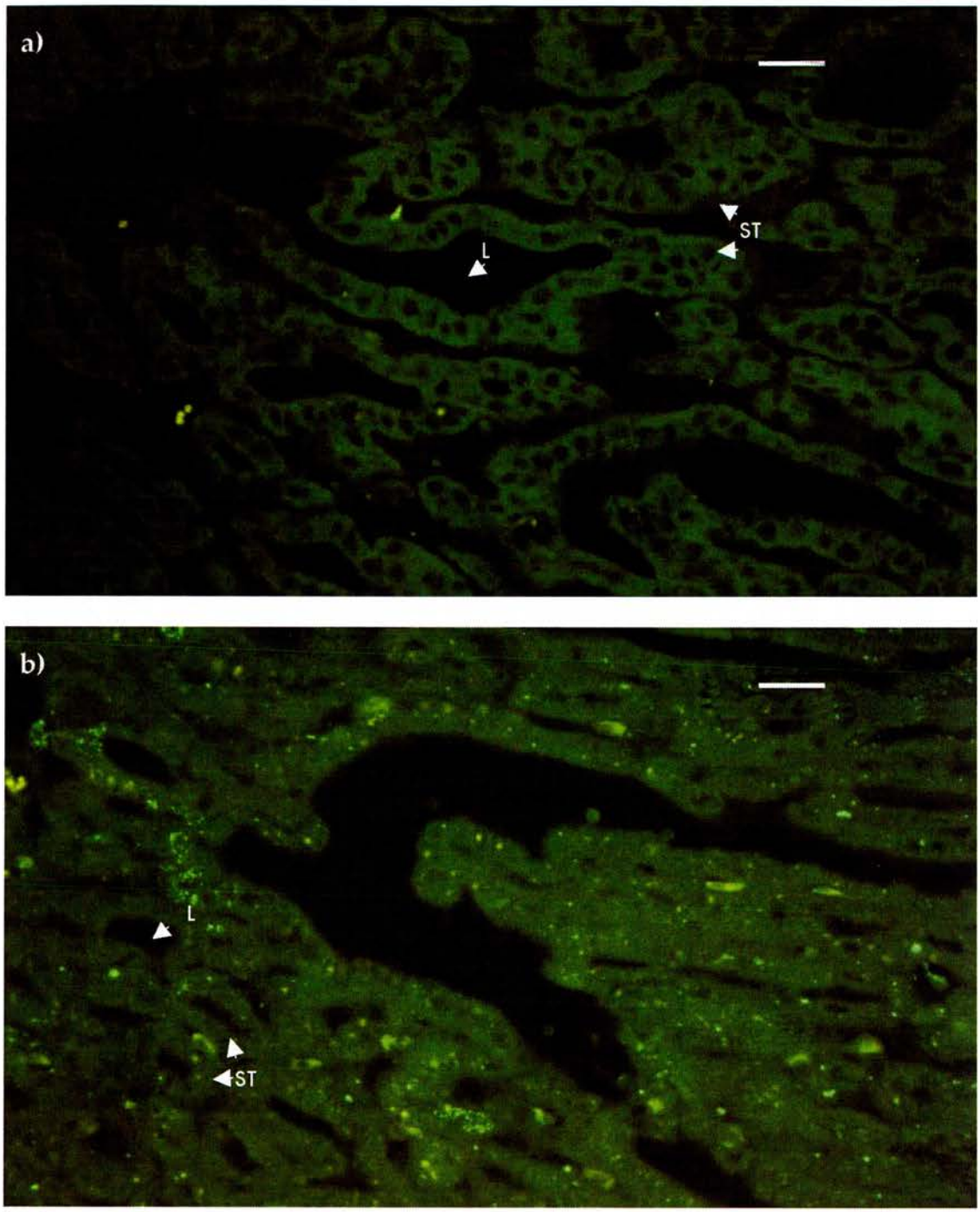

Figure 5.16: Central tubular region rectal gland sections from bull sharks acclimated to SW. a) Incubated with Na^+, K^+-ATPase α_1 subunit antibody diluted 1:10. **b)** Incubated with pre-immune serum diluted 1:10. ST, secretory tubule; L, tubule lumen. Bars 25 μm.

5.8: Expression of Na^+, K^+-ATPase α_1 and β_1 subunit protein in osmoregulatory tissues of FW- and SW-acclimated bull sharks

Immunopositive bands of around 95 kDa can be seen on Western blots supporting *C. leucas* kidney, gill, intestine and rectal gland protein samples, and probed with the Na^+, K^+-ATPase α_1 subunit isoform antibody. Although the actual molecular weight of the protein inferred from the amino acid sequence is 112.9 kDa, it is common for Na^+, K^+-ATPase α subunits to separate on an SDS PAGE gel anywhere from 90 to 112 kDa (Lee *et al.*, 1998; Hwang *et al.*, 1998; Piermarini *et al.*, 1999; Guynn *et al.*, 2002; Lin *et al.*, 2003; Lin *et al.*, 2004). Na^+, K^+-ATPase α_1 subunit protein was isolated from the rectal gland of the dusky shark, *Carcharhinus obscurus*, and found to have a molecular weight of 106 kDa (Hastings and Reynolds, 1979). The absence of bands on the blot probed with pre-immune serum indicates the validity of the bands seen on the former blot. The Na^+, K^+-ATPase α_1 subunit isoform antibody was raised specifically against the amino acid sequence of the *C. leucas* Na^+, K^+-ATPase α_1 subunit isoform, and is unlikely to cross-react with the other Na^+, K^+-ATPase α subunit isoforms. The results from Section 5.1 reveal that Na^+, K^+-ATPase α_1 subunit isoform protein is expressed strongly in the rectal gland and kidney, and also at lower levels in the gill and intestine. This concurs with the results of the Na^+, K^+-ATPase mRNA expression studies in Chapter 4.

The Na^+, K^+-ATPase α subunit gene is highly conserved across all vertebrate phyla (*Figure 3.3*), therefore many investigators have used antibodies raised to mammalian or avian Na^+, K^+-ATPase sequences in order to examine expression of this protein in fish tissues (Lee *et al.*, 1998; D'Cotta *et al.*, 2000; Piermarini and Evans, 2000) without first establishing the Na^+, K^+-ATPase α subunit sequence of these fish species. However, the isoform-specific region of the α subunit isoforms (*Figure 3.10*) can be highly variable between phyla (Pressley, 1992) and therefore antibodies raised to this region in mammalian species may not cross-react. As discussed previously in Section 3.4, Hansen (1999) performed Western blots using antibodies raised against mammalian Na^+, K^+-ATPase α subunit isoforms to determine the expression of α subunit isoforms in the rectal gland of *S. acanthias*. This led to the incorrect

conclusion that only the α_3 isoform was expressed in the rectal gland. This experiment highlights the importance of using species specific antisera.

It is possible that the discovery of additional isoforms in many fish species has been held back by the assumption that antibodies designed to mammalian Na^+, K^+-ATPase subunit isoforms will be sufficiently similar to the study species. In *S. salar,* Western blots using mammalian Na^+, K^+-ATPase subunit isoform specific antibodies found no immunoreactivity for Na^+, K^+-ATPase α_1 and α_2 subunit isoforms (D'Cotta *et al.,* 2000). However, similar to the findings of Hansen's study of *S. acanthias,* (1999), the antibody raised to mammalian α_3 did cross-react with the Na^+, K^+-ATPase α subunit *S. salar* indicating that the isoform expressed in *S. salar* was α_3. The authors suggest that this is most likely to be explained by differences in the mammalian and teleost Na^+, K^+-ATPase α subunit sequences resulting in cross-reaction with the α_3 antibody rather than the α_1 antibody (D'Cotta *et al.,* 2000). In *O. mossambicus,* an antibody raised against an avian Na^+, K^+-ATPase α_1 subunit gene was used for Western blotting, whereas the Na^+, K^+-ATPase α_2 and α_3 subunit isoform specific antibodies were both raised to the gene sequence of the rat. Immunopositive bands were expressed in the gills and kidney of *O. mossambicus* using the Na^+, K^+-ATPase α_1 subunit antibody. The anti-rat Na^+, K^+-ATPase α_3 subunit isoform antibody detected immunoreactive bands in the brain, heart and gills, but not kidney, whereas the anti-rat α_2 isoform specific antibody produced no immunoreactive bands in *O. mossambicus* (Lee *et al.,* 1998). In a more recent study, all three Na^+, K^+-ATPase α subunit isoforms were detected in the brain, gill, and kidney of *T. bernacchii* and *N. angustata* by Western blotting using isoform-specific antibodies (Guynn *et al.,* 2002). Since the antibody used in the present study was raised to the gene sequence of the *C. leucas,* the results observed are entirely reliable. Antibodies raised to the sequence of *C. leucas* Na^+, K^+-ATPase α_2 and α_3 subunit isoforms were not produced in this study, although these isoform proteins are likely to be expressed mainly in the brain with only low levels expected in the osmoregulatory tissues.

The immunopositive bands seen on Western blots supporting kidney, gill intestine and rectal gland protein samples from *C. leucas,* and probed with Na^+, K^+-ATPase β_1 subunit antibody ranged in size from 45 to 55 kDa. The

molecular weight inferred from the cloned sequence is 35.2 kDa. This discrepancy is probably accounted for by the variable states of glycosylation of the β_1 subunit as described in Section 1.6.2. The Na^+, K^+-ATPase β subunit from another shark from the same genus, *C. obscurus*, has a non-glycosylated molecular weight of 37 kDa, rising to 52 kDa when glycosylated (Hastings and Reynolds, 1979).

On comparison of Na^+, K^+-ATPase α_1 and β_1 subunit isoform protein expression in kidney, gill and intestine of *C. leucas* acclimated to FW and SW, no significant differences in expression were found. It was not possible to compare the expression of Na^+, K^+-ATPase subunits in the rectal gland of *C. leucas* since rectal gland samples from SW-acclimated sharks were not available for protein analysis. The results of the protein expression studies mirror the results of the mRNA expression studies in Chapter 4, where there was no significant difference in Na^+, K^+-ATPase α_1 and β_1 subunit mRNA expression. It was suggested in the previous chapter that the change in Na^+, K^+-ATPase activity in the kidney and rectal gland of SW-acclimated *C. leucas* observed by Pillans *et al.*, (2005) may be due to post-transcriptional regulation. However, since there is no difference in Na^+, K^+-ATPase subunit protein expression in the kidneys of FW- and SW-acclimated *C. leucas*, the reported differences in enzyme activity in this tissue must be du to post-translational factors. Since Na^+, K^+-ATPase α_1 and β_1 subunit protein expression was not examined in the rectal gland of *C. leucas* acclimated to FW and SW, it is unknown whether salinity-dependent regulation of protein expression contributes to the reported change in rectal gland Na^+, K^+-ATPase activity (Pillans *et al.*, 2005). Branchial and intestinal Na^+, K^+-ATPase activities were unchanged by SW transfer (Pillans *et al.*, 2005), and this is consistent with our finding that Na^+, K^+-ATPase α_1 and β_1 subunit protein expression was also found to remain constant following SW-acclimation.

Studies of Na^+, K^+-ATPase α_1 subunit protein expression in the branchial cells of the teleost, *O. mossambicus*, have reported conflicting results. Using an antibody raised to the avian Na^+, K^+-ATPase α_1 subunit sequence, Na^+, K^+-ATPase α_1 subunit protein expression in the gills of *O. mossambicus* was found to be significantly greater in FW-acclimated fish, compared to SW-acclimated fish (Lee *et al.*, 1998). Subsequently, a specific antibody raised to

the Na^+, K^+-ATPase α_1 subunit gene sequence identified in *O. mossambicus* revealed higher levels of expression of the α_1 subunit in the gills of SW-acclimated *O. mossambicus* compared to FW-acclimated fish (Hwang *et al.*, 1998; Hwang *et al.*, 1999). Although the results of these studies are in direct contrast to each other, it is more likely that the later studies using antibodies raised against the *O. mossambicus* Na^+, K^+-ATPase α_1 subunit sequence are accurate.

When transferred from brackish water (BW; 10 ppt) to FW or SW, the Na^+, K^+-ATPase α subunit protein expression in the gills of *C. chanos* was highest in FW conditions (Lin *et al.*, 2003). Expression of Na^+, K^+-ATPase α subunit protein also increased in the gills of *T. nigroviridis* after transfer of fish from BW to FW, but the highest levels of Na^+, K^+-ATPase α subunit expression were found in fish transferred to SW. In contrast to the gill, Na^+, K^+-ATPase α subunit protein expression in the kidney of *T. nigroviridis* was greatest in FW-acclimated fish and decreased with increased salinity (Lin *et al.*, 2004). The patterns of Na^+, K^+-ATPase α subunit protein expression in these tissues paralleled the pattern of Na^+, K^+-ATPase activity (Lin *et al.*, 2004), therefore in *T. nigroviridis*, Na^+, K^+-ATPase activity appears to be regulated primarily by the expression of the α subunit. This is in contrast with the findings from the present *C. leucas* study.

In an experiment bearing many similarities to the present study, Piermarini and Evans (2000) examined Na^+, K^+-ATPase α subunit protein expression in *D. sabina* native to FW and SW environments, and FW *D. sabina* which were subsequently acclimated to SW for 7 days. Branchial Na^+, K^+-ATPase α subunit protein expression was highest in the FW group, significantly reduced in the SW-acclimated group, and further reduced in the native SW group. Conversely, Na^+, K^+-ATPase α subunit expression in the rectal gland was highest in the native SW group, significantly lower in the SW-acclimated group, and lowest in the native FW group. Na^+, K^+-ATPase activities were also highest in FW gill and SW rectal gland, matching the trends for Na^+, K^+-ATPase protein expression. It is possible that *D. sabina* and *C. leucas* evolved different strategies for euryhalinity since there is a marked change in both protein expression and activity in branchial Na^+, K^+-ATPase, and no such

difference was detected in *C. leucas*. Euryhalinity in fish has arisen several times in members of various classes, leading to the suggestion that many different mechanisms of FW osmoregulation may have evolved (Marshall, 2002). In *D. sabina*, the activity of Na^+, K^+-ATPase in the gills and rectal gland may be regulated primarily by increased translation of functional protein subunits, whereas there was no change in branchial Na^+, K^+-ATPase expression or activity in *C. leucas* (Pillans *et al.*, 2005).

The data presented in Sections 5.1-5.2 suggest that Na^+, K^+-ATPase protein expression is unchanged in *C. leucas* kidney, gill and intestine after transfer from FW to SW, and that any changes in Na^+, K^+-ATPase activity occur downstream of translational regulation.

5.9: Immunolocalisation of Na^+, K^+-ATPase α_1 subunit protein in osmoregulatory tissues of FW- and SW-acclimated bull sharks

Na^+, K^+-ATPase α_1 subunit immunoreactive cells were present in all bull shark tissues examined. Observed changes in Na^+, K^+-ATPase α_1 subunit distribution between tissues of FW- and SW-acclimated sharks will be discussed below. It must be noted that the intensity of immunoreactivity was not quantified so any remarks on signal strength were determined purely by visual observation.

A potential complication in the interpretation of these results is the association of the Na^+, K^+-ATPase α subunit with FXYD proteins. These FXYDs are likely to associate with the N-terminal of the Na^+, K^+-ATPase α_1 subunit (Cornelius *et al.*, 2005) which is the region to which the antibody was raised. This may result in reduced immunostaining in regions where FXYDs are associated with the Na^+, K^+-ATPase since the antibody recognition sequence would be masked by the FXYD. This might explain the discrepancies between the levels of α_1 subunit protein expression in the Western blots of the membrane preparations and the apparent α_1 subunit protein expression in the fixed tissues. Immunoreactivity appeared to be much stronger in the gill where FXYDs are known not to occur in elasmobranchs, compared with the relatively weaker immunoreactivity seen in the kidney, rectal gland and intestine where PLMS is expressed

(Mahmmoud *et al.*, 2003). The gill and intestine of *C. leucas* show a similar level of α_1 subunit expression in Western blots, but in fixed sections, the gill appears to shows a much higher expression of Na^+, K^+-ATPase than the intestine. This could be explained by the fact that the intestinal enterocytes exhibited a uniform distribution of Na^+, K^+-ATPase, whereas in the gill, expression of Na^+, K^+-ATPase is largely associated with certain cells, such as MR cells, displaying strong immunoreactivity. However, since PLMS can be found in the intestine, and not the gill, it is possible that PLMS in the intestine is interfering with the antibody binding and giving a weaker signal than expected. If PLMS also associates with Na^+, K^+-ATPase in the rectal gland and kidney, this would explain the low levels of expression in the fixed samples of kidney and rectal gland compared to the high levels of expression in these tissues on Western blots.

There was a noticeable difference in the Na^+, K^+-ATPase α_1 subunit distribution within the gills of FW and SW-acclimated sharks. In FW-acclimated *C. leucas*, MR cells on both the lamellae and filaments were Na^+, K^+-ATPase immunoreactive. However, in SW-acclimated *C. leucas*, Na^+, K^+-ATPase immunoreactivity is only found in cells within the filament. It is unclear as to whether the lack of Na^+, K^+-ATPase immunoreactivity on the secondary lamellae of SW-acclimated sharks is caused by a decrease in Na^+, K^+-ATPase staining intensity or a decrease in lamellar MR cell number. This shift in Na^+, K^+-ATPase immunoreactivity distribution might be due to different types of MR cell, all of which express Na^+, K^+-ATPase on the basolateral membrane, but which support a different array of transporters dependent on whether they are to be functional in FW, and perform ion uptake, or functional in SW for ion excretion (Section 1.5). The changes observed may be less to do with osmoregulation and more associated with acid-base exchange (Evans, 1984; as discussed in Section 1.4.3).

As is the case for Na^+, K^+-ATPase protein expression, the majority of studies into the distribution and localisation of Na^+, K^+-ATPase in teleosts has focused on the gill, since this is the primary site of osmoregulation in these fish. Na^+, K^+-ATPase is differentially distributed according to environmental salinity. Numerous studies have observed Na^+, K^+-ATPase staining in MR

cells situated on both the lamellae and filaments of FW fish. However, Na^+, K^+-ATPase is only found in MR cells within the filament and interlamellar region within the gills of marine fish (Uchida *et al.*, 1996; Shikano and Fujio, 1998[a]; Piermairini and Evans, 2000; Lin *et al.*, 2003). Even *O. keta* transferred from FW to brackish water (BW; 25 ppt) and then reintroduced to FW only displayed Na^+, K^+-ATPase specific staining in MR cells on the secondary lamellae when in FW, and not in BW (Shikano and Fujio, 1998[a]). The high level of Na^+, K^+-ATPase protein expression observed in the gills of FW fish (discussed in Section 5.8) is likely to be due to the increase in Na^+, K^+-ATPase expression in these lamellar MR cells (Lin *et al.*, 2004). Copper exposure also causes an increase in secondary lamellar MR cell Na^+, K^+-ATPase immunoreactivity in FW *O. mossambicus* (Dang *et al.*, 1999). The same pattern of Na^+, K^+-ATPase immunoreactive cells described in euryhaline teleosts was also observed in the gills of a euryhaline elasmobranch, *D. sabina* (Piermarini and Evans, 2000). Strong immunoreactivity was found in lamellar MR cells, and weak immunoreactivity in the filamental MR cells of FW-acclimated fish. However, in SW-acclimated fish, Na^+, K^+-ATPase immunoreactive cells were greatly reduced in number and/or staining intensity along the lamellae, but increased in number within the primary filament, especially at the base of the secondary lamellae. In *D. sabina* collected from SW, Na^+, K^+-ATPase was found to be only located within the filaments, in the interlamellar regions (Piermarini and Evans, 2000). The findings of the present study concur with these observations.

Studies on the gills of *P. reticulata* indicate that the MR cells classified as α and β MR cells show different Na^+, K^+-ATPase immunoreactivity (Shikano and Fujio, 1998[c]). The α MR cells, situated within the secondary lamellae show strong immunoreactivity, whereas the β cells of the interlamellar regions have weaker Na^+, K^+-ATPase immunoreactivities. In addition, the α MR cells became larger and increased in number, therefore increasing the percentage area of α MR cells on SW adaptation. In contrast, the β MR cells became smaller and less numerous (Shikano and Fujio 1998[c]; Shikano and Fujio, 1998[b]). The present study was unable to classify MR cell type, but the change in *C. leucas* branchial Na^+, K^+-ATPase protein localisation is consistent

with the concept of the expression of different MR cell types according to environmental salinity.

There were no observable differences in Na^+, K^+-ATPase protein distribution in the intestine of *C. leucas* acclimated to FW and SW. As described in Section 1.4.4, the elasmobranch intestine is unlikely to have a major role in osmoregulation apart from during extensive feeding events and acclimation to hypersaline water, so it was unsurprising that no differences were observed in Na^+, K^+-ATPase distribution in this tissue.

In the sinus zone of both FW- and SW-acclimated *C. leucas* kidneys, Na^+, K^+-ATPase is located on the basolateral membrane of intermediate tubule sections. Strong Na^+, K^+-ATPase immunoreactivity was also observed in the flagellar ribbons of proximal tubule cells. In addition, proximal tubule cells bearing flagellar ribbons, and the basolateral membrane of some cells of the proximal tubules were Na^+, K^+-ATPase immunoreactive, but this observation only occurred in kidneys from FW-acclimated *C. leucas*. Visually, the Na^+, K^+-ATPase immunofluorescence was reduced in SW-acclimated *C. leucas* compared to FW-acclimated sharks. The cell specific staining observed in the proximal tubules of FW-acclimated sharks may be due to Na^+, K^+-ATPase being recruited to the plasma membrane from a diffuse cytoplasmic distribution. Given the relationship between Na^+, K^+-ATPase and several members of the FXYD family in the vertebrate kidney, it is possible that FXYDs may be associated to the Na^+, K^+-ATPase α subunit hence blocking the antibody recognition site. This would evidently result in an inaccurate picture of Na^+, K^+-ATPase expression. In *T. nigroviridis*, although Na^+, K^+-ATPase was localised to the basolateral membrane of cells within the proximal tubules, immunoreactivity also appeared to locate to the cytoplasm of the cells comprising the distal and collecting tubules. It was suggested that different tubules may have distinct patterns of basolateral membrane infoldings, causing Na^+, K^+-ATPase immunoreactivity to appear to be cytoplasmic, when in fact it is located on the membrane (Lin *et al.*, 2004).

In the rectal gland of both FW- and SW-acclimated sharks, Na^+, K^+-ATPase immunofluorescence predominates in the sub-capsular region, and gradually diminishes towards the central/luminal tubular region.

Immunofluorescence was observed throughout the secretory tubules of the rectal gland, but not the capsule enclosing the gland. In the rectal glands of FW-acclimated sharks, Na^+, K^+-ATPase immunoreactivity was localised to the basolateral membrane of cells within the tubules, whereas in the glands from SW-acclimated *C. leucas*, immunoreactivity appears to spread throughout the cytoplasm of the tubule cells. This is likely to be due to extensive infoldings of the basolateral and lateral membranes of these cells, and hence staining which appears to by cytoplasmic is localised to the highly complex basolateral and lateral membranes. A study of Na^+, K^+-ATPase localisation in the rectal gland of *S. acanthias* revealed that the enzyme was located on the basolateral and lateral membranes of the tubule cells, and more specifically, that the distribution of the enzyme on the membrane was linked to areas with abundant mitochondria (Eveloff *et al.*, 1979). Confocal microscopy would enable the precise distribution of Na^+, K^+-ATPase immunoreactivity to be determined in the rectal glands of *C. leucas*. As reported for the kidney, FXYDs have also been discovered in the elasmobranch rectal gland, (Cornelius *et al.*, 2000), and it is possible that these may be masking the true expression and distribution of Na^+, K^+-ATPase. This may be particularly true in the central tubular region of the gland where there are much lower levels of Na^+, K^+-ATPase immunoreactivity. No obvious differences in gross morphology of the gland were observed in this study, which is contrary to previous studies which report a decrease in tubule number in FW-acclimated *C. leucas* (Oguri, 1964).

6

Amplification, cloning, sequencing and expression of additional proteins:

- Phospholemman-like protein from shark (PLMS)
- Sodium, potassium, 2 chloride cotransporter (NKCC)
- Cystic fibrosis transmembrane conductance regulator (CFTR)
- Aquaporin (AQP)
- β-actin

Results

6.1: Amplification, cloning and expression of additional proteins

Although this project aimed to fully characterise and examine expression of Na^+, K^+-ATPase in *C. leucas*, several other additional proteins have been investigated during the course of these studies. Since osmoregulation depends on the functions of many different proteins including Na^+, K^+-ATPase, it was useful to know whether other key transporting or regulating proteins were also found in *C. leucas* osmoregulatory tissues. The proteins examined were the phospholemman-like protein from shark (PLMS, also called FXYD10), the sodium, potassium, 2 chloride cotransporter (NKCC), the cystic fibrosis transmembrane conductance regulator (CFTR) and aquaporin (AQP). It was also necessary to obtain a partial DNA sequence for *C. leucas* β-actin, in order to use the expression of this protein as a control for RT-PCR quantification analysis. Due to time and material constraints it was not possible to fully characterise and examine the expression of these proteins, however this chapter will summarise the results from our preliminary studies.

6.2: PLMS (FXYD10)

The success of obtaining the partial amino acid sequence of FXYDs from other elasmobranch species (Cornelius *et al.*, 2000; Schuurmans Stekhoven *et al.*, 2001) prompted a brief attempt to clone this gene from *C. leucas*. RT-PCR, Northern and Western blotting were carried out using primers, DNA probes and antibodies which were specific to the PLMS sequence reported for *S. acanthias* (SqPLMS; Mahmmoud *et al.*, 2003). RT-PCR failed to amplify any FXYDs from *C. leucas* cDNAs. A DNA probe specific to the sequence of SqPLMS in *S. acanthias* (NCBI/GenBank accession no. AJ556170) was hybridised to a Northern blot supporting RNAs from various tissues of *S. acanthias*, and the rectal gland of *C. leucas* and *S. canicula* (*Figure 6.1*). A PLMS mRNA transcript of ~3.6 kb was expressed in rectal gland, heart, brain, intestine and kidney, but not in gill, of *S. acanthias*. Although a similar sized transcript was also weakly expressed in *S. canicula* rectal gland, there was no expression of PLMS mRNA transcript in *C. leucas*. A weak signal from an unknown transcript of ~8 kb was found in *C. leucas* rectal gland when hybridised with the SqPLMS probe. *Figure 6.2* shows a Western blot

performed using *C. leucas* tissue homogenates and primary a polyclonal antibody raised against SqPLMS (courtesy of F. Cornelius and Y. Mahmmoud) which suggested the possibility of expression of a PLMS-like protein in *C. leucas*. Immunopositive bands of 15 kDa were found in kidney and rectal gland samples taken from *C. leucas* which were similar to the reported size of PLMS found in *S. acanthias* (Mahmmoud *et al.*, 2003).

6.3: NKCC

A 764 bp cDNA fragment of the NKCC gene was amplified from *C. leucas* gill cDNA using RT-PCR and degenerate primers (NKCC primers, Appendix 3). *Figure 6.3* shows the 764 bp RT-PCR product which was subsequently purified, cloned and sequenced (Sections 2.10-2.15). The interleaved nucleotide and putative amino acid sequence of the *C. leucas* NKCC fragment is shown in *Figure 6.4*. Within this region of the gene, this sequence shares 96% amino acid homology with *S. canicula* NKCC, 95% with *S. acanthias* NKCC, 70% with human NKCC1, and 44% with human NKCC2 (NCBI accession numbers Y18919, U05958, P55011 and Q13621 respectively). A purified clone of this fragment was used as a DNA probe in Northern blotting to examine NKCC mRNA expression in various tissues. A ~5 kb NKCC mRNA transcript was expressed in rectal gland, kidney, intestine, interrenal gland, atrium, ventricle and brain from both FW- and SW-acclimated *C. leucas* (*Figure 6.5*).

6.4: CFTR

A 839 bp fragment of CFTR DNA was amplified from *C. leucas* rectal gland cDNA using RT-PCR and degenerate primers (CFTR primers, Appendix 3; *Figure 6.6*). These fragments were purified, cloned and sequenced (Sections 2.10-2.15), and the resulting nucleotide and putative amino acid sequences are shown in *Figure 6.7*. The sequence is 90% homologous to the amino acid sequence reported for *S. acanthias* and 73% homologous to human CFTR (NCBI accession numbers P26362 and DQ356261.1 respectively). A purified clone of this fragment was used as a DNA probe in Northern blotting to examine CFTR mRNA expression in various tissues of FW- and SW-acclimated *C. leucas*. Two different sized CFTR mRNA transcripts (approximately 4 and 5 kb) were expressed in rectal gland, whereas only the

larger transcript was expressed in kidney. There was no expression of CFTR in any of the other tissues examined (*Figure 6.8*).

6.5: AQP

A 394 bp cDNA fragment of AQP was amplified from SW-acclimated *C. leucas* kidney cDNA using RT-PCR and degenerate primers (AQP1e primers, Appendix 3). *Figure 6.9* shows the amplified 394 bp fragment which was subsequently purified, cloned and sequenced (Sections 2.10-2.15). The full sequence of 1095 nucleotides encoding for a 256 amino acid protein was obtained using RACE RT-PCR by C. Cutler (Cutler *et al.*, 2005), and is shown in *Figure 6.10*. The amino acid sequence of *C. leucas* AQP shares similar homologies with the human isoforms AQP1 (46%), AQP2 (48%) and AQP5 (48%; NCBI accession numbers BC022486.1, BC042496.1 and NM_001651.1 respectively). Using a purified clone of the original fragment as a DNA probe, Northern blotting was used to examine AQP mRNA expression in various tissues. A ~1.1 kb AQP mRNA transcript was expressed in SW-acclimated *C. leucas* kidney, but not in FW-acclimated *C. leucas*. No expression was found in any other tissues examined *(Figure 6.11)*.

6.6: β-actin

As discussed in Section 4.2, *C. leucas* β-actin was used as a control "housekeeping" gene in the evaluation of Na^+, K^+-ATPase α subunit isoform expression in tissues from fish acclimated to FW and SW. Initially, a 795 bp fragment of β-actin was amplified, using RT-PCR and degenerate primers (β-actin primer, Appendix 3), from cDNAs prepared from *C. leucas* rectal gland, kidney, gill and intestine. This fragment (shown in *Figure 6.12*), was purified, cloned and sequenced (Sections 2.10-2.15). The sequences revealed the expression of two distinct isoforms as shown in *Figures 6.13 - 6.15*. The β-actin isoform A cDNA sequence is 81% identical to the β-actin isoform B. However, these sequences encode two proteins which are only distinguishable from each other at two amino acid positions (^{126}Gly/Ala and ^{144}Leu/Met; as illustrated in *Figures 6.13* and *6.14*). The β-actin isoform A amino acid sequence shares 97% homology with both human β-actin and *T. scyllium* β-actin (NCBI accession numbers BC014861 and AB084472 respectively). The β-actin isoform B amino acid sequence of *C. leucas* shares

98% homology with a human β-actin variant, but also 98% with β-actin of human and *T. scyllium* (NCBI accession numbers AK223055, BC014861 and AB084472 respectively). In order to use β-actin as a control gene for the Na^+, K^+-ATPase α subunit isoforms, the fragment to be amplified needed to be of a comparable size to the α subunit isoform fragments being amplified. A specific primer set was designed which would amplify a 425 bp fragment of both A and B isoforms (*C. leucas* β-actin, Appendix 3) and this can be seen in *Figure 4.1* along with the Na^+, K^+-ATPase α subunit isoform fragments.

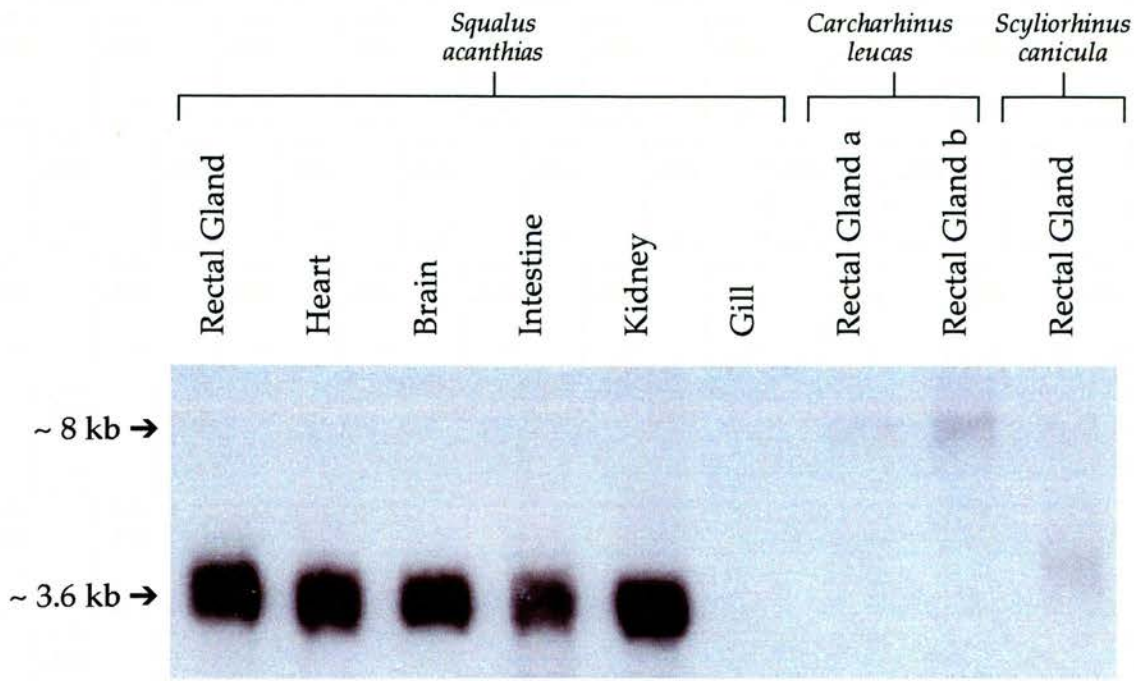

Figure 6.1: Expression of SqPLMS in *S. acanthias*, *C. leucas* and *S. canicula*. Northern blot using a fragment of SqPLMS as a DNA probe to examine expression of SqPLMS in rectal gland, heart, brain, intestine, kidney and gill of *S. acanthias*, and rectal gland of *C. leucas* and *S. canicula*. For *C. leucas*, rectal gland a and b denote RNA samples isolated from two different fish. With the exception of the gill, all tissues from *S. acanthias* express a SqPLMS mRNA transcript of ~3.6 kb. *S. canicula* rectal gland also expresses a transcript of ~3.6 kb, whereas *C. leucas* does not express a transcript of this size, but instead does express a transcript of ~8 kb.

Figure 6.2: Expression of SqPLMS in *C. leucas* using Western blotting. 100 μg protein from of each tissue homogenate was blotted and the resulting blots were probed with SqPLMS antiserum, diluted 1:5000. Two immunopositive bands within the expected size range of SqPLMS were identified.

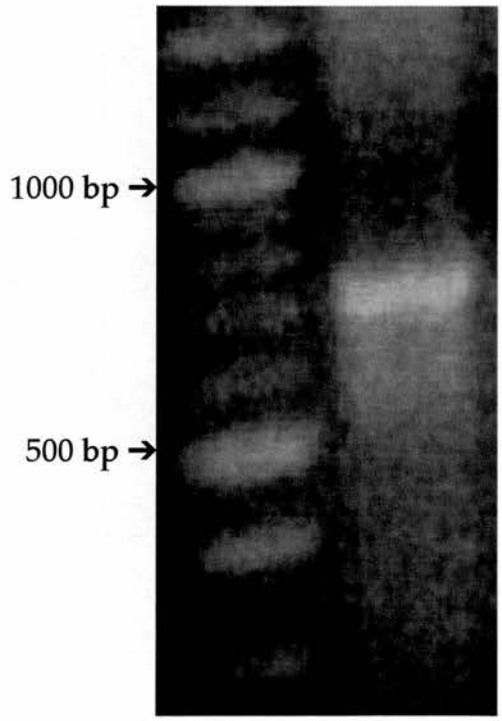

Figure 6.3: RT-PCR amplification of a NKCC cDNA fragment. A cDNA fragment of NKCC, of 764 bp, was amplified using a *C. leucas* gill cDNA template as described in Section 6.3.

```
    Glu Asp His Met Lys Asn Phe Arg Pro Gln Cys Leu Leu Met Thr Gly Ala Pro Thr Ser     20
  1 GAG GAT CAC ATG AAA AAC TTC AGG CCC CAA TGC CTG TTG ATG ACA GGT GCT CCT ACA TCC
    Arg Pro Ala Leu Leu His Leu Val His Ala Phe Thr Lys Asn Val Gly Leu Val Val Cys     40
 61 CGT CCA GCT TTG CTC CAT CTA GTT CAT GCC TTT ACC AAA AAT GTT GGA CTG GTG GTC TGT
    Gly His Val His Thr Gly Pro Arg Arg Gln Ala Leu Lys Glu Ile Ser Thr Asp Gln Ala     60
121 GGA CAT GTT CAT ACG GGA CCT CGT AGA CAA GCC TTG AAG GAA ATT TCT ACT GAT CAA GCC
    Lys Tyr Gln Arg Trp Leu Ile Lys Asn Lys Met Lys Ala Phe Tyr Ala Pro Val Tyr Ala     80
181 AAG TAT CAA CGG TGG TTA ATC AAA AAC AAA ATG AAA GCC TTC TAC GCG CCT GTA TAT GCA
    Glu Asp Leu Arg Glu Gly Thr Gln Phe Leu Leu Gln Ala Val Gly Leu Gly Arg Met Arg    100
241 GAA GAT CTG CGT GAG GGA ACA CAG TTC TTG CTT CAG GCT GTA GGA CTT GGT CGA ATG CGT
    Pro Asn Thr Leu Val Leu Gly Phe Lys Lys Asp Trp His Gln Ala Leu Met Lys Asp Val    120
301 CCC AAC ACG CTT GTT CTT GGC TTT AAA AAA GAC TGG CAC CAA GCC CTT ATG AAG GAT GTG
    Glu Asn Tyr Ile Asn Thr Ile His Asp Ala Phe Asp Tyr Gln Tyr Gly Val Val Val Ile    140
361 GAA AAT TAC ATC AAT ACT ATT CAT GAT GCA TTT GAC TAT CAG TAT GGA GTA GTT GTC ATT
    Arg Leu Lys Glu Gly Phe Asn Ile Ser His Leu Gln Ala Gln Glu Glu Leu Cys Thr Ser    160
421 AGA CTA AAG GAA GGC TTT AAT ATT TCT CAC CTA CAA GCA CAA GAA GAA CTG TGC ACT TCT
    Gln Glu Lys Ser Ala His Pro Lys Asp Ile Val Val Asn Leu Glu His Ser Asp Ala Asp    180
481 CAG GAG AAA TCT GCT CAT CCT AAG GAT ATA GTA GTA AAT CTG GAG CAC TCT GAT GCA GAC
    Ser Ser Lys Pro Ser Ser Lys Ser Val Ser Glu Thr Asn Ser Pro Ala Val Ser Gln Asp    200
541 TCT TCC AAG CCA TCT TCT AAA TCA GTG AGT GAA ACC AAC AGC CCA GCA GTG TCA CAA GAC
    Gln Lys Asp Glu Glu Asp Asp Gly Lys Ala Ser Thr Gln Pro Leu Leu Lys Lys Glu Ala    220
601 CAA AAA GAT GAA GAA GAT GAC GGA AAG GCG TCA ACC CAG CCA CTC TTG AAA AAA GAG GCT
    Lys Gly Pro Ser Val Pro Leu Thr Met Thr Asp Gln Lys Leu Leu Gln Ala Ser Ser Arg    240
661 AAA GGT CCA TCT GTG CCT TTG ACT ATG ACC GAT CAG AAG CTG CTT CAG GCC AGC TCT CGC
    Phe Gln Lys Lys Gln Gly Lys Asp Thr Ile Asp Ile Trp Gly                            254
721 TTC CAG AAG AAA CAG GGC AAG GAC ACG ATC GAC ATC TGG GGG BT
```

Figure 6.4: Interleaved sequence of the *C. leucas* NKCC cDNA fragment. Nucleotide and amino acid sequences of *C. leucas* NKCC.

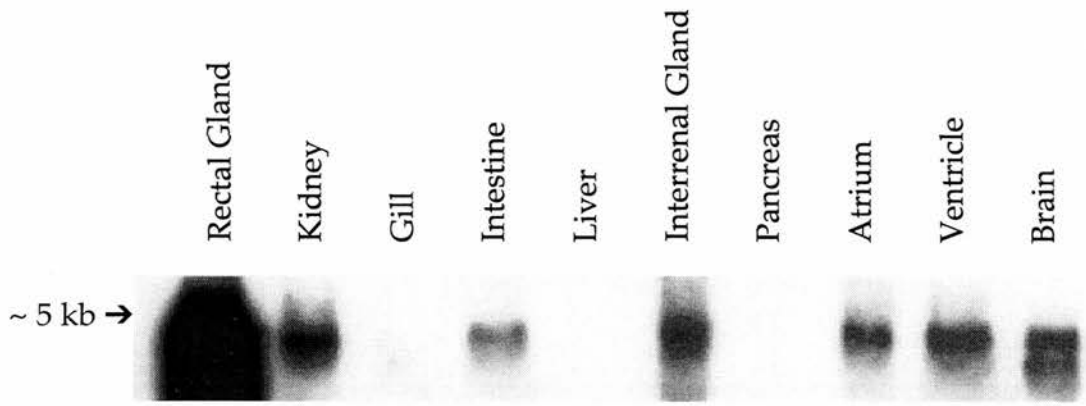

Figure 6.5: Expression of NKCC mRNA in bull shark tissues determined by Northern blotting. This figure shows the relative levels of NKCC in various bull shark tissues. Autoradiographs were exposed for 18-hours to the blot –80°C. All mRNA transcripts were ~5 kb in size. NKCC was highly expressed in rectal gland, with lower levels found in the kidney, intestine, interrenal gland, atrium, ventricle and brain. Since the blots for FW- and SW-acclimated *C. leucas* were identical, only the blot from FW-acclimated fish is shown.

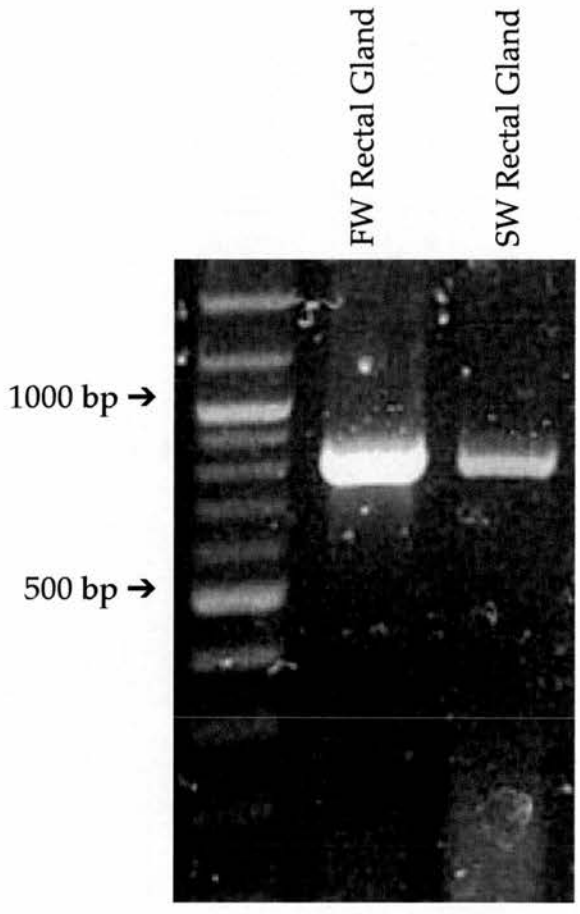

Figure 6.6: RT-PCR amplification of a CFTR cDNA fragment. A cDNA fragment of 839 bp was amplified using rectal gland cDNA templates and degenerate sense and antisense CFTR primers (Appendix 3) from both FW- and SW-acclimated *C. leucas* as described in Section 6.4.

```
    Tyr Phe Glu Thr Leu Phe His Lys Ala Leu Asn Leu His Thr Ala Asn Trp Phe Leu Tyr     20
  1 TAC TTT GAA ACG CTG TTC CAC AAG GCT CTG AAC CTT CAC ACT GCA AAC TGG TTT CTC TAC
    Leu Ser Thr Leu Arg Trp Phe Gln Met Arg Ile Asp Ile Val Phe Val Leu Phe Phe Ile     40
 61 CTC TCA ACG CTG CGC TGG TTC CAG ATG AGG ATT GAT ATT GTA TTT GTT CTC TTC TTT ATT
    Ala Ile Thr Phe Ile Ser Ile Ala Thr His Asn Ile Arg Glu Gly Lys Val Gly Ile Ile     60
121 GCA ATT ACT TTC ATC TCC ATA GCA ACA CAC AAT ATC AGA GAA GGA AAA GTT GGA ATT ATC
    Leu Thr Leu Ala Met Thr Ile Met Ser Thr Leu Gln Trp Ala Val Asn Ser Ser Ile Asp     80
181 CTG ACC TTA GCC ATG ACC ATT ATG AGC ACT CTG CAG TGG GCT GTC AAT TCA AGC ATA GAC
    Val Asp Ser Leu Met Arg Ser Val Ser Arg Val Phe Lys Tyr Ile Asp Ile Pro Pro Glu    100
241 GTG GAT AGT CTG ATG AGG TCT GTA AGT CGT GTT TTT AAA TAC ATT GAC ATA CCT CCG GAA
    Gly Ser Glu Phe Lys Asn Gln His His Leu Ser Asn Pro Ser Asp Val Leu Val Ile Glu    120
301 GGA TCG GAA TTC AAG AAC CAA CAT CAT CTC AGC AAC CCC TCG GAT GTG CTC GTA ATT GAA
    Asn Lys Tyr Leu Thr Asn Glu Trp Pro Ser Gly Gly Gln Met Met Val Asn Asn Leu Thr    140
361 AAC AAG TAT CTA ACC AAT GAA TGG CCA TCA GGA GGC CAG ATG ATG GTG AAT AAC CTC ACA
    Ala Lys Tyr Thr Asn Asp Gly Arg Pro Val Leu Gln Asp Leu Ser Phe Phe Val Asn Ala    160
421 GCC AAG TAT ACC AAT GAT GGG CGC CCA GTT CTT CAG GAC CTT TCC TTC TTT GTA AAT GCA
    Gly Gln Arg Val Gly Leu Leu Gly Arg Thr Gly Ala Gly Lys Ser Thr Leu Leu Ser Ala    180
481 GGA CAA CGG GTT GGA TTG CTG GGA CGG ACA GGT GCT GGA AAG AGC ACA TTG CTT TCT GCT
    Leu Leu Arg Leu Leu Ser Thr Glu Gly Glu Ile Gln Ile Asp Gly Ile Ser Trp Asn Ser    200
541 CTT CTG CGT CTC TTG TCA ACT GAA GGG GAA ATC CAG ATT GAT GGG ATA TCC TGG AAT TCA
    Val Ser Leu Gln Lys Trp Arg Lys Ala Phe Gly Val Ile Pro Gln Lys Val Phe Val Phe    220
601 GTC TCC TTA CAA AAG TGG AGA AAA GCA TTT GGC GTC ATT CCA CAG AAA GTC TTT GTG TTC
    Ser Gly Thr Phe Arg Lys Asn Leu Asp Pro Tyr Glu Gln Trp Ser Asp Glu Glu Ile Trp    240
661 TCT GGA ACC TTC CGG AAG AAC TTG GAT CCT TAC GAA CAA TGG AGC GAT GAG GAA ATC TGG
    Asn Val Thr Glu Glu Val Gly Leu Lys Ser Val Ile Glu Gln Phe Pro Asp Asn Leu Asn    260
721 AAT GTC ACT GAA GAG GTT GGT TTG AAA TCA GTG ATT GAG CAG TTT CCA GAT AAT CTT AAC
    Phe Val Leu Val Asp Gly Gly Tyr Ile Leu Ser Xxx Gly His Xxx Xxx Phe Met Cys        279
781 TTT GTT TTG GTG GAT GGC GGC TAC ATT CTC AGC AAY GGC CAC AAR CAR TTC ATG TGC YT
```

Figure 6.7: Interleaved sequence of the *C. leucas* CFTR cDNA fragment. Nucleotide and putative amino acid sequences of *C. leucas* CFTR.

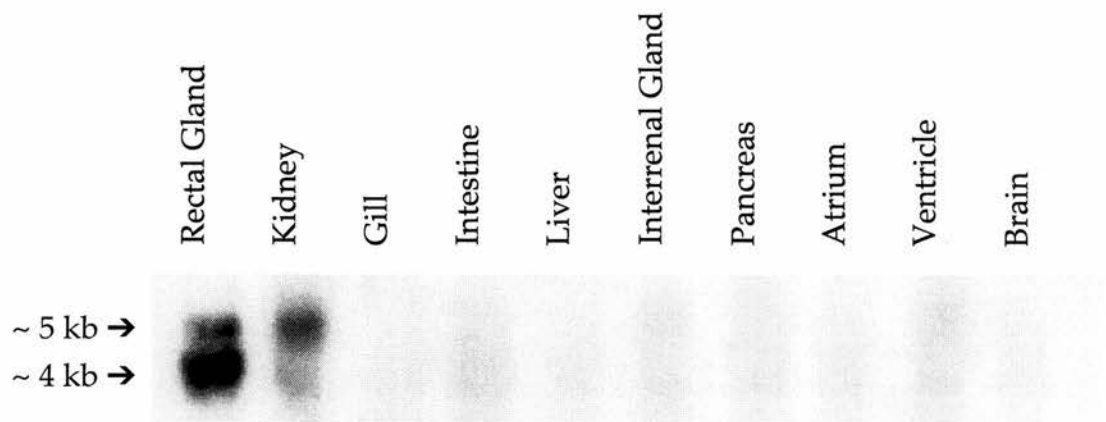

Figure 6.8: Expression of CFTR mRNA in tissues from bull sharks acclimated to FW determined by Northern blotting. This figure shows the relative levels of CFTR in various bull shark tissues. Autoradiographs were exposed for 18-hours to the blot –80°C. A CFTR mRNA transcript of ~5 kb was expressed in both rectal gland and kidney, and a smaller transcript of ~4 kb was expressed only in the rectal gland. An identical pattern of expression was observed for SW-acclimated fish (data not shown).

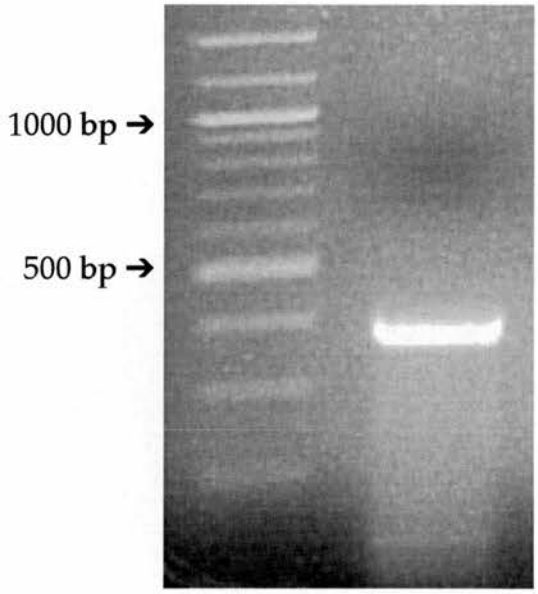

Figure 6.9: RT-PCR amplification of an AQP cDNA fragment. An AQP cDNA fragment of 394 bp was amplified using a kidney cDNA template prepared from SW-acclimated *C. leucas* as described in Section 6.5.

```
   1                                                                AAACACGACTCAGAG
     Met Lys Leu Leu Lys Glu Glu Ile Leu Ser Glu Leu Phe Trp Arg Ala Leu Thr Ala Glu     20
  16 ATG AAA CTG CTG AAA GAG GAA ATT CTC AGC GAG TTA TTC TGG AGG GCC CTG ACT GCC GAA
     Phe Leu Gly Thr Ala Val Phe Val Phe Ser Ser Leu Ala Cys Ala Leu Gly Trp Ser Gly     40
  76 TTC CTG GGG ACT GCA GTC TTT GTG TTC TCC AGC TTG GCC TGT GCC TTG GGC TGG TCG GGA
     Gly Gly Pro Ser Thr Leu Gln Ile Ala Leu Gly Phe Gly Leu Gly Val Ala Ala Val Ser     60
 136 GGA GGT CCC AGC ACC CTG CAG ATT GCC CTG GGC TTT GGT CTG GGG GTA GCT GCT GTC TCT
     Val Phe Thr Gln Gly Val Ser Gly Ala Gln Leu Asn Pro Ala Val Ser Leu Ala Leu Leu     80
 196 GTC TTC ACC CAG GGA GTG AGC GGG GCT CAG CTG AAC CCC GCG GTC AGC CTC GCC CTG CTC
     Leu Gly Leu Arg Ile Ser Pro Leu Arg Ala Leu Leu Tyr Thr Ile Val Gln Ser Leu Gly    100
 256 CTT GGT TTG CGC ATC AGT CCA CTC CGA GCT CTG CTC TAC ACG ATC GTG CAA AGC CTG GGG
     Ala Ile Ala Ala Cys Ala Leu Leu Ser Val Leu Thr Pro Glu Asp Ile His Gly Asp Leu    120
 316 GCC ATC GCA GCT TGT GCC CTC CTC TCT GTA CTC ACA CCT GAG GAT ATC CAC GGA GAC CTG
     Gly Leu Asn Gln Pro Ser Pro Gly Val Thr Gln Ser Gln Ala Leu Gly Val Glu Ile Ile    140
 376 GGG CTC AAC CAG CCT TCT CCG GGA GTT ACA CAG AGC CAG GCT CTG GGA GTG GAG ATC ATT
     Ile Thr Phe Gln Leu Val Met Cys Val Phe Thr Ile Ser His Lys Asp Ser Asn Phe Lys    160
 436 ATC ACC TTC CAG CTC GTT ATG TGT GTA TTC ACC ATT TCC CAC AAG GAC AGC AAC TTC AAA
     Gly Cys Ala His Met Ala Ile Gly Ala Ser Val Thr Leu Gly His Leu Val Ala Ile Gly    180
 496 GGC TGT GCA CAC ATG GCG ATT GGA GCA TCT GTG ACT CTT GGA CAT CTA GTG GCA ATT GGA
     Tyr Thr Gly Cys Ser Met Asn Pro Ala Arg Ser Leu Gly Pro Ala Val Ile Thr Thr Asn    200
 556 TAT ACT GGG TGC AGT ATG AAC CCT GCT CGA TCT TTG GGG CCA GCT GTC ATT ACA ACA AAC
     Phe Ser His Leu Trp Ile Phe Trp Val Gly Pro Leu Leu Gly Gly Val Leu Ala Ala Ile    220
 616 TTC AGC CAT CTT TGG ATT TTT TGG GTC GGG CCC CTC CTT GGA GGA GTC TTG GCT GCA ATT
     Val Tyr Asn Leu Leu Leu Arg Thr Lys Arg Met Gly Cys Arg Asp Cys Leu Asn Ser Leu    240
 676 GTG TAC AAT TTA CTA TTG AGG ACA AAG AGG ATG GGG TGC AGA GAC TGC CTG AAC TCA CTG
     Lys Thr Asp Gln Lys Val Glu Phe Asn Leu Glu Ser Gln Pro Ser Thr Stop              256
 736 AAG ACT GAT CAA AAG GTG GAA TTC AAC CTG GAA TCA CAG CCA TCA ACT TAA ATGTTGTTCCT
 798 GCAGCTTCTGGCCAGCAAATCAATCATCTGGCAATAAATAAGGCAGCGTCATCTATCAACCTTTCTATGTCAGTATGTT
 877 TCTAAAGTTGGTCAACTTTGTAAATAAAAATCAGGTCTTTTGTTTTCTTTGTGAAACACTTTATTGAAATTGTATTTGA
 956 GTAAATGAGAGTTCTGCTGTTGTGTTTAGTAAGTGCAGAAGGACAGGGACACACTGTGGTAATGTTCTGATATTTCACT
1035 GTATCGTGTAATAAAATCAAATCTGGATCACCAAAAAAAAAAAAAAAAAAAAAAAAAAAAA
```

Figure 6.10: Interleaved sequence of the *C. leucas* AQP cDNA. Nucleotide and putative amino acid sequences of the full length *C. leucas* AQP cDNA.

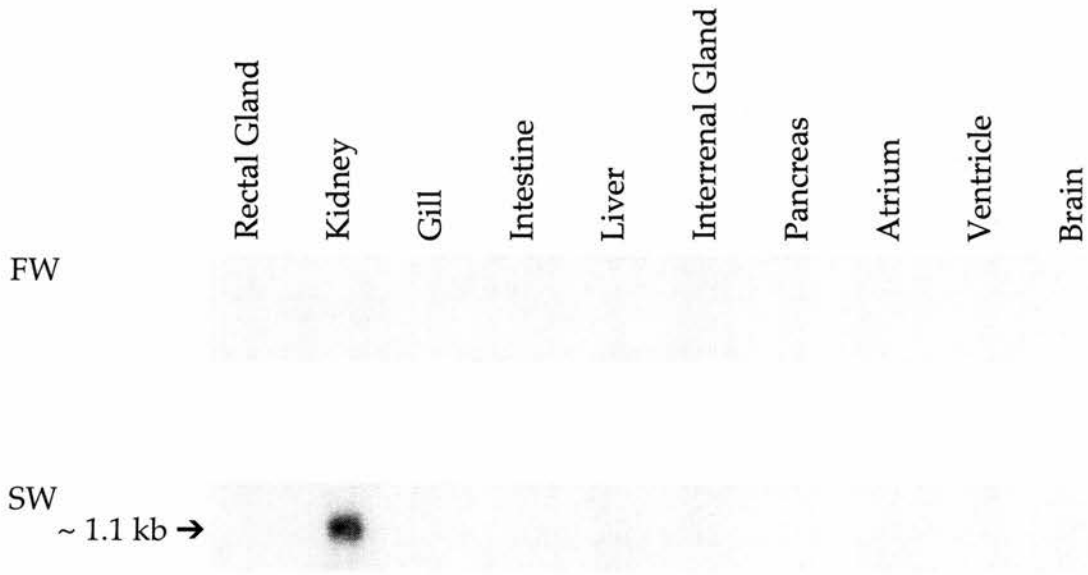

Figure 6.11: Expression of AQP mRNA in bull shark tissues determined by Northern blotting. Autoradiograph indicating the levels of expression of AQP mRNA in various bull shark tissues. Autoradiograph was exposed at –80°C for 18-hours. An AQP mRNA transcript of ~1.1 kb was expressed only in kidney from SW-acclimated *C. leucas*.

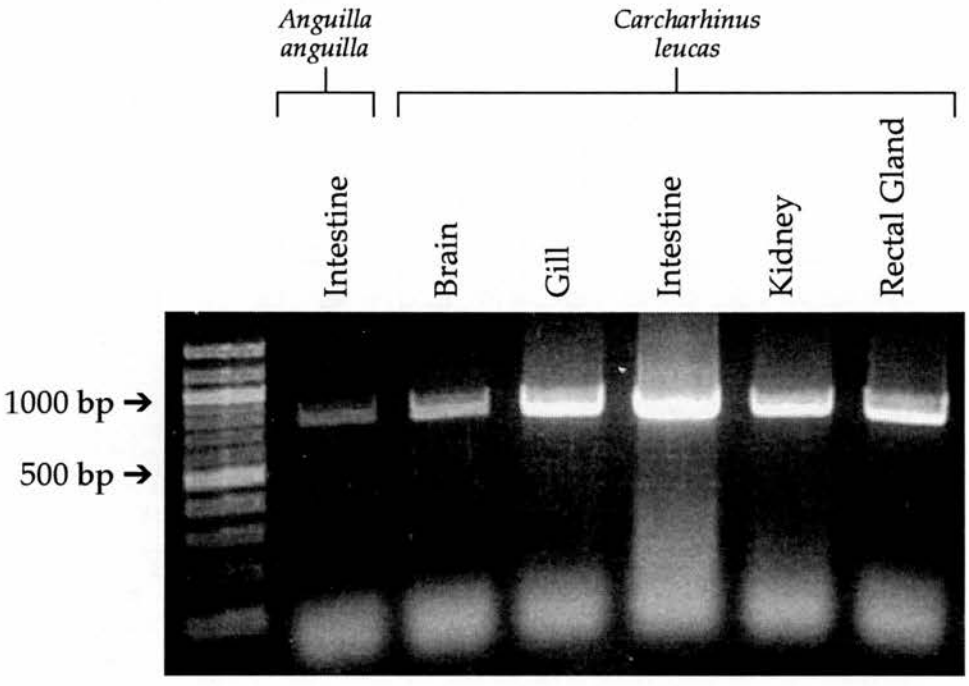

Figure 6.12: RT-PCR amplification of a β-actin cDNA fragment. A cDNA fragment of β-actin (795 bp) was amplified from eel (*Anguilla anguilla*) intestine and *C. leucas* brain, gill, intestine, kidney and rectal gland cDNA templates.

```
    Val Asp Asn Gly Ser Gly Met Cys Glu Ala Gly Phe Ala Gly Asp Asp Ala Pro Arg Ala     20
  1 GTC GAT AAT GGG TCG GGG ATG TGT GAG GCC GGA TTC GCC GGA GAT GAC GCA CCC CGT GCG
    Val Phe Pro Ser Ile Val Gly Arg Pro Arg His Gln Gly Val Met Val Gly Met Gly Gln     40
 61 GTT TTT CCT TCC ATC GTA GGA AGG CCA CGT CAC CAA GGT GTG ATG GTC GGT ATG GGT CAG
    Lys Asp Ser Tyr Val Gly Asp Glu Ala Gln Ser Lys Arg Gly Ile Leu Thr Leu Lys Tyr     60
121 AAG GAC AGT TAC GTT GGT GAT GAA GCC CAG TCT AAA CGT GGT ATC CTC ACG CTC AAG TAT
    Pro Ile Glu His Gly Ile Val Thr Asn Trp Asp Asp Met Glu Lys Ile Trp His His Thr     80
181 CCT ATT GAG CAC GGT ATC GTC ACC AAC TGG GAT GAC ATG GAG AAG ATT TGG CAC CAC ACC
    Phe Tyr Asn Glu Leu Arg Val Ala Pro Glu Glu His Pro Val Leu Leu Thr Glu Ala Pro    100
241 TTC TAC AAC GAG TTG CGT GTC GCC CCC GAG GAG CAC CCC GTG CTT CTT ACC GAA GCC CCG
    Leu Asn Pro Lys Ala Asn Arg Glu Lys Met Thr Gln Ile Met Phe Glu Thr Phe Asn Thr    120
301 TTG AAC CCT AAG GCC AAC CGC GAG AAA ATG ACC CAG ATC ATG TTC GAG ACC TTC AAC ACG
    Pro Ala Met Tyr Val Gly Ile Gln Ala Val Leu Ser Leu Tyr Ala Ser Gly Arg Thr Thr    140
361 CCC GCC ATG TAC GTT GGT ATT CAG GCG GTG CTC TCT CTG TAT GCC TCT GGT CGT ACC ACC
    Gly Ile Val Leu Asp Ser Gly Asp Gly Val Thr His Thr Val Pro Ile Tyr Glu Gly Tyr    160
421 GGT ATT GTG CTC GAC TCC GGA GAC GGT GTC ACT CAC ACT GTG CCC ATT TAC GAA GGT TAC
    Ala Leu Pro His Ala Ile Leu Arg Leu Asp Leu Ala Gly Arg Asp Leu Thr Asp Tyr Leu    180
481 GCT CTG CCC CAC GCC ATT CTG CGT CTT GAC TTG GCC GGT CGT GAT TTG ACC GAC TAC TTG
    Met Lys Ile Leu Thr Glu Arg Gly Tyr Ser Phe Thr Thr Thr Ala Glu Arg Glu Ile Val    200
541 ATG AAA ATC CTC ACC GAG CGT GGT TAC AGT TTC ACC ACC ACG GCC GAG CGT GAA ATT GTC
    Arg Asp Ile Lys Glu Lys Leu Cys Tyr Val Ala Leu Asp Phe Glu Gln Glu Met Ala Thr    220
601 CGT GAC ATC AAG GAG AAG CTC TGC TAC GTC GCC TTG GAC TTT GAA CAG GAA ATG GCT ACT
    Ala Ala Ser Ser Ser Ser Leu Glu Lys Ser Tyr Glu Leu Pro Asp Gly Gln Val Ile Thr    240
661 GCC GCT TCC AGC TCA TCT TTA GAG AAG AGC TAC GAA TTG CCC GAT GGT CAG GTT ATC ACC
    Ile Gly Asn Glu Arg Phe Arg Cys Pro Glu Ala Leu Phe Gln Pro Ser Phe Leu Gly Met    260
721 ATC GGT AAC GAG CGT TTC CGT TGT CCC GAG GCT CTG TTC CAG CCC AGC TTC CTC GGC ATG
    Glu Ser Cys Gly Ile                                                              265
781 GAA TCG TGC GGA ATC
```

Figure 6.13: Interleaved sequence of *C. leucas* β-actin A isoform. Nucleotide and amino acid sequences of a fragment of the *C. leucas* β-actin A isoform. ^{126}Gly and ^{144}Leu are the only amino acid residues which vary between the two β-actin isoforms (highlighted in red).

```
  1                                                                   G
    Xxx Xxx Xxx Gly Xxx Gly Met Xxx Glu Ala Gly Phe Ala Gly Asp Asp Ala Pro Arg Ala     20
  2 GTS GAH AWK GGG TCS GGG ATG TGY GAG GCT GGC TTT GCT GGG GAT GAT GCC CCT CGT GCT
    Val Phe Pro Ser Ile Val Gly Arg Pro Arg His Gln Gly Val Met Val Gly Met Gly Gln     40
 62 GTC TTC CCT TCC ATT GTT GGT CGC CCA AGA CAC CAG GGT GTA ATG GTT GGT ATG GGG CAG
    Lys Asp Ser Tyr Val Gly Asp Glu Ala Gln Ser Lys Arg Gly Ile Leu Thr Leu Lys Tyr     60
122 AAG GAC AGC TAC GTT GGT GAT GAG GCT CAG AGC AAA AGA GGT ATC CTG ACC CTG AAG TAC
    Pro Ile Glu His Gly Ile Val Thr Asn Trp Asp Asp Met Glu Lys Ile Trp His His Thr     80
182 CCC ATT GAG CAC GGT ATT GTC ACC AAC TGG GAT GAC ATG GAG AAG ATC TGG CAT CAC ACT
    Phe Tyr Asn Glu Leu Arg Val Ala Pro Glu Glu His Pro Val Leu Leu Thr Glu Ala Pro    100
242 TTC TAC AAT GAA CTG CGA GTT GCT CCT GAA GAA CAC CCA GTC CTG CTC ACA GAA GCC CCC
    Leu Asn Pro Lys Ala Asn Arg Glu Lys Met Thr Gln Ile Met Phe Glu Thr Phe Asn Thr    120
302 CTG AAC CCC AAA GCC AAC AGA GAA AAA ATG ACA CAG ATT ATG TTT GAG ACT TTC AAT ACC
    Pro Ala Met Tyr Val Ala Ile Gln Ala Val Leu Ser Leu Tyr Ala Ser Gly Arg Thr Thr    140
362 CCT GCC ATG TAT GTT GCC ATC CAG GCT GTG CTG TCA CTC TAT GCC TCT GGT AGA ACC ACT
    Gly Ile Val Met Asp Ser Gly Asp Gly Val Thr His Thr Val Pro Ile Tyr Glu Gly Tyr    160
422 GGT ATT GTG ATG GAC TCT GGT GAT GGT GTC ACC CAC ACT GTG CCC ATC TAT GAA GGT TAT
    Ala Leu Pro His Ala Ile Leu Arg Leu Asp Leu Ala Gly Arg Asp Leu Thr Asp Tyr Leu    180
482 GCC CTC CCC CAT GCT ATT CTG CGT CTG GAT TTG GCT GGT CGT GAT CTG ACA GAC TAC CTC
    Met Lys Ile Leu Thr Glu Arg Gly Tyr Ser Phe Thr Thr Thr Ala Glu Arg Glu Ile Val    200
542 ATG AAG ATT CTG ACA GAA AGA GGC TAC TCT TTC ACC ACC ACA GCT GAG AGA GAA ATT GTC
    Arg Asp Ile Lys Glu Lys Leu Cys Tyr Val Ala Leu Asp Phe Glu Gln Glu Met Ala Thr    220
602 CGT GAC ATC AAG GAG AAG CTC TGC TAT GTT GCA CTG GAC TTT GAA CAG GAG ATG GCC ACT
    Ala Ala Ser Ser Ser Ser Leu Glu Lys Ser Tyr Glu Leu Pro Asp Gly Gln Val Ile Thr    240
662 GCT GCT TCC TCT TCT TCC CTT GAG AAG AGC TAT GAA CTG CCT GAT GGG CAG GTA ATC ACC
    Ile Gly Asn Glu Arg Phe Arg Cys Pro Glu Ala Leu Phe Gln Pro Ser Phe Xxx Gly Met    260
722 ATT GGT AAT GAG CGA TTC AGA TGC CCA GAG GCC CTC TTC CAG CCA TCT TTC YTS GGC ATG
    Glu Xxx Cys Xxx Ile                                                             265
782 GAA TCS TGC GGW ATC
```

Figure 6.14: Interleaved sequence of *C. leucas* β-actin B isoform. Nucleotide and amino acid sequences of a fragment of the *C. leucas* β-actin B isoform. ^{126}Ala and ^{144}Met are the only amino acid residues which vary between the two β-actin isoforms (highlighted in red).

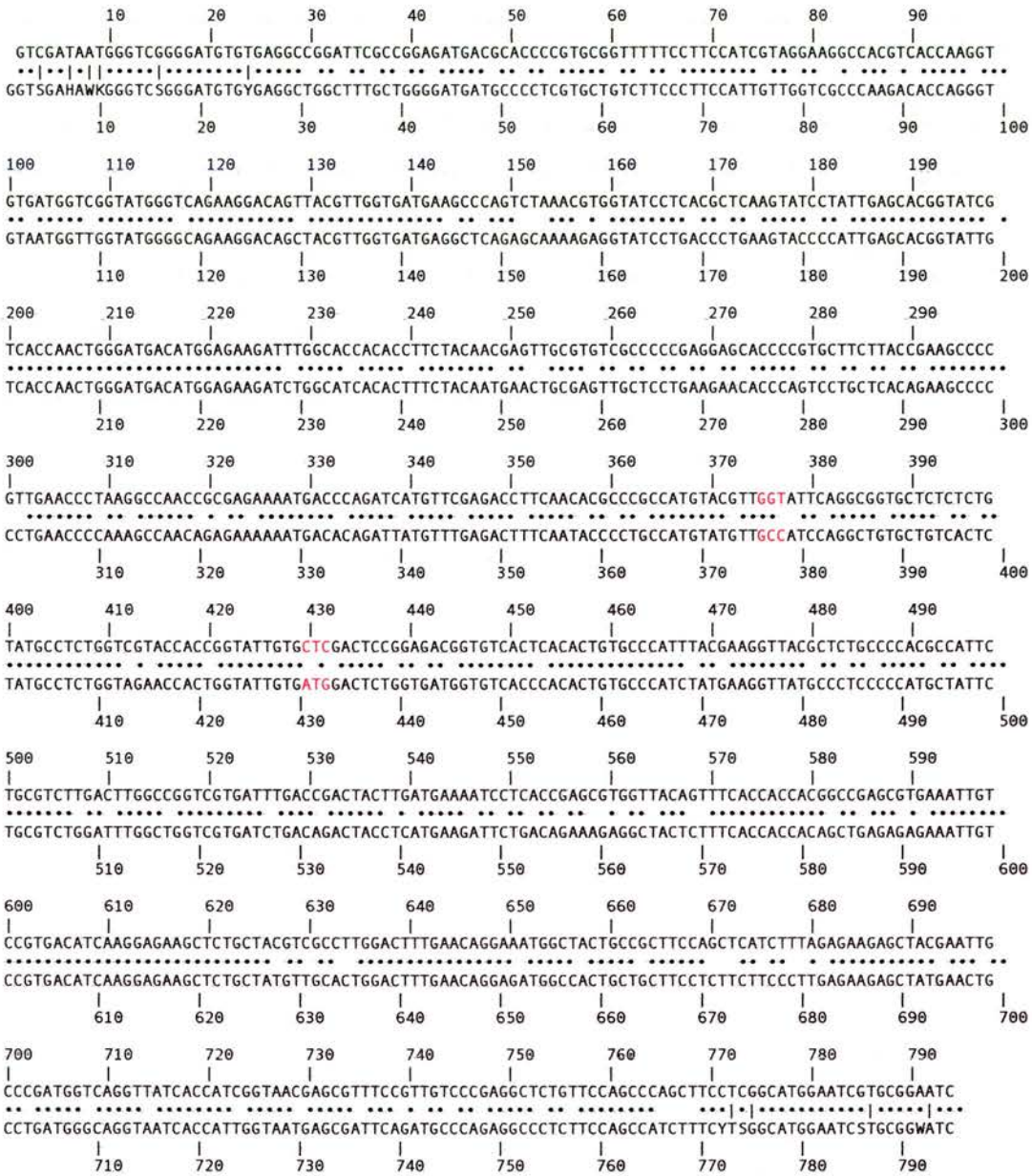

Figure 6.15: Alignment of the *C. leucas* β-actin A isoform cDNA fragment (top) with the *C. leucas* β-actin B isoform cDNA fragment (bottom). Nucleotide sequences of both isoforms of the *C. leucas* β-actin gene. The cDNA sequences are 81% identical but encode proteins which only vary at two amino acid positions (as shown in *Figures 6.13* and *6.14*). The codons which encode the variable residues are highlighted in red.

6.7: Expression of additional proteins in *C. leucas*

Using the SqPLMS antibody, Western blots indicated the presence a bull shark homologue of SqPLMS in various tissue homogenates. However, several cloning techniques failed to amplify PLMS cDNA from *C. leucas* tissues and Northern blot analysis using a SqPLMS probe also failed to identify potential PLMS mRNA transcripts. Due to the high interspecific variability of FXYDs, it is likely that the primers used for PCR amplification and the DNA probe synthesised from the *S. acanthias* cDNA were not of sufficient homology to match any possible FXYDs expressed in *C. leucas*. However, the results of the protein expression studies, carried out using the polyclonal antibody raised to the PLMS sequence from *S. acanthias* did yield immunopositive bands in *C. leucas* of around 15 kDa which is a similar size to the SqPLMS protein. Further studies would be required to verify whether this band is *C. leucas* PLMS.

NKCC was expressed at detectable levels on Northern blots supporting *C. leucas* RNA extracted from rectal gland, kidney, intestine, interrenal gland, atrium, ventricle and brain. Although on Northern blots expression in the gill was undetectable, NKCC was amplified using RT-PCR and cDNA from *C. leucas* gill. The *C. leucas* NKCC mRNA transcript was ~5 kb in size in all tissues, contrary to *S. acanthias*, in which a 5.2 kb transcript is found only in the kidney, with a 7.4 kb transcript present in rectal gland, brain, gill, heart, intestine and testis (Xu *et al.*, 1994). A 7.2 kb NKCC mRNA transcript was also discovered in the rectal gland of *S. canicula* (MacKenzie *et al.*, 2002). These transcripts correspond to the sizes of the mammalian secretory NKCC1 (~7.4 kb) and absorptive NKCC2 (~5 kb) isoforms (Russell, 2000). This would indicate that the mRNA transcript expressed in *C. leucas* is the smaller absorptive NKCC2 isoform, however the amino acid homologies of human NKCC1 and NKCC2 with the short section of *C. leucas* NKCC which has been sequenced would indicate otherwise (70% and 44% respectively). The entire sequence of *C. leucas* NKCC must be elucidated in order to state which NKCC isoform is present in this species.

In *C. leucas*, CFTR was expressed at detectable levels only in the rectal gland and kidney. Two different sized transcripts of ~5kb and ~4kb were expressed in the rectal gland, both of which are smaller than the mammalian CFTR mRNA which is ~6.5 kb (Fuller and Benos, 1992). A 4.59 kb CFTR cDNA has been cloned from the rectal gland of *S. acanthias*, which encodes for a protein of 1492 amino acids (Marshall *et al.*, 1991). In *F. heteroclitus*, two transcripts of ~7.5 and ~5.5 kb were expressed in the intestine and gill, and it was suggested that this was either an additional cross-reactive homologue of human CFTR, or an alternatively spliced form (Singer *et al.*, 1998). The CFTR mRNA transcript expressed in *S. canicula* is 6.4 kb (MacKenzie *et al.*, 2002), which is much larger than the transcripts expressed in *C. leucas*.

AQP has been identified in many vertebrate tissues, including the kidney, intestinal tract, respiratory epithelia and brain, however *C. leucas* AQP was only detected in the kidney of SW-acclimated sharks. No transcripts were detectable in any other tissues, in FW- or SW-acclimated sharks. This appears to be contrary to the expression of AQP1 in the kidney of *A. anguilla*, which decreases after transfer to SW (Martinez *et al.*, 2005b). The present study examined expression in only a single RNA sample from a FW- and SW-acclimated shark. Additional Northern blots supporting multiple RNA samples would determine whether this trend is maintained. The similarity of *C. leucas* AQP to AQP1, AQP2 and AQP5 in other vertebrates may suggest that these AQP isoforms evolved from a common ancestral gene. It is likely that AQP1 is the common ancestral gene, since AQP2 and AQP5 have not yet been identified in teleost fish, but homologues of AQP1 have been identified in many species (Cutler *et al.*, 2005).

β-actin is a major constituent of the cell cytoskeleton, not only interacting with other actin molecules to form cellular microfilaments but also interacting with a wide variety of other proteins. It is one of the most highly conserved proteins and since it is one of the few proteins which are presumed to be expressed at similar levels in any particular tissue irrespective of the external environment, it is often referred to as a "housekeeping" gene (Erba *et al.*, 1988). It can be used to standardise experiments as it provides a control; a consistently expressed gene throughout the experimental conditions. As would be expected, expression

of this protein was identified in all *C. leucas* tissues examined. Two isoforms of the β-actin gene were identified in *C. leucas,* both of which shared high amino acid homology with other vertebrate β-actin proteins sequences. This gene was not fully sequenced in the present study since it was simply required as a control for the experiments determining the effect of environmental salinity on Na^+, K^+-ATPase expression.

7

Final conclusions and future work

7.1: Final Conclusions

The osmoregulatory tissues of the euryhaline bull shark, *C. leucas*, express several transport proteins, including Na^+, K^+-ATPase, which are essential for the maintenance of osmotic balance of the body fluids when fish are in FW or SW environments. With respect to Na^+, K^+-ATPase, three α subunit isoforms and one β subunit isoform were found to be expressed in the major osmoregultory tissues, the rectal gland, kidney, gill and intestine. Using RT-PCR and Northern and Western blotting, the levels of Na^+, K^+-ATPase subunit mRNA expression and protein abundance were studied in tissues isolated from FW- and SW-acclimated fish.

When euryhaline fish move between FW and SW, Na^+, K^+-ATPase activities in the osmoregulatory organs show a salinity-dependent regulation. Na^+, K^+-ATPase activity can be regulated at the gene level, resulting in a change in mRNA expression which is usually accompanied by a proportionate increase in translation of protein subunits. In the gill and kidney of *S. sarba* acclimated to a range of salinities, Na^+, K^+-ATPase α_1 and β_1 protein abundance were consistent with changes in expression of α_1 and β_1 mRNAs (Deane and Woo, 2004). These proteins must then be translocated from the endoplasmic reticulum to the plasma membrane in order to function as ion transporters. Additional proteins may associate with the Na^+, K^+-ATPase α subunit, such as FXYD proteins, which are able to regulate the activity of the enzyme.

A recent study reported a change in Na^+, K^+-ATPase activity in the rectal gland and kidney, but not in the gill or intestine, of juvenile *C. leucas* transferred from FW to SW (Pillans *et al.*, 2005). After a 7-day acclimation period to SW, Na^+, K^+-ATPase activity increased in the rectal gland, and decreased in the kidney. In the present study where *C. leucas* were acclimated under identical conditions, no changes in Na^+, K^+-ATPase α and β subunit mRNA expression were found in any tissues from FW- and SW-acclimated fish. This suggests that the reported changes in Na^+, K^+-ATPase activity within the kidney and rectal gland were not caused by transcriptional regulation. In addition, no changes in the amount of Na^+, K^+-ATPase α and β subunit protein expression were found in kidney, gill or intestine following SW-acclimation. Therefore, it is possible to conclude that

in the kidney of *C. leucas*, Na^+, K^+-ATPase activity must be able to be regulated at some point after translation, possibly by differential recruitment of subunits to the plasma membrane, direct phosphorylation of the alpha subunit or by interactions with other molecules, including FXYD proteins such as PLMS. This conclusion cannot be made for the rectal gland since only protein expression in FW-acclimated sharks was examined during this study.

Differences were observed, however, in the distribution of Na^+, K^+-ATPase α_1 subunit in some osmoregulatory tissues of FW- and SW-acclimated *C. leucas*. The major difference in Na^+, K^+-ATPase α_1 subunit distribution was found in the gills, where the pattern of Na^+, K^+-ATPase distribution matches that seen in many teleost (summarised in Section 1.4.3) and one other elasmobranch species (Piermarini and Evans, 2000), whereby filamental MR cells express Na^+, K^+-ATPase in SW-acclimated fish, but both filamental and lamellar MR cells are Na^+, K^+-ATPase immunoreactive in FW-acclimated fish. As discussed in Sections 1.5 and 5.9, the MR cells in the different areas of the *C. leucas* gill may express different transporters (Hiroi *et al.*, 2005), resulting in the specialisation of these cells for either ion absorption or excretion.

The rectal glands of both FW- and SW-acclimated *C. leucas* exhibited greater levels of immunoreactivity for the α_1 subunit in the subcapsular region of the glands compared to the more central tubular regions. As suggested in Section 5.9, it is possible that expression of FXYD proteins associated with the Na^+, K^+-ATPase α_1 subunit may have prevented antibody binding, and thus masked the true levels of Na^+, K^+-ATPase α_1 subunit expression in the central regions of the gland. This may also be associated with the 'switching on and off' of the secretory activity of the rectal gland by promoting Na^+, K^+-ATPase activity during periods of high salt intake but suppressing Na^+, K^+-ATPase activity at other times. In rectal gland tubule cells, Na^+, K^+-ATPase is localised to the basolateral membrane, with more intense staining appearing throughout the cell in the glands of SW-acclimated fish. This phenomena may to be due to more extensive infolding of the basolateral and lateral membranes of cells in rectal glands of SW-acclimated sharks. Alternatively,

there may be more FXYD proteins expressed in the glands of FW-acclimated sharks, therefore reducing immunoreactivity.

Bull sharks, like most large active predatory sharks, are intermittent feeders, often ingesting large amounts of food and possibly also SW during individual feeding events (Holmgren and Nilsson, 1999). This strategy requires the osmoregulatory tissues to respond rapidly and transiently following a feeding event. In *C. leucas*, there is evidence that this tight regulation may be achieved, at least in part, by the actions of FXYD proteins, particularly in the rectal gland. This theory is supported by observations in *S. canicula* where Na^+, K^+-ATPase activity was transiently increased following a feeding event but this was not dependent on an increase in mRNA expression (MacKenzie *et al.*, 2002).

The results of this study consistently indicate that post-translational regulatory processes are very important for both the short and long term regulation of Na^+, K^+-ATPase activity in *C. leucas* tissues. This is contrary to the findings in teleost fish (as discussed in Sections 1.4.3). Teleosts and elasmobranchs employ markedly different osmoregulatory strategies whereby elasmobranchs supplement their total plasma osmolality by retaining urea, unlike teleosts which must precisely regulate the Na^+ and Cl^- composition of the plasma (Section 1.1). Since elasmobranchs are largely reliant on urea synthesis and retention in order to maintain plasma osmolality, the control of Na^+, K^+-ATPase activity by regulation of expression in elasmobranchs is likely to be of less importance than in teleost fish. However, the findings of the current study also differ from the findings of a study in another euryhaline elasmobranch, *D. sabina* (Piermarini and Evans, 2000) where the reported changes in branchial Na^+, K^+-ATPase activity were paralleled by a change in Na^+, K^+-ATPase α subunit protein expression. No change in *C. leucas* branchial Na^+, K^+-ATPase α or β subunit mRNA or protein expression were observed in the current study, nor were any changes reported in branchial Na^+, K^+-ATPase activity (Pillans *et al.*, 2005). It seems likely that these euryhaline elasmobranch species have evolved different osmoregulatory strategies. The evolutionary distance between the two species (separated at the Subdivision level) would presumably be great

enough to permit the evolution of two distinct osmoregulatory strategies as suggested in Sections 1.5. and 5.8.

7.2: Future Work

C. leucas is a model organism for the study of osmoregulation since it can tolerate a broad range of environmental salinities. This study has investigated the expression of a single transport protein which is intimately involved in the physiological processes which allow the shark to inhabit these varied salinities. Some additional proteins have also been identified in osmoregulatory tissues from *C. leucas*, but the expression of these deserves more comprehensive study.

There are many questions yet to be answered concerning the expression and more importantly regulation of Na^+, K^+-ATPase. It is possible that an additional Na^+, K^+-ATPase α subunit isoform (a homologue of mammlian α_4; Lingrel *et al.*, 2003) might be present in the testis of *C. leucas*. As this is thought to be involved with sperm motility it therefore may not be present the testes of juvenile sharks. Two additional Na^+, K^+-ATPase β subunit isoforms are present in other vertebrates (Blanco and Mercer, 1998), so it is likely that homologues of these isoforms are also present in *C. leucas*. Further cloning of RT-PCR products using degenerate primers and brain and testis cDNA from *C. leucas* would demonstrate the existence of these isoforms in *C. leucas*.

The mRNA expression of Na^+, K^+-ATPase α and β subunits has been well characterised in this study, including the expression of all three α isoforms. However, protein expression was not fully examined in the rectal gland, due to insufficient tissue supply. The expression of the α_1 subunit protein should be a priority of future studies. Antibodies could also be raised against the Na^+, K^+-ATPase α_2 and α_3 isoform sequences for use in both western blotting and immunohistochemistry techniques. The impact of possible FXYD proteins on the expression and activity of Na^+, K^+-ATPase would be an interesting area of study. The cloning of FXYD proteins, raising of antibodies and co-localisation studies would be of particularly interest in the rectal gland, where it is thought these proteins may be associating with and regulating the activity of Na^+, K^+-ATPase. The use of an antibody raised

against the C-terminal of the Na^+, K^+-ATPase α_1 subunit sequence which is not thought to be occluded by FXYD proteins would establish whether FXYD association might be related to the differences in immunoreactivity throughout the rectal gland. Electron microscopy would also help define the precise localisation of the Na^+, K^+-ATPase α and β subunits within the cells of the osmoregulatory tissues from FW- and SW-acclimated sharks, and would confirm whether the cells in the rectal glands of SW-acclimated bull sharks have more complex basolateral membranes than those of FW-acclimated sharks.

Unlike the study by Piermarini and Evans (2000), this study did not evaluate Na^+, K^+-ATPase protein expression in *C. leucas* caught in SW. The subjects of the present study were all juvenile sharks which do not move into SW until they are larger in size and therefore individuals caught in SW would not have been directly comparable to the FW juveniles. However, it would be of interest to know whether these sharks adopt a different osmoregulatory strategy than the potentially short term measures displayed by the juvenile sharks in the current study.

Perhaps the most exciting direction for future work lies in the evaluation of the mechanisms of regulation of Na^+, K^+-ATPase activity, since the present study indicates activity changes associated with FW-SW transfer are not regulated by changes in expression of Na^+, K^+-ATPase mRNA or protein. The recruitment of the Na^+, K^+-ATPase protein complexes appears to be key in regulation of activity in some organs (Bertorello *et al.*, 2003). Further Na^+, K^+-ATPase localisation studies may reveal a shift from cytoplasmic to membrane bound distribution. FXYD proteins (Section 1.4.3) have already been shown to play a major role in the regulation of Na^+, K^+-ATPase activity in several tissues and further investigations into this family of proteins would hopefully provide more insight into how complex tissues like the kidney can perform both ion excretion and absorption so efficiently. Phosphorylation and glycosylation of the Na^+, K^+-ATPase subunits may also play a role in the synthesis, distribution and functional activity of this enzyme. In addition, other proteins which associate with either the α or β protein subunits may also have regulatory roles (Section 1.4.4). Na^+, K^+-ATPase is reported to be regulated by many hormones via the activation of

various intracellular messengers, most of which are accompanied by changes in the phosphorylation state of the Na^+, K^+-ATPase α subunits (Section 1.4.4). Understanding the chemical cascade resulting from the release of hormones which in turn regulates the activity of the Na^+, K^+-ATPase will require an integrative approach, encompassing studies at every level from hormone release to the molecular events leading to changes in activity or location of the enzyme.

References

Agre, P., King, L. S., Yasui, M., Guggino, W. B., Ottersen, O. P., Fujiyoshi, Y., Engel, A. and Nielsen, S. (2002). "Aquaporin water channels-from atomic structure to clinical medicine." *Journal of Physiology* **542**(1): 3-16.

Al-Khalili, L., Krook, A. and Chibalin, A. V. (2003). "Phosphorylation of the Na^+, K^+-ATPase in skeletal muscle: potential mechanism for changes in pump cell-surface abundance and activity." *Annals of the New York Academy of Sciences* **986**: 449-452.

Alberts, B., Bray, D., Lewis, J., Raff, M., Roberts, K. and Watson, J. D. (1994). *Molecular Biology of the Cell*. New York, Garland Publishing, Inc.

Aller, S. G., Lombardo, I. D., Bhanot, S. and Forrest, J. N. (1999). "Cloning, characterization, and functional expression of a CNP receptor regulating CFTR in the shark rectal gland." *American Journal of Physiology* **276**(1): C442-C449.

Almansa, E., Sanchez, J. J., Cozzi, S., Casariego, M., Cejas, J. and Diaz, M. (2001). "Segmental heterogeneity in the biochemical properties of the Na^+-K^+-ATPase along the intestine of the gilthead seabream (*Sparus aurata* L.)." *Journal of Comparative Physiology* **171B**(7): 557-568.

Anderson, W. G., Conlon, J. M. and Hazon, N. (1995). "Characterization of the endogenous intestinal peptide that stimulates the rectal gland of *Scyliorhinus canicula*." *American Journal of Physiology* **268**(2): R1359.

Anderson, W. G., Cerra, M. C., Wells, A., Tierney, M. L., Tota, B., Takei, Y. and Hazon, N. (2001[a]). "Angiotensin and angiotensin receptors in cartilaginous fishes." *Comparative Biochemistry and Physiology* **128A**(1): 31-40.

Anderson, W. G., Takei, Y. and Hazon, N. (2001[b]). "The dipsogenic effect of the renin-angiotensin system in elasmobranch fish." *General and Comparative Endocrinology* **124**(3): 300-307.

Anderson, W. G., Good, J. P. and Hazon, N. (2002[a]). "Changes in chloride secretion rate and vascular perfusion in the rectal gland of the European lesser-spotted dogfish in response to environmental and hormonal stimuli." *Journal of Fish Biology* **60**(6): 1580-1590.

Anderson, W. G., Takei, Y. and Hazon, N. (2002[b]). "Osmotic and volaemic effects on drinking rate in elasmobranch fish." *Journal of Experimental Biology* **205**(8): 1115-1122.

Anderson, W. G., Good, J. P., Franklin, C. E. and Hazon, N. (2003). "Scaling of rectal gland mass in the European lesser-spotted dogfish." *Journal of Fish Biology* **62**(3): 749-751.

Anderson, W. G., Hyodo, S., Tsukada, T., Meischke, L., Pillans, R. D., Good, J. P., Takei, Y., Cramb, G., Franklin, C. E. and Hazon, N. (2005). "Sequence, circulating levels, and expression of C-type natriuretic peptide in a euryhaline elasmobranch, *Carcharhinus leucas*." *General and Comparative Endocrinology* **144**(1): 90-98.

Ando, M. (1992). "Regulatory Mechansims of Ion and Water Transport Across The Intestine of the Seawater Fish." *Trends in Comparative Physiology & Biochemistry Proceedings*(8th International Symposium): 51-56.

Armour, K. J., O'Toole, L. B. and Hazon, N. (1993[a]). "The effect of dietary protein restriction on the secretory dynamics of 1 alpha-hydroxycorticosterone and urea in the dogfish, *Scyliorhinus canicula*: a possible role for 1 alpha-hydroxycorticosterone in sodium retention." *Journal of Endocrinology* **138**(2): 275-282.

Armour, K. J., O'Toole, L. B. and Hazon, N. (1993[b]). "Mechanisms of ACTH- and angiotensin II-stimulated 1 alpha-hydroxycorticosterone secretion in the dogfish, *Scyliorhinus canicula*." *Journal of Molecular Endocrinology* **10**(3): 235-244.

Arnesen, A. M., Johnsen, H. K., Mortensen, A. and Jobling, M. (1998). "Acclimation of Atlantic salmon (*Salmo salar* L.) smolts to `cold' sea water following direct transfer from fresh water." *Aquaculture* **168**: 351-367.

Arystarkhova, E. and Sweadner, K. J. (1997). "Tissue-specific expression of the Na, K-ATPase β3 subunit. The presence of β3 in lung and liver addresses the problem of the missing subunit." *Journal of Biological Chemistry* **272**(36): 22405-22408.

Arystarkhova, E., Donnet, C., Asinovski, N. K. and Sweadner, K. J. (2002). "Differential regulation of renal Na, K-ATPase by splice variants of the gamma subunit." *Journal of Biological Chemistry* **277**(12): 10162-10172.

Arystarkhova, E. and Wetzel, R. K. (2003). "Gamma structural variants differentially regulate Na, K-ATPase properties." *Annals of the New York Academy of Sciences* **986**: 416-419.

Attali, B., Latter, H., Rachamim, N. and Garty, H. (1995). "A corticosteroid-induced gene expressing an "IsK-like" K^+ channel activity in *Xenopus* oocytes." *Proceedings of the National Academy of Sciences of the United States of America* **92**(13): 6092-6096.

Avella, M., Masoni, A., Bornancin, M. and Mayer-Gostan, N. (1987). "Gill Morphology and Sodium Influx in the Rainbow Trout (*Salmo gairdneri*) Acclimated to Artificial Freshwater Environments." *Journal of Experimental Zoology* **241**: 159-170.

Avella, M. and Bornancin, M. (1989). "A new analysis of ammonia and sodium transport through the gills of the freshwater rainbow trout (*Salmo gairdneri*)." *Journal of Experimental Biology* **142**: 155-176.

Ballantyne, J. S., Moyes, C. D. and Moon, T. W. (1987). "Compatible and counteracting solutes and the evolution of ion and osmoregulation in fishes." *Canadian Journal of Zoology* **65**: 1883-1888.

Ballantyne, J. S. (1997). "Jaws: The inside story. The metabolism of elasmobranch fishes." *Comparative Biochemistry and Physiology* **118B**(4): 703-742.

Bass, A. J., D'Aubrey, J. D. and Kistnasamy, N. (1973). Sharks of the east cost of southern Africa. I. The genus *Carcharhinus* (Carcharhinidae). *Oceanographic Research Institute Investigational Report*, South African Association for Marine Biological Research: 1-168.

Beggah, A. T., Jaunin, P. and Geering, K. (1997). "Role of glycosylation and disulfide bond formation in the beta subunit in the folding and functional expression of Na, K-ATPase." *Journal of Biological Chemistry* **272**(15): 10318-10326.

Beguin, P., Wang, X., Firsov, D., Puoti, A., Claeys, D., Horisberger, J. D. and Geering, K. (1997). "The gamma subunit is a specific component of the Na, K-ATPase and modulates its transport function." *Embo Journal* **16**(14): 4250-4260.

Beguin, P., Hasler, U., Beggah, A., Horisberger, J. D. and Geering, K. (1998). "Membrane integration of Na, K-ATPase alpha-subunits and beta-subunit assembly." *Journal of Biological Chemistry* **273**(38): 24921-24931.

Beguin, P., Crambert, G., Guennoun, S., Garty, H., Horisberger, J. D. and Geering, K. (2001). "CHIF, a member of the FXYD protein family, is a regulator of Na, K-ATPase distinct from the gamma-subunit." *Embo Journal* **20**(15): 3993-4002.

Beguin, P., Crambert, G., Monnet-Tschudi, F., Uldry, M., Horisberger, J. D., Garty, H. and Geering, K. (2002). "FXYD7 is a brain-specific regulator of Na, K-ATPase alpha1-beta isozymes." *Embo Journal* **21**(13): 3264-3273.

Benz, E. J., Scofield, P., Appel, J. Z., Benz, J., Boyd, C., Chai, J., Devarajan, P. and Su, L. (1992). "Cloning and characterization of sequences encoding the major isoform of Na, K-ATPase in shark rectal gland." *Bulletin of the Mount Desert Island Biological Laboratory* **31**: 103-104.

Bertorello, A. and Aperia, A. (1989). "Regulation of Na^+-K^+-ATPase activity in kidney proximal tubules: involvement of GTP binding proteins." *American Journal of Physiology* **256**(1): F57-62.

Bertorello, A. M., Aperia, A., Walaas, S. I., Nairn, A. C. and Greengard, P. (1991). "Phosphorylation of the catalytic subunit of Na^+, K^+-ATPase inhibits the activity of the enzyme." *Proceedings of the National Academy of Sciences of the United States of America.* **88**(24): 11359-11362.

Bertorello, A. M., Komarova, Y., Smith, K., Leibiger, I. B., Efendiev, R., Pedemonte, C. H., Borisy, G. and Sznajder, J. I. (2003). "Analysis of Na^+, K^+-ATPase motion and incorporation into the plasma membrane in response to G protein-coupled receptor signals in living cells." *Molecular Biology of the Cell* **14**(3): 1149-1157.

Biemesderfer, D., Payne, J. A., Lytle, C. Y. and Forbush, B., 3rd (1996). "Immunocytochemical studies of the Na-K-Cl cotransporter of shark kidney." *American Journal of Physiology* **270**(6): F927-936.

Bittner, A. and Lang, S. (1980). "Some aspects of the osmoregulation of amazonian freshwater stingrays (*Potamotrygon hystrix*) - I. Serum osmolality, sodium and chloride content, water content, hematocrit and urea level." *Comparative Biochemistry and Physiology* **67A**: 9-13.

Blanco, G. and Mercer, R. W. (1998). "Isozymes of the Na-K-ATPase: heterogeneity in structure, diversity in function." *American Journal of Physiology* **275**(5): F633-650.

Blanco, G., Melton, R. J., Sanchez, G. and Mercer, R. W. (1999). "Functional Characterization of a Testes-Specific α-Subunit Isoform of the Sodium/Potassium Adenosinetriphosphatase." *Biochemistry* **38**(41): 13661-13669.

Bleckmann, H. and Hofmann, M. H. (1999). Special senses. *Sharks, skates and rays: The biology of elasmobranch fish*. Hamlett, W. C. Baltimore, John Hopkins University Press: 300-328.

Bleich, M., Heitzmann, D., Hug, M. J., Hoffmann, E. K., Greger, R. and Warth, R. (2000). "Regulation of the Na^+ 2Cl- K^+ co-transporter--mechanisms in the rectal gland of Squalus acanthias with implications for the thick ascending limb of Henle." *Nephrology Dialysis Transplantation* **15**(Supplement 6): 16-18.

Boisier, P., Ranaivoson, G., Rasolofonirina, N., Andriamahefazafy, B., Roux, J., Chanteau, S., Satake, M. and Yasumoto, T. (1995). "Fatal mass poisoning in Madagascar following ingestion of a shark (*Carcharhinus leucas*): clinical and epidemiological aspects and isolation of toxins." *Toxicon* **33**(10): 1359-1364.

Bone, Q., Marshall, N. B. and Blaxter, J. H. S. (1999). *Biology of fishes*. Cheltenham, Stanley Thornes.

Bonting, S. L. (1966). "Studies on sodium-potassium-activated adenosinetriphosphatase. XV. The rectal gland of the elasmobranchs." *Comparative Biochemistry and Physiology* **17**(3): 953-966.

Boron, W. F. and Boulpaep, E. L. (2005). *Medical Physiology*. Philadelphia, Elsevier Saunders.

Boylan, J. W. (1972). "A model for passive urea reabsorption in the elasmobranch kidney." *Comparative Biochemistry and Physiology* **42A**(1): 27-30.

Branstetter, S. and Stiles, R. (1987). "Age and growth estimates of the bull shark, *Carcharhinus leucas*, from the northern Gulf of Mexico." *Environmental Biology of Fishes* **20**(3): 169-181.

Brown, J. A. and Green, C. (1987). "Single nephron function of the lesser spotted dogfish, *Scyliorhinus canicula*, and the effects of adrenaline." *Journal of Experimental Biology* **129**: 265-278.

Bulger, R. E. (1963). "Fine Structure of the Rectal (Salt-Secreting) Gland of the spiny dogfish, *Squalus acanthias*." *Anatomical Record* **147**: 95-127.

Burger, J. W. and Hess, W. N. (1960). "Function of the rectal gland in the spiny dogfish." *Science* **131**: 670-671.

Burgess, G. H. (2005). *International Shark Attack File, Florida Museum of Natural History, University of Florida*. http://www.flmnh.ufl.edu/fish/sharks/statistics/species2.htm Accessed 2005.

Burke, J. (1996). *PCR: Essential Techniques*. Chichester, John Wiley and Sons.

Burns, J. and Copeland, D. E. (1950). "Chloride excretion in the head region of *Fundulus heteroclitus*." *Biological Bulletin* **99**(3): 381-385.

Capurro, C., Coutry, N., Bonvalet, J. P., Escoubet, B., Garty, H. and Farman, N. (1996). "Cellular localization and regulation of CHIF in kidney and colon." *American Journal of Physiology* **271**(3): C753-762.

Carrier, J. C. and Evans, D. H. (1973). "Ion and water turnover in the fresh-water elasmobranch *Potamotrygon sp.*" *Comparative Biochemistry and Physiology* **45A**(2): 667-670.

Chan, D. K. and Phillips, J. G. (1966). "The embryology of the rectal gland of the spiny dogfish *Squalus acanthias* L." *Journal of Anatomy* **100**(4): 899-903.

Chan, D. K. and Phillips, J. G. (1967). "The anatomy, histology and histochemistry of the rectal gland in the lip-shark *Hemiscyllium plagiosum* (Bennett)." *Journal of Anatomy* **101**(1): 137-157.

Choe, K. P., Edwards, S., Morrison-Shetlar, A. I., Toop, T. and Claiborne, J. B. (1999). "Immunolocalization of Na^+/K^+-ATPase in mitochondrion-rich cells of the atlantic hagfish (*Myxine glutinosa*)." *Comparative Biochemistry and Physiology* **124A**: 161-168.

Choe, K. P., Morrison-Shetlar, A. I., Wall, B. P. and Claiborne, J. B. (2002). "Immunological detection of Na^+/H^+ exchangers in the gills of a hagfish, *Myxine glutinosa*, an elasmobranch, *Raja erinacea*, and a teleost, *Fundulus heteroclitus*." *Comparative Biochemistry and Physiology* **131A**(2): 375-385.

Choe, K. P. and Evans, D. H. (2003). "Compensation for Hypercapnia by a Euryhaline Elasmobranch: Effect of Salinity and Roles of Gills and Kidneys in Fresh Water." *Journal of Experimental Zoology* **297**(1): 52-63.

Choe, K. P., O Brien, S., Evans, D. H., Toop, T. and Edwards, S. L. (2004). "Immunolocalization of Na^+/K^+-ATPase, Carbonic Anhydrase II, and Vacuolar H^+-ATPase in the Gills of Freshwater Adult Lampreys, *Geotria australis*." *Journal of Experimental Zoology* **301**(8): 654-665.

Chomczynski, P. and Sacchi, N. (1987). "Single-step method of RNA isolation by acid guanidinium thiocyanate-phenol-chloroform extraction." *Analytical Biochemistry* **162**(1): 156-159.

Chomczynski, P. and Mackey, K. (1995). "Substitution of chloroform by bromo-chloropropane in the single-step method of RNA isolation." *Analytical Biochemistry* **225**(1): 163-164.

Clarke, R. J., Humphrey, P. A., Lupfert, C., Apell, H. J. and Cornelius, F. (2003). "Kinetic Investigations of the Mechanism of the Rate-Determining Step of the Na^+, K^+-ATPase Pump Cycle." *Annals of the New York Academy of Sciences* **986**: 159-162.

Cliff, G. (1991). "Shark attacks on the South African coast between 1960 and 1990." *South African Journal of Science* **87**: 513-518.

Cliff, G. and Dudley, S. F. J. (1991). "Shark caught in the protective gill nets off Natal, South Africa. 4. The bull shark *Carcharhinus leucas* Valenciennes." *South African Journal of Marine Science* **10**: 253-270.

Collin, S. P. and Whitehead, D. (2004). "The functional roles of passive electroreception in non-electric fishes." *Animal Biology* **54**: 1-26.

Colonna, T., Kostich, M., Hamrick, M., Hwang, B., Rawn, J. D. and Fambrough, D. M. (1997). "Subunit interactions in the sodium pump." *Annals of the New York Academy of Sciences* **834**: 498-513.

Compagno, L. J. V. (1984). *FAO Species Catalogue: An Annotated and Illustrated Catalogue of Shark Species Known to Date.* Rome, FAO.

Compagno, L. J. V., Dando, M. and Fowler, S. (2005). *A Field Guide to the Sharks of the World.* London, Harper Collins Publishers Ltd.

Conlon, J. M., Deacon, C. F., O'Toole, L. and Thim, L. (1986). "Scyliorhinin I and II: two novel tachykinins from dogfish gut." *FEBS Letters* **200**(1): 111-116.

Conley, D. M. and Mallatt, J. (1988). "Histochemical localization of Na^+-K^+ ATPase and carbonic anhydrase activity in gills of 17 fish species." *Canadian Journal of Zoology* **66**: 2398-2405.

Cooper, A. R. and Morris, S. (1998). "Osmotic, ionic and haematological response of the Port Jackson shark *Heterodontus portusjacksoni* and the common stingaree *Trygonoptera testacea* upon exposure to diluted seawater." *Marine Biology* **132**(1): 29-42.

Cooper, A. R. and Morris, S. (2004). "Osmotic, sodium, carbon dioxide and acid-base state of the Port Jackson shark, *Heterodontus portusjacksoni*, in response to lowered salinity." *Journal of Comparative Physiology* **174B**(3): 211-222.

Copeland, D. E. (1948). "The cytological basis of chloride transfer in the gills of *Fundulus heteroclitus*." *Journal of Morphology* **82**: 201-227.

Cornelius, F. (1995). "Cholesterol modulation of molecular activity of reconstituted shark Na^+, K^+-ATPase." *Biochimica et Biophysica Acta* **1235(2)**: 205-212.

Cornelius, F., Mahmmoud, Y. A. and Vorum, H. (2000). "Phospholemman as a putative regulatory protein of shark Na, K-ATPase." *International Congress Series* **1207**: 555-558.

Cornelius, F., Mahmmoud, Y. A. and Christensen, H. R. Z. (2001). "Modulation of Na, K-ATPase by Associated Small Transmembrane Regulatory Proteins and by Lipids." *Journal of Bioenergetics and Biomembranes* **33**(5): 415-424.

Cornelius, F. and Mahmmoud, Y. A. (2003). "Functional Modulation of the Sodium Pump: The Regulatory Proteins "Fixit"." *News in Physiological Sciences* **18**: 119-124.

Cornelius, F., Mahmmoud, Y. A., Meischke, L. and Cramb, G. (2005). "Functional Significance of the Shark Na, K-ATPase N-Terminal Domain. Is the Structurally Variable N-Terminus Involved in Tissue-Specific Regulation by FXYD Proteins?" *Biochemistry* **44**: 13051-13062.

Crambert, G., Fuzesi, M., Garty, H., Karlish, S. and Geering, K. (2002). "Phospholemman (FXYD1) associates with Na, K-ATPase and regulates its transport properties." *Proceedings of the National Academy of Sciences of the United States of America* **99**(17): 11476-11481.

Crambert, G., Beguin, P., Uldry, M., Monnet-Tschudi, F., Horisberger, J. D., Garty, H. and Geering, K. (2003). "FXYD7, the first brain- and isoform-specific regulator of Na, K-ATPase: biosynthesis and function of its posttranslational modifications." *Annals of the New York Academy of Sciences* **986**: 444-448.

Crambert, G., Li, C., Claeys, D. and Geering, K. (2005). "FXYD3 (Mat-8), a New Regulator of Na, K-ATPase." *Molecular Biology of the Cell* **16**: 2363-2371.

Crawford, M. B. (1899). "On the Rectal Gland of the Elasmobranchs." *Proceedings of the Royal Society of Edinburgh* **23**: 55-61.

Crespo, S. (1981). "Zinc and Copper Distribution in Excretory Organs of the Dogfish *Scyliorhinus canicula* and Chloride Cell Response Following Treatment with Zinc Sulphate." *Marine Biology* **65**: 117-123.

Crespo, S. (1982). "Surface Morphology of Dogfish (*Scyliorhinus canicula*) Gill Epithelium, and Surface Morphological Changes Following Treatment with Zinc Sulphate: A Scanning Electron Microscope Study." *Marine Biology* **67**: 159-166.

Crespo, S. and Sala, R. (1986). "Ultrastructural alterations of the dogfish (*Scyliorhinus canicula*) gill filament related to experimental aquatic zinc pollution." *Diseases of Aquatic Organisms* **1**: 99-104.

Cutler, C. P., Sanders, I. L., Hazon, N. and Cramb, G. (1995[a]). "Primary sequence, tissue specificity and expression of the Na^+, K^+-ATPase α1 subunit in the European eel (*Anguilla anguilla*)." *Comparative Biochemistry and Physiology* **111B**(4): 567-573.

Cutler, C. P., Sanders, I. L., Hazon, N. and Cramb, G. (1995[b]). "Primary sequence, tissue specificity and mRNA expression of the Na^+/K^+-ATPase β1 subunit in the European eel (*Anguilla anguilla*)." *Fish Physiology and Biochemistry* **14**(5): 423-429.

Cutler, C. P., Brezillon, S., Bekir, S., Sanders, I. L., Hazon, N. and Cramb, G. (2000). "Expression of the duplicate Na, K-ATPase β_1-isoform in the European eel (*Anguilla anguilla*)." *American Journal of Physiology* **279**: R222-R229.

Cutler, C. P. and Cramb, G. (2000). Water Transport and Aquaporin Expression in Fish. *Molecular Biology and Physiology of Water and Solute Transport*. Hohmann, S. and Nielsen, S. London, UK, Kluwer academic press: 431-441.

Cutler, C. P. and Cramb, G. (2002[a]). "Two isoforms of the $Na^+/K^+/2Cl^-$ cotransporter are expressed in the European eel (*Anguilla anguilla*)." *Biochimica et Biophysica Acta* **1566**(1-2): 92-103.

Cutler, C. P. and Cramb, G. (2002[b]). "Branchial expression of an aquaporin 3 (AQP-3) homologue is downregulated in the European eel *Anguilla anguilla* following seawater acclimation." *Journal of Experimental Biology* **205**(17): 2643-2651.

Cutler, C. P., Meischke, L. and Cramb, G. (2005). "Evolutionary and comparative analysis of aquaporin watter channel genes in fish." *Bulletin of the Mount Desert Island Biological Laboratory* **44**: 55.

D'Cotta, H., Valotaire, C., Gac, F. L. and Prunet, P. (2000). "Synthesis of gill Na^+-K^+-ATPase in Atlantic salmon smolts: differences in α-mRNA and α-protein levels." *American Journal of Physiology* **278**: R101-R110.

Dahan, D., Evagelidis, A., Hanrahan, J. W., Hinkson, D. A., Jia, Y., Luo, J. and Zhu, T. (2001). "Regulation of the CFTR channel by phosphorylation." *Pflugers Archiviv* **443**: S92-S96.

Dang, Z., Lock, R. A. C., Flik, G. and Wendelaar-Bonga, S. E. (2000). "Na^+/K^+-ATPase Immunoreactivity in branchial chloride cells of *Oreochromis mossambicus* exposed to copper." *Journal of Experimental Biology* **203**: 379-387.

Darman, R. B., Flemmer, A. and Forbush, B. (2001). "Modulation of ion transport by direct targeting of protein phosphatase type 1 to the Na-K-Cl cotransporter." *Journal of Biological Chemistry* **276**(37): 34359-34362.

Davies, D. T. and Rankin, J. C. (1973). "Adrenergic receptors and vascular responses to catecholamines of perfused dogfish gills." *Comparative and General Pharmacology* **4**(14): 139-147.

Davis, L., Dibner, M. and Battey, J. (1986). *Basic Methods in Molecular Biology*, Elsevier.

De Boeck, G., Grosell, M. and Wood, C. (2001). "Sensitivity of the spiny dogfish (*Squalus acanthias*) to waterborne silver exposure." *Aquat Toxicol* **54**(3-4): 261-275.

De Vlaming, V. L. and Sage, M. (1973). "Osmoregulation in the Euryhaline Elasmobranch, *Dasyatis sabina*." *Comparative Biochemistry and Physiology* **45A**: 31-44.

Dean, R. B. (1941). "Theories of Electrolyte Equilibrium in Muscle." *Biological Symposium* **3**: 331-348.

Deane, E. E., Kelly, S. P. and Woo, N. Y. S. (1999). "Hormonal modulation of branchial Na^+-K^+-ATPase subunit mRNA in a marine teleost *Sparus sarba*." *Life Sciences* **64**(20): 1819-1829.

Deane, E. E. and Woo, N. Y. (2004). "Differential gene expression associated with euryhalinity in sea bream (*Sparus sarba*)." *American Journal of Physiology* **287**(5): R1054-1063.

Deen, P. M. T. and Van Os, C. H. (1998). "Epithelial aquaporins." *Current Opinion in Cell Biology* **10**(4): 435-442.

Diaz, M., Cozzi, S., Almansa, E., Casariego, M., Bolaños, A., Cejas, J. and Lorenzo, A. (1998). "Characterization of intestinal Na^+ - K^+ -ATPase in the gilthead seabream (*Sparus aurata* L.). Evidence for a tissue-specific heterogeneity." *Comparative Biochemistry and Physiology* **121B**(1): 65-76.

Donald, J. A., Toop, T. and Evans, D. H. (1997). "Distribution and characterization of natriuretic peptide receptors in the gills of the spiny dogfish, *Squalus acanthias*." *General and Comparative Endocrinology* **106**(3): 338-347.

Doyle, W. L. (1962). "Tubule cells of the rectal salt-gland of *Urolophus*."*American Journal of Anatomy* **111**: 223-237.

Edwards, S. L., Claiborne, J. B., Morrison-Shetlar, A. I. and Toop, T. (2001). "Expression of Na^+/H^+ exchanger mRNA in the gills of the Atlantic hagfish (*Myxine glutinosa*) in response to metabolic acidosis." *Comparative Biochemistry and Physiology* **130A**(1): 81-91.

Edwards, S. L., Donald, J. A., Toop, T., Donowitz, M. and Tse, C. M. (2002). "Immunolocalisation of sodium/proton exchanger-like proteins in the gills of elasmobranchs." *Comparative Biochemistry and Physiology* **131A**(2): 257-265.

Endo, M. (1984). "Histological and Enzymatic Studies of the Renal Tubules of Some Marine Elasmobranchs." *Journal of Morphology* **182**: 63-69.

Erba, H. P., Eddy, R., Shows, T., Kedes, L. and Gunning, P. (1988). "Structure, chromosome location, and expression of the human gamma-actin gene: differential evolution, location, and expression of the cytoskeletal β- and γ-actin genes." *Molecular and Cellular Biology* **8**(4): 1775-1789.

Ernst, S. A., Hootman, S. R., Schreiber, J. H. and Riddle, C. V. (1981). "Freeze-fracture and morphometric analysis of occluding junctions in rectal glands of elasmobranch fish." *Journal of Membrane Biology* **58**(2): 101-114.

Esmann, M. (1992). "Properties of oligomycin-induced occlusion of Na^+ by detergent-solubilized Na, K-ATPase from pig kidney or shark rectal gland." *Biochimica et Biophysica Acta* **1106**(1): 1-12.

Evans, D. H., Oikari, A., Kormanik, G. A. and Mansberger, L. (1982). "Osmoregulation by the prenatal spiny dogfish, *Squalus acanthias*." *Journal of Experimental Biology* **101**: 295-305.

Evans, D. H. (1984[a]). The Roles of Gill Permeability and Transport Mechanisms in Euryhalinity. *Fish Physiology*. Hoar, W. S. and Randall, D. J. New York, Academic Press, Inc. X Part B: 239-283.

Evans, D. H. (1984[b]). "Gill Na^+/H^+ and Cl-/HCO3- exchange systems evolved before the vertebrates entered fresh water." *Journal of Experimental Biology* **113**: 465-469.

Evans, D. H. and Kormanik, G. A. (1985). "Urea efflux from the *Squalus acanthias* pup: the effect of stress." *Journal of Experimental Biology* **119**: 375-379.

Evans, D. H., Piermarini, P. M. and Potts, W. T. W. (1999). "Ionic Transport in the Fish Gill Epithelium." *Journal of Experimental Zoology* **283**(7): 641-652.

Evans, D. H. and Piermarini, P. M. (2001). "Contractile properties of the elasmobranch rectal gland." *Journal of Experimental Biology* **204**(1): 59-67.

Evans, D. H., Piermarini, P. M. and Choe, K. P. (2005). "The Multifunctional Fish Gill: Dominant Site of Gas Exchange, Osmoregulation, Acid-Base Regulation, and Excretion of Nitrogenous Waste." *Physiological Reviews* **85**: 97-178.

Eveloff, J., Karnaky, K. J., Silva, P., Epstein, F. H. and Kinter, W. B. (1979). "Elasmobranch Rectal Gland Cell: Autoradiographic localization of [^{3}H] Ouabain-Sensitive Na, K-ATPase in rectal gland of dogfish, *Squalus acanthias*." *Journal of Cell Biology* **83**: 16-32.

Ewart, H. S. and Klip, A. (1995). "Hormonal regulation of the Na^+-K^+-ATPase: mechanisms underlying rapid and sustained changes in pump activity." *American Journal of Physiology* **269**: C295-C311.

Ewing, R. D., Ewing, G. S. and Satterthwaite, T. D. (2001). "Changes in gill Na^+, K^+-ATPase specific activity during seaward migration of wild juvenile chinook salmon." *Journal of Fish Biology* **58**: 1414-1426.

Farman, N., Fay, M. and Cluzeaud, F. (2003). "Cell-specific expression of three members of the FXYD family along the renal tubule." *Annals of the New York Academy of Sciences* **986**: 428-436.

Feraille, E. and Doucet, A. (2001). "Sodium-Potassium-Adenosinetriphosphate-Dependent Sodium Transport in the Kidney: Hormonal Control." *Physiological Reviews* **81**(1): 345-418.

Feraille, E., Mordasini, D., Gonin, S., Deschãenes, G., Vinciguerra, M., Doucet, A., Vandewalle, A., Summa, V., Verrey, F. and Martin, P. Y. (2003). "Mechanism of control of Na, K-ATPase in principal cells of the mammalian collecting duct." *Annals of the New York Academy of Sciences* **986**: 570-578.

Feschenko, M. S., Wetzel, R. K. and Sweadner, K. J. (1997). "Phosphorylation of Na, K-ATPase by protein kinases. Sites, susceptibility, and consequences." *Annals of the New York Academy of Sciences* **834**: 479-488.

Fines, G. A., Ballantyne, J. S. and Wright, P. A. (2001). "Active urea transport and an unusual basolateral membrane composition in the gills of a marine elasmobranch." *American Journal of Physiology* **280**(2): R16-R24.

Fishelson, L., Baranes, A. and Delarea, Y. (2004). "Morphogenesis of the salt gland in the viviparous Oman shark, *lago omanensis* (Triakidae) from the Gulf of Aqaba (Red Sea)." *Journal of Marine Biological Association of the United Kingdom* **84**(2): 433-438.

Flemmer, A. W., Gimenez, I., Dowd, B. F., Darman, R. B. and Forbush, B. (2002). "Activation of the Na-K-Cl cotransporter NKCC1 detected with a phospho-specific antibody." *Journal of Biological Chemistry* **277**(40): 37551-37558.

Fontainhas-Fernandes, A., Russell-Pinto, F., Gomes, E., Reis-Henriques, M. and Coimbra, J. (2000). "The effect of dietary sodium chloride on some osmoregulatory parameters of the teleost, *Oreochromis niloticus*, after transfer from freshwater to seawater." *Fish Physiology and Biochemistry* **23**(4): 307-316.

Forbush, B., 3rd, Haas, M. and Lytle, C. (1992). "Na-K-Cl cotransport in the shark rectal gland. I. Regulation in the intact perfused gland." *American Journal of Physiology* **262**(4): C1000-1008.

Forrest, J. N., Cohen, A. D., Schon, D. A. and Epstein, F. H. (1973). "Na transport and Na-K-ATPase in gills during adaptation to seawater: effects of cortisol." *American Journal of Physiology* **224**(3): 709-713.

Forrest, J. N., Jr., Boyer, J. L., Ardito, T. A., Murdaugh, H. V., Jr. and Wade, J. B. (1982). "Structure of tight junctions during Cl secretion in the perfused rectal gland of the dogfish shark." *American Journal of Physiology* **242**(5): C388-392.

Foskett, J. K. and Scheffey, C. (1982). "The chloride cell: definitive identification as the salt-secretory cell in teleosts." *Science* **215**(4529): 164-166.

Friedman, P. A., Hebert, S. C. and Mt Desert Island Biological Laboratory, S. C. M. (1990). "Diluting segment in kidney of dogfish shark. I. Localization and characterization of chloride absorption." *American Journal of Physiology* **258**(2): R398-408.

Fu, X. and Kamps, M. P. (1997). "E2a-Pbx1 induces aberrant expression of tissue-specific and developmentally regulated genes when expressed in NIH 3T3 fibroblasts." *Molecular and Cellular Biology* **17**(3): 1503-1512.

Fuller, C. M. and Benos, D. J. (1992). "CFTR!" *American Journal of Physiology* **263**(2): C267-286.

Fuzesi, M., Goldshleger, R., Garty, H. and Karlish, S. J. (2003). "Defining the nature and sites of interaction between FXYD proteins and Na, K-ATPase." *Annals of the New York Academy of Sciences* **986**: 532-533.

Gagnon, E., Forbush, B., Flemmer, A. W., Gimenez, I., Caron, L. and Isenring, P. (2002). "Functional and molecular characterization of the shark renal Na-K-Cl cotransporter: novel aspects." *American Journal of Physiology* **283**(2): F1046-1055.

Gallis, J. L., Belloc, F., Lasserre, P. and Boisseau, J. (1979). "Freshwater adaptation in the euryhaline teleost, *Chelon labrosus*. II. Effects of continuance of adaptation, cortisol treatment, and environmental calcium on water influx in isolated gill." *General and Comparative Endocrinology.* **38**(1): 11-20.

Garty, H., Lindzen, M., Scanzano, R., Aizman, R., Fuzesi, M., Goldshleger, R., Farman, N., Blostein, R. and Karlish, S. J. D. (2003). "A functional interaction between CHIF and Na-K-ATPase: implication for regulation by FXYD proteins." *American Journal of Physiology* **283**(2): F607-F615.

Geering, K. (2001). "The Functional Role of β Subunits in Oligomeric P-Type ATPases." *Journal of Bioenergetics and Biomembranes* **33**(5): 425-438.

Geering, K., Bâeguin, P., Garty, H., Karlish, S., Fèuzesi, M., Horisberger, J. D. and Crambert, G. (2003). "FXYD proteins: new tissue- and isoform-specific regulators of Na, K-ATPase." *Annals of the New York Academy of Sciences* **986**: 388-394.

Gerst, J. W. and Thorson, T. B. (1977). "Effects of saline acclimation on plasma electrolytes, urea excretion, and hepatic urea biosynthesis in a freshwater stingray, *Potamotrygon sp.* Garman, 1877." *Comparative Biochemistry and Physiology* **56A**(1): 87-93.

Gerzeli, G., De Stefano, G. F., Bolognani, L., Koenig, K. W., Gervaso, M. V. and Omodeo-Sale, M. F. (1976). The rectal gland in relation to the osmoregulatory mechanisms of marine and freshwater elasmobranchs. *Investigations of the Ichthyofauna of Nicaraguan Lakes*. Thorson, T. B. Lincoln, School of Life Sciences, University of Nebraska.

Gjevre, A. and Naess, L. I. M. (1996). "Intestinal Na^+/K^+-ATPase Activity in Salmonids." *Comparative Biochemistry and Physiology* **115A**(2): 159-168.

Goertmiller, C. C., Jr. and Ellis, R. A. (1976). "Localization of ouabain-sensitive, potassium-dependent nitrophenyl phosphatase in the rectal gland of the spiny dogfish, *Squalus acanthias*." *Cell and Tissue Research* **175**(1): 101-112.

Gogelein, H., Greger, R. and Schlatter, E. (1987[a]). "Potassium channels in the basolateral membrane of the rectal gland of *Squalus acanthias*. Regulation and inhibitors." *Pflugers Archiv* **409**(1-2): 107-113.

Gogelein, H., Schlatter, E. and Greger, R. (1987[b]). "The "small" conductance chloride channel in the luminal membrane of the rectal gland of the dogfish (*Squalus acanthias*)." *Pflugers Archiv* **409**(1-2): 122-125.

Goldstein, L. and Forster, R. P. (1971). "Osmoregulation and urea metabolism in the little skate *Raja erinacea*." *American Journal of Physiology* **220**(3): 742-746.

Gonzalez, R. J., Cooper, J. and Head, D. (2005). "Physiological responses to hyper-saline waters in sailfin mollies (*Poecilia latipinna*)." *Comparative Biochemistry and Physiology* **142A**(4): 397-403.

Good, J. P. (2005). The rectal gland and euryhalinity in elasmobranch fish. *Biology Ph. D. Thesis*, University of St Andrews.

Goss, G. G., Perry, S. F., Fryer, J. N. and Laurent, P. (1998). "Gill morphology and acid-base regulation in freshwater fishes." *Comparative Biochemistry and Physiology* **119A**(1): 107-116.

Greger, R. and Schlatter, E. (1984[a]). "Mechanism of NaCl secretion in the rectal gland of spiny dogfish (*Squalus acanthias*). I. Experiments in isolated in vitro perfused rectal gland tubules." *Pflugers Archiv* **402**(1): 63-75.

Greger, R. and Schlatter, E. (1984[b]). "Mechanism of NaCl secretion in rectal gland tubules of spiny dogfish (*Squalus acanthias*). II. Effects of inhibitors." *Pflugers Archiv* **402**(4): 364-375.

Greger, R., Schlatter, E., Wang, F. and Forrest, J. N., Jr. (1984). "Mechanism of NaCl secretion in rectal gland tubules of spiny dogfish (*Squalus acanthias*). III. Effects of stimulation of secretion by cyclic AMP." *Pflugers Archiv* **402**(4): 376-384.

Greger, R., Schlatter, E. and Gogelein, H. (1987[b]). "Chloride channels in the luminal membrane of the rectal gland of the dogfish (*Squalus acanthias*). Properties of the "larger" conductance channel." *Pflugers Archiv* **409**(1-2): 114-121.

Greger, R., Gogelein, H. and Schlatter, E. (1987). "Potassium channels in the basolateral membrane of the rectal gland of the dogfish (*Squalus acanthias*)." *Pflugers Archiv* **409**(1-2): 100-106.

Greger, R., Gèogelein, H. and Schlatter, E. (1988). "Stimulation of NaCl secretion in the rectal gland of the dogfish *Squalus acanthias*." *Comparative Biochemistry and Physiology* **90A**(4): 733-737.

Greger, R., Mall, M., Bleich, M., Ecke, D., Warth, R., Riedemann, N. and Kunzelmann, K. (1996). "Regulation of epithelial ion channels by the cystic fibrosis transmembrane conductance regulator." *Journal of Molecular Medicine* **74**(9): 527-534.

Greger, R., Schreiber, R., Mall, M., Wissner, A., Hopf, A., Briel, M., Bleich, M., Warth, R. and Kunzelmann, K. (2001). "Cystic fibrosis and CFTR." *Pflugers Archiviv* **443**: S3-S7.

Griffith, R. W., Pang, P. K. T., Srivastava, A. K. and Pickford, G. E. (1973). "Serum composition of freshwater stingrays (Potamotrygonidae) adapted to fresh and dilute seawater." *Biological Bulletin* **144**: 304-320.

Gunning, M., Cuero, C., Solomon, R. and Silva, P. (1993). "C-type natriuretic peptide receptors and signaling in rectal gland of *Squalus acanthias*." *American Journal of Physiology* **264**(2): F300-305.

Guynn, S. R., Scofield, M. A. and Petzel, D. H. (2002). "Identification of mRNA and protein expression of the Na/K-ATPase α1-, α2- and α3-subunit isoforms in Antarctic and New Zealand nototheniid fishes." *Journal of Experimental Marine Biology and Ecology* **273**: 15-32.

Haas, M. and Forbush, B. (1998). "The Na-K-Cl Cotransporters." *Journal of Bioenergetics and Biomembranes* **30**(2): 161-172.

Haas, M. and Forbush, B. (2000). "The Na-K-Cl Cotransporter of Secretory Epithelia." *Annual Review of Physiology* **62**: 515-534.

Hamann, S., Zeuthen, T., La Cour, M., Nagelhus, E. A., Ottersen, O. P., Agre, P. and Nielsen, S. (1998). "Aquaporins in complex tissues: distribution of aquaporins 1-5 in human and rat eye." *American Journal of Physiology* **274**(5): C1332-1345.

Hannafin, J., Kinne-Saffran, E., Friedman, D. and Kinne, R. (1983). "Presence of a sodium-potassium chloride cotransport system in the rectal gland of *Squalus acanthias*." *Journal of Membrane Biology* **75**(1): 73-83.

Hanrahan, J. W., Duguay, F., Sansom, S., Alon, N., Jensen, T., Riordan, J. R. and Grzelczak, Z. (1993). "Low-conductance chloride channel activated by cAMP in the rectal gland of the shark *Squalus acanthias* and in cells heterologously expressing shark CFTR." *Bulletin of the Mount Desert Island Biological Laboratory* **32**: 48-49.

Hansen, O. (1999). "Heterogeneity of Na^+/K^+-ATPase from rectal gland of *Squalus acanthias* is not due to alpha isoform diversity." *Pflugers Archiv.* **437**(4): 517-222.

Hasler, U., Wang, X., Crambert, G., Beguin, P., Jaisser, F., Horisberger, J. D. and Geering, K. (1998). "Role of beta-subunit domains in the assembly, stable expression, intracellular routing, and functional properties of Na, K-ATPase." *Journal of Biological Chemistry* **273**(46): 30826-30835.

Hasler, U., Greasley, P. J., von Heijne, G. and Geering, K. (2000). "Determinants of topogenesis and glycosylation of type II membrane proteins. Analysis of Na, K-ATPase beta 1 and beta 3 subunits by glycosylation mapping." *Journal of Biological Chemistry* **275**(37): 29011-29022.

Hastings, D. F. and Reynolds, J. A. (1979). "Molecular weight of (Na^+, K^+)ATPase from shark rectal gland." *Biochemistry.* **18**(5): 817-821.

Hayslett, J. P., Jampol, L. M., Forrest, J. N., Epstein, M., Murdaugh, H. V. and Myers, J. D. (1973). "Role of Na-K-ATPase in the renal reabsorption of sodium in the elasmobranch, Squalus acanthias." *Comparative Biochemistry and Physiology* **44A**(2): 417-422.

Haywood, G. P. (1975). "A preliminary investigation into the roles played by the rectal gland and kidneys in the osmoregulation of the striped dogfish *Poroderma africanum*." *Journal of Experimental Zoology.* **193**(2): 167-175.

Hazon, N., Balment, R. J., Perrott, M. and O'Toole, L. B. (1989). "The renin-angiotensin system and vascular and dipsogenic regulation in elasmobranchs." *General and Comparative Endocrinology* **74**(2): 230-236.

Hazon, N., Tierney, M., Anderson, G., MacKenzie, S., Cutler, C. P. and Cramb, G. (1997[a]). Ion and Water Balance in Elasmobranch Fish. *Ionic Regulation in Animals.* Hazon, N., Eddy, F. B. and Flik, G., Springer Verlag: 70-86.

Hazon, N., Cerra, M. C., Tierney, M. L. and Tota, B. (1997[b]). Elasmobranch renin angiotensin system and the angiotensin receptor. *Comparative endocrinology,* Yokohama; Japan, Bologna.

Hazon, N., Tierney, M. L. and Takei, Y. (1999). "Renin-angiotensin system in elasmobranch fish: A review." *Journal of Experimental Zoology* **284**(5): 526-534.

Hazon, N., Wells, A., Pillans, R. D., Good, J. P., Gary Anderson, W. and Franklin, C. E. (2003). "Urea based osmoregulation and endocrine control in elasmobranch fish with special reference to euryhalinity." *Comparative Biochemistry and Physiology* **136B**(4): 685-700.

Hebert, S. C. and Friedman, P. A. (1990). "Diluting segment in kidney of dogfish shark. II. Electrophysiology of apical membranes and cellular resistances." *American Journal of Physiology* **258**(2): R409-417.

Heijden, A., Verbost, P., Eygensteyn, J., Li, J., Bonga, S. and Flik, G. (1997). "Mitochondria-rich cells in gills of tilapia (*Oreochromis mossambicus*) adapted to fresh water or sea water: quantification by confocal laser scanning microscopy." *Journal of Experimental Biology* **200**(1): 55-64.

Henderson, I. W., O'Toole, L. B. and Hazon, N. (1988). Kidney Function. *Physiology of Elasmobranch Fishes*. Shuttleworth, T. J., Springer-Verlag: 204-214.

Hentschel, H. (1978). "The kidney of the prussian carp, *Carassius auratus gibelio* (Cyprinidae). III. Glycogen-rich cells in the distal segment of nephronic tubule." *Tissue and Cell* **10**(2): 319-330.

Heupel, M. R. and Simpfendorfer, C. A. (2005). "Using Acoustic Monitoring to Evaluate MPAs for Shark Nursery Areas: The Importance of Long-term Data." *Marine Technology Society Journal* **39**: 10-18.

Heupel, M. R., Simpfendorfer, C. A. and Hueter, R. E. (2003). "Running before the storm: blacktip sharks respond to falling barometric pressure associated with Tropical Storm Gabrielle." *Journal of Fish Biology* **63**(5): 1357-1363.

Hill, W. G., Mathai, J. C., Gensure, R. H., Zeidel, J. D., Apodaca, G., Saenz, J. P., Kinne-Saffran, E., Kinne, R. and Zeidel, M. L. (2004). "Permeabilities of teleost and elasmobranch gill apical membranes: evidence that lipid bilayers alone do not account for barrier function." *American Journal of Physiology* **287**(1): C235-242.

Hiroi, J., McCormick, S. D., Ohtani-Kaneko, R. and Kaneko, T. (2005). "Functional classification of mitochondrion-rich cells in euryhaline Mozambique tilapia (*Oreochromis mossambicus*) embryos, by means of triple immunofluorescence staining for Na^+/K^+-ATPase, $Na^+/K^+/2Cl$- cotransporter and CFTR anion channel." *Journal of Experimental Biology* **208**(11): 2023-2036.

Hirose, S., Kaneko, T., Naito, N. and Takei, Y. (2003). "Molecular biology of major components of chloride cells." *Comparative Biochemistry and Physiology* **136B**(4): 593-620.

Holmgren, S. and Nilsson, S. (1983). "Bombesin-, gastrin/CCK-, 5-hydroxytryptamine-, neurotensin-, somatostatin-, and VIP-like immunoreactivity and catecholamine fluorescence in the gut of the elasmobranch, *Squalus acanthias*." *Cell and Tissue Research* **234**(3): 595-618.

Holmgren, S. and Nilsson, S. (1999). Digestive System. *Sharks, Skates and Rays: The Biology of Elasmobranch Fishes*. Hamlett, W. C. Baltimore, The John Hopkins University Press: 144-173.

Holt, W. F. and Idler, D. R. (1975). "Influence of the interrenal gland on the rectal gland of a skate." *Comparative Biochemistry and Physiology* **50C**(1): 111-119.

Humphrey, P. A., Lupfert, C., Apell, H. J., Cornelius, F. and Clarke, R. J. (2002). "Mechanism of the Rate-Determining Step of the Na^+, K^+-ATPase Pump Cycle." *Biochemistry* **41**(30): 9496-9507.

Hwang, P. P., Fang, M. J., Tsai, J. C., Huang, C. J. and Chen, S. T. (1998). "Expression of mRNA and protein of Na^+-K^+-ATPase alpha subunit in gills of tilpia (*Oreochromis mossambicus*)." *Fish Physiology and Biochemistry* **18**: 363-373.

Hwang, P. P., Lee, T. H., Weng, C. F., Fang, M. J. and Cho, G. Y. (1999). "Presence of Na-K-ATPase in mitochondria-rich cells in the yolk-sac epithelium of larvae of the teleost *Oreochromis mossambicus*." *Physiological and Biochemical Zoology* **72**(2): 138-144.

Hyodo, S., Katoh, F., Kaneko, T. and Takei, Y. (2004). "A facilitative urea transporter is localized in the renal collecting tubule of the dogfish *Triakis scyllia*." *Journal of Experimental Biology* **207**(2): 347-356.

Ino, Y., Gotoh, M., Sakamoto, M., Tsukagoshi, K. and Hirohashi, S. (2002). "Dysadherin, a cancer-associated cell membrane glycoprotein, down-regulates E-cadherin and promotes metastasis." *Proceedings of the National Academy of Sciences of the United States of America* **99**(1): 365-370.

Ip, Y. K., Tam, W. L., Wong, W. P., Loong, A. M., Hiong, K. C., Ballantyne, J. S. and Chew, S. F. (2003). "A comparison of the effects of environmental ammonia exposure on the Asian freshwater stingray *Himantura signifer* and the Amazonian freshwater stingray *Potamotrygon motoro*." *Journal of Experimental Biology* **206**(20): 3625-3633.

Isenring, P. and Forbush, B. (1997). "Ion and Bumetanide Binding by the Na-K-Cl Cotransporter." *Journal of Biological Chemistry* **272**(39): 24556-24562.

Isenring, P., Jacoby, S. C. and Forbush, B. (1998[a]). "The role of transmembrane domain 2 in cation transport by the Na-K-Cl cotransporter." *Proceedings of the National Academy of Sciences USA* **95**(12): 7179-7184.

Isenring, P., Jacoby, S. C., Chang, J. and Forbush, B. (1998[b]). "Mutagenic mapping of the Na-K-Cl cotransporter for domains involved in ion transport and bumetanide binding." *Journal of General Physiology* **112**(5): 549-558.

Isenring, P. and Forbush, B. (2001). "Ion transport and ligand binding by the Na-K-Cl cotransporter, structure-function studies." *Comparative Biochemistry and Physiology* **130A**(3): 487-497.

Ishibashi, K., Kuwahara, M., Kageyama, Y., Tohsaka, A., Marumo, F. and Sasaki, S. (1997). "Cloning and functional expression of a second new aquaporin abundantly expressed in testis." *Biochemistry and Biophysical Research Communications* **237**(3): 714-718.

Jaisser, F., Jaunin, P., Geering, K., Rossier, B. C. and Horisberger, J. D. (1994). "Modulation of the Na, K-pump function by beta subunit isoforms." *Journal of General Physiology* **103**(4): 605-623.

Jampol, L. M. and Epstein, F. H. (1979). "Sodium-potassium-activated adenosine triphosphate and osmotic regulation by fishes." *American Journal of Physiology* **218**(2): 607-611.

Janech, M. G. and Piermarin, P. M. (2002). "Renal water and solute excretion in the Atlantic stingray in fresh water." *Journal of Fish Biology* **61**(4): 1053-1057.

Janech, M. G., Fitzgibbon, W. R., Chen, R., Nowak, M. W., Miller, D. H., Paul, R. V. and Ploth, D. W. (2003). "Molecular and functional characterization of a urea transporter from the kidney of the Atlantic stingray." *American Journal of Physiology* **284**(2): F996-1005.

Jensen, M. K., Madsen, S. S. and Kristiansen, K. (1998). "Osmoregulation and Salinity Effects on the Expression and Activity of Na^+, K^+-ATPase in the Gills of European Sea Bass, *Dicentrarchus labrax* (L.)." *Journal of Experimental Zoology* **282**: 290-300.

Jiang, G., Klein, J. D. and O'Neill, W. C. (2001). "Growth factors stimulate the Na-K-2Cl cotransporter NKCC1 through a novel Cl(-)-dependent mechanism." *American Journal of Physiology* **281**(6): C1948-1953.

Jobling, M. (1995). *Environmental Biology of Fishes*. London, Chapman and Hall Publishers.

Jones, D. H., Golding, M. C., Barr, K. J., Fong, G. H. and Kidder, G. M. (2001). "The mouse Na^+-K^+-ATPase gamma-subunit gene (Fxyd2) encodes three developmentally regulated transcripts." *Physiological Genomics* **6**(3): 129-135.

Jorgensen, P. L., Hakansson, K. O. and Karlish, S. J. (2003). "Structure and mechanism of Na, K-ATPase: functional sites and their interactions." *Annual Review of Physiology*. **65**. 817-849.

Kanoh, S., Niwa, E., Osaka, Y. and Watabe, S. (1999). "Effects of urea on actin-activated Mg^{2+}-ATPase of requiem shark myosin." *Comparative Biochemistry and Physiology* **122B**(3): 333-338.

Kaplan, J. H., Arguello, J. M., Ellis-Davies, G. C. R. and Lutsenko, S. (1994). The Stabilization of Cation Binding and its Relation to Na^+/K^+-ATPase Structure and Function. *The Sodium Pump, Structural Mechanism, Hormonal Control and Its Role in Disease*. Bamberg, E. and Schoner, W. New York, Steinkopff, Springer & Darmstadt: 321-229.

Kaplan, J., Hu, Y. and Gatto, C. (2001). "Conformational Coupling: The Moving Parts of an Ion Pump." *Journal of Bioenergetics and Biomembranes* **33**(5): 379-385.

Karnaky, K. J. (1986). "Structure and Function of the Chloride Cell of *Fundulus heteroclitus* and Other Teleosts." *American Zoology* **26**: 209-224.

Karnaky, K. J. (1998). Osmotic and Ionic Regulation. *The Physiology of Fishes*. Evans, D. H., CRC Press: 157-176.

Karnaky, K. J., Jr., Ernst, S. A. and Philpott, C. W. (1976[a]). "Teleost Chloride Cell: I. Response of pupfish *Cyprinodon variegatus* gill Na, K-ATPase and chloride cell fine structure to various high salinity environments." *Journal of Cell Biology* **70**(1): 144-156.

Karnaky, K. J., Kinter, L. B., Kinter, W. B. and Stirling, C. E. (1976[b]). "Teleost Chloride Cell: II. Autoradiographic localization of gill Na, K-ATPase in killifish *Fundulus heteroclitus* adapted to low and high salinity environments." *Journal of Cell Biology* **70**: 157-177.

Karnaky, K. J., Piermarini, P. M. and Forte, L. R. (1999). "Guanylin/Uroguanylin Regulation of Dogfish Shark (*Squalus acanthias*) Rectal Gland Chloride Secretion." *Bulletin of the Mount Desert Island Biological Laboratory* **38**: 70-71.

Kawakami, K., Noguchi, S., Noda, M., Takahashi, H., Ohta, T., Kawamura, M., Nojima, H., Nagano, K., Hirose, T., Inayama, S., Hayashida, H., Miyata, T. and Numa, S. (1985). "Primary structure of the α-subunit of *Torpedo californica* (Na^+K^+)ATPase deduced from cDNA sequence." *Nature* **316**(22): 733-736.

Kawamura, M., Noguchi, S., Ueno, S., Kusaba, M. and Takeda, K. (1994). Functional Analysis of the Disulfide Bonds of Na^+/K^+-ATPase β-subunit by Site Directed Mutagenesis. *The Sodium Pump, Structural Mechanism, Hormonal Control and Its Role in Disease*. Bamberg, E. and Schoner, W. New York, Steinkopff, Springer & Darmstadt: 287-297.

Kelly, S. P., Chow, I. N. K. and Woo, N. Y. S. (1999). "Haloplasticity of Black Seabream (*Mylio macrocephalus*): Hypersaline to Freshwater Acclimation." *Journal of Experimental Zoology* **283**(3): 226-241.

Kempton, R. T. (1962). "Studies on the elasmobranch kidney. III. The kidney of the lesser electric ray, *Narcine brasiliensis*." *Journal of Morphology* **111**: 217-25.

Kent, B. and Olson, K. R. (1982). "Blood flow in the rectal gland of *Squalus acanthias*." *American Journal of Physiology* **243**(3): R296-303.

Kerem, B., Rommens, J. M., Buchanan, J. A., Markiewicz, D., Cox, T. K., Chakravarti, A., Buchwald, M. and Tsui, L. C. (1989). "Identification of the cystic fibrosis gene: genetic analysis." *Science* **245**(4922): 1073-1080.

Kerst, G., Beschorner, U., Unsold, B., von Hahn, T., Schreiber, R., Greger, R., Gerlach, U., Lang, H. J., Kunzelmann, K. and Bleich, M. (2001). "Properties and function of KCNQ1 K^+ channels isolated from the rectal gland of *Squalus acanthias*." *Pflugers Archiv* **443**(1): 146-154.

Keys, A. and Willmer, E. N. (1932). ""Chloride secreting cells" in the gill of fishes, with special reference to the common eel." *Journal of Physiology* **76**: 368-378.

King, L. S. and Agre, P. (1996). "Pathophysiology of the aquaporin water channels." *Annual Review of Physiology* **58**: 619-648.

Kinne-Saffran, E. and Kinne, R. K. (2001). "Inhibition by mercuric chloride of Na-K-2Cl cotransport activity in rectal gland plasma membrane vesicles isolated from *Squalus acanthias*." *Biochimica et Biophysica Acta* **1510**(1-2): 442-451.

Kisen, G., Gallais, C., Auperin, B., Klungand, H., Sandra, O., Prunet, P. and Andersen, O. (1994). "Northern blot analysis of the Na^+, K^+-ATPase alpha-subunit in salmonids." *Comparative Biochemistry and Physiology* **107B**(2): 255-259.

Kleinzeller, A. (1985). "Trimethylamine oxide and the maintenance of volume of dogfish shark rectal gland cells." *Journal of Experimental Zoology.* **236**(1): 11-17.

Kleizen, B., Braakman, I. and de Jonge, H. R. (2000). "Regulated trafficking of the CFTR chloride channel." *European Journal of Cell Biology* **79**(8): 544-556.

Knepper, M. A., Kim, G. H. and Masilamani, S. (2003). "Renal tubule sodium transporter abundance profiling in rat kidney: response to aldosterone and variations in NaCl intake." *Annals of the New York Academy of Sciences* **986**: 562-569.

Ko, Y. H. and Pedersen, P. L. (1997). "Frontiers in Research on Cystic Fibrosis: Understanding Its Molecular and Chemical Basis and Relationship to the Pathogenesis of the Disease." *Journal of Bioenergetics and Biomembranes* **29**(5): 417-428.

Kormanik, G. A. (1993). "Ionic and osmotic environment of developing elasmobranch embryos." *Environmental Biology of Fishes* **38**: 233.

Kritzler, H. and Wood, L. (1961). "Provisional audiogram for the shark, *Carcharhinus leucas*." *Science.* **133**: 1480-1482.

Krogh, A. (1938). "The active transport of ions in some freshwater animals." *Zeitschrift fur Vergleichende Physiologie* **25**: 335-350.

Kultz, D. and Jurss, K. (1993). "Biochemical characterization of isolated branchial mitochondria-rich cells of *Oreochromis mossambicus* acclimated to fresh water or hypersaline sea water." *Journal of Comparative Physiology* **163B**: 406-412.

Kurihara, K., Nakanishi, N., Moore-Hoon, M. L. and Turner, R. J. (2002). "Phosphorylation of the salivary $Na^{(+)}$-$K^{(+)}$-$2Cl^{(-)}$ cotransporter." *American Journal of Physiology* **282**(4): C817-823.

Kuriyama, H., Kawamoto, S., Ishida, N., Ohno, I., Mita, S., Matsuzawa, Y., Matsubara, K. and Okubo, K. (1997). "Molecular cloning and expression of a novel human aquaporin from adipose tissue with glycerol permeability." *Biochemistry and Biophysical Research Communications* **241**(1): 53-58.

Kuster, B., Shainskaya, A., Pu, H. X., Goldshleger, R., Blostein, R., Mann, M. and Karlish, S. J. (2000). "A new variant of the gamma subunit of renal Na, K-ATPase. Identification by mass spectrometry, antibody binding, and expression in cultured cells." *Journal of Biological Chemistry* **275**(24): 18441-18446.

Lacy, E. R., Reak, E., Schlusselberg, D. S., Smith, W. K. and Woodward, D. J. (1985). "A renal countercurrent system in marine elasmobranch fish: a computer-assisted reconstruction." *Science.* **227**(4692): 1351-1354.

Lacy, E. R. and Reale, E. (1985[a]). "The elasmobranch kidney. I. Gross anatomy and general distribution of the nephrons." *Anatomy and Embryology (Berl)* **173**(1): 23-34.

Lacy, E. R. and Reale, E. (1985[b]). "The elasmobranch kidney. II. Sequence and structure of the nephrons." *Anatomy and Embryology (Berl)* **173**(2): 163-186.

Lacy, E. R. and Reale, E. (1986). "The elasmobranch kidney. III. Fine structure of the peritubular sheath." *Anatomy and Embryology (Berl)* **173**(3): 299-305.

Lacy, E. R., Castellucci, M. and Reale, E. (1987). "The elasmobranch renal corpuscle: fine structure of Bowman's capsule and the glomerular capillary wall." *The Anatomical Record.* **218**(3): 294-305.

Lacy, E. R., Luciano, L. and Reale, E. (1989). "Flagellar cells and ciliary cells in the renal tubule of elasmobranchs." *Journal of Experimental Zoology* (Supplement 2):186-192.

Lacy, E. R. and Reale, E. (1991[a]). "Fine structure of the elasmobranch renal tubule: neck and proximal segments of the little skate."*American Journal of Anatomy* **190**(2): 118-132.

Lacy, E. R. and Reale, E. (1991[b]). "The fine structure of the elasmobranch renal tubule: intermediate, distal, and collecting duct segments of the little skate."*American Journal of Anatomy* **192**(4): 478-497.

Lacy, E. J. and Reale, E. (1999). Urinary System. *Sharks, Skates and Rays: The Biology of Elasmobranch Fishes.* Hamlett, W. C. Baltimore, The John Hopkins University Press: 353-397.

Lagios, M. D. and Stasko-Concannon, S. (1979). "Ultrastructure and ATPase activity of the rectal gland of the chondrichthyean fish *Hydrolagus colliei* (Holocephali)." *Cell and Tissue Research* **198**(2): 287-294.

Laughery, M. D., Todd, M. L. and Kaplan, J. H. (2003). "Mutational analysis of alpha-beta subunit interactions in the delivery of Na, K-ATPase heterodimers to the plasma membrane." *Journal of Biological Chemistry* **278**(37): 34794-34803.

Lear, S., Coen, B. J., Silva, P., Lechene, C. and Epstein, F. H. (1992). "cAMP activates the sodium pump in cultured cells of the elasmobranch rectal gland." *Journal of the American Society of Nephrology* **2**: 1523-1528.

Lee, M. D., King, L. S. and Agre, P. (1997). "The aquaporin family of water channel proteins in clinical medicine." *Medicine (Baltimore)* **76**(3): 141-156.

Lee, T., Tsai, J., Fang, M., Yu, M. and Hwang, P. (1998). "Isoform expression of Na^+-K^+-ATPase α-subunit in gills of the teleost *Oreochromis mossambicus*." *American Journal of Physiology* **275**: R926-R932.

Li, C., Grosdidier, A., Crambert, G., Horisberger, J. D., Michielin, O. and Geering, K. (2004). "Structural and functional interaction sites between Na, K-ATPase and FXYD proteins." *Journal of Biological Chemistry* **279**(37): 38895-38902.

Lignot, J. H., Cutler, C. P., Hazon, N. and Cramb, G. (2002). "Immunolocalisation of aquaporin 3 in the gill and the gastrointestinal tract of the European eel *Anguilla anguilla* (L.)." *Journal of Experimental Biology* **205**(17): 2653-2663.

Lin, Y. M., Chen, C. N. and Lee, T. H. (2003). "The expression of gill Na, K-ATPase in milkfish, *Chanos chanos*, acclimated to seawater, brackish water and fresh water." *Comparative Biochemistry and Physiology* **135A**: 489-497.

Lin, C. H., Tsai, R. S. and Lee, T. H. (2004). "Expression and distribution of Na, K-ATPase in gill and kidney of the spotted green pufferfish, *Tetraodon nigroviridis*, in response to salinity challenge." *Comparative Biochemistry and Physiology.* **138A**(3): 287-295.

Lingrel, J. B. and Kuntzweiler, T. (1994). "Na^+, K^+-ATPase." *Journal of Biological Chemistry.* **269**(31): 19659-19662.

Lingrel, J. B., Argèuello, J. M., Van Huysse, J. and Kuntzweiler, T. A. (1997). "Cation and cardiac glycoside binding sites of the Na, K-ATPase." *Annals of the New York Academy of Sciences* **834**: 194-206.

Lingrel, J., Moseley, A., Dostanic, I., Cougnon, M., He, S., James, P., Woo, A., O'Connor, K., and Neumann, J. (2003). "Functional roles of the alpha isoforms of the Na, K-ATPase." *Annals of the New York Academy of Sciences* **986**: 354-359.

Liu, H., Hooper, S. B., Armugam, A., Dawson, N., Ferraro, T., Jeyaseelan, K., Thiel, A., Koukoulas, I. and Wintour, E. M. (2003). "Aquaporin gene expression and regulation in the ovine fetal lung." *Journal of Physiology* **551**(2): 503-514.

Lopez, L. B., Quintas, L. E. M. and Noel, F. (2002). "Influence of development on Na^+/K^+-ATPase expression: isoform- and tissue-dependancy." *Comparative Biochemistry and Physiology* **131A**: 323-333.

Lopina, O. D. (2001). "Interaction of Na, K-ATPase catalytic subunit with cellular proteins and other endogenous regulators." *Biochemistry (Mosc)* **66**(10): 1122-1131.

Lubarski, I., Pihakaski-Maunsbach, K., Karlish, S. J., Maunsbach, A. B. and Garty, H. (2005). "Interaction with the Na, K-ATPase and tissue distribution of FXYD5 (related to ion channel)." *Journal of Biological Chemistry* **280**(45): 37717-37724.

Lupfert, C., Grell, E., Pintschovius, V., Apell, H. J., Cornelius, F. and Clarke, R. J. (2001). "Rate Limitation of the Na^+, K^+-ATPase Pump Cycle." *Biophysical Journal* **81**(4): 2069-2081.

Lutsenko, S. and Kaplan, J. H. (1992). "Evidence of a Role for the Na, K-ATPase α-Subunit in Active Cation Transport." *Annals of New York Academy of Sciences* **671**: 147.

Lutsenko, S. and Kaplan, J. H. (1993). "An essential role for the extracellular domain of the Na, K-ATPase beta-subunit in cation occlusion." *Biochemistry.* **32**(26): 6737-6743.

Lutsenko, S. and Kaplan, J. H. (1994). "Molecular events in close proximity to the membrane associated with the binding of ligands to the Na, K-ATPase." *Journal of Biological Chemistry.* **269**(6): 4555-4564.

Lutsenko, S. and Kaplan, J. H. (1995). "Organization of P-type ATPases: significance of structural diversity." *Biochemistry.* **34**(48): 15607-15613.

Lytle, C., Xu, J. C., Biemesderfer, D., Haas, M. and Forbush, B., 3rd (1992). "The Na-K-Cl cotransport protein of shark rectal gland. I. Development of monoclonal antibodies, immunoaffinity purification, and partial biochemical characterization." *Journal of Biological Chemistry* **267**(35): 25428-25437.

Lytle, C. and Forbush, B. (1992[a]). "The Na-K-Cl cotransport protein of shark rectal gland. II. Regulation by direct phosphorylation." *Journal of Biological Chemistry* **267**(35): 25438-25443.

Lytle, C. and Forbush, B., 3rd (1992[b]). "Na-K-Cl cotransport in the shark rectal gland. II. Regulation in isolated tubules." *American Journal of Physiology* **262**(4): C1009-1017.

Lytle, C. and Forbush, B. (1996). "Regulatory phosphorylation of the secretory Na-K-Cl cotransporter: modulation by cytoplasmic Cl." *American Journal of Physiology* **270**(1): C437-C448.

Ma, T., Yang, B. and Verkman, A. S. (1996). "Gene structure, cDNA cloning, and expression of a mouse mercurial-insensitive water channel." *Genomics* **33**(3): 382-388.

MacKenzie, S. (1996). The effect of feeding of ion transport in the rectal gland of the European dogfish (*Scyliorhinus canicula*). *Biology Ph. D. Thesis*, University of St Andrews.

MacKenzie, S., Cutler, C. P., Hazon, N. and Cramb, G. (2002). "The effects of dietary sodium loading on the activity and expression of Na, K-ATPase in the rectal gland of the European Dogfish (*Scyliorhinus canicula*)." *Comparative Biochemistry and Physiology* **131B**: 185-200.

Madsen, S. S., Jensen, M. K., Nohr, J. and Kristiansen, K. (1995). "Expression of Na^+-K^+-ATPase in the brown trout, *Salmo trutta*: in vivo modulation by hormones and seawater." *American Journal of Physiology* **269**: R1339-R1345.

Mahmmoud, Y. A. and Cornelius, F. (2000). "Variable protein kinase C targeting to the N- and C-terminal domains of shark Na, K-ATPase induced by detergent." *International Congress Series* **1207**: 591-594.

Mahmmoud, Y. A., Vorum, H. and Cornelius, F. (2000). "Identification of a phospholemman-like protein from shark rectal glands. Evidence for indirect regulation of Na, K-ATPase by protein kinase C via a novel member of the FXYDY family." *Journal of Biological Chemistry* **275**(46): 35969-35977.

Mahmmoud, Y. A. and Cornelius, F. (2002). "Protein Kinase C Phosphorylation of Purified Na, K-ATPase: C-Terminal Phosphorylation Sites at the alpha- and gamma-subunits Close to the Inner Face of the Plasma Membrane." *Biophysical Journal* **82**(4): 1907-1919.

Mahmmoud, Y. A., Cramb, G., Maunsbach, A. B., Cutler, C. P., Meischke, L. and Cornelius, F. (2003). "Regulation of Na, K-ATPase by PLMS, the phospholemman-like protein from shark: molecular cloning, sequence, expression, cellular distribution, and functional effects of PLMS." *Journal of Biological Chemistry* **278**(39): 37427-37438.

Mahmmoud, Y. A. (2005). "Curcumin modulation of Na, K-ATPase: phosphoenzyme accumulation, decreased K^+ occlusion, and inhibition of hydrolytic activity." *British Journal of Pharmacology* **145**(2): 236-245.

Mancera, J. M. and McCormick, S. D. (2000). "Rapid activation of gill Na^+, K^+-ATPase in the euryhaline teleost *Fundulus heteroclitus*." *Journal of Experimental Zoology.* **287**(4): 263-274.

Manire, C., Hueter, R., Hull, E. and Spieler, R. (2001). "Serological Changes Associated with Gill-Net Capture and Restraint in Three Species of Sharks." *Transactions of the American Fisheries Society* **130**(6): 1038-1048.

Marshall, J., Martin, K. A., Picciotto, M., Hockfield, S., Nairn, A. C. and Kaczmarek, L. K. (1991). "Identification and localization of a dogfish homolog of human cystic fibrosis transmembrane conductance regulator." *Journal of Biological Chemistry* **266**(33): 22749-22754.

Marshall, W. S., Bryson, S. E., Darling, P., Whitten, C., Patrick, M., Wilkie, M., Wood, C. M. and Buckland-Nicks, J. (1997). "NaCl Transport and Ultrastructure of Opercular Epithelium From a Fresh-water-Adapted Euryhaline Teleost, *Fundulus heteroclitus*." *Journal of Experimental Zoology* **277**(1): 23-37.

Marshall, W. S. and Bryson, S. E. (1998). "Transport mechanisms of seawater teleost chloride cells: an inclusive model of a multifunctional cell." *Comparative Biochemistry and Physiology* **119A**(1): 97-106.

Marshall, W. S., Emberley, T. R., Singer, T. D., Bryson, S. E. and McCormick, S. D. (1999). "Time course of salinity adaptation in a strongly euryhaline estuarine teleost, *Fundulus heteroclitus*: a multivariable approach." *Journal of Experimental Biology* **202** (11): 1535-1544.

Marshall, W. S. (2002). "Na^+, Cl^-, Ca^{2+} and Zn^{2+} Transport by Fish Gills: Retrospective Review and Prospective Synthesis." *Journal of Experimental Zoology* **293**(3): 264-283.

Marshall, W. S. and Singer, T. D. (2002). "Cystic fibrosis transmembrane conductance regulator in teleost fish." *Biochimica Et Biophysica Acta* **1566**(1-2): 16-27.

Martin, R. A. (2005). "Conservation of freshwater and euryhaline elasmobranchs: a review." *Journal of Marine Biological Association of the United Kingdom* **85**: 1049-1074.

Marshall, W. S., Lynch, E. M. and Cozzi, R. R. F. (2002[a]). "Redistribution of immunofluorescence of CFTR anion channel and NKCC cotransporter in chloride cells during adaptation of the killifish *Fundulus heteroclitus* to sea water." *Journal of Experimental Biology* **205**(9): 1265-1273.

Marshall, W. S., Howard, J. A., Cozzi, R. R. and Lynch, E. M. (2002[b]). "NaCl and fluid secretion by the intestine of the teleost *Fundulus heteroclitus*: involvement of CFTR." *Journal of Experimental Biology* **205**(6): 745-758.

Martinez, A. S., Cutler, C. P., Wilson, G. D., Phillips, C., Hazon, N. and Cramb, G. (2005[a]). "Regulation of expression of two aquaporin homologs in the intestine of the European eel: effects of seawater acclimation and cortisol treatment." *American Journal of Physiology* **288**(6): R1733-1743.

Martinez, A. S., Cutler, C. P., Wilson, G. D., Phillips, C., Hazon, N. and Cramb, G. (2005[b]). "Cloning and expression of three aquaporin homologues from the European eel (*Anguilla anguilla*): effects of seawater acclimation and cortisol treatment on renal expression." *Biology of the Cell* **97**(8): 615-627.

Martinez, A. S., Wilson, G., Phillips, C., Cutler, C., Hazon, N. and Cramb, G. (2005[c]). "Effect of Cortisol on Aquaporin Expression in the Esophagus of the European Eel, *Anguilla anguilla*." *Annals of the New York Academy of Sciences* **1040**: 395-398.

Marver, D., Lear, S., Marver, L. T., Silva, P. and Epstein, F. H. (1986). "Cyclic AMP-dependent stimulation of Na, K-ATPase in shark rectal gland." *Journal of Membrane Biology.* **94**(3): 205-215.

McCormick, S. D., Sundell, K., Bjèornsson, B. T., Brown, C. L. and Hiroi, J. (2003). "Influence of salinity on the localization of Na^+/K^+-ATPase, $Na^+/K^+/2Cl$- cotransporter (NKCC) and CFTR anion channel in chloride cells of the Hawaiian goby (*Stenogobius hawaiiensis*)." *Journal of Experimental Biology* **206**(24): 4575-4583.

McKendry, J. E., Bernier, N. J., Takei, Y., Duff, D. W., Olson, K. R. and Perry, S. F. (1999). "Natriuretic peptides and the control of catecholamine release in two freshwater teleost and a marine elasmobranch fish." *Fish Physiology and Biochemistry* **20**(1): 61-77.

Mercer, R. W., Biemesderfer, D., Bliss, D. P. and Collins, J. H. (1993). "Molecular cloning and immunological characterization of the gamma polypeptide, a small protein associated with the Na, K-ATPase." *Journal of Cell Biology* **121**(3): 579-586.

Metcalfe, J. D. and Butler, P. J. (1986). "The Functional Anatomy of the Gills of the Dogfish (*Scyliorhinus canicula*)." *Journal of Zoology* **208A**: 519-530.

Miller, D. S., Masereeuw, R., Henson, J. and Karnaky, K. J. (1998). "Excretory transport of xenobiotics by dogfish shark rectal gland tubules." *American Journal of Physiology* **275**(3): R697-705.

Miller, D. S., Masereeuw, R. and Karnaky, K. J., Jr. (2002). "Regulation of MRP2-mediated transport in shark rectal salt gland tubules." *American Journal of Physiology* **282**(3): R774-781.

Montoya, R. V. and Thorson, T. B. (1982). "The bull shark (*Carcharhinus leucas*) and largetooth sawfish (*Pristis perotteti*) in Lake Bayano, a tropical man-made impoundment in Panama." *Environmental Biology of Fishes* **7**(4): 341-347.

Moorman, J. R., Ackerman, S. J., Kowdley, G. C., Griffin, M. P., Mounsey, J. P., Chen, Z., Cala, S. E., O'Brian, J. J., Szabo, G. and Jones, L. R. (1995). "Unitary anion currents through phospholemman channel molecules." *Nature* **377**(6551): 737-740.

Moorman, J. R. and Jones, L. R. (1998). "Phospholemman: a cardiac taurine channel involved in regulation of cell volume." *Advances in Experimental Medical and Biology* **442**: 219-228.

Morales, M. M., Capella, M. A. M. and Lopes, A. C. (1999). "Structure and function of the cystic fibrosis transmembrane conductance regulator." *Brazilian Journal of Medical and Biological Research* **32**(8): 1021-1028.

Morgan, R. L., Ballantyne, J. S. and Wright, P. A. (2003[a]). "Regulation of a renal urea transporter with reduced salinity in a marine elasmobranch, *Raja erinacea*." *Journal of Experimental Biology* **206**(18): 3285-3292.

Morgan, R. L., Wright, P. A. and Ballantyne, J. S. (2003[b]). "Urea transport in kidney brush-border membrane vesicles from an elasmobranch, *Raja erinacea*." *Journal of Experimental Biology* **206**(18): 3293-3302.

Morrison, B. W., Moorman, J. R., Kowdley, G. C. and Kobayashi, Y. M. (1995). "Mat-8, a novel phospholemman like protein expressed in human breast tumors, induces a chloride conductance in *Xenopus* oocytes." *Journal of Biological Chemistry* **270**(5): 2176-2182.

Motais, R. and Garcia-Romeu, F. (1972). "Transport mechanisms in the teleostean gill and amphibian skin." *Annual Review of Physiology* **34**: 141-176.

Mulders, S. M., Preston, G. M., Deen, P. M., Guggino, W. B., van Os, C. H. and Agre, P. (1995). "Water channel properties of major intrinsic protein of lens." *Journal of Biological Chemistry* **270**(15): 9010-9016.

Newbound, D. R. and O'Shea, J. E. (2001). "The microanatomy of the rectal salt gland of the Port Jackson Shark, *Heterodontus portusjacksoni* (Meyer) (Heterodontidae): suggestions for a counter-current exchange system." *Cells Tissues Organs* **169**(2): 165-175.

Nielsen, S., King, L. S., Christensen, B. M. and Agre, P. (1997). "Aquaporins in complex tissues. II. Subcellular distribution in respiratory and glandular tissues of rat." *American Journal of Physiology* **273**(5): C1549-1561.

Noaillac Depeyre, J. and Gas, N. (1976). "Electron microscopic study on gut epithelium of the tench (*Tinca tinca* L.) with respect to its absorptive functions." *Tissue and Cell* **8**(3): 511-530.

Oguri, M. (1964). "Rectal glands of marine and fresh-water sharks: comparative histology." *Science* **144**: 1151-1152.

Okamura, H., Denawa, M., Ohniwa, R. and Takeyasu, K. (2003). "P-type ATPase superfamily: evidence for critical roles for kingdom evolution." *Annals of the New York Academy of Sciences* **986**: 219-223.

Palmer, C. J., Scott, B. T. and Jones, L. R. (1991). "Purification and complete sequence determination of the major plasma membrane substrate for cAMP-dependent protein kinase and protein kinase C in myocardium." *Journal of Biological Chemistry* **266**(17): 11126-11130.

Park, Y. S. and Hong, S. K. (1976). "Properties of toad skin Na-K-ATPase with special reference to effect of temperature." *American Journal of Physiology* **231**(5): 1356-1363.

Pärt, P., Wright, P. A. and Wood, C. M. (1998). "Urea and water permeability in dogfish (*Squalus acanthias*) gills." *Comparative Biochemistry and Physiology* **119A**(1): 117-124.

Payan, P., Goldstein, L. and Forster, R. P. (1973). "Gills and kidneys in ureosmotic regulation in euryhaline skates." *American Journal of Physiology* **224**(2): 367-372.

Payan, P. and Maetz, J. (1973). "Branchial sodium transport mechanisms in *Scyliorhinus canicula*: evidence for Na^+/NH_4^+ and Na^+H^+ exchanges and for a role of carbonic anhydrase." *Journal of Experimental Biology* **58**: 487-502.

Pelis, R. M., Zydlewski, J. and McCormick, S. D. (2001[a]). "Gill Na^+-K^+-$2Cl^-$ cotransporter abundance and location in Atlantic salmon: effects of seawater and smolting." *American Journal of Physiology* **280**(6): R1844-1852.

Pelis, R. M. and McCormick, S. D. (2001[b]). "Effects of growth hormone and cortisol on Na^+-K^+-$2Cl^-$ cotransporter localization and abundance in the gills of Atlantic salmon." *General and Comparative Endocrinology* **124**(2): 134-143.

Perry, S. F. (1998). "Relationships between branchial chloride cells and gas transfer in freshwater fish." *Comparative Biochemistry and Physiology* **119A**(1): 9-16.

Philpott, C. W. and Copeland, D. E. (1963). "Fine Structure of Chloride Cells from Three Species of Fundulus." *Journal of Cell Biology* **18**: 389-404.

Philpott, C. W. (1980). "Tubular system membranes of teleost chloride cells: osmotic response and transport sites." *American Journal of Physiology* **238**(3): R171-184.

Piermarini, P. M. and Evans, D. H. (1998). "Osmoregulation of the Atlantic stingray (*Dasyatis sabina*) from the freshwater Lake Jesup of the St. Johns River, Florida." *Physiological Zoology* **71**(5): 553-560.

Piermarini, P. M., Choe, K. P. and Karnaky, K. J. (1999). "Effect of Rectal Gland Removal on Na, K-ATPase Expression in the Gills and Kidneys of *Raja erinacea*." *Bulletin of the Mount Desert Island Biological Laboratory* **38**: 35-36.

Piermarini, P. M. and Evans, D. H. (2000). "Effects of environmental salinity on Na^+/K^+-ATPase in the gills and rectal gland of a euryhaline elasmobranch (*Dasyatis sabina*)." *Journal of Experimental Biology* **203**: 2957-2966.

Piermarini, P. M. and Evans, D. H. (2001). "Immunochemical analysis of the vacuolar proton-ATPase B-subunit in the gills of a euryhaline stingray (*Dasyatis sabina*): effects of salinity and relation to Na^+/K^+-ATPase." *Journal of Experimental Biology* **204**: 3251-3259.

Piermarini, P. M., Verlander, J. W., Royaux, I. E. and Evans, D. H. (2003). "Pendrin immunoreactivity in the gill epithelium of a euryhaline elasmobranch." *American Journal of Physiology* **283**(2): R983-R992.

Pierre, S. V., Duran, M., Carr, D. L. and Pressley, T. A. (2002). "Structure/function analysis of Na^+-K^+-ATPase central isoform-specific region: involvement in PKC regulation." *American Journal of Physiology* **283**: F1066-F1074.

Pierre, S. V., Duran, M. J., Carr, D. L. and Pressley, T. A. (2003). "Structure/function analysis of Na, K-ATPase $\alpha 1$ and $\alpha 2$ central isoform-specific regions reveals their involvement in regulation by protein kinase C." *Annals of the New York Academy of Sciences* **986**: 260-262.

Pillans, R. D. and Franklin, C. E. (2004). "Plasma osmolyte concentrations and rectal gland mass of bull sharks *Carcharhinus leucas*, captured along a salinity gradient." *Comparative Biochemistry and Physiology* **138A**(3): 363-371.

Pillans, R. D., Good, J. P., Anderson, W. G., Hazon, N. and Franklin, C. E. (2005). "Freshwater to seawater acclimation of juvenile bull sharks (*Carcharhinus leucas*): plasma osmolytes and Na^+/K^+-ATPase activity in gill, rectal gland, kidney and intestine." *Journal of Comparative Physiology* **175B**: 37-44.

Pisam, M., Caroff, A. and Rambourg, A. (1987). "Two types of chloride cells in the gill epithelium of a freshwater-adapted euryhaline fish: *Lebistes reticulatus*; their modifications during adaptation to saltwater."*American Journal of Anatomy* **179**(1): 40-50.

Pisam, M., Prunet, P., Boeuf, G. and Rambourg, A. (1988). "Ultrastructural features of chloride cells in the gill epithelium of the Atlantic salmon, *Salmo salar*, and their modifications during smoltification."*American Journal of Anatomy* **183**(3): 235-244.

Pisam, M., Massa, F., Jammet, C. and Prunet, P. (2000). "Chronology of the appearance of beta, A, and alpha mitochondria-rich cells in the gill epithelium during ontogenesis of the brown trout (*Salmo trutta*)." *Anatomical Record* **259**(3): 301-311.

Pressley, T. A. (1992). "Phylogenetic conservation of isoform-specific regions within alpha-subunit of Na^+-K^+-ATPase." *American Journal of Physiology* **262**(3): C743-751.

Pritchard, J. B. (2003). "The gill and homeostasis: transport under stress." *American journal of physiology* **285**(6): R1269-1271.

Pu, H. X., Cluzeaud, F., Goldshleger, R., Karlish, S. J., Farman, N. and Blostein, R. (2001). "Functional role and immunocytochemical localization of the gamma α and gamma β forms of the Na, K-ATPase gamma subunit." *Journal of Biological Chemistry* **276**(23): 20370-20378.

Randall, D. J. and Brauner, C. (1998). "Interactions between ion and gas transfer in freshwater teleost fish." *Comparative Biochemistry and Physiology* **119A**(1): 3-8.

Randall, J. E. (1986). *Sharks of Arabia.* London, Immel Publishing.

Raschi, W. and Mackanos, L. A. (1989). "The Structure of the Ampullae of Lorenzini in *Dasyatis garouaensis* and its implications on the evolution of freshwater electroreceptive systems." *Journal of Experimental Zoology* (Supplement 2): 101-111.

Raschi, W., Keithan, E. D. and Rhee, W. C. H. (1997). "Anatomy of the Ampullary Electroreceptor in the Freshwater Stingary, *Himantura signifer*." *Copeia*(1): 101-107.

Reader's Digest (1994). *Sharks: Silent Hunters of the Deep.* Surry Hills, NSW, Reader's Digest.

Rice, W. J., Young, H. S., Martin, D. W., Sachs, J. R. and Strokes, D. L. (2001). "Structure of Na^+, K^+-ATase at 11-Å Resolution: Comparison with Ca^{2+}-ATPase in E_1 and E_2 states." *Biophysical Journal* **80**: 2187-2197.

Richards, J. G., Semple, J. W., Bystriansky, J. S. and Schulte, P. M. (2003). "Na^+/K^+-ATPase alpha-isoform switching in gills of rainbow trout (*Oncorhynchus mykiss*) during salinity transfer." *Journal of Experimental Biology* **206**(24): 4475-4486.

Riordan, J. R., Rommens, J. M., Kerem, B., Alon, N., Rozmahel, R., Grzelczak, Z., Zielenski, J., Lok, S., Plavsic, N., Chou, J. L. (1989). "Identification of the cystic fibrosis gene: cloning and characterization of complementary DNA." *Science* **245**(4922): 1066-1073.

Riordan, J. R., Forbush, B. and Hanrahan, J. W. (1994). "The molecular basis of chloride transport in shark rectal gland." *Journal of Experimental Biology* **196**: 405-418.

Romao, S., Freire, C. A. and Fanta, E. (2001). "Ionic regulation and Na^+, K^+-ATPase activity in gills and kidney of the Antarctic aglomerular cod icefish exposed to dilute seawater." *Journal of Fish Biology* **59**: 463-468.

Russell, J. M. (2000). "Sodium-potassium-chloride cotransport." *Physiological Reviews* **80**(1): 211-276.

Sabolic, I., Katsura, T., Verbavatz, J. M. and Brown, D. (1995). "The AQP2 Water Channel: Effect of Vasopressin Treatment, Microtubule Disruption, and Distribution in Neonatal Rats." *Journal of Membrane Biology* **143**(3): 165-175.

Saito, S., Matoba, R., Kato, K. and Matsubara, K. (2001). "Expression of a novel member of the ATP1G1/PLM/MAT8 family, phospholemman-like protein (PLP) gene, in the developmental process of mouse cerebellum." *Gene* **279**(2): 149-155.

Sambrook, J., Fritsch, E. F. and Maniatis, T. (1989). *Molecular Cloning: A Laboratory Manual.* USA, Cold Spring Harbor Laboratory Press.

Sanger, F., Nicklen, S. and Coulson, A. R. (1977). "DNA sequencing with chain-terminating inhibitors." *Proceedings of the National Academy of Sciences of the United States of America* **74**(12): 5463-5467.

Sawyer, D. B. and Beyenbach, K. W. (1985). "Mechanism of fluid secretion in isolated shark renal proximal tubules." *American Journal of Physiology* **249**(6): F884-890.

Schmid, T. H., Murru, F. L. and McDonald, F. (1990). "Feeding habits and growth rates of bull (*Carcharhinus leucas* (Valenciennes)), sandbar (*Carcharhinus plumbeus* (Nardo)), sandtiger (*Eugomphodus taurus* (Rafinesque)) and nurse (*Ginglymostoma cirratum* (Bonnaterre)) sharks maintained in captivity." *Journal of Aquariculture and Aquatic Sciences* **5**(4): 100-105.

Schmid, T. H. and Murru, F. L. (1994). "Bioenergetics of the Bull Shark, *Carcharhinus leucas*, Maintained in Captivity." *Zoo Biology* **13**(2): 177-185.

Schneider, J. W., Mercer, R. W., Gilmore-Hebert, M., Utset, M. F., Lai, C., Greene, A. and Benz, E. J., Jr. (1988). "Tissue specificity, localization in brain, and cell-free translation of mRNA encoding the α3 isoform of Na^+, K^+-ATPase." *Proceedings of the National Academy of Sciences of the United States of America* **85**(1): 284-288.

Schuurmans Stekhoven, F. M., Flik, G. and Wendelaar Bonga, S. E. (2001). "N-terminal sequences of small ion channels in rectal glands of sharks: a biochemical hallmark for classification and phylogeny?" *Biochemistry and Biophysical Research Communications* **288**(3): 670-675.

Schuurmans Stekhoven, F. M., Grell, E., Atsma, W., Flik, G. and Wendelaar Bonga, S. E. (2003). "Organ-related distribution of phospholemman in the spiny dogfish *Squalus acanthias*." *Biochemical and biophysical research communications.* **303**(4): 1008-1011.

Scott, G. R., Richards, J. G., Forbush, B., Isenring, P. and Schulte, P. M. (2004). "Changes in gene expression in gills of the euryhaline killifish *Fundulus heteroclitus* after abrupt salinity transfer." *American Journal of Physiology* **287**(1): C300-C335.

Scott, G. R., Claiborne, J. B., Edwards, S. L., Schulte, P. M. and Wood, C. M. (2005). "Gene expression after freshwater transfer in gills and opercular epithelia of killifish: insight into divergent mechanisms of ion transport." *Journal of Experimental Biology* **208**: 2719-2729.

Segall, L., Lane, L. K. and Blostein, R. (2002). "New insights into the role of the N terminus in conformational transitions of the Na, K-ATPase." *Journal of Biological Chemistry* **277**(38): 35202-35209.

Seibel, B. A. and Walsh, P. J. (2002). "Trimethylamine oxide accumulation in marine animals: relationship to acylglycerol storage." *Journal of Experimental Biology* **205**(3): 297-306.

Seidelin, M., Madsen, S. S., Cutler, C. P. and Cramb, G. (2001). "Expression of gill vacuolar-type H^+-ATPase B subunit, and Na+,K^+-ATPase α_1 and β_1 subunit messenger RNAs in smolting *Salmo salar*." *Zoological Science* **18**: 315-324.

Shikano, T. and Fujio, Y. (1998[a]). "Immunolocalization of Na^+/K^+-ATPase in branchial epithelium of chum salmon fry during seawater and freshwater acclimation." *Journal of Experimental Biology* **201**: 3031-3040.

Shikano, T. and Fujio, Y. (1998[b]). "Relationships of salinity tolerance to immunolocalization of Na^+, K^+-ATPase in the gill epithelium during seawater and freshwater adaptation of the guppy, *Poecilia reticulata*." *Zoological Science* **15**: 35-41.

Shikano, T. and Fujio, Y. (1998[c]). "Immunolocalization of Na^+, K^+-ATPase and Morphological Changes in Two Types of Chloride Cells in the Gill Epithelium During Seawater and Freshwater Adaptation in the Euryhaline Teleost *Poecilia reticulata*." *Journal of Experimental Zoology* **281**: 80-89.

Shikano, T. and Fujio, Y. (1999). "Changes in Salinity Tolerance and Branchial Chloride Cells of Newborn Guppy During Freshwater and Seawater Adaptation." *Journal of Experimental Zoology* **284**(2): 137-146.

Shrimpton, J. M. and McCormick, S. D. (1999). "Responsiveness of gill Na^+/K^+-ATPAse to cortisol is related to gill corticosteroid receptor concentration in juvenile ranboiw trout." *Journal of Experimental Biology* **202**: 987-995.

Shumaker, H. and Soleimani, M. (1999). "CFTR upregulates the expression of the basolateral Na^+-K^+-$2Cl^-$ cotransporter in cultured pancreatic duct cells." *American Journal of Physiology* **277**(1): C1100-C1110.

Shuttleworth, T. J. and Thompson, J. L. (1980). "Oxygen consumption in the rectal gland of the dogfish *Scyliorhinus canicula* and the effects of cyclic AMP." *Journal of Comparative Physiology* **136**: 39-43.

Shuttleworth, T. J. and Thorndyke, M. C. (1984). "An endogenous peptide stimulates secretory activity in the elasmobranch rectal gland." *Science* **225**(4659): 319-321.

Shuttleworth, T. J. (1988). Salt and Water Balance - Extrarenal Mechanisms. *Physiology of Elasmobranch Fishes*. Shuttleworth, T. J., CRC Press: 171-199.

Silva, P., Stoff, J., Field, M., Fine, L., Forrest, J. N. and Epstein, F. H. (1977). "Mechanism of active chloride secretion by shark rectal gland: role of Na-K-ATPase in chloride transport." *American Journal of Physiology* **233**(4): F298-F306.

Silva, P., Stoff, J. S., Leone, D. R. and Epstein, F. H. (1985). "Mode of action of somatostatin to inhibit secretion by shark rectal gland." *American Journal of Physiology* **249**(3): R329-334.

Silva, P., Lear, S., Reichlin, S. and Epstein, F. H. (1990). "Somatostatin mediates bombesin inhibition of chloride secretion by rectal gland." *American Journal of Physiology* **258**(6): R1459-1463.

Silva, P. and Epstein, F. H. (1993[a]). "Secretion of nitrate by rectal gland of *Squalus acanthias*." *Comparative Biochemistry and Physiology* **104A**(2): 255-259.

Silva, P., Epstein, F. H. and Solomon, R. J. (1993[b]). "C-type Natriuretic Peptide (CNP) Stimulates Chloride Secretion by the Rectal Gland of the Shark via a Dual Mechanism of Action Involving Protein Kinase C." *Clinical Research* **41**(2): 327A.

Silva, P., Solomon, R. J. and Epstein, F. H. (1996). "The rectal gland of *Squalus acanthias*: A model for the transport of chloride." *Kidney International* **49**(6): 1552-1556.

Silva, P., Solomon, R. J. and Epstein, F. H. (1999). "Mode of activation of salt secretion by C-type natriuretic peptide in the shark rectal gland." *American Journal of Physiology* **277**(6): R1725-1732.

Simmerman, H. K. B. and Jones, L. R. (1998). "Phospholamban: Protein Structure, Mechanism of Action, and Role in Cardiac Function." *Physiological Reviews* **78**(4): 921-948.

Simpfendorfer, C. A. and Milward, N. E. (1993). "Utilisation of a tropical bay as a nursery area by sharks of the families Carcharhinidae and Sphyrnidae." *Environmental Biology of Fishes* **37**(4): 337-245.

Simpfendorfer, C. A. (2005). "Threatened fishes of the world: Pristis pectinata Latham, 1794 (Pristidae)." *Environmental Biology of Fishes* **73**(1): 20.

Simpfendorfer, C. A., Freitas, G. G., Wiley, T. R. and Heupel, M. R. (2005). "Distribution and Habitat Partitioning of immature Bull Sharks (*Carcharhinus leucas*) in a Southwest Florida Estuary." *Estuaries* **28**: 78-85.

Singer, T. D., Tucker, S. J., Marshall, W. S. and Higgins, C. F. (1998). "A divergent CFTR homologue: highly regulated salt transport in the euryhaline teleost *F. heteroclitus*." *American Journal of Physiology* **274**(3): C715-723.

Skou, J. C. (1957). "The influence of some cations on an adenosine triphosphate from peripheral nerves." *Biochimica Et Biophysica Acta* **23**: 354-401.

Skou, J. C. and Esmann, M. (1992). "The Na, K-ATPase." *Journal of Bioenergetics and Biomembranes* **24**(3): 249-260.

Smith, C. P. and Wright, P. A. (1999). "Molecular characterization of an elasmobranch urea transporter." *American Journal of Physiology* **276**(2): R622-626.

Snelson, F. F., Mulligan, T. J. and Williams, S. E. (1984). "Food habits, occurrence, and population structure of the bull shark, *Carcharhinus leucas*, in Florida coastal lagoons." *Bulletin of Marine Science* **34**(1): 71-80.

Solomon, R., Taylor, M., Stoff, J. S., Silva, P. and Epstein, F. H. (1984[a]). "In vivo effect of volume expansion on rectal gland function. I. Humoral factors." *American Journal of Physiology* **246**(1): R63-66.

Solomon, R. J., Taylor, M., Rosa, R., Silva, P. and Epstein, F. H. (1984[b]). "In vivo effect of volume expansion on rectal gland function. II. Hemodynamic changes." *American Journal of Physiology* **246**(1): R67-71.

Solomon, R., Taylor, M., Dorsey, D., Silva, P. and Epstein, F. H. (1985). "Atriopeptin stimulation of rectal gland function in *Squalus acanthias*." *American Journal of Physiology* **249**(3): R348-354.

Solomon, R., Protter, A., McEnroe, G., Porter, J. G. and Silva, P. (1992). "C-type natriuretic peptides stimulate chloride secretion in the rectal gland of *Squalus acanthias*." *American Journal of Physiology* **262**(4): R707-711.

Sosa-Nishizaki, O., Taniuchi, T., Ishihara, H. and Shimizu, M. (1998). "The bull shark, *Carcharhinus leucas* (Valenciennes, 1841), from the Usumacinta River, Tabasco, Mexico, with notes on its serum composition and osmolarity." *Ciencias Marinas* **24**(2): 183-192.

Steele, S. L., Yancey, P. H. and Wright, P. A. (2004). "Dogmas and controversies in the handling of nitrogenous wastes: Osmoregulation during early embryonic development in the marine little skate *Raja erinacea*; response to changes in external salinity." *Journal of Experimental Biology* **207**(12): 2021-2031.

Steele, S. L., Yancey, P. H. and Wright, P. A. (2005). "The Little Skate *Raja erinacea* Exhibits an Extrahepatic Ornithine Urea Cycle in the Muscle and Modulates Nitrogen Metabolism during Low-Salinity Challenge." *Physiological and Biochemical Zoology* **78**: 216-226.

Stoff, J. S., Silva, P., Field, M., Forrest, J., Stevens, A. and Epstein, F. H. (1977). "Cyclic AMP regulation of active chloride transport in the rectal gland of marine elasmobranchs." *Journal of Experimental Zoology* **199**(3): 443-438.

Stoff, J. S., Rosa, R., Hallac, R., Silva, P. and Epstein, F. H. (1979). "Hormonal regulation of active chloride transport in the dogfish rectal gland." *American Journal of Physiology* **237(2)**: F138-144.

Stoff, J. S., Silva, P., Lechan, R., Solomon, R. and Epstein, F. H. (1988). "Neural control of shark rectal gland." *American Journal of Physiology* **255**(2): R212-216.

Stolte, H., Galaske, R. G., Eisenbach, G. M., Lechene, C., Schmidt-Nielson, B. and Boylan, J. W. (1977). "Renal tubule ion transport and collecting duct function in the elasmobranch little skate, *Raja erinacea*." *Journal of Experimental Zoology* **199**(3): 403-410.

Sulikowski, J. A. and Maginniss, L. A. (2001). "Effects of environmental dilution on body fluid regulation in the yellow stingray, *Urolophus jamaicensis*." *Comparative Biochemistry and Physiology* **128A**(2): 223-232.

Sulikowski, J. A., Treberg, J. R. and Howell, W. H. (2003). "Fluid Regulation and Physiological Adjustments in the Winter Skate, *Leucoraja ocellata*, Following Exposure to Reduced Environmental Salinities." *Environmental Biology of Fishes* **66**(4): 339-348.

Suzuki, R., Togashi, K., Ando, K. and Takei, Y. (1994). "Distribution and molecular forms of C-type natriuretic peptide in plasma and tissue of a dogfish, *Triakis scyllia*." *General and Comparative Endocrinology* **96**(3): 378-384.

Sweadner, K. J. and Rael, E. (2000). "The FXYD gene family of small ion transport regulators or channels: cDNA sequence, protein signature sequence, and expression." *Genomics* **68**(1): 41-56.

Sweadner, K. J., Arystarkhova, E., Donnet, C. and Wetzel, R. K. (2003). "FXYD proteins as regulators of the Na, K-ATPase in the kidney." *Annals of the New York Academy of Sciences* **986**: 382-387.

Tam, W. L., Wong, W. P., Loong, A. M., Hiong, K. C., Chew, S. F., Ballantyne, J. S. and Ip, Y. K. (2003). "The osmotic response of the Asian freshwater stingray (*Himantura signifer*) to increased salinity: a comparison with marine (*Taeniura lymma*) and Amazonian freshwater (*Potamotrygon motoro*) stingrays." *Journal of Experimental Biology* **206**(17): 2931-2940.

Teixeira, V. L., Katz, A. I., Pedemonte, C. H. and Bertorello, A. M. (2003). "Isoform-specific regulation of Na^+, K^+-ATPase endocytosis and recruitment to the plasma membrane." *Annals of the New York Academy of Sciences* **986**: 587-594.

Therien, A. G., Goldshleger, R., Karlish, S. J. and Blostein, R. (1997). "Tissue-specific distribution and modulatory role of the gamma subunit of the Na, K-ATPase." *Journal of Biological Chemistry* **272**(51): 32628-34.

Therien, A. G., Pu, H. X., Karlish, S. J. D. and Blostein, R. (2001). "Molecular and Functional Studies of the Gamma Subunit of the Sodium Pump." *Journal of Bioenergetics and Biomembranes* **33**(5): 407-414.

Thomas, S. and Egee, S. (1998). "Fish red blood cells: characteristics and physiological role of the membrane ion transporters." *Comparative Biochemistry and Physiology* **119A**(1): 79-86.

Thorndyke, M. C. and Shuttleworth, T. J. (1985). "Biochemical and physiological studies on peptides from the elasmobranch gut." *Peptides* **6** (Supplement 3): 369-372.

Thorson, T. B. (1962). "Partitioning of body fluids in the Lake Nicaragua shark and three marine sharks." *Science* **138**: 688-690.

Thorson, T. B. (1967). Osmoregulation in fresh-water elasmobranchs. *Sharks, Skates and Rays*: 265-270.

Thorson, T. B., Cowan, C. M. and Watson, D. E. (1967). "*Potamotrygon spp.*: elasmobranchs with low urea content." *Science* **158**(799): 375-377.

Thorson, T. B. and Gerst, J. W. (1972). "Comparison of some parameters of serum and uterine fluid of pregnant, viviparous sharks (*Carcharhinus leucas*) and serum of their near-term young." *Comparative Biochemistry and Physiology* **42A**(1): 33-40.

Thorson, T. B., Cowan, C. M. and Watson, D. E. (1973). "Body fluid solutes of juveniles and adults of the euryhaline bull shark *Carcharhinus leucas* from freshwater and saline environments." *Physiological Zoology* **46**: 29-42.

Thorson, T. B., Wotton, R. M. and Georgi, T. A. (1978). "Rectal gland of freshwater stingrays, *Potamotrygon spp.* (Chondrichthyes: Potamotrygonidae)." *Biological Bulletin* **154**: 508-516.

Thorson, T. B. (1982). "Life history implications of a tagging study of the largetooth sawfish, *Pristis perotteti*, in the Lake Nicaragua-Rio San Juan system." *Environmental Biology of Fishes* **7**(3): 207-228.

Thorson, T. B. and Lacy, E. J. (1982). "Age, growth rate and longevity of *Carcharhinus leucas* estimated from tagging and vertebral rings." *Copeia* **1982**(1): 110-116.

Thorson, T. B., Brooks, D. R. and Mayes, M. A. (1983). "The evolution of freshwater adaptation in stingrays." *National Geographic Research Reports* **15**: 663-674.

Tierney, M. L., Hamano, K., Anderson, G., Takei, Y., Ashida, K. and Hazon, N. (1997[a]). "Interactions between the renin-angiotensin system and catecholamines on the cardiovascular system of elasmobranchs." *Fish Physiology and Biochemistry* **17**: 333-337.

Tierney, M., Takei, Y. and Hazon, N. (1997[b]). "The presence of angiotensin II receptors in elasmobranchs." *General and Comparative Endocrinology* **105**(1): 9-17.

Tolentino, P. J., DeFord, S. M., Notterpek, L., Glenn, C. C., Pike, B. R., Wang, K. K. and Hayes, R. L. (2002). "Up-regulation of tissue-type transglutaminase after traumatic brain injury." *Journal of Neurochemistry* **80**(4): 579-588.

Treberg, J. R. and Driedzic, W. R. (2002). "Elevated Levels of Trimethylamine Oxide in Deep-Sea Fish: Evidence for Synthesis and Intertissue Physiological Importance." *Journal of Experimental Zoology* **293**(1): 39-45.

Uchida, K., Kaneko, T., Yamaguchi, A., Ogasawara, T. and Hirano, T. (1997). "Reduced hypoosmoregulatory ability and alteration in gill chloride cell distribution in mature chum salmon (*Oncorhynchus keta*) migrating upstream for spawning." *Marine Biology* **129**(2): 247-254.

Ura, K., Mizuno, S., Okubo, T., Chida, Y., Misaka, N., Adachi, S. and Yamauchi, K. (1997). "Immunohistochemical study of changes in gill Na^+/K^+-ATPase α-subunit during smoltification in the wild masu salmon, *Oncorhynchus masou*." *Fish Physiology and Biochemistry* **17**: 397-403.

Valentich, J. D., Karnaky, K. J. and Ecay, T. W. (1996). "Ultrastructural and cytochemical characterization of cultured dogfish shark rectal gland cells." *American Journal of Physiology* **271**(6): C1993-2003.

Van Os, C. H., Deen, P. M. T. and Dempster, J. A. (1994). "Aquaporins: water selective channels in biological membranes. Molecular structure and tissue distribution." *Biochimica Et Biophysica Acta* **1197**(3): 291-309.

Varsamos, S., Diaz, J. P., Charmantier, G., Flik, G., Blasco, C. and Connes, R. (2002). "Branchial chloride cells in sea bass (*Dicentrarchus labrax*) adapted to fresh water, seawater, and doubly concentrated seawater." *Journal of Experimental Zoology* **293**(1): 12-26.

Veillette, P. A. and Young, G. (2004). "Temporal changes in intestinal Na^+, K^+-ATPase activity and in vitro responsiveness to cortisol in juvenile chinook salmon." *Comparative Biochemistry and Physiology* **138A**(3): 297-303.

Verkman, A. S. and Mitra, A. K. (2000). "Structure and function of aquaporin water channels." *American Journal of Physiology* **278**(1): F13-28.

Vilsen, B., Ramlov, D. and Andersen, J. P. (1997). "Functional consequences of mutations in the transmembrane core region for cation translocation and energy transduction in the Na^+, K^+-ATPase and the SR $Ca(2^+)$-ATPase." *Annals of the New York Academy of Sciences* **834**: 297-309.

Voet, J., G. and Voet, D. (1990). *Biochemistry*. New York, Wiley.

Waldegger, S., Fakler, B., Bleich, M., Barth, P., Hopf, A., Schulte, U., Busch, A. E., Aller, S. G., Forrest, J. N., Jr., Greger, R. and Lang, F. (1999). "Molecular and functional characterization of s-KCNQ1 potassium channel from rectal gland of *Squalus acanthias*." *Pflugers Archiv* **437**(2): 298-304.

Wetzel, R. K. and Sweadner, K. J. (2001). "Immunocytochemical localization of Na-K-ATPase alpha- and gamma-subunits in rat kidney." *American Journal of Physiology* **281**(2): F531-F545.

Whitehead, D. L. (2002). "Ampullary organs and electroreception in freshwater *Carcharhinus leucas*." *Journal of Physiology Paris* **96**(5-6): 391-395.

Wilkie, M. P. (1997). "Mechanisms of ammonia excretion across fish gills." *Comparative Biochemistry and Physiology* **118A**(1): 39-50.

Wilson, E. D., McGuinn, M. R. and Goldstein, L. (1999). "Trimethylamine Oxide Transport Across Plasma Membranes of Elasmobranch Erythrocytes." *Journal of Experimental Zoology* **284**(6): 605-609.

Wilson, J. M., Randall, D. J., Vogl, A. W., Harris, J., Sly, W. S. and Iwama, G. K. (2000). "Branchial carbonic anhydrase is present in the dogfish, *Squalus acanthias*." *Fish Physiology and Biochemistry* **22**(4): 329-336.

Wilson, J. M., Morgan, J. D., Vogl, A. W. and Randall, D. J. (2002). "Branchial mitochondria-rich cells in the dogfish *Squalus acanthias*." *Comparative Biochemistry and Physiology* **132A**(2): 365-374.

Wintner, S. P., Dudley, S. F. J., Kistnasamy, N. and Everett, B. (2002). "Age and growth estimates for the Zambezi shark, *Carcharhinus leucas*, from the east coast of South Africa." *Marine and Freshwater Research* **53**(2): 557-566.

Withers, P. C. (1992). *Comparative Animal Physiology*. Forth Worth, Saunders College Publishing.

Withers, P. C., Morrison, G. and Guppy, M. (1994). "Buoyancy Role of Urea and TMAO in an Elasmobranch Fish, the Port Jackson Shark, *Heterodontus portusjacksoni*." *Physiological Zoology* **67**(3): 693-705.

Witters, H., Berckmans, P. and Vangenechten, C. (1996). "Immunolocalization of Na+,K^+-ATPase in the gill epithelium of rainbow trout, *Oncorhynchus mykiss*." *Cell and Tissue Research* **283**: 461-468.

Wong, C. K. and Chan, D. K. (1999). "Isolation of viable cell types from the gill epithelium of Japanese eel *Anguilla japonica*." *American Journal of Physiology* **276**(2): R363-372.

Wong, T. M. and Chan, D. K. O. (1977). "Physiological adjustments to dilution of the external medium in the Lip-shark *Hemiscyllium plagiosum* (Bennett)." *Journal of Experimental Zoology* **200**: 85-96.

Wood, C., Pärt, P. and Wright, P. (1995). "Ammonia and urea metabolism in relation to gill function and acid-base balance in a marine elasmobranch, the spiny dogfish (*Squalus acanthias*)." *Journal of Experimental Biology* **198**(7): 1545-1558.

Wood, C. M., Matsuo, A. Y., Gonzalez, R. J., Wilson, R. W., Patrick, M. L. and Val, A. L. (2002). "Mechanisms of ion transport in *Potamotrygon*, a stenohaline freshwater elasmobranch native to the ion-poor blackwaters of the Rio Negro." *Journal of Experimental Biology* **205**(19): 3039-3054.

Wright, P. A. and Land, M. D. (1998). "Urea production and transport in teleost fishes." *Comparative Biochemistry and Physiology* **119A**(1): 47-54.

Wu, Y. C., Lin, L. Y. and Lee, T. H. (2003). "Na+,K^+,2Cl^--cotransporter: A Novel Marker for Identifying Freshwater- and Seawater-type Mitochondria-rich Cells in Gills of the Euryhaline Tilapia, *Oreochromis mossambicus*." *Zoological Studies* **42**(1): 186-192.

Xu, J. C., Lytle, C., Zhu, T. T., Payne, J. A., Benz, E., Jr. and Forbush, B., 3rd (1994). "Molecular cloning and functional expression of the bumetanide-sensitive Na-K-Cl cotransporter." *Proceedings of the National Academy of Sciences of the United States of America* **91**(6): 2201-2205.

Yamaguchi, F., Yamaguchi, K., Tai, Y., Sugimoto, K. and Tokuda, M. (2001). "Molecular cloning and characterization of a novel phospholemman-like protein from rat hippocampus." *Molecular Brain Research* **86**(1-2): 189-192.

Yancey, P. H. and Somero, G. N. (1979). "Counteraction of urea destabilization of protein structure by methylamine osmoregulatory compounds of elasmobranch fishes." *Biochemical Journal* **183**(2): 317-323.

Yancey, P. H. and Somero, G. N. (1980). "Methylamine osmoregulatory solutes of elasmobranch fishes counteract urea inhibition of enzymes." *Journal of Experimental Zoology* **212**: 205-213.

Yoshikawa, J. S. M., McCormick, S. D., Young, G. and Bern, H. A. (1993). "Effects of salinity of chloride cells and Na^+, K^+-ATPase activity in the teleost *Gillichthys mirabilis*." *Comparative Biochemistry and Physiology* **105A**(2): 311-317.

Yoshimura, S. H. and Takeyasu, K. (2003). "Differential degradation of the Na^+/K^+-ATPase subunits in the plasma membrane." *Annals of the New York Academy of Sciences* **986**: 378-381.

Zeidel, J. D., Mathai, J. C., Campbell, J. D., Ruiz, W. G., Apodaca, G. L., Riordan, J. and Zeidel, M. L. (2005). "Selective permeability barrier to urea in shark rectal gland." *American Journal of Physiology* **289**(1): F83-89.

Appendices

Appendix 1: List of species cited, in alphabetical order

Scientific name	Common name
Anguilla anguilla	European eel
Carcinus maenas	shore crab
Carcharhinus leucas	bull shark
Carcharhinus limbatus	blacktip shark
Carcharhinus obscurus	dusky shark
Carcharias taurus	sandtiger shark/grey nurse shark/spotted raggedtooth
Carcharodon carcharias	white shark
Centroscyllium fabricii	black dogfish
Chanos chanos	milkfish
Chelon labrosus	thick-lipped grey mullet
Chiloscyllium plagiosum	whitespotted bambooshark
Cyprinodon variegatus	pupfish/sheepshead minnow
Cyprinus carpio	common carp
Dasyatis garouaensis	smooth freshwater stingray
Dasyatis sabina	Atlantic stingray
Dicentrarchus labrax	European seabass
Fundulus chrysotus	golden topminnow
Fundulus heteroclitus	killifish, mummichog
Fundulus similis	longnose killifish
Geotria australis	pouched lamprey
Gillichthys mirabilis	longjawed mudsucker
Glyphis spp.	freshwater sharks of the genus *Glyphis*
Heterodontus portusjacksoni	Port Jackson shark
Himantura signifer	Asian white-edge freshwater whip ray
Himantura uarnak	honeycomb stingray
Latimeria chalumnae	coelacanth
Leucoraja ocellata	winter skate
Manta birostris	manta ray
Mugil cephalus	striped mullet
Mustelus canis	dusky smoothhound
Mylio macrocephalus	black sea bream
Myxine glutinosa	hagfish
Narcine brasiliensis	lesser electric ray
Negaprion brevirostris	lemon shark
Nematolosa erebi	bony bream
Notothenia angustata	New Zealand black cod
Notothenia neglecta	Antarctic fish
Oreochromis mossambicus	Mozambique tilapia
Oreochromis niloticus	Nile tilapia
Oncorhynchus keta	chum salmon
Oncorhynchus mykiss	rainbow trout
Oncorhynchus tshawytscha	chinook salmon
Paralichthys dentatus	summer flounder
Periophthalmodon schlosseri	giant mudskipper
Platichthys flesus	European flounder
Poecilia latipinna	sailfin molly
Poecilia reticulata	guppy
Poroderma africanum	pyjama shark/striped catshark
Potamotrygon spp.	Amazonian freshwater rays
Pristis microdon	freshwater sawfish
Pristis pectinata	smalltooth sawfish
Pristis perotteti	largetooth sawfish
Raja erinacea	little skate
Raja radiata	thorny skate/starry skate
Salmo salar	Atlantic salmon

Salmo trutta	brown trout
Scyliorhinus canicula	European lesser spotted dogfish/ smallspotted catshark
Sparus aurata	gilthead sea bream
Sparus sarba	silver sea bream
Squalus acanthias	piked dogfish/spiny dogfish
Stenogobius hawaiiensis	Hawaiian goby
Tetraodon nigroviridis	spotted green pufferfish
Torpedo californica	Pacific electric ray
Trematomus bernacchii	emerald notothen/emerald rockcod
Triakis scyllium	banded houndshark
Triakis semifasciata	leopard shark
Trygonoptera testacea	common stingaree
Urolophus jamaicensis	yellow stingray

N. B. Latin and common names may differ from those specified in the publications cited. Where possible, the nomenclature used reflects the most current classification of each species.

Appendix 2: List of suppliers of equipment and chemicals.

Ambion Inc., Abingdon, Oxfordshire, UK
Amersham Pharmacia Biotech, Little Chalfont, Buckinghamshire, UK
Applied Biosystems, Foster City, California, USA
Aquasonic, Wauchope, NSW, Australia
Baird and Tatlock (London) Ltd., London, UK
Beckman Instruments Inc. Palo Alto, California, USA
BD Biosciences, Erembodegem, Belgium
Bibby Stuart, Staffordshire, UK
BIO 101 Inc., Anachem Ltd, Luton, UK
Biogene Ltd., Anachem Ltd., Luton, UK
Bio-Rad Laboratories, Hercules, California, USA
Biosoft, Cambridge, UK
Calor, Warwick, UK
Canberra Packard, Meridan, California, USA
Clontech, Basingstoke, UK
Eastman Kodak Co., Rochester, New York, USA
Edge Biosystems, Gaithersburg, USA
Genbank®, NCBI, Bethesda, Maryland, USA
Gibco Life Technologies Ltd., Paisley, UK
Helena Biosciences Europe, Sunderland, Tyne and Wear, UK
Herolab GMBH laboratory, Weisloch, Germany
Invitrogen, Groningen, The Netherlands
Jackson ImmunoResearch Europe Ltd., Cambridgeshire, UK
Kinematica Ltd., Lucerne, Switzerland
Leec Ltd., Nottingham, UK
Leitz, Oberkochen, Germany
Millipore, Watford, UK
MWG Biotech, Milton Keynes, UK
New England Biolabs, Hitchin, Hertfordshire, UK
Oxoid, Unipath Ltd, UK
Packard Instruments, Pangbourne, Berkshire, UK
PE Applied Biosystems, Perkin Elmer Ltd, Chesire, UK
Pharmacia Ltd., Morpeth, UK
PNACL, Universityof Leicester, Leicester, UK
Polaroid (UK) Ltd., Luton, UK
Polytech, Brisbane, QLD, Australia
Promega Corporation UK, Southampton, UK
Qbiogene Inc., Irvine, California, USA
SAS Institute Inc., Cary, North Carolina, USA
Scie-Plas, Southam, Warwickshire, UK
Scotlab, Coatbridge, Strathclyde, UK
Sigma Aldrich Ltd., Poole, Dorset
Sigma Genosys, Cambridgeshire, UK
Spectronics Corporation, Westbury, New York, USA
Syngene, Cambridge, UK
Techne Ltd., Cambridge, UK
VWR Laboratory Supplies, Poole, Dorset, UK
Weiss-Gallenkamp, Loughborough, UK
Zeiss, Oberkochen, Germany

Appendix 3: Primer Sequences

All primers are listed in standard IUPAC (International Union of Pure and Applied Chemistry) code format. N = I/C wobble.

Clontech Marathon™ cDNA Amplification Kit Primers

BD Smart II™ A Oligonucleotide	5' AAG CAG TGG TAT CAA CGC AGA GTA CGC GGG 3'
Marathon™ cDNA synthesis primer	5' GGA ACA AAC GGC ATG TGA GC 3'
Marathon adaptor primer 1 (AP1)	5' CCA TCC TAA T AC GAC TCAC T AT AGG GC 3'
Marathon adaptor primer 2 (AP2)	5' ACT CAC TAT AGG GCT CGA GCG GC 3'

Degenerate Primers

P-type ATPase sense	5' ATY TGY TCN GAY AAR ACN GGN ACN YTN AC 3'
P-type ATPase antisense	5' SMR TCR TTN RYN CCR TCN CCN GT 3'
All Na, K-ATPase α sense	5' CCN ACN ACN CCN SAR TGG RTN AAR TTY TG 3'
All Na, K-ATPase α antisense	5' GTN ARN GTN CCN GTY TTR TCN GAR CAD AT 3'
All Na, K-ATPase β sense	5' TTY TWY GGN TGY YTN GYN GSN RTH TTY RT 3'
All Na, K-ATPase β antisense	5' TGN ARN WDN YKN CCR TAR TAN GGR TAR TA 3'
PLMS sense	5' CGN TTC ACT TAC GAC TAC TAC 3'
PLMS antisense	5' CCG CCT GCG GGT GGA CAG ACG GCG 3'
NKCC sense	5' GAR GAY CAY RTN AAR AAY TWY MGN CCN CAR TG 3'
NKCC antisense	5' ARC CAN YAN AYR TCN ATN GTN YYY TTN CCY TG 3'
CFTR sense	5' TAY TTY GAR ACN YTN TTY CAY AAR GC 3'
CFTR antisense	5' ARR CAC ATN ARY TGY TTR TGN CCR T 3'
AQP1e sense	5' GGN GAR ATG AGY GGN GCN CAR GTN AAY CC 3'
AQP1e antisense	5' GCN GGN CCN ARN GAN CKN GCN GGR TTC AT 3'
β-actin sense	5' GTN GAY AAY GGN TCN GGN ATG TGY AA 3'
β-actin antisense	5' GAT WCC RCA NGA YTC CAT RCC NAR GA 3'

Specific primers

C. leucas α mid 1 sense	5' CTG TCC CTC ATC CTT GGA TAC A 3'
C. leucas α mid 1 antisense	5' AGC ATC TCC AGC AAC ACT TCG 3'
C. leucas α 2 sense	5' CAG CAC TCT CCC AGT TGA GCA GTT CC 3'
C. leucas α 2 antisense	5' TCA ACC ATG TCC TTC AGG TCA GTG CCG 3'
C. leucas α 2 mid antisense	5' CTG TTA CAG AGG GCA GCA ATC CGC 3'
C. leucas α 3 sense 1	5' GGC TTC GGG ATT GGA CAC TGG GAA 3'
C. leucas α 3 sense 2	5' ACT GGC TAC AGT AAC GGT CTG CCT G 3'
C. leucas β actin sense	5' GTC ACC AAC TGG GAT GAC ATG GAG AAG 3'
C. leucas β actin antisense	5' GCA GAG CTT CTC CTT GAT GTC ACG GAC 3'

5' RACE Primers

C. leucas α 1 5' Race 1	5' GCA ACC ATG TGC AGA GAT GAT TCG CAG 3'
C. leucas α 1 5' Race 2	5' CTC CCA GGT ATA AAT TAT CAT TGG CTG GC 3'
C. leucas α 2 5' Race 1	5' GGA ATC CAT AAT TCG GGA ACT CTT TGA C 3'
C. leucas α 2 5' Race 2	5' GAT CAT CAC GAC CGC AGC CAG AAC G 3'
C. leucas α 3 5' Race 1	5' CGG TGA TGA TGA CTA CAG CCG ACA GC 3'
C. leucas α 3 5' Race 2	5' GTC TCC GGC TGG ACT GTC TTC AG 3'
C. leucas β 1 5' Race 1	5' CCA CTA GGA GAG TCA GAA CAG TCC TC 3'
C. leucas β 1 5' Race 2	5' CTT ACG TAG GAT GTT GGG TTC GAC ATG C 3'
C. leucas AQP1e 1 5' Race 1	5' GCA ACC ATG TGC AGA GAT GAT TCG CAG 3'
C. leucas AQP1e 1 5' Race 2	5' GCC TGG CTC TGT GTA ACT CCC 3'

3′ RACE Primers

C. leucas α 1 3′ Race 1	5′ GCA AGT GCA GAA GTG CTG GAA TCA AG 3′
C. leucas α 1 3′ Race 2	5′ CTC AGA ACA GCT AGA CGA CAT CTT ACA GT 3′
C. leucas α 2 3′ Race 1	5′ ACG GCA CTG ACC TGA AGG ACA TGG TTG A 3′
C. leucas α 2 3′ Race 2	5′ GAA GAA CAG CTC GAT CAG ATT TTG GCC A 3′
C. leucas α 3 3′ Race 1	5′ CGG AGA TCG TCT TCG CTC GGA 3′
C. leucas α 3 3′ Race 2	5′ CTC CCC TCA ACA GAA ACT CAT CAT CGT GGA 3′
C. leucas α 3 3′ Race 1b	5′ GAG TGG CGA GCA GAT TGA CGA CAT TCT GCG 3′
C. leucas β 1 3′ Race 1	5′ CCG CAT CTT ATT CCT ATT CAT TGT GCA GC 3′
C. leucas β 1 3′ Race 2	5′ CAT GGG AGG GTT CGC TGG CTT TCC 3′
C. leucas AQP1e 1 3′ Race 1	5′ GCA AGT GCA GAA GTG CTG GAA TCA AG 3′
C. leucas AQP1e 1 3′ Race 2	5′ CTC AGA ACA GCT AGA CGA CAT CTT ACA GT 3′

Cloning and Sequencing Primers

M13 forward	5′ GGA ACA AAC GGC ATG TGA GC 3′
M13 reverse	5′ AAG CAG TGG TAA CAA CGC AGA GTA CGC GGG3′
T7	5′ CCA TCC TAA T AC GAC TCA CT A TAG GGC 3′
T3	5′ ACT CAC TAT AGG GCT CGA GCG GC 3′
C. leucas α 1 3′ Race seq 1	5′ CTC CGT CTT CCA ACA AGG AAT GAA G 3′
C. leucas β 1 3′ Race seq 1	5′ CAG TAC TGT AGT GCA TTC ATT GGT CC 3′
C. leucas β 3′ seq	5′ CCT TGA GTA TTG CTG CCT TGT GCC TC 3′
C. leucas α 2 3′ Race seq 1	5′ GGC TTA TGA AGC AGC CGA GAG TGA CAT C 3′
C. leucas α 2 3′ Race seq 2	5′ ACT GAA GCC CCG CTC ATG TTC TC 3′

Primers for amplification of DNA probes for Northern blotting

C. leucas α 1 5′ antisense 1 (used with T7 and clone)	5′ GCT TTC TTA CTT TTC TTC TTG GAT TTG G 3′
C. leucas α 2 5′ antisense 1 (used with T7 and clone)	5′ AAC CTT CTT CTT CTT GGC ATT TTC CG 3′
C. leucas α 3 5′ antisense 1 (used with T7 and clone)	5′ CCT GTA CAC AAT CAG CAT TGT GCT TC 3′

Primers for semi-quantitative PCR

C. leucas α 1 sense	5′ CGA GGG ACG AAA GCC CAA AGA TAG TG 3′
C. leucas α 1 antisense	5′ GGA TAA CCT TCT GTA TAT GTG TCG TCA GGC 3′
C. leucas α 2 sense	5′ CTC CAT CTC CAA GCG GGA AAC AGC C 3′
C. leucas α 2 antisense	5′ GGG ATC TCT CCT CGC CAC TGC CCG CC 3′
C. leucas α 3 sense	5′ CCA TTC ATG AGA CAG AGG ACC CGA ATG 3′
C. leucas α 3 antisense	5′ CAC ATC ATC GGT GTC AAA GGC GAA TC 3′

Animation Notes

These animations were created by myself during the course of my Ph. D. studies. I have used them in several international conference presentations where I have used them to introduce my study and help the audience understand what is taking place at the organ and cell level when a bull shark is acclimated to FW or SW. The file will open in Microsoft Powerpoint (PC or Mac computers, although a PC is preferable) and the animations will work fully when viewed as a slide show. Slides 1 and 2 focus on the roles of the osmoregulatory organs and these require the viewer to click to see each stage of the animation. Slides 3 and 4 concentrate on the movement of ions across the epithelia of osmoregulatory tissues and will animate automatically. The notes below will help the viewer fully appreciate and understand the animations.

Slide 1
Here is a bull shark swimming along in seawater, where the salt levels outside are greater than inside, but sharks maintain a plasma concentration slightly higher than the external medium by retaining urea. Water is taken up across the diffusion gradient of the gills, so the kidney has to get rid of this water with isoosmotic urine. Salts are also taken in from seawater, absorbed across the gut during feeding and these are largely excreted via the rectal gland.

Slide 2
In freshwater, the situation is more similar to teleost fish where plasma osmolality and salt concentrations are much higher than the external environment leading to water uptake and ion loss. Urea is no longer retained in an effort to reduce the body fluid concentration. Water is taken up by diffusion, particularly during feeding and at the gills. The kidney has to work really hard to excrete all this extra water taken up and produces copious urine. Because the rectal gland is a purely salt secreting organ, this must be switched off when in freshwater. But salts are still going to be lost across the diffusion gradient, in the urine and across the gills. So there needs to be active ion uptake mechanisms, notably at the gills, to replenish lost ions. Water and ion transport is largely accomplished via specialised mitochondria rich cells found in the osmoregulatory organs, and these differ in mechanism depending on salinity.

Slide 3
Na is transported across the basolateral membrane, out of the cell by Na, K-ATPase. This gradient draws sodium into the cell, with chloride and potassium, across the basolateral NKCC cotransporter. Potassium exits via basolateral potassium channels, and chloride passively exits via a luminal chloride channel, the CFTR, creating an electrochemical potential. This potential forces sodium along a paracellular pathway between chloride cells. The Na, K-ATPase reaction is the only step requiring energy.

Slide 4
In freshwater, carbonic anhydrase catalyses the reaction converting water and carbon dioxide to hydrogen and bicarbonate ions. These then allow sodium and chloride into the cell via sodium hydrogen and chloride bicarbonate ion exchangers. Chloride passes into the body fluids via a basolateral chloride channel, and the sodium builds up on the Na, K-ATPase. Potassium ions from the body fluids are transported into the cell by the NaKATPase. This then flows back into the body fluids via a basolateral potassium channel. All of the transporters in the chloride cell must be working to create a net movement of ions, and the Na, K-ATPase provides the energy which drives the whole system.